ATOM TRANSFER RADICAL POLYMERIZATION WITH LOW CATALYST CONCENTRATION IN CONTINUOUS PROCESSES

by

NICKY C. F. CHAN

A thesis submitted to the

Department of Chemical Engineering

In conformity with the requirements for

the degree of Doctor of Philosophy

Queen's University

Kingston, Ontario, Canada

April, 2012

Abstract

Atom transfer radical polymerization (ATRP) is a dynamic technique that possesses tremendous potential for the synthesis of novel polymeric materials not possible through conventional free radical polymerization. However, its use on an industrial scale has been limited by the high level of transition metal complex required. Significant advances have been made in the last 5 years towards lowering the level of copper complexes used in ATRP, resulting in novel variants called "activator regenerated by electron transfer" (ARGET) and "single electron transfer-living radical polymerization" (SET-LRP).

To fully realize the potential of ATRP, its use in industrially relevant processes must be studied. Continuous processes such as tubular flow reactors and stirred tank reactors (CSTR) can reduce waste, improve productivity and facilitate process scale-up when compared to common batch reactors. The combination of low copper concentration ATRP techniques and continuous processes are especially attractive towards the design of a commercially viable process. This thesis presents a study into ARGET ATRP and SET-LRP as applied to continuous tubular and stirred tank reactors for the production of acrylic and methacrylic polymers.

The equilibrium which governs polymerization rate and control over molecular architecture is studied through batch ARGET ATRP experiments. The improved understanding of ARGET ATRP enabled the reduction of ligand from a 3 to 10 fold excess used previously down to a stoichiometric ratio to copper salts. ARGET ATRP was then adapted to a continuous tubular reactor, as well as to a semi-automated CSTR. The design of the reactors and the effect of reaction conditions such as reducing agent concentration and residence time are discussed.

The use of common elemental copper(0) such as copper wire and copper tubing is also investigated with SET-LRP for room temperature polymerization of methyl acrylate. SET-LRP is adapted to a CSTR to observe the effects of residence time on reaction rate, molecular weight

control as well as copper consumption rate. The use of copper tubing as a catalyst source for SET-LRP is demonstrated and the design of a continuous tubular reactor using a combination of copper and stainless steel tubing is discussed.

Co-Authorship

The bulk of the research in this thesis was conducted independently under the supervision of Dr. Michael Cunningham and Dr. Robin Hutchinson at Queen's University. The material presented in Chapters 3, 4, 6, 7, and 8 have been accepted and published in a variety of peer-reviewed and respected journals as detailed later on in the thesis.

The experimental work in Chapter 4 on ARGET ATRP in a continuous tubular reactor was conducted at Queen's University with the help of Dr. Salima Boutti, who also assisted in the editing of the manuscript and subsequent publication.

The adaptation of ARGET ATRP to a CSTR in Chapter 5 was done in collaboration with Dr. Jan Meuldijk at the Eindhoven University of Technology. The preliminary experimental work was done in Eindhoven, and Dr. Meuldijk is also assisting with the preparation of the manuscript to be submitted.

Acknowledgements

I would like to express my gratitude towards my supervisors, Dr. Michael Cunningham and Dr. Robin Hutchinson, for their guidance, support, and encouragement throughout my graduate studies at Queen's University. They have been instrumental in my growth as a researcher and as a person, and I am thankful for the opportunities for learning and development that I have been given in the last 5 years.

I would also like to thank Dr. Jan Meuldijk for the opportunity to work in the Eindhoven University of Technology as part of my Ph.D. studies. It was a great research opportunity, and I also made some good friends who share a love of beer and Greek food. Homies for life, respect no disrespect. On the subject of friends, I also need to thank the many friends and colleagues at Queen's University who have made my time here so memorable. There are just too many bros and honorary bros to list.

Finally, to my family and loved ones, thanks for everything. Especially the parts where you tried to get me to explain what it is I've been doing in school for so many years. I've learned a great deal about ATRP, but I still don't know what the Chinese translation is.

"If you can fill the unforgiving minute
With sixty seconds' worth of distance run,
Yours is the Earth and everything that's in it,
And – which is more – you'll be a Man, my son!"

– Rudyard Kipling, *If*

Table of Contents

List of Figures

List of Tables

List of Schemes

Nomenclature

$[Cu^{II}(TPMA)Br][Br]$	Copper(II) bromide bound to TPMA
AGET	Activator generated by Electron Transfer
AIBN	azobisisobutyronitrile
ARGET	Activator Regenerated by Electron Transfer
BA	Butyl acrylate
BMA	Butyl methacrylate
BPMODA	Bis(2-pyridylmethyl)octadecylamine
CRP	Controlled Radical Polymerization
CSTR	Continuous stirred tank reactor
CuBr	Copper (I) bromide
$CuBr_2$	Copper (II) bromide
DMF	Dimethylformamide
DMSO	Dimethyl sulfoxide
EBiB	Ethyl 2-bromoisobutyrate
Et_6TREN	tris[2-(diethylamino)ethyl]amine
FRP	Free Radical Polymerization
GPC	Gel permeation chromatography
HMTETA	Hexamethyltriethylenetetramine
ICAR	Initiators for Continuous Activator Regeneration
ISET	Inner sphere electron transfer
k_{act}	ATRP activation rate constant
K_{ATRP}	ATRP equilibrium constant
K_{BH}	Rate constant of alkyl halide bond homolysis

k_{deact}	ATRP deactivation rate constant
K_{EA}	Rate constant of reduction of halogen to a halide ion
K_{ET}	Rate constant of oxidation of metal complex
k_p	Rate constant of propagation in free radical polymerization
k_p	Rate constant of termination in free radical polymerization
K_X	Rate constant of association of halide ion to metal complex
MA	Methyl acrylate
Me_6TREN	tris[2-(dimethylamino)ethyl]amine
MMA	Methyl methacrylate
M_n	Number-average molecular weight
MWD	Molecular weight distribution
NMP	Nitroxide mediated polymerization
OSET	Outer sphere electron transfer
PBR	Packed bed reactor
PDI	Polydispersity index
PMDETA	N,n,n',n',n-Pentamethyldiethylenetriamine
ppm	Parts per million
PRE	Persistent radical effect
RAFT	reversible addition fragmentation chain transfer (RAFT)
RTD	Residence time distribution
R-X	Alkyl halide initiator, or halogen capped polymer chain in dormant state
$R^{\bullet}$	Active radical species
SET-LRP	Single Electron Transfer-Living Radical Polymerization
$Sn(EH)_2$	Tin(II) 2-ethylhexanoate
τ	Mean residence time

List of Publications

Chan, N.; Cunningham, M. F.; Hutchinson, R. A. ARGET ATRP of Methacrylates and Acrylates with Stoichiometric Ligand to Copper Ratios. *Macromolecular Chemistry and Physics* **2008**, *209*, 1797-1805.

Chan, N.; Boutti, S.; Cunningh**a**m, M. F.; Hutchinson, R. A. Continuous atom transfer radical polymerization with low catalyst concentration in a tubular reactor. *Macromolecular Reaction Engineering* **2009**, *3*, 222-231.

Chan, N.; Cunningham, M. F.; Hutchinson, R. A. Reducing ATRP Catalyst Concentration in Batch, Semibatch and Continuous Reactors. *Macromolecular Reaction Engineering* **2010**, *4*, 369-380.

Chan, N.; Cunningham, M. F.; Hutchinson, R. A. Continuous controlled radical polymerization of methyl acrylate in a copper tubular reactor. *Macromolecular Rapid Communications* **2011**, *32*, 604-609.

Chan, N.; Cunningham, M. F.; Hutchinson, R.A. Continuous controlled radical polymerization of methyl acrylate with copper wire in a CSTR. *Polymer Chemistry* **2012**, *3*, 486-497.

Chan, N.; Cunningham, M. F.; Hutchinson, R.A. Copper mediated controlled radical polymerization in the presence of ascorbic acid in a continuous tubular reactor. *Polymer Chemistry* **2012**, *3*, 1322-1333.

Chapter 1

Introduction

Controlled radical polymerization (CRP) has emerged as a promising route for the synthesis of novel macromolecules with well-controlled microstructure. Atom transfer radical polymerization (ATRP) in particular has received extensive academic and industrial interest as it is able to polymerize a wide range of monomers under relatively mild conditions with good control, leading to a variety of value-added polymeric materials with innovative applications. Despite the ability to tailor polymer structure to an extent not possible with conventional free radical polymerization (FRP), few examples can be found where ATRP is employed on a large scale. Widespread adoption of ATRP has been hindered by practical concerns over low polymerization rates, material costs of metal complexes and other components, toxicity of the compounds involved, as well as post-polymerization purification costs associated with metal complex removal.

Recent advances in the understanding of the ATRP equilibrium have allowed for significant reduction in the level of copper metal complexes used in ATRP down to almost negligible parts per million (ppm) levels. The improved ATRP systems are called "activator regenerated by electron transfer" (ARGET), "initiators for continuous activator regeneration" (ICAR), and "single electron transfer-living radical polymerization" (SET-LRP) and will be discussed in more detail in Chapter 2.

In order to fully realize the commercial potential of ATRP, an emphasis must be placed on the development of more industrially viable processes such as continuous reactors due to their increased efficiency and economic viability compared to conventional batch processes. Although there have been a few studies of ATRP in continuous reactors, no investigations have been made combining the use of continuous processes and low copper concentration variants of ATRP.

1.1 Thesis Objectives

ATRP provides a facile route towards the production of well-controlled low molecular weight polymer chains with targeted placement of desired functional groups. These polymers may be of commercial interest for automotive coatings due to ongoing environmental regulations to reduce the volatile organic content in solvent borne acrylic coatings. Current industrial practice is to produce functionalized low molecular weight polymer (<5000 $g \cdot mol^{-1}$) via high temperature semi-batch polymerization in order to decrease solvent content to 30 wt% while maintaining acceptable solution viscosity. As such, the studies in this thesis targeted the synthesis of well-controlled low molecular weight polymer chains at low solvent content. The purpose of this thesis was to investigate the low copper concentration variants of ATRP in batch systems, and then integrate that knowledge into common industrial processes like continuous tubular reactors and continuous stirred tank reactors (CSTR). The primary goals of the study were:

1. Gain improved understanding of ARGET ATRP and SET-LRP through batch polymerizations; identify limitations and areas for improvement.
2. Design and build a viable continuous tubular reactor for ARGET ATRP based on previous experimental designs with conventional ATRP, and demonstrate the use of ARGET ATRP in a continuous tubular reactor with a model methacrylic monomer.
3. Design and build a CSTR system for ARGET ATRP from a semi-automated Chemspeed reaction platform, and demonstrate the use of ARGET ATRP in a CSTR with an acrylic and methacrylic monomer.
4. Design and build a CSTR system for SET-LRP from a semi-automated Chemspeed reaction platform, and demonstrate the use of SET-LRP in a CSTR with an acrylic monomer
5. Design and build a continuous tubular reactor for SET-LRP capable of room temperature polymerization of acrylic monomers at a fast polymerization rate.

6. Demonstrate the use of SET-LRP in a continuous tubular process for the production of homo and copolymers.

1.2 Thesis Outline

This thesis is presented in manuscript format, and is based on the publications previously listed. Chapter 2 presents a literature review of the relevant technical areas for the research conducted. A general overview of the factors that govern the ATRP equilibrium, the rate of reaction and the control over a polymerization are given. An introduction is provided towards the different low copper concentration ATRP systems, and a brief review of the use of ATRP in continuous systems is presented.

Chapter 3 focuses on the batch study of ARGET ATRP with methyl methacrylate (MMA), butyl methacrylate (BMA), as well as butyl acrylate (BA) to provide representative kinetics of methacrylic and acrylic classes of monomers. Through careful consideration of the factors governing the activity of the copper complex which mediates the ATRP equilibrium, a reduction in ligand concentration is achieved for solution polymerization. The ARGET ATRP system utilized in Chapter 3 is applied towards a continuous tubular reactor in Chapter 4 for the polymerization of BMA. The process of designing the reactor, troubleshooting the initial experiments, and the effects of reducing agent concentration are described.

The use of a CSTR for CRP is generally avoided as the residence time distribution in a CSTR has a broadening effect on the molecular weight distribution of the polymer produced via controlled techniques. However, broadening due to residence time effects does not necessitate a negative impact on the livingness or controlled structure of the polymer produced. Chapter 5 and Chapter 6 address the design of a CSTR using a semi-automated Chemspeed reaction platform for ARGET ATRP and SET-LRP. Polymerizations of MMA and BA are conducted using ARGET ATRP, and the different reaction kinetics and its impact on the polydispersity of the molecular weight distribution are discussed. Methyl acrylate (MA) is used as a model acrylic monomer for

SET-LRP in a CSTR. The effects of residence time on steady state properties of the outlet polymer as well as copper consumption rate are reported.

Chapter 7 examines the use of copper tubing as both reactor and catalyst source for continuous polymerization of methyl acrylate. An initial all copper reactor design is introduced and its use is successfully demonstrated for methyl acrylate polymerization. The effects of residence time and reactor flow rate on the steady state conversion and outlet polymer properties are investigated. Chapter 8 builds upon the all copper reactor design introduced in Chapter 7, and the use of copper and stainless steel tubing in constructing a tubular reactor are discussed. The use of ascorbic acid as a reducing agent for SET-LRP is also investigated for the first time. The improved design in Chapter 8 eliminates some of the inherent flaws in the original all copper reactor design, and its use for the production of multiblock copolymers are considered.

An overall summary of the work conducted in this thesis is provided in Chapter 9. Some recommendations for future work based on the experience and knowledge gained from this thesis are also provided.

1.3 Summary of Original Contributions

Given the novelty of low copper ATRP and the scarcity of literature focusing on ATRP in different reactor designs, the research conducted in this thesis represents the first time ARGET ATRP and SET-LRP have been applied to a commercially relevant continuous process. Some of the original contributions include:

- Improved understanding of ARGET ATRP and the importance of ligand concentration when applied towards polymerization of acrylics and methacrylics. The ligand concentration required was reduced from a 3-10 fold excess down to only a stoichiometric ratio with regard to copper salt.

- First ever experimental demonstration of ARGET ATRP or SET-LRP in any type of continuous process.
- Design and the first experimental demonstration of ARGET ATRP in a continuous tubular reactor. The results demonstrated the robustness of ARGET ATRP towards impurities in the polymerization system, and how increasing the amount of reducing agent can lead to an increase in polymerization rate without a negative impact on livingness.
- Design and the first experimental investigation into ARGET ATRP or any type of ATRP in a CSTR. Solvent effects on ATRP kinetics and the effect of reducing agent concentration in a CSTR on polymerization rate compared to a batch reactor are discussed.
- Design and the first experimental demonstration of SET-LRP in a CSTR. The effects of residence time on copper consumption and the use of two CSTR's in series are shown.
- First experimental proof of concept using copper tubing as reactor and catalyst source for SET-LRP to continuously produce well-controlled and living acrylic polymers.
- Improved reactor design using a combination of copper and stainless steel tubing along with ascorbic acid as an environmentally friendly reducing agent for SET-LRP. The improved reactor concept can be used to continuously produce multiblock gradient copolymers with high livingness and very low residual copper concentration.

Chapter 2

Background and Literature Review

2.1 Controlled Radical Polymerization

Free radical polymerization (FRP) is one of the most common and practical techniques for producing commodity polymers. FRP possesses great tolerance to material and operational impurities, along with high compatibility with a wide range of vinyl monomers making it a very robust and cost effective process that accounts for a significant portion of polymer production. Mechanistically, FRP with a thermal initiator can be broken down into three basic steps – initiator decomposition and initiation, propagation, and termination by combination or disproportionation as shown in Scheme 2.1.

Initiator dissociation	$I \overset{k_\mathrm{d}}{\rightarrow} 2R\cdot$
Initiation	$R\cdot + M \overset{k_\mathrm{i}}{\rightarrow} P_{1}\cdot$
Propagation	$P_n\cdot + M \overset{k_\mathrm{p}}{\rightarrow} P_{n+1}\cdot$
Termination by combination	$P_n\cdot + P_m\cdot \overset{k_\mathrm{tc}}{\rightarrow} D_{n+m}$
Termination by disproportionation	$P_n\cdot + P_m\cdot \overset{k_\mathrm{td}}{\rightarrow} D_n + D_m$

Scheme 2.1: General mechanism for free radical polymerization.

Due to the high reactivity of transient radical species, polymer chain lifetimes are short with unavoidable termination and transfer reactions that yield a broad molecular weight distribution with statistical polymer architecture. This makes it difficult to generate more complex and defined structures which are required for advanced applications. In the last 20 years, several methods of controlled radical polymerization (CRP) have been introduced that allow for much greater control over polymer microstructure. The most studied methods of CRP are stable free

radical polymerization/nitroxide mediated polymerization (SFRP/NMP),[1] reversible addition-fragmentation chain transfer polymerization (RAFT),[2,3] and atom transfer radical polymerization (ATRP).[4,5] The central principle between all forms of CRP is to suppress bimolecular termination by maintaining a low radical concentration throughout the polymerization. This is accomplished through an equilibrium between dormant polymer chains which are capped by a mediating species, and active polymer chains which are free to undergo propagation and other FRP mechanisms. In order to successfully suppress termination, the equilibrium must favour the formation of dormant chains, and the formation of a dormant chain should be fast.

2.2 Atom Transfer Radical Polymerization

The pioneering work on ATRP was conducted independently by two groups in 1995. Kato *et al.* demonstrated the polymerization of MMA using a ruthenium based complex,[4] while at the same time Wang and Matyjaszewski showed the polymerization of styrene using a copper based mediator.[5] Since then, an immense amount of literature has been published on ATRP in bulk and solution, mostly using copper bound to a nitrogen based ligand as the mediating species due to its low cost and versatility compared to other transition metals.[6,7]

In ATRP, growing radicals can be reversibly activated or deactivated via a dynamic equilibrium with a transition metal complex (Mt^n-Y/Ligand) with an exchange of halide species (X) between the chain end and metal complex, as shown in Scheme 2.2. As the rate coefficient for deactivation (k_{deact}) is much higher than the activation rate coefficient (k_{act}), the majority of chains exist in a dormant (halogen capped) state (R-X), thereby suppressing bimolecular radical termination and enabling control over polymer microstructure. In addition, unavoidable termination between radicals will lead to a build-up of deactivating species. This shifts the equilibrium towards the dormant state and further lowers the active radical concentration to suppress termination. This is also known as the persistent radical effect (PRE).[8] In addition, k_{deact}

is of a similar order of magnitude as that for k_t; as deactivator concentration is much higher than radical concentration, deactivation becomes the dominant chain ending reaction.

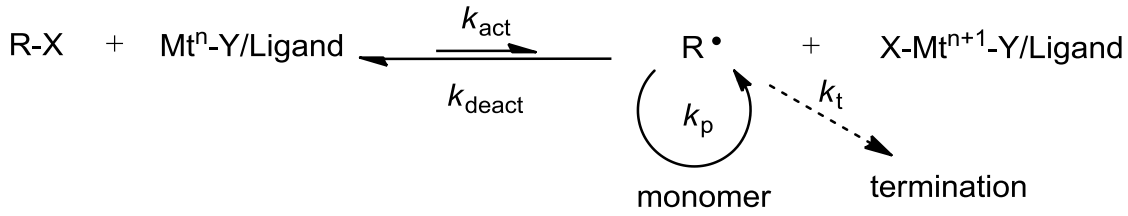

Scheme 2.2: General mechanism for ATRP.

Traditionally, the transition metal complex which governs the ATRP equilibrium is used in stoichiometric or slightly sub-stoichiometric ratio to the initiating alkyl halide species. The ratio of monomer to initiator provides the target molecular weight (MW), and for the desired MW in most applications this results in a high level of residual metal in the final polymer. The mediating metal complex can be present on the order of 10^4 parts per million (ppm). This metal complex can often be expensive, as the nitrogen based ligands commonly used with copper can cost upwards of one hundred dollars per gram. In addition, the metal can be toxic and adds undesired colour to the polymer such that separation (and recycle) from the final product may be required. This additional level of post-process purification can add significantly to production costs, and is a considerable hurdle towards commercial scale applications of ATRP.[9–11]

2.2.1 Understanding the ATRP Equilibrium

The dynamics of the ATRP equilibrium are very important to the polymerization rate and control imposed over the final macromolecular structure. As briefly discussed, the deactivation of growing chains must be fast in order to suppress unwanted radical termination. In addition, fast activation is required in order to maintain a reasonable rate of polymerization as well as to ensure that all chains are initiated at the same time. This ensures that all polymer chains grow at the same rate and undergo similar numbers of activation/deactivation cycle, statistically leading to a narrow final molecular weight distribution. As copper complexes are most often used in ATRP,

the rate of polymerization for an ATRP system assuming negligible bimolecular termination can be approximated as:[6]

$$R_p = k_p[M][P^\bullet] = k_p[M]\frac{k_{act}}{k_{deact}}[R-X]_0\frac{[Cu^I]}{[Cu^{II}X]} \qquad \textbf{Equation 2-1}$$

where: k_p is the monomer propagation rate coefficient; $[M]$, $[P^\bullet]$, $[R\text{-}X]_0$ are monomer, propagating chain, and alkyl halide initiator concentrations respectively; k_{act} and k_{deact} are the rate constants of activation and deactivation which combine to form the ATRP equilibrium constant; and $[Cu^I]$ and $[Cu^{II}X]$ are the concentrations of the activator and deactivator species. Of the variables in Equation 2-1, the rate constants of activation (k_{act}) and deactivation (k_{deact}) exhibit the largest variance with polymerization conditions and are the key to successfully controlling the final molecular structure using ATRP.

The ATRP equilibrium can be theoretically broken down into 4 separate reversible reactions as shown in Scheme 2.3. It is important to note that while analysis of the ATRP equilibrium as dissected into these four elementary steps can generate useful trends, the physical relevance to how the reaction proceeds is less meaningful. The four reversible reactions are: oxidation of the metal complex (electron transfer, K_{ET}), alkyl halide bond homolysis (K_{BH}), reduction of a halogen to a halide ion (electron affinity, K_{EA}), and association of the halide ion to metal complex (halidophilicity, K_X).[12] The product of these four elementary rate constants gives rise to the overall ATRP equilibrium (K_{ATRP}).

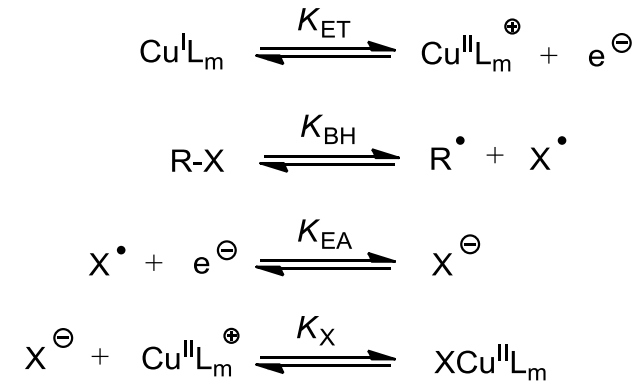

Scheme 2.3: Breakdown of the ATRP equilibrium.[12]

2.2.1.1 Alkyl halide and copper halide bond strength

The effect of alkyl halide structure on the ATRP equilibrium can be generalized in order of radical stability (tertiary > secondary > primary). Tertiary radicals formed from methacrylic polymer chain ends or corresponding alkyl halides analogues have the greatest radical stability due to hyperconjugation with adjacent bonds and as such possess the highest k_{act}. Substituent effects on radical stability also apply, and electron rich α-substituents capable of stabilizing the radical will increase the activation rate constant.[13,14] The effect of halide on the ATRP equilibrium is more complex, and in general K_{ATRP} of alkyl bromides are an order of magnitude higher than the corresponding chloride complex. This is the summation of several factors, the first being the strength of the carbon-halide bond. Carbon-chloride bonds are stronger than carbon-bromide bonds, and as such the higher bond dissociation energy for C-Cl bonds will lower K_{BH} and decrease K_{ATRP}. At the same time, chlorine has a greater electron affinity than bromine as it is more electronegative, and K_{EA} for chlorine will be higher. Finally copper chloride bonds are stronger than copper bromide bonds, making the formation of the higher oxidation state complex more likely and thus increasing K_{ATRP}.[12,14,15]

2.2.1.2 Halidophilicity of metal center

In general, a metal center with higher affinity for halides forms more active ATRP complexes. A comparison between copper, ruthenium and osmium complexes used for ATRP found that ruthenium and osmium complexes with similar ATRP activities were generally much less reducing when compared to copper complexes. The halide affinities (halidophilicity) of the ruthenium and osmium compounds were calculated to be 7-9 orders of magnitude stronger than typical copper ATRP complexes in order to compensate for the more positive reduction potentials.[16]

2.2.1.3 Reduction potential of the mediating complex

The electron transfer equilibrium (K_{ET}) is mostly affected by ligand selection and has the largest influence on the ATRP equilibrium. There are a number of ligands available for copper mediated ATRP, and a selection of the ligands that have been studied are shown in Figure 2.1, with corresponding equilibrium constants spanning over 7 orders of magnitude.[14,17] As k_{deact} is generally fast with small variability between mediating species, the shift in ATRP equilibrium comes from changes in the activation rate constant. It is difficult to directly relate ligand structure to the ATRP equilibrium, as small changes can have large effects on the activation kinetics likely due to steric constraints on copper/ligand complex geometry. This is best illustrated by comparing tris[2-(dimethylamino)ethyl]amine (Me_6TREN, highlighted in green), used to form one of the most active ATRP complexes, to tris[2-(diethylamino)ethyl]amine (Et_6TREN, highlighted in orange), a structurally similar ligand with similar electron donating substituents. Me_6TREN has a K_{ATRP} of 1.5 x 10^{-4}, while Et_6TREN has a K_{ATRP} of 9.4 x 10^{-10} under the same conditions, a difference of over 5 orders of magnitude.

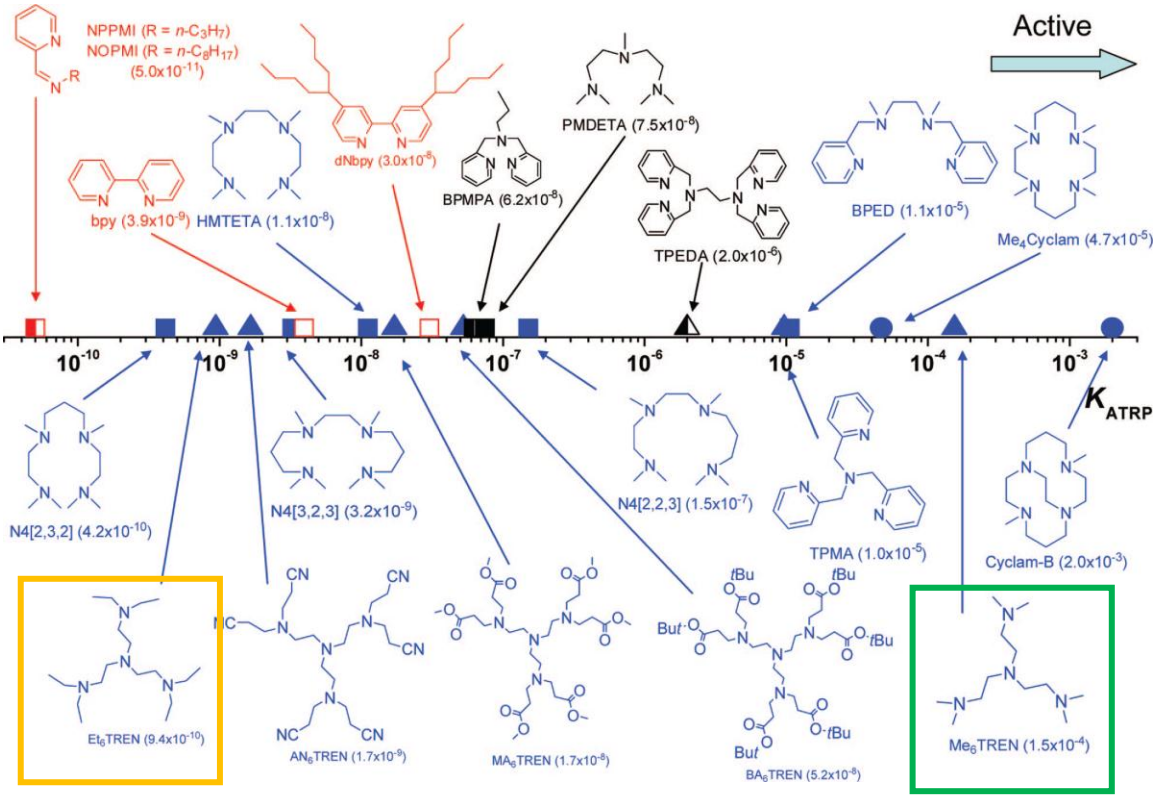

Figure 2.1: ATRP equilibrium constants (K_{ATRP}) for various nitrogen based ligands as measured with CuBr in acetonitrile at 22 °C.[14]

Even with the apparent discrepancies, the general order of activity for copper complexes based on ligand structure increases with denticity.[14] A better way to identify the activity of a copper complex for ATRP is through its reduction potential. Complexes with lower (more negative) reduction potentials are more reducing and therefore more active than complexes with higher reduction potentials. This is illustrated in Figure 2.2, which shows a linear relationship between K_{ATRP} and redox potential for different copper complexes. Lower reduction potentials result in higher ATRP equilibrium constants and therefore higher polymerization rate.

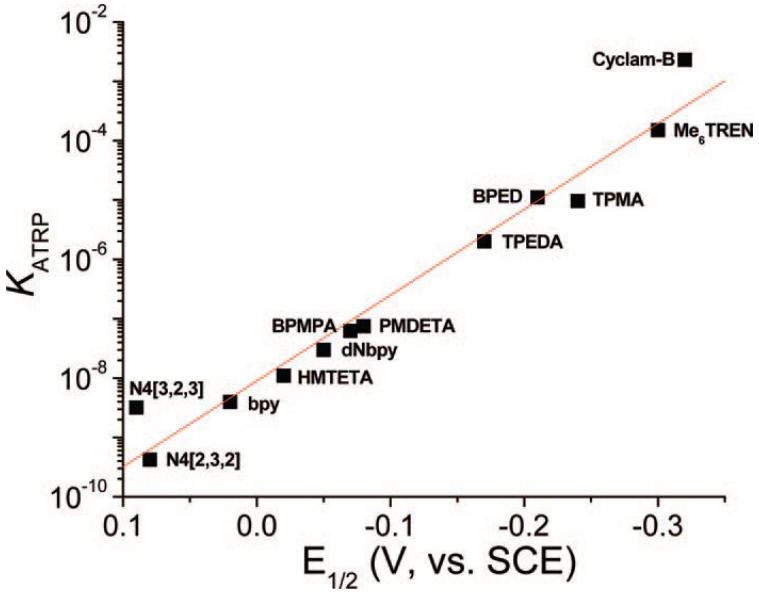

Figure 2.2: Plot of K_{ATRP} vs. redox potential for copper complexes shown in Figure 2.1.[14]

Another method of predicting the activity of a copper complex for ATRP is to compare the stability constants of the metal complex. A complex with a low reduction potential should be more stable in its oxidized state. In other words, the more stable the high oxidation state is compared to the low oxidation state, the lower the reduction potential between the two oxidation states and the more active the copper complex becomes. Omitting the oxidation state for simplicity, the overall stability constant can be generally defined as:[18]

$$\beta_{k,L} = \frac{[CuL_k]}{[Cu][L]^k} \qquad \textbf{Equation 2-2}$$

Where: CuL_k is the concentration of the copper complex, Cu is the concentration of free copper species, and L is the concentration of free ligand. The redox potential of the copper complex can be approximated by the following relationship:[12]

$$E \approx E^\circ + \frac{RT}{F}\left(\ln\frac{[Cu^{II}]_{tot}}{[Cu^{I}]_{tot}} - \ln\frac{\beta^{II}}{\beta^{I}}\right) \qquad \textbf{Equation 2-3}$$

where: E° is the standard potential of the Cu^{II}/Cu^{I} couple, R is the universal gas constant, T is temperature, F is Faraday's constant, and β^j is the stability constant of the Cu^jL complex in the

relevant oxidation state. As the stability constants are easily measured and readily available, it is possible to use the stability constant of each oxidation state to predict ATRP activity and the overall ATRP equilibrium.

The ATRP equilibrium and stability constants for some common ligands are given in Table 2.1. The stability constant of copper(I) and copper(II) complexes can be used to generate an estimate of the activity of the complex.[12] A high ratio of β^{II}/β^{I} indicates that the copper(II) oxidation state is more stable than the copper(I) state, and as such the complex should have a high activation rate constant. The ratio $\beta^{II}/(\beta^{I})^2$ can be used to estimate a complex's tendency to disproportionation and is discussed later during the overview of SET-LRP.

Table 2.1: Comparison between stability constants and ATRP activity,[12] for ligand structures see Figure 2.1.

Copper complex	β^{I}	β^{II}	$\log(\beta^{II}/\beta^{I})$	$\log(\beta^{II}/(\beta^{I})^2)$	K_{ATRP}
CuBr/bpy	8.9×10^{12}	4.5×10^{13}	0.70	-12.25	3.93×10^{-9}
CuBr/HMTETA	1×10^{11}	3.98×10^{12}	1.60	-9.40	8.38×10^{-9}
CuBr/PMDETA	$<1 \times 10^{8}$	1.45×10^{12}	4.16	-3.38	7.46×10^{-8}
CuBr/TPMA	7.94×10^{12}	3.89×10^{17}	4.69	-8.21	9.65×10^{-6}
CuBr/Me_6TREN	6.3×10^{8}	2.69×10^{15}	6.63	-2.17	1.54×10^{-4}

2.2.1.4 Solvent effects on ATRP equilibrium constant

Solvent choice can heavily impact polymerization kinetics in FRP through solvent interactions with monomer and transition state radical structures. In ATRP, solvent can affect the rate of polymerization and control over polymerization by impacting the propagation rate constant as in FRP, in addition to other properties of the transition metal complex. In general, it has been found that activation rate constants increase with solvent polarity. Using the four elementary reactions presented in Scheme 2.3, solvent effects can be broken down into its specific impact on each mechanism.

Without going into detailed calculations, solvent effects can be qualitatively analyzed in terms of stability. The electron affinity (K_{EA}) is affected by charge localization and ion solvation. Solvents which promote ion solvation and stabilize halide ions will give larger K_{ATRP}'s.

Halidophilicity (K_X) is influenced by similar factors, and the more poorly a halide ion is solvated, the more strongly it will bind to the metal center, and the more reducing the complex becomes. The solvent effect on electron transfer (K_{ET}) can likewise be characterized by its impact on complex stability at each oxidation state. As previously discussed, a copper complex that is more stable in its higher oxidation state will be more reducing and more active. Therefore, solvents which preferentially stabilize the copper(II) oxidation state will increase the ATRP equilibrium and the rate of polymerization. It should be noted that K_{ET} is still dominated by ligand choice, as the degrees of freedom afforded by the ligand will shape complex sensitivity to various solvents. This is due to possible reorganization of the coordination sphere upon oxidation and more rigid ligands like Me_4-cyclam make this process more difficult compared to a branched ligand with higher degree of freedom like Me_6TREN (see Figure 2.1 for ligand structures).

The Kamlet-Taft expression is a linear solvation energy relationship that has been used to describe and predict properties in solution such as solubility, free energy and enthalpy of equilibria, and redox potentials. The Kamlet-Taft equation is defined as:[19]

$$XYZ = XYZ_0 + a \propto + b\beta + s\pi^* + h(\delta_H)^2 \qquad \textbf{Equation 2-4}$$

where: XYZ is the property of interest, XYZ_0, a, b, s, and h are solvent independent coefficients characteristic of the process; α is the hydrogen bond donor ability of the solvent, β is the hydrogen bond acceptor ability, π^* is the dipolarity/polarizability parameter (ability of solvent to stabilize charge or dipole by its dielectric effect), and δ_H is the Hildebrand solubility parameter, which is a measure of the solvent-solvent interactions that are disrupted in creating a cavity for the solute. Kamlet-Taft relationships have been used by Coullerez *et al.*[20] and Brauecker *et al.*[21] to analyze and predict solvent effects on the ATRP equilibrium with good accuracy. ATRP equilibrium constants spanning over 7 orders of magnitude were predicted and compared to experimental results with strong agreement. Figure 2.3 shows a plot of predicted log(K_{ATRP})

compared to experimentally derived log(K_{ATRP}), and it can be seen that polar solvents like DMSO possess substantially higher equilibrium constants than toluene or acetone.

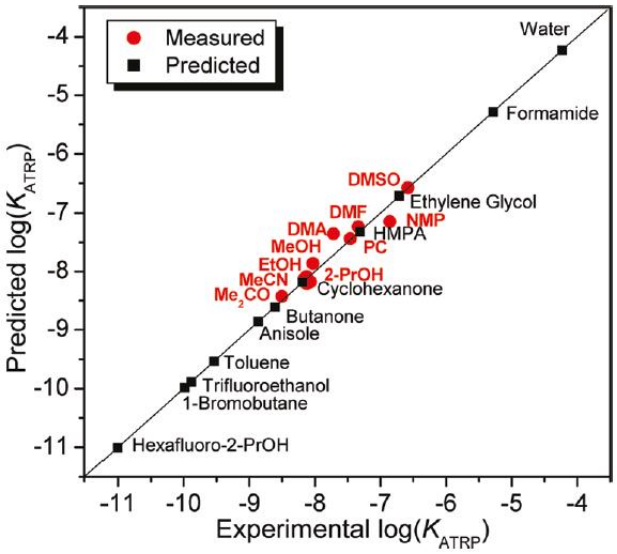

Figure 2.3: log(K_{ATRP}) as predicted using the Kamlet-Taft relationship vs. experimental log(K_{ATRP}).[21]

2.2.2 Activator Regenerated by Electron Transfer (ARGET) ATRP

There are two benefits for the development of new ligands which generate copper complexes with higher ATRP equilibrium constants. Looking at Equation 2-1, it can be seen that the overall polymerization rate is dependent on K_{ATRP} which can be increased by increasing k_{act}, or decreasing k_{deact}. A higher K_{ATRP} achieved through an increase in activation rate will yield faster polymerizations and reduced operation times, which has long been a disadvantage for CRP when compared to conventional FRP. Although a higher K_{ATRP} can be beneficial, it is important that this is done without a decrease in k_{deact} as this will lower the probability of chain capping as a chain ending event. This subsequently increases the radical concentration, leading to a higher level of bimolecular termination and reduced livingness in the final polymer. This can also be

explained by looking at the polydispersity of the molecular weight distribution as defined by Equation 2-5:[22]

$$PDI = \frac{M_w}{M_n} = 1 + \frac{1}{DP_n} + \left(\frac{[R-X]_0 k_p}{k_{deact}[Cu^{II}X]} \right)\left(\frac{2}{X} - 1 \right) \qquad \textbf{Equation 2-5}$$

where X represents conversion and the other symbols are as previously defined. The equation shows that polydispersity is dependent on deactivator concentration and the deactivation rate constant. To maintain low polydispersity and high livingness, the mediator needs to have fast deactivation kinetics and ideally fast activation kinetics as well to promote activation/deactivation cycles. Undergoing more activation/deactivation cycles will give a higher statistical probability that all chains have added the same number of units and are the same length.

Another substantial benefit from increasing the ATRP equilibrium is the reduction in concentration of mediating species required to maintain control over the polymerization. As the overall rate of polymerization is dependent only on the ratio of copper complexes, and not on the absolute concentration present, it is theoretically possible to significantly reduce the amount of metal used if the ATRP equilibrium value is high. This can dramatically reduce material and post-polymerization processing costs, making ATRP much more attractive from an industrial perspective. However, this is not possible in practice as at low mediator concentration, a small amount of irreversible radical terminations will lead to relatively large build-up of copper(II) deactivators. This dramatically shifts the copper(I)/copper(II) (activator/deactivator) ratio and ultimately stops the reaction before it can reach completion.

Given this limitation in deactivator build-up by the persistent radical effect, another technique was required to reduce mediator concentration down to more industrially acceptable levels. This led to the development of “activator generated by electron transfer” (AGET) and “activators regenerated by electron transfer” (ARGET); through which mediator concentration

can be lowered to ppm levels with respect to monomer. The proposed mechanism for these two methods are shown in Scheme 2.4

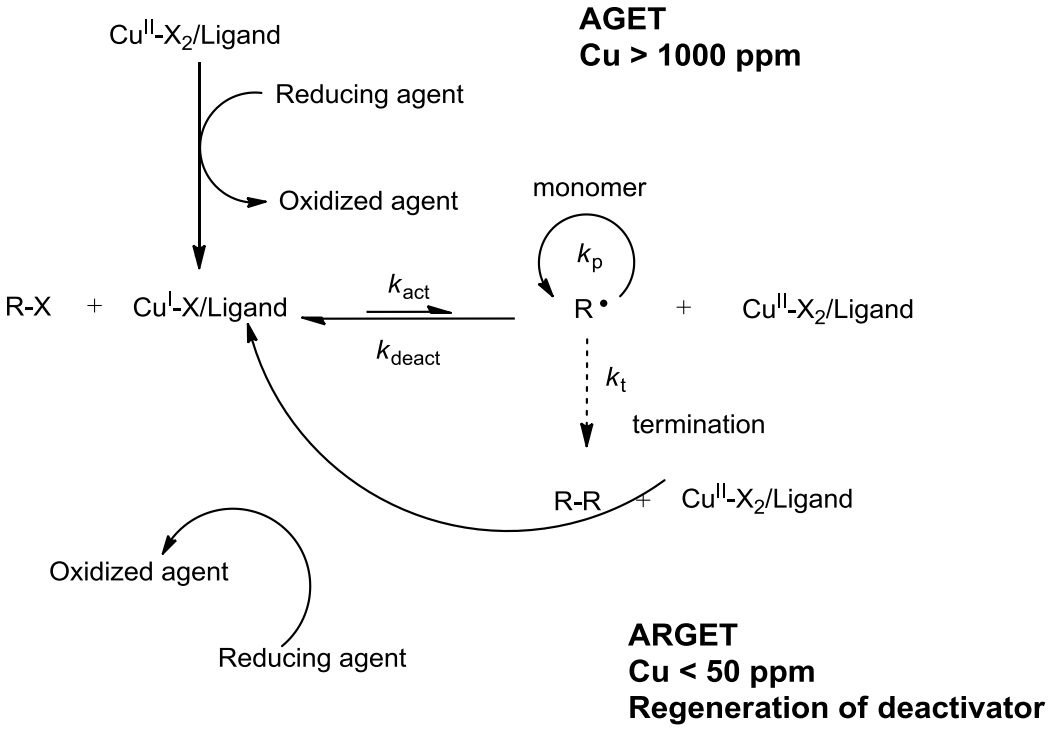

Scheme 2.4: Proposed mechanism for AGET and ARGET ATRP.

From the proposed mechanism, it can be seen that AGET and ARGET ATRP share a great deal of similarities. Both techniques employ the more oxidatively stable copper(II) species as a starting material. This can simplify handling procedures as active copper complexes are readily oxidized in the presence of air from copper(I) to copper(II). The difference between the two methods lies in the amount of mediator and reducing agent added. AGET ATRP utilizes a stoichiometric amount of reducing agent in order to convert the initial population of copper(II) deactivators into copper(I) activators in order to initiate polymerization. AGET ATRP can be conducted using low activity mediators, and its primary advantage over conventional ATRP is in material storage and improved handling. With ARGET ATRP, an excess of reducing agent is added to both initiate polymerization and convert copper(II) deactivating species, which have

accumulated due to bimolecular termination, back into copper(I) activators. Through this mechanism, a reasonable rate of polymerization can be attained at low mediator concentration.

Both AGET[23] and ARGET[24,25] were discovered by Jakubowski *et al.* when researching the combination ring opening polymerization with ATRP to synthesize poly(ε-caprolactone)-b-poly(n-octadecyl methacrylate) copolymers. Tin (II) 2-ethylhexanoate ($Sn(EH)_2$) was added to initiate the ring opening mechanism, but $Sn(EH)_2$ had the unexpected effect of reducing copper(II) into copper(I) during copolymerization. This enabled polymerization at low mediator concentrations as $Sn(EH)_2$ continually regenerated copper(I) activator and polymerization of styrene was successful with only 15 ppm of copper relative to monomer when using Me_6TREN as ligand.

ARGET ATRP is also compatible with a variety of other reducing agents. Glucose, ascorbic acid, hydrazine, phenols, and tertiary amines have all been successfully used to produce a wide variety of polymers with varying microstructure and properties.[25–35] The choice of reducing agent impacts the rate of reduction, and a strong reducing agent like ascorbic acid can only be used in a heterogeneous system to limit the concentration of reducing agent in solution so that an appropriate amount of deactivators will remain to control the polymerization.[29] The concentration of reducing agent can also affect the copper(I)/copper(II) ratio in the system and thus polymerization rate. As well, reducing agents have varying levels of toxicity, and should be carefully selected as they may not be suitable for certain applications.

The principal disadvantage of ARGET ATRP as first introduced[25,26] was the requirement for ligand concentrations in 3 to 10 times molar excess to metal in order to achieve a controlled polymerization. As ligands such as Me_6TREN and TPMA which are commonly used for ARGET are expensive and not widely available, these factors present considerable barriers to industrial scale up.

An excess of ligand to metal helps preserve the copper complex concentration and protect it from destabilizing side reactions. At low mediator concentration, dissociation of the copper complex becomes more pronounced and can account for destabilization of a significant percent of total mediator concentration. This becomes more pronounced at elevated temperatures during polymerization. From 25 °C to 110 °C, the stability constant of common copper complexes can vary by 2-3 orders of magnitude.[12] As the nitrogen based ligands used are basic, protonation can occur if the reaction media becomes acidic. When $Sn(EH)_2$ is used a reducing agent, a Lewis acid can be formed during the redox process, and is thought to destabilize the copper complex.[25,26] Competitive complexation from solvent and monomer is also an issue at low mediator concentrations.[36] While the ligand binds more strongly, the relative abundance of solvent and monomer present can gradually displace bound ligand. Depending on the solvent, halide dissociation from mediator is also a concern. In polar protic solvents, halides are more prone to dissociation from copper(II), forming the copper(I) complex.[37] If dissociation occurs to a significant extent, there can be loss of control over the polymerization due to insufficient deactivator concentration. Finally, disproportionation (reversible generation of copper(II) and copper(0) species from two copper(I) species) is enhanced in protic solvents, and can affect the reaction kinetics and possibly the mechanism of reaction.

The extent of disproportionation can be estimated from the previously introduced stability constants, as calculated by $\beta^{II/} (\beta^{I})^{2}$.[18] Figure 2.4 shows a plot of ATRP activity (estimation of K_{ATRP}) and the overall stability of the copper complex. An ideal complex should have high activity as well as high stability constants in both oxidation states to minimize the effect of side reactions. From the stability constants available in Table 2.1 and the relationship in Figure 2.4, it can be seen that TPMA is an ideal ligand for low mediator concentration ATRP.

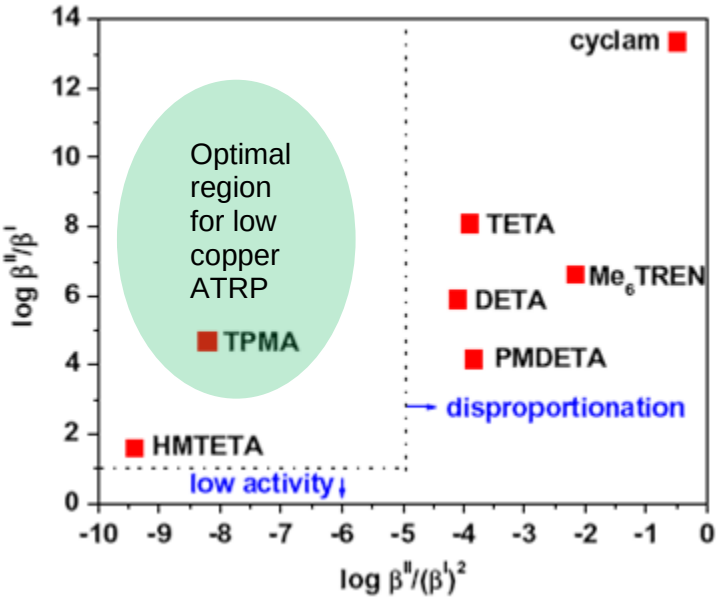

Figure 2.4: Map of ATRP activity (y-axis) and extent of disproportionation (x-axis).[11]

In addition to requiring substantially less mediator than conventional ATRP, reducing mediator concentration can decrease the frequency of unwanted side reactions between active species and growing radicals. Radicals with α-electron withdrawing substituents (cyano or carboxy groups) are likely to be reduced by copper(I) activator to carbanions. Likewise, electron donating radicals can be oxidized to carbocations. These two mechanisms are thought to be the reason for the limited conversion and molecular weight observed in acrylonitrile[38] and styrene[39] polymerizations. Using ARGET ATRP, Pietrasik *et al.* were able to prepare styrene-acrylonitrile copolymers reaching a high molecular weight of 2×10^5 $g\cdot mol^{-1}$ with low polydispersity.[28] Likewise, Jakubowski *et al.* were able to synthesize high molecular weight polystyrene via ARGET ATRP with improved chain end functionality. When targeting low molecular weight polystyrene, chain end functionality (amount of chains which are still halogen capped) was found to be almost double that of conventional ATRP (87% vs. 48%).[33]

ARGET ATRP has also been used to synthesize materials that are not feasible with conventional ATRP. Yamamoto *et al*. used ARGET ATRP to polymerize di(ethylene glycol) methyl ether.[40] As the monomer possesses a strong electron withdrawing group, under conventional ATRP conversion is limited to 50%. With ARGET ATRP, 80% conversion was reached at 6 hours, and polymerization was successful even with a limited amount of air if the amount of reducing agent is increased. The reducing agent acted as an oxygen scavenger, by repeatedly reducing copper(II) which has been oxidized into copper(I) until all the oxygen is consumed. A similar effect was observed by Matyjaszewski *et al*. in the polymerization of surface grafted polymer brushes with ARGET ATRP in the presence of air.[32]

The copolymerization of 1-alkenes with other more polar vinyl monomers is also a problem with conventional FRP and ATRP. Although not a side reaction, halogen transfer to an active alkene radical forms a dormant polymer chain with a carbon-halide bond that is too strong to be cleaved by ATRP mediators. As there is a much lower mediator concentration in ARGET ATRP, generation of these irreversible chain ends is suppressed, and Tanaka *et al*. were able to copolymerize 1-alkenes with butyl acrylate and methyl methacrylate.[41,42] Higher conversion and higher alkene incorporation was reached when compared with conventional ATRP.

2.2.3 Initiators for Continuous Activator Regeneration (ICAR) ATRP

Matyjaszewski *et al.* also developed another method of regenerating activators to enable low copper concentration ATRP called "initiators for continuous activator regeneration" (ICAR).[26] In ICAR ATRP, a small amount of thermal free radical initiator is used instead of a reducing agent to regenerate activators from accumulated deactivating species. Unfortunately, the use of a free radical initiator in ICAR is also its primary flaw, as the constant generation of radicals over the course of the polymerization generates additional polymer chains, which will broaden the molecular weight distribution and give unwanted homopolymer when synthesizing block copolymers. However, copper complex stability is improved in ICAR as side reactions caused by

reducing agents do not occur. As such, ligand can be added in a stoichiometric ratio to metal which lowers material costs. With ICAR, the polymerization rate can depend heavily on the decomposition kinetics of the additional initiator, as decomposition can dominate the active radical concentration. However, control over the polymerization is still heavily dependent on ligand choice, as ligand will affect copper complex stability and deactivation kinetics. Mueller *et al*. successfully used ARGET and ICAR ATRP to chain extend polyacrylate and polystyrene macroinitiators with methyl methacrylate.[31]

2.3 Single Electron Transfer-Living Radical Polymerization

Around the same time that ARGET and ICAR ATRP were being developed, Percec *et al.* proposed another low copper concentration method of controlled radical polymerization utilizing ligands and initiators that are commonly used in conventional ATRP. This process was named "single electron transfer-living radical polymerization" (SET-LRP),[43] and utilized elemental copper as an activating species in place of copper salts as in ATRP. The proposed schematic for SET-LRP is shown in Scheme 2.5.

In SET-LRP, polymer chains are activated through a copper(0) mediated outer-sphere electron transfer (OSET) process of heterolytic carbon-halide bond dissociation. Active chains may then undergo propagation, termination or deactivation via halogen exchange with a copper(II) species as in ATRP. Both the activation and deactivation step generate copper(I) species, which undergo near instantaneous disproportionation into copper(0) and copper(II) when appropriate ligand and solvent combinations are used. The use of ligands that favour disproportionation (Me_6TREN, TREN, PMDETA), and certain polar or coordinating solvents (DMSO,[43] alcohols,[44] binary mixtures of water and other organic solvents[45]) are required to complete the SET-LRP cycle.

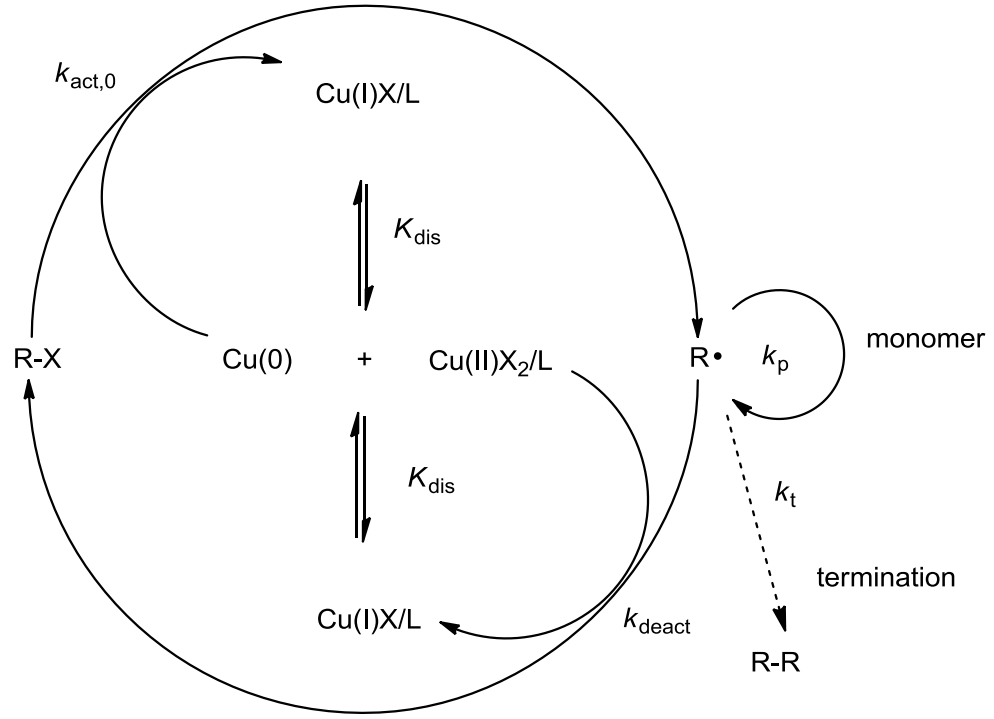

Scheme 2.5: Proposed SET-LRP mechanism.

SET-LRP possesses several advantages over conventional ATRP and other forms of low copper concentration ATRP. As with ARGET or ICAR ATRP, only a small amount of copper is present in solution, and the residual copper concentration is much lower than conventional ATRP. The use of elemental copper enables simple removal of the bulk of the metal as it is heterogeneous to the reaction media. The polymerization rates are higher than in comparable ATRP systems, and polymerizations are often conducted at room temperature. This is due to faster activation ($k_{act,0}$) through the OSET process mediated by copper(0) when compared to the inner sphere electron transfer (ISET) process in conventional ATRP. SET-LRP has been successfully demonstrated for the synthesis of acrylates,[43,46,47] methacrylates[43,48,49] and acrylamides[50] with well-controlled molecular weights and polymer structure.

Control and retention of chain end fidelity is also improved when compared with ATRP. In ATRP, control is maintained by the persistent radical effect and a small amount of termination is required to generate a regulating concentration of deactivating species. The proposed SET-LRP

mechanism provides one deactivator for every two activations by copper(0) and the concentration of copper(II) deactivators is regulated by disproportionation instead of the PRE. As such, SET-LRP is theorized to provide greater retention of chain end fidelity, leading to a polymer that has higher livingness compared to ATRP or other forms of CRP.[43,46,51] This high degree of livingness enables the synthesis of high molecular weight polymer not possible with ATRP, as well as facile generation of multiblock copolymers[52] or dendrimers[53] through an iterative polymerization process without the need for purification and isolation of macroinitiator.

Despite the many advances SET-LRP offers, its mechanism is still heavily debated in literature. In particular, it is reasoned that SET-LRP cannot occur via an OSET process, and that the accelerated polymerization rates observed are a result of a traditional ISET ATRP process with additional rate enhancement due to solvent effects as dictated by the use of polar protic solvents. Evidence for both OSET and ISET will be briefly discussed.

2.3.1 The Role of Copper(0)

The role of copper(0) as an activator via OSET has been a point of contention in literature since the discovery of SET-LRP. One of the stronger pieces of evidence towards OSET is the use of SET-LRP for controlled polymerization of vinyl chloride (VC).[43,54] There are two major challenges towards controlled polymerization of VC. In FRP of VC, chain transfer to monomer is several orders of magnitude higher than with other common vinyl monomers and dominates over bimolecular termination. As CRP relies on the persistent radical effect to regulate the population of mediators, chain transfer in VC polymerization poses a problem in the establishment of sufficient deactivating species. In addition, VC dormant chain reactivation is not possible when conventional ATRP mediators are used, and deactivation of chains by halogen transfer becomes an irreversible chain ending event.

These two problems were eliminated through the use of SET-LRP. Reactivation of dormant chains was possible with copper(0) due to more energetically favourable OSET

activation. In addition, the concentration of deactivating copper(II) species was generated by disproportionation and therefore independent of chain transfer or termination. These two factors enabled the controlled polymerization of VC via SET-LRP with predictable molecular weights. Block copolymers could also be formed with VC and other vinyl monomers.

Despite this experimental evidence, Matyjaszewski *et al.* initially contended that copper(0) acts primarily as a reducing agent, to regenerate copper(I) activators through comportionation with copper(II) species.[55] *Ab initio* calculations of alkyl halides and their subsequent radicals in gas and solution phase found that OSET activation may occur via a concerted dissociative electron transfer, rather than a stepwise process. However, the rate constant of this hypothetical concerted OSET reaction for a model alkyl halide was found to be on the order of 10^{-11} M^{-1} s^{-1}, which was significantly lower than the experimentally measured ATRP rate constant (~82 M^{-1} s^{-1}).[56]

2.3.2 Copper(0) Surface Dependent Kinetics

The use of elemental copper in the form of copper powder or copper wire in SET-LRP in place of copper halide salts simplifies addition and removal of the transition metal complex as the majority of the metal remains heterogeneous. Copper powder with particles ranging from the micrometer[43] to nanoscale (< 100 nm)[57] have been used in SET-LRP, and it was found that using smaller copper particles greatly increased the surface area available for activation and as such resulted in faster polymerizations, although it was difficult to draw a linear relationship between particle size and overall polymerization rate due to the dispersity in particle size. A slight decrease in chain end fidelity was also observed when using nanosized powder due to the substantially larger radical flux in the initial stages of polymerization.[57] More interestingly, an experiment was designed to verify the nature of copper(0) as an activator by decanting the solution from heterogeneous copper powder during the polymerization. It was found that polymerization stopped once copper powder was removed from the reaction media, and

polymerization restarted as soon as the powder was added back in. It was concluded that copper(0) was the dominant activating species and that transient copper(I) activators played a negligible role in the reaction kinetics.[57]

The use of copper wire provided a more uniform and readily calculated surface area for activation. It was found that the observed rate of polymerization was proportional to the copper surface area with a reaction order of 0.44 and was suggested to be evidence for a surface mediated activation process.[58] Coincidentally, a similar rate order has been observed in ARGET ATRP with respect to reducing agent,[32] as well as with ICAR ATRP[59] with respect to thermal initiator. The rate of polymerization with copper wire can be enhanced by a pre-polymerization treatment to remove copper oxides on the surface. Copper oxides are hypothesized to be slower activators than elemental copper, and the cause for variability between polymerizations conducted at the same conditions with copper wire.[60] Hydrazine[61] and various acids[62] have been used to enhance the polymerization rate in SET-LRP of methyl acrylate with good effect.

2.3.3 Use of Nonpolar Solvent with Copper(0)

As disproportionation of copper(I) complexes are an integral component of SET-LRP, several studies have been carried out in nonpolar solvents where disproportionation is negligible while using copper(0) as an activation source. Lligadas and Percec performed a comparison of copper(0) mediated polymerization in DMSO and toluene.[51] The use of DMSO, a solvent that favours disproportionation, resulted in rapid polymerization with near complete conversion in under 45 minutes. When toluene was used as a solvent, a limiting conversion of 60% was observed even after a polymerization period of 17 hours. A similar result was observed when comparing copper(0) mediated polymerizations in DMSO and acetonitrile,[63] and it was concluded that disproportionation was essential for a successful SET-LRP and that solvent choice differentiates between the established ATRP mechanism and the proposed SET-LRP mechanism.

Wright *et al.* first reported successful copper(0) mediated controlled radical polymerization of methyl acrylate in a non-polar solvent.[64] Polymerizations were conducted in toluene with the addition of various phenols to drive disproportionation of copper species. Increasing the phenol concentration to 20 fold excess over initiator gave higher polymerization rates with improved control. Copper(0) mediated CRP in toluene has also been reported for methyl methacrylate[65] and styrene.[66] In both studies, uncontrolled polymerization was observed early in the reaction. This was attributed to generation of radicals by electron transfer mediated by copper(0). As disproportionation is not favoured in toluene, electron transfer generates copper(I) species which also act as activators, increasing the radical concentration in solution. This led to an increased amount of bimolecular termination before a sufficiently large population of copper(II) deactivators is established to control the polymerization.[67] The proposed schematic for copper(0) mediated CRP without disproportionation is shown in Scheme 2.6.

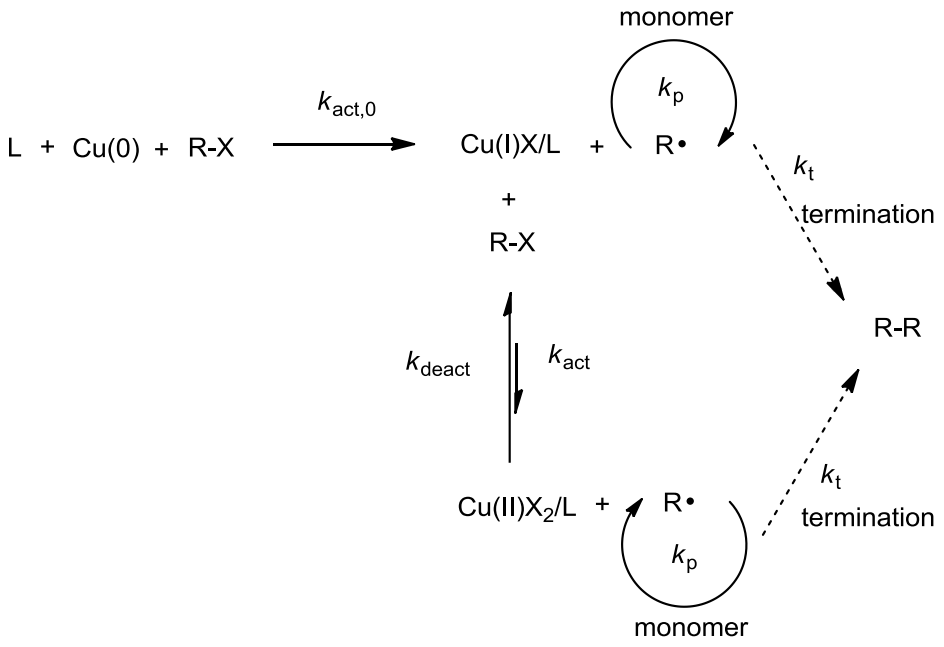

Scheme 2.6: Proposed mechanism of copper(0) mediated CRP in nonpolar solvent.

The studies in nonpolar solvents indicate that copper(0) must behave as an activator, and that it likely has a dual role as activator and reducing agent. Similar results have been observed

for other zero valent metals (zinc, magnesium, iron) used in conjunction with copper complexes for conventional ATRP.[68,69] It is proposed that copper(0) behaves as a reducing agent and supplemental activator, and that the process should be called "supplemental activator and reducing agent" (SARA) ATRP.[70]

2.4 ATRP in Continuous Processes

2.4.1 ATRP in Continuous Tubular Reactors

Continuous reactors offer several advantages when compared to simple batch processes. Inconsistencies during start-up are eliminated in continuous processes, and once at steady state, continuous reactors yield more consistent product quality than batch reactors. The elimination of downtime between reactions, and the reduction of off-spec products give continuous processes a tremendous advantage in productivity and efficiency over comparable batch reactors. Continuous tubular reactors, or plug flow reactors (PFR), in particular are ideal for scale up due to their large surface area to volume ratio. This greatly improves the heat removal capacity of a reactor and facilitates better temperature control.

Despite the advantages, there are relatively few reports in literature on controlled radical polymerization in continuous processes. Enright *et al.* have reported the NMP of styrene,[71] as well as synthesis of styrene and butyl acrylate block copolymers by NMP in a continuous tubular reactor.[72] Russem *et al.* investigated the RAFT miniemulsion polymerization in a series of tubular reactors.[73–75] Investigations on ATRP in tubular reactors are hampered by the limitations with mediator recycling, handling, and cost discussed before. In addition, commercially available ligands that can be used in ATRP often form heterogeneous complexes, adding another complication when studying PFR's or continuous stirred tank reactors (CSTR).

Shen *et al.* were the first to report on the bulk ATRP of methyl methacrylate on a silica supported mediator in a batch reactor.[76] CuBr was mixed with hexamethyltriethylenetetramine

(HMTETA), toluene and silica particles. The mediator readily adsorbed onto the silica particles, possibly due to the complex's high affinity for the hydroxyl group on the silica particle. The particles were used in solution polymerization of MMA in toluene at 80 °C, and showed similar behaviour to conventional ATRP solution polymerization. The mediator was separated, reused and showed 80% of the initial activity on the first recycle, and 50% of the initial activity on the third use. The silica particles were then packed into a stainless steel column to form a packed bed reactor (PBR).[77,78] By using a PBR, Shen *et al.* were able to reduce the problems associated with high metal concentrations and post-process recycling, although there was still a loss of mediator activity with reaction time. The column used was 900 mm long with an inner diameter of 3.75 mm. The reactor showed good stability (stable operational time of over 100 hours before loss of activity), and conversion was directly proportional to flow rate (residence time in the reactor). Compared to batch polymerization, there was some broadening in the molecular weight distribution (MWD), and this was attributed to possible back mixing in the reactor or trapping of polymer in silica gel pores. Block copolymer of methyl methacrylate and n-butyl methacrylate was synthesized by adding another identical packed column to extend the original reactor and feeding monomer into the junction. The final polymer had a much higher polydispersity index (PDI) than the equivalent batch reaction due to the broad residence time distribution (RTD) of the reactor. As polymerization time is directly proportional to chain length, having a broadened RTD will resulted in a broadening of the molecular weight distribution. Low conversion on the second methacrylate feed was also observed due to insufficient reaction time.

Noda *et al.* reported the synthesis of MMA homo and block copolymers in a 10 mL continuous microreactor.[79] The reactor was made from Teflon tubing with a 1.6 mm inner diameter. Two different N-alkyl-2-pyridylmethanimines were synthesized and used in these experiments. Presumably, these ligands formed homogeneous copper complexes, and as such reactor clogging was not observed. The use of a microreactor rendered the amount of copper use

negligible, and so ligand recycling or synthesis was not a concern. Polymerizations were conducted at 90 ℃ and showed good control (i.e. no observed PDI broadening). An additional feed point was added to synthesize copolymers of methacrylates and acrylates. While the copolymerization of two methacrylates was successful, low conversion was observed when butyl acrylate was fed in as the second monomer. This was also attributed to insufficient reaction time to polymerize BA to high conversion.

Müller *et al.* also investigated the ATRP of butyl acrylate and styrene in a continuous tubular reactor.[80] Unlike Noda, the approach was to demonstrate industrially feasibility by utilizing a large stainless steel reactor (volume of approximately 500 mL, 150 m of stainless steel tubing with an ID of 2.1 mm), and to modify copper solubility through monomer and solvent choice. The polymerization of butyl acrylate using acetonitrile as solvent at 80 °C was homogeneous and the tubular experiments showed good agreement with batch experiments. Polymerization of styrene at 110 °C in the tubular reactor was slightly faster than in batch. However, reactor clogging was an issue, possibly due to precipitation of copper(II) complex.

2.4.2 ATRP in Continuous Stirred Tank Reactors

Continuous stirred tank reactors (CSTR) are commonly used in industry, and are sometimes preferred over tubular reactors as they are less prone to fouling. The use of ATRP in a CSTR has not been studied experimentally. Part of this can be attributed to mediator solubility and the difficulties with operating a heterogeneous CSTR. Another possible reason is that, unlike a tubular or plug flow reactor where all reactants share a similar residence time, reactants in a CSTR will have a broad residence time distribution. Since polymer chains in controlled radical polymerization can have a lifetime of several hours and chain length is proportional to reaction time, there will be considerable broadening of the molecular weight distribution.[81] As one of the traditional advantages of CRP has been narrowly dispersed polymer chains, producing them in a CSTR seems to be counterproductive. However, a narrow polydispersity index is only one way to

measure livingness in living polymerization, and a wide molecular weight distribution due to a residence time effect does not necessitate poor control or livingness. Zhang and Ray[82] modeled conventional ATRP of styrene and BA at 110 °C in a series of 4, 8, or 16 tanks and found that as the number of CSTRs increased, the PDI decreased from 1.6 to 1.3 as the residence time distribution tightened. Since the composition in each tank was different, a tapered gradient polymer was theorized as the final product.

Schork *et al.* have investigated RAFT miniemulsion polymerization in a series of CSTRs. They were able to produce styrene homopolymer in a series of three CSTR's with a mean residence time of approximately two hours per stirred tank.[83,84] While the polymer exhibited living characteristics, the PDI was higher than in batch polymerizations partly due to residence time effects. The production of styrene and butyl acrylate block copolymer was also reported in a series of four CSTR's with a similar residence time.[85]

References

(1) Georges, M. K.; Veregin, R. P. N.; Kazmaier, P. M.; Hamer, G. K. *Macromolecules* **1993**, *26*, 2987–2988.

(2) Chiefari, J.; Y. K. Chong; Ercole, F.; Krstina, J.; Jeffery, J.; Le, T. P. T.; Mayadunne, R. T. A.; Meijs, G. F.; Moad, C. L.; Moad, G.; others *Macromolecules* **1998**, *31*, 5559–5562.

(3) Mayadunne, R. T. A.; Rizzardo, E.; Chiefari, J.; Chong, Y. K.; Moad, G.; Thang, S. H. *Macromolecules* **1999**, *32*, 6977–6980.

(4) Kato, M.; Kamigaito, M.; Sawamoto, M.; Higashimura, T. *Macromolecules* **1995**, *28*, 1721-1723.

(5) Wang, J. S.; Matyjaszewski, K. *Journal of the American Chemical Society* **1995**, *117*, 5614-5615.

(6) Matyjaszewski, K.; Xia, J. *Chemical Reviews* **2001**, *101*, 2921-2990.

(7) Ouchi, M.; Terashima, T.; Sawamoto, M. *Chemical reviews* **2009**, *109*, 4963-5050.

(8) Fischer, H. *Chemical Reviews* **2001**, *101*, 3581-3610.

(9) Shen, Y.; Tang, H.; Ding, S. *Progress in Polymer Science* **2004**, *29*, 1053-1078.

(10) Tsarevsky, N. V.; Matyjaszewski, K. *Journal of Polymer Science Part A: Polymer Chemistry* **2006**, *44*, 5098-5112.

(11) Tsarevsky, N. V.; Matyjaszewski, K. *Chemical reviews* **2007**, *107*, 2270-2299.

(12) Tsarevsky, N. V.; Braunecker, W. A.; Matyjaszewski, K. *Journal of Organometallic Chemistry* **2007**, *692*, 3212-3222.

(13) Tang, W.; Matyjaszewski, K. *Macromolecules* **2007**, *40*, 1858-1863.

(14) Tang, W.; Kwak, Y.; Braunecker, W.; Tsarevsky, N. V.; Coote, M. L.; Matyjaszewski, K. *Journal of the American Chemical Society* **2008**, *130*, 10702-10713.

(15) di Lena, F.; Matyjaszewski, K. *Progress in Polymer Science* **2010**, *35*, 959-1021.

(16) Braunecker, W. A.; Brown, W. C.; Morelli, B. C.; Tang, W.; Poli, R.; Matyjaszewski, K. *Macromolecules* **2007**, *40*, 8576-8585.

(17) Tang, W.; Tsarevsky, N. V.; Matyjaszewski, K. *Journal of the American Chemical Society* **2006**, *128*, 1598-1604.

(18) Tsarevsky, N. V.; Braunecker, W. A.; Vacca, A.; Gans, P.; Matyjaszewski, K. *Macromolecular Symposia* **2007**, *248*, 60-70.

(19) Marcus, Y.; Kamlet, M. J.; Taft, R. W. *The Journal of Physical Chemistry* **1988**, *92*, 3613-3622.

(20) Coullerez, G.; Malmström, E.; Jonsson, M. *The Journal of Physical Chemistry A* **2006**, *110*, 10355-10360.

(21) Braunecker, W. A.; Tsarevsky, N. V.; Gennaro, A.; Matyjaszewski, K. *Macromolecules* **2009**, *42*, 6348-6360.

(22) Litvinenko, G.; Müller, A. H. E. *Macromolecules* **1997**, *30*, 1253-1266.

(23) Jakubowski, W.; Matyjaszewski, K. *Macromolecules* **2005**, *38*, 4139-4146.

(24) Jakubowski, W.; Matyjaszewski, K. *Macromolecular Symposia* **2006**, *240*, 213-223.

(25) Jakubowski, W.; Min, K.; Matyjaszewski, K. *Macromolecules* **2006**, *39*, 39-45.

(26) Matyjaszewski, K.; Jakubowski, W.; Min, K.; Tang, W.; Huang, J.; Braunecker, W. A.; Tsarevsky, N. V. *Proceedings of the National Academy of Sciences of the United States of America* **2006**, *103*, 15309-15314.

(27) Jakubowski, W.; Matyjaszewski, K. *Angewandte Chemie* **2006**, *45*, 4482-6.

(28) Pietrasik, J.; Dong, H.; Matyjaszewski, K. *Macromolecules* **2006**, *39*, 6384-6390.

(29) Min, K.; Gao, H.; Matyjaszewski, K. *Macromolecules* **2007**, *40*, 1789-1791.

(30) Dong, H.; Tang, W.; Matyjaszewski, K. *Macromolecules* **2007**, *40*, 2974-2977.

(31) Mueller, L.; Jakubowski, W.; Tang, W.; Matyjaszewski, K. *Macromolecules* **2007**, *40*, 6464-6472.

(32) Matyjaszewski, K.; Dong, H.; Jakubowski, W.; Pietrasik, J.; Kusumo, A. *Langmuir* **2007**, *23*, 4528-4531.

(33) Jakubowski, W.; Kirci-Denizli, B.; Gil, R. R.; Matyjaszewski, K. *Macromolecular Chemistry and Physics* **2008**, *209*, 32-39.

(34) Dong, H.; Matyjaszewski, K. *Macromolecules* **2008**, *41*, 6868-6870.

(35) Tang, H.; Shen, Y.; Li, B. G.; Radosz, M. *Macromolecular Rapid Communications* **2008**, *29*, 1834-1838.

(36) Braunecker, W. A.; Tsarevsky, N. V.; Pintauer, T.; Gil, R. R.; Matyjaszewski, K. *Macromolecules* **2005**, *38*, 4081-4088.

(37) Tsarevsky, N. V.; Pintauer, T.; Matyjaszewski, K. *Macromolecules* **2004**, *37*, 9768-9778.

(38) Matyjaszewski, K.; Jo, S. M.; Paik, H.-jong; Shipp, D. A. *Macromolecules* **1999**, *32*, 6431-6438.

(39) Lutz, J. F.; Matyjaszewski, K. *Journal of Polymer Science Part A: Polymer Chemistry* **2005**, *43*, 897-910.

(40) Yamamoto, S.; Matyjaszewski, K. *Polymer Journal* **2008**, *40*, 496-497.

(41) Tanaka, K.; Matyjaszewski, K. *Macromolecules* **2007**, *40*, 5255-5260.

(42) Tanaka, K.; Matyjaszewski, K. *Macromolecular Symposia* **2008**, *261*, 1-9.

(43) Percec, V.; Guliashvili, T.; Ladislaw, J. S.; Wistrand, A.; Stjerndahl, A.; Sienkowska, M. J.; Monteiro, M. J.; Sahoo, S. *Journal of the American Chemical Society* **2006**, *128*, 14156-14165.

(44) Lligadas, G.; Percec, V. *Journal of Polymer Science Part A: Polymer Chemistry* **2008**, *46*, 2745-2754.

(45) Nguyen, N. H.; Rosen, B. M.; Jiang, X.; Fleischmann, S.; Percec, V. *Journal of Polymer Science Part A: Polymer Chemistry* **2009**, *47*, 5577-5590.

(46) Lligadas, G.; Percec, V. *Journal of Polymer Science Part A: Polymer Chemistry* **2007**, *45*, 4684-4695.

(47) Fleischmann, S.; Rosen, B. M.; Percec, V. *Journal of Polymer Science Part A: Polymer Chemistry* **2010**, *48*, 1190-1196.

(48) Fleischmann, S.; Percec, V. *Journal of Polymer Science Part A: Polymer Chemistry* **2010**, *48*, 2236-2242.

(49) Fleischmann, S.; Percec, V. *Journal of Polymer Science Part A: Polymer Chemistry* **2010**, *48*, 2243-2250.

(50) Nguyen, N. H.; Rosen, B. M.; Percec, V. *Journal of Polymer Science Part A: Polymer Chemistry* **2010**, *48*, 1752-1763.

(51) Lligadas, G.; Percec, V. *Journal of Polymer Science Part A: Polymer Chemistry* **2008**, *46*, 6880-6895.

(52) Soeriyadi, A. H.; Boyer, C.; Nyström, F.; Zetterlund, P. B.; Whittaker, M. R. *Journal of the American Chemical Society* **2011**, *133*, 11128-11131.

(53) Rosen, B. M.; Lligadas, G.; Hahn, C.; Percec, V. *Journal of Polymer Science Part A: Polymer Chemistry* **2009**, *47*, 3940-3948.

(54) Hatano, T.; Rosen, B. M.; Percec, V. *Journal of Polymer Science Part A: Polymer Chemistry* **2010**, *48*, 164-172.

(55) Matyjaszewski, K.; Tsarevsky, N. V.; Braunecker, W. A.; Dong, H.; Huang, J.; Jakubowski, W.; Kwak, Y.; Nicolay, R.; Tang, W.; Yoon, J. A. *Macromolecules* **2007**, *40*, 7795-7806.

(56) Lin, C. Y.; Coote, M. L.; Gennaro, A.; Matyjaszewski, K. *Journal of the American Chemical Society* **2008**, *130*, 12762-12774.

(57) Lligadas, G.; Rosen, B. M.; Bell, C. a.; Monteiro, M. J.; Percec, V. *Macromolecules* **2008**, *41*, 8365-8371.

(58) Nguyen, N. H.; Rosen, B. M.; Lligadas, G.; Percec, V. *Macromolecules* **2009**, *42*, 2379-2386.

(59) Zhong, M.; Matyjaszewski, K. *Macromolecules* **2011**, *44*, 2668-2677.

(60) Levere, M. E.; Willoughby, I.; O'Donohue, S.; de Cuendias, A.; Grice, A. J.; Fidge, C.; Becer, C. R.; Haddleton, D. M. *Polymer Chemistry* **2010**, *1*, 1086-1094.

(61) Nguyen, N. H.; Percec, V. *Journal of Polymer Science Part A: Polymer Chemistry* **2010**, *48*, 5109-5119.

(62) Nguyen, N. H.; Percec, V. *Journal of Polymer Science Part A: Polymer Chemistry* **2011**, *49*, 4241-4252.

(63) Lligadas, G.; Rosen, B. M.; Monteiro, M. J.; Percec, V. *Macromolecules* **2008**, *41*, 8360-8364.

(64) Wright, P. M.; Mantovani, G.; Haddleton, D. M. *Journal of Polymer Science Part A: Polymer Chemistry* **2008**, *46*, 7376-7385.

(65) Hornby, B. D.; West, A. G.; Tom, J. C.; Waterson, C.; Harrisson, S.; Perrier, S. *Macromolecular Rapid Communications* **2010**, *31*, 1276-1280.

(66) Tom, J.; Hornby, B.; West, A.; Harrisson, S.; Perrier, S. *Polymer Chemistry* **2010**, *1*, 420-422.

(67) West, A. G.; Hornby, B.; Tom, J.; Ladmiral, V.; Harrisson, S.; Perrier, S. *Macromolecules* **2011**, *44*, 8034-8041.

(68) Matyjaszewski, K.; Coca, S.; Gaynor, S. G.; Wei, M.; Woodworth, B. E. *Macromolecules* **1997**, *30*, 7348-7350.

(69) Zhang, Y.; Wang, Y.; Matyjaszewski, K. *Macromolecules* **2011**, *44*, 683-685.

(70) Zhang, Y.; Wang, Y.; Peng, C.-how; Zhong, M.; Zhu, W.; Konkolewicz, D.; Matyjaszewski, K. *Macromolecules* **2012**, *45*, 78-86.

(71) Enright, T. E.; Cunningham, M. F.; Keoshkerian, B. *Macromolecular Rapid Communications* **2005**, *26*, 221-225.

(72) Enright, T. E.; Cunningham, M. F.; Keoshkerian, B. *Macromolecular Reaction Engineering* **2010**, *4*, 186-196.

(73) Russum, J. P.; Jones, C. W.; Schork, F. J. *Macromolecular Rapid Communications* **2004**, *25*, 1064-1068.

(74) Russum, J. P.; Jones, C. W.; Schork, F. J. *Industrial & Engineering Chemistry Research* **2005**, *44*, 2484-2493.

(75) Russum, J. P.; Jones, C. W.; Schork, F. J. *AIChE Journal* **2006**, *52*, 1566-1576.

(76) Shen, Y.; Zhu, S.; Zeng, F.; Pelton, R. H. *Macromolecules* **2000**, *33*, 5427-5431.

(77) Shen, Y.; Zhu, S.; Pelton, R. *Macromolecular Rapid Communications* **2000**, *21*, 956–959.

(78) Shen, Y.; Zhu, S. *AIChE Journal* **2002**, *48*, 2609-2619.

(79) Noda, T.; Grice, A. J.; Levere, M. E.; Haddleton, D. M. *European Polymer Journal* **2007**, *43*, 2321-2330.

(80) Müller, M.; Cunningham, M. F.; Hutchinson, R. A. *Macromolecular Reaction Engineering* **2008**, *2*, 31-36.

(81) Schork, F. J.; Smulders, W. *Journal of Applied Polymer Science* **2004**, *92*, 539–542.

(82) Zhang, M.; Ray, W. H. *Journal of Applied Polymer Science* **2002**, *86*, 1047-1056.

(83) Smulders, W. W.; Jones, C. W.; Schork, F. J. *AIChE Journal* **2005**, *51*, 1009-1021.

(84) Qi, G.; Jones, C. W.; Schork, J. F. *Industrial & Engineering Chemistry Research* **2006**, *45*, 7084-7089.

(85) Smulders, W. W.; Jones, C. W.; Schork, F. J. *Macromolecules* **2004**, *37*, 9345-9354.

Chapter 3

Reducing Ligand use in ARGET ATRP

Preface

From the literature review, it can be seen ARGET and ICAR both have their own advantages and disadvantages. ARGET is a more elegant and cleaner polymerization technique, especially for the preparation of block copolymers, but the requirement for excess ligand can be a considerable hurdle for scale up as the ligands used are quite expensive. As such, the first step towards scale up of ARGET ATRP should be to reduce the amount of ligand required. In this section, results from ARGET ATRP of butyl acrylate (BA), butyl methacrylate (BMA), and methyl methacrylate (MMA) homopolymerizations using only stoichiometric amounts of ligand to copper in a variety of solvents, and under industrially relevant conditions where monomer and solvent purification are bypassed are discussed. The results demonstrate the robustness of ARGET ATRP under a wide variety of experimental conditions, and its potential for industrial adoption. The work in this section has been published as a full paper in Macromolecular Chemistry and Physics (2008, vol. 209, 1797-1805).

Abstract

Atom transfer radical polymerizations of butyl methacrylate, methyl methacrylate, and butyl acrylate have been conducted using only ppm amounts of catalyst through the regeneration of activator via the ARGET mechanism. The polymers produced were nearly colourless, and exhibited living characteristics with copper catalyst levels as low as 6.4 ppm relative to monomer. Polymerizations were well controlled at temperatures up to 110 °C and, contrary to previous studies, ARGET ATRP was successfully carried out using only a stoichiometric amount of ligand to catalyst. As ligand can account for a considerable portion of catalyst cost, these results demonstrate the robustness of ARGET ATRP, and its potential for industrial adoption.

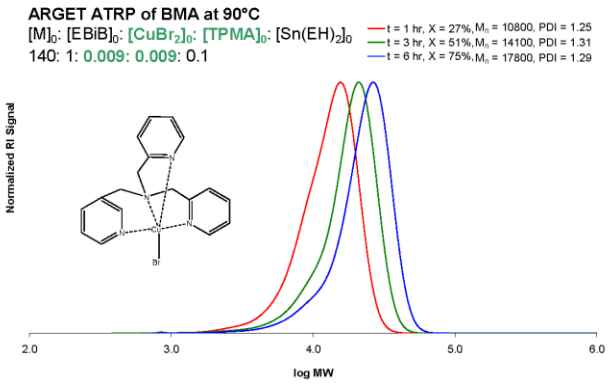

3.1 Introduction

Controlled or living polymerization techniques (L/CRP) present an interesting alternative to traditional free radical polymerization by allowing for excellent control over molecular microstructure to produce specialty polymers. In particular, atom transfer radical polymerization (ATRP)[1-4] provides a simple way to synthesize polymers with controlled microstructure and narrow molecular weight distributions. ATRP proceeds via standard free radical polymerization mechanisms. However, growing radicals can be reversibly activated or deactivated via a dynamic equilibrium with a transition metal catalyst complex (typically copper bound to a nitrogen based ligand) with an exchange of halogen between the chain end and metal complex. The majority of chains exist in a dormant (halogen capped) state, and irreversible termination of propagating free radicals is statistically suppressed to give polymer synthesized via ATRP its living nature.

Traditionally, the transition metal catalyst employed in ATRP is used in stoichiometric or slightly sub-stoichiometric ratio to the initiator, leading to a high catalyst level in the final polymer. This catalyst can often be expensive, especially in cases where a ligand must be specially synthesized. In addition, the catalyst can be harmful, and adds undesired colour to the polymer so that catalyst separation from the final product (and recycle) may be required. This can add significantly to production costs, and has so far contributed to making ATRP economically less viable for most applications.

A more desirable approach would be to reduce the catalyst level through tuning catalyst activity to maintain a reasonable polymerization rate at lower metal levels. The rate of reaction for an ATRP system assuming negligible bimolecular termination can be approximated as:

$$R_p = k_p[M][P^\bullet] = k_p[M]\frac{k_a}{k_{da}}[R-X]\frac{[Cu^I]}{[Cu^{II}X]} \qquad \textbf{Equation 3-1}$$

where: k_p is the monomer propagation rate coefficient; [*M*], [$P^\bullet$], [*R-X*] are monomer, propagating chain, and alkyl halide initiator concentrations respectively; k_a and k_{da} are the rate constants of

activation and deactivation which combine to form the ATRP equilibrium constant; and [Cu^{I}] and [$Cu^{II}X$] are the concentrations of the activator and deactivator species. The rate constants of activation and deactivation can be dramatically altered through ligand choice. Two examples of such ligands are tris[2-(dimethylamino)ethyl]amine (Me_6TREN), and tris(2-pyridylmethyl)amine (TPMA). Complexes formed using these ligands have ATRP equilibrium constants several orders of magnitude higher than when using other ligands.[5,6] Nonetheless, it is not possible to reduce catalyst concentration by the same scale, as irreversible radical termination will lead to a buildup of deactivator species. This shifts the activator/deactivator ratio, and ultimately stops the reaction before it can reach completion.

In order to circumvent this limitation, Matyjaszewski *et al.* recently developed two methods by which activator can be regenerated in-situ from deactivator whose concentration has built up due to termination.[7] Both these procedures allow for catalyst concentration to be lowered to parts per million (ppm) levels with respect to monomer. In addition, they allow for the use of the more oxidatively stable Cu(II) species as a starting material, which simplifies the handling procedures. The first technique is called "activators regenerated by electron transfer" (ARGET), and utilizes a reducing agent to convert copper(II) deactivating species into copper(I) activating species. A variety of reducing agents, such as tin(II) 2-ethylhexanoate ($Sn(EH)_2$), glucose, ascorbic acid, hydrazine, or phenols have been successfully used to synthesize a wide variety of polymers with varying architecture and reactivity.[7-16]

One of the drawbacks of ARGET is that ligand must be added to metal in 3 to 10 times molar excess in order to achieve a controlled polymerization. The excess ligand helps to maintain the catalyst complex and protect it from destabilizing side reactions. These side reactions vary depending on reaction conditions, but generally include monomer complexation to catalyst,[8,10] and destabilization or complexation of catalyst to Lewis acid formed from the reduction

mechanism.[7,8] As these ligands are expensive and not widely available, these factors present considerable hurdles to industrial scale up.

The second method developed by Matyjaszewski *et al.* is called "initiators for continuous activator regeneration" (ICAR), and uses a small amount of thermal free radical initiator to reduce Cu(II) deactivator into Cu(I) activator. The chief limitation to ICAR is the generation of additional chains due to the radical source, which will broaden the molecular weight distribution and give new homopolymer in a block copolymerization. However, since there is no generation of acid or other reactions with reducing agents, the catalyst is more stable and ligand can be added in a stoichiometric ratio to metal.[7,14] Evidently, ARGET ATRP is a more feasible system for the preparation of block copolymers as there is no additional radical source, and it would be even more attractive if ligand levels could be reduced.

Herein, we report results of ARGET ATRP of butyl acrylate (BA), butyl methacrylate (BMA), and methyl methacrylate (MMA) homopolymers using only stoichiometric amounts of ligand to copper under a variety of solvents, and under industrially relevant conditions where monomer and solvent purification are bypassed. The results demonstrate the robustness of ARGET ATRP under a wide variety of experimental conditions.

3.2 Experimental

3.2.1 Materials

Butyl methacrylate (BMA) (99%, Aldrich), butyl acrylate (BA) (99%, Aldrich), and styrene (99%, Aldrich) were purified by elution through a column packed with inhibitor remover (Aldrich). The compounds methyl methacrylate (MMA) (99%, Aldrich), copper(II) bromide ($CuBr_2$, 99% Aldrich), 2-(aminomethyl)pyridine (99%, Aldrich), sodium triacetoxyborohydride (95%, Aldrich), pyridine-2-carboxaldehyde (99%, Aldrich), sodium hydrogen carbonate (99.7%,

Aldrich), magnesium sulphate (99%, Aldrich), ethyl acetate (99.8%, Aldrich), dichloromethane (99.5% Aldrich), petroleum ether (40-60 °C, Acros), anisole (99%, Aldrich), benzonitrile (99%, Aldrich), toluene (99%, Acros), ethyl 2-bromoisobutyrate (EBiB) (98%, Aldrich), and tin(II) 2-ethylhexanoate ($Sn(EH)_2$) (95%, Aldrich) were used as received.

3.2.2 Synthesis of tris(2-pyridylmethyl)amine (TPMA)

Tris(2-pyridylmethyl)amine (TPMA) was synthesized according to published procedure.[17] 1.62 g (15.78 mmol) of 2-(aminomethyl)pyridine and 9.36 g (44.1 mmol) of sodium triacetoxyborohydride were combined in 225 mL of dichloromethane in an ice bath. 3.00 mL (31.5 mmol) of pyridine-2-carboxaldehyde was slowly added to the cooled mixture. Upon complete addition, stirring was continued for a further 18 hours. Subsequently, a saturated aqueous sodium hydrogen carbonate solution was added and after 15 min of stirring the solution was extracted with ethyl acetate. The organic fraction was dried with magnesium sulfate, and then the solvent was removed by vacuum. The residue was washed several times with small quantities of petroleum ether (spec 40-60C) then dried under vacuum. Yield 3.30 g of yellow solid (72%). ^{1}H NMR (CDCl3): δ8.53 (d, 3H, 6-Py*H*), 7.63 (m, 6H, 3-Py*H* and 4-Py*H*), 7.14 (t, 3H, 5-Py*H*), 3.88 (s, 6H, NCH_2).

The copper(II) bromide TPMA complex, [Cu^{II}(TPMA)Br][Br] was prepared according to literature procedure,[18] and dissolved in benzonitrile to form a stock solution. $CuBr_2$ (0.878 g, 3.93 mmol) was combined with TPMA (1.141 g, 3.93 mmol) and dichloromethane (2 mL) in a small vial. The mixture was stirred at room temperature for 30 minutes, and the product precipitated by slow addition of n-pentane. The supernatant liquid was decanted and the green powder was washed with 2 x 10 mL of n-pentane and dried under vacuum. Yield 1.93 g (96%) of a light green powder. 0.0805 g of the complex was dissolved in 10 mL of benzonitrile to make a stock solution.

3.2.3 ARGET ATRP polymerization procedure

1.00 g of benzonitrile/[Cu^{II}(TPMA)Br][Br] stock solution was diluted by 9 g of toluene and mixed with BMA (35 g, 0.246 mol) in a 100 mL two neck round bottom flask. The mixture was purged under nitrogen for one hour, before being heated to 70 ºC. EBiB (0.341 g, 1.75 mmol) dissolved in 2.5 g of toluene was purged with nitrogen for ten minutes, was then added to the round bottom flask via a degassed syringe. After approximately 10 minutes, $Sn(EH)_2$ (0.071 g, 0.175 mmol) dissolved in 2.5 g of toluene purged with nitrogen was injected. Samples were withdrawn using a deoxygenated syringe and placed into an ice bath to stop polymerization. The target molecular weight of the polymerization was 20000 $g \cdot mol^{-1}$ (DP_n = 140). Solvent content was 30% by mass, and concentration of $CuBr_2$ was 100 ppm on a mass basis, or 64 ppm on a molar basis with respect to monomer. Polymerizations of other monomers were carried out following the same procedure.

3.2.4 Characterization

Sample conversion was determined by gravimetry. Gel permeation chromatography (GPC) was used to determine the molecular weight distribution of the polymer samples. Dried polymer samples were dissolved in tetrahydrofuran (THF) and passed through a column packed with basic alumina to remove remaining copper. The GPC was equipped with a Waters 2960 separation module containing four Styragel columns of pore sizes 100, 500, 10^3, 10^4 Å, coupled with a refractive index detector operating at 40 ºC. THF was used as eluant and the flow rate was set to 1.0 $mL \cdot min^{-1}$. The detector was calibrated with eight narrow polystyrene standards ranging from 347 to 355 000 $g \cdot mol^{-1}$. The molecular weights of poly(BMA), poly(MMA), and poly(BA) samples were obtained by universal calibration using known Mark-Houwink parameters for polystyrene ($K = 11.4 \cdot 10^{-5}$ $dL \cdot g^{-1}$, a = 0.716),[19] poly(BMA) ($K = 14.8 \cdot 10^{-5}$ $dL \cdot g^{-1}$, a = 0.664),[19] poly(MMA) ($K = 9.44 \cdot 10^{-5}$ $dL \cdot g^{-1}$, a = 0.719),[19] and poly(BA) ($K = 7.4 \cdot 10^{-5}$ $dL \cdot g^{-1}$, a = 0.750).[20]

3.3 Results and Discussion

3.3.1 ARGET ATRP of methacrylates

The experimental conditions of poly(BMA) produced by ARGET ATRP are summarized in Table 3.1. While there is a slightly higher molar concentration of catalyst relative to monomer for experiments 3-5 than for experiments 1-2, the ratio between initiator (chain) and catalyst concentration is actually higher for experiments 3-6 (112 chains : 1 catalyst, except for experiment 6, which has a ratio of 1117:1) than for experiments 1-2 (100 chains : 1 catalyst). The catalyst concentration was calculated on a mass basis for the later experiments in order to ensure a constant concentration regardless of the monomer being used.

Table 3.1: Experimental conditions of PBMA prepared by ARGET ATRP at 70 °C.

exp.	$[M]_0$: $[EBiB]_0$: $[CuBr_2]_0$:$[TPMA]_0$: $[Sn(EH)_2]_0$	solvent [c]
1	200:1:0.01:0.01:0.1	anisole
2	200:1:0.01:0.05:0.1	anisole
3	140:1:0.009:0.009:0.1	benzonitrile
4 [a]	140:1:0.009:0.009:0.1	benzonitrile
5 [a, b]	140:1:0.009:0.009:0.1	toluene
6 [a, b]	140:1:0.0009:0.0009:0.1	toluene

[a] monomer was not purified before use. [b] benzonitrile was used in the stock solution, with final ratio benzonitrile:toluene 1:14 by mass. [c] solvent content is 30% by mass in all cases.

In all experiments, the use of $[Cu^{II}(TPMA)Br][Br]$ as catalyst produced nearly colourless polymer with living characteristics. The final properties of PBMA produced by ARGET ATRP are summarized in Table 3.2. Figure 3.1(a) shows the evolution of number-aveage molecular weights (M_n) and polydispersities (PDI) for several representative BMA polymerizations. In all cases M_n increased linearly while PDI decreased with conversion. Experiments 1 and 2 were done in anisole at conditions similar to those previously reported in literature.[10] The use of TPMA in 5 times molar excess to copper in experiment 2 gave higher polymerization rate than when using TPMA at a stoichiometric ratio, which may be attributed to the fact that amine based ligands are basic and can function as reducing agents.[7] The presence of excess reducing agent would increase

the copper(I):copper(II) ratio and enhance polymerization rate. Surprisingly, the use of only a stoichiometric amount of ligand in experiment 1 produced a well-controlled living system. In previous studies, polymerization of styrene using $Sn(EH_2)$ as reducing agent was found to require excess ligand to stabilize the catalyst against complexation or dissociation due to side reactions with a Lewis acid formed from $Sn(EH_2)$, as well as the high temperature required for polymerization of styrene.[8] The stability of copper(II) complexes formed with TPMA have been previously measured as a function of temperature, and can decrease by as much as two orders of magnitude from room temperature to reaction temperatures.[21] Polymerizations of methacrylates and acrylates using $Sn(EH_2)$ as reducing agent were also conducted with an excess of ligand.[10]

Table 3.2: Final properties of PBMA prepared by ARGET ATRP at 70 °C.

exp.	Cu [a] (ppm)	t (min)	conv (%)	$M_{n,theo}$ [b] ($g \cdot mol^{-1}$)	$M_{n,GPC}$ ($g \cdot mol^{-1}$)	PDI
1	50	300/1330	45/88	9500/18700	17760/29300	1.38/1.22
2	50	300/1330	59/92	11800/18400	18500/27000	1.36/1.29
3	64	300/1130	36/52	7170/10430	11300/13200	1.28/1.39
4	64	300/1130	49/73	9800/14600	12400/15400	1.36/1.51
5	64	300/1680	50/96	10600/19000	13300/20700	1.28/1.24
6	6.4	300/1400	29/74	5600/15000	21600/32400	1.46/1.46

[a] molar ratio vs. monomer. [b] $M_{n,theo} = ([M]_0/[EBiB]_0) \times conv. \times MW_M$.

It was observed that the catalyst was not fully soluble in anisole at room temperature in experiments 1 and 2. Even upon heating to reaction temperatures, the catalyst in copper(II) form remained insoluble in the reaction mixture. However, once the reducing agent $Sn(EH_2)$ was injected, the solution became homogeneous. As copper(I) is known to have greater solubility in organic media than copper(II), an increased copper(I):copper(II) ratio solubilizes the catalyst. It has been previously reported that only soluble catalyst participates in the ATRP equilibrium.[22-25] As such, it was hypothesized that by increasing solvent polarity, it would be possible to enhance catalyst solubility and possibly enhance absolute copper concentration. Benzonitrile was chosen due to its high boiling point, and nitrile functional group (like acetonitrile) which has been known to complex to copper as a "fifth ligand".[26]

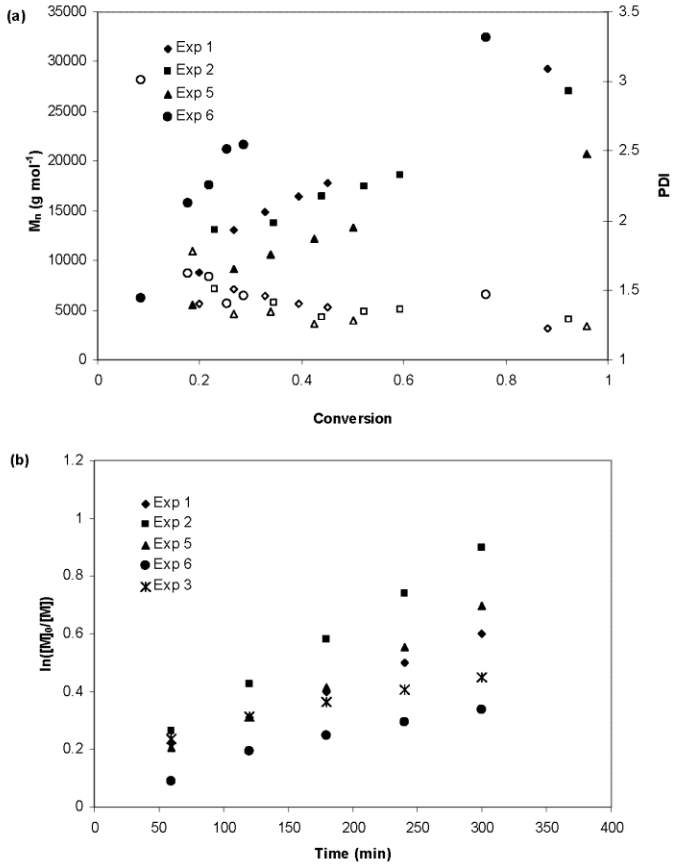

Figure 3.1: Evolution of number-average molecular weight (M_n, filled symbols) and polydispersity index (PDI, open symbols) with conversion (a), and normalized conversion vs. time (b) for butyl methacrylate ARGET ATRP at 70 °C. Experimental conditions are summarized in Table 3.1.

The results from this strategy were mixed. Using only benzonitrile as solvent (experiments 3 and 4) produced a slower polymerization than in anisole with similar control. Solvent choice can heavily influence polymerization rate in ATRP not only through changing catalyst solubility, but through stabilization of either copper(I) or copper(II) complexes. If the stability of the copper(I) species is enhanced in benzonitrile, then the ATRP equilibrium constant will decrease, lowering polymerization rate. The curvature in the kinetic plot for experiment 3 in Figure 3.1(b) indicates that the number of active chains decreases as the polymerization

progresses, which could be due to slow destabilization of the catalyst by side reactions with the oxidized reducing agent. In experiment 4, the use of unpurified monomer and unpurified solvent did not seem to negatively impact the final results. In fact, the use of unpurified monomer gave a higher rate of polymerization. This might be attributed to trace quantities of phenol inhibitor in the monomer, which may reduce copper(II) to increase the copper(I):copper(II) ratio, enhancing polymerization rate.[27] A reduction of copper(II) concentration in the system would also account for the higher PDI in experiment 4.

However, if benzonitrile is only used in small quantities in a co-solvent system with toluene as in experiments 5 and 6, reaction rate is higher (similar to when using anisole) and the number of active chains remains constant with unpurified monomer and solvents. The use of toluene most likely changed the polarity of the solvent system, changing the ATRP equilibrium or catalyst stability. Even at extremely low catalyst concentrations (experiment 6), the system was controlled and living, as seen by the GPC traces shown in Figure 3.2. The polydispersity of the molecular weight distribution is defined by Equation 3-2:

$$PDI = \frac{M_w}{M_n} = 1 + \frac{1}{DP_n} + \left(\frac{[R-X]_0 k_p}{k_{da}[Cu^{II}X]} \right) \left(\frac{2}{X} - 1 \right) \qquad \textbf{Equation 3-2}$$

where X represents conversion and the other symbols are as previously defined. Given that there are over 1000 polymer chains (defined by $[R\text{-}X]_0$) per single catalyst complex, the ability of the catalyst to maintain a living system is quite impressive.

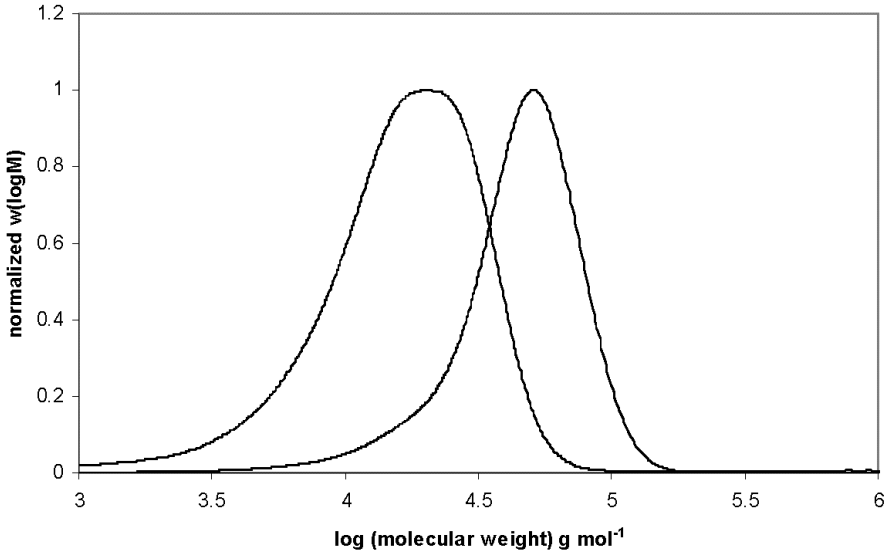

Figure 3.2: Gel permeation chromatography traces for pBMA produced in experiment 6 (6.4 ppm catalyst, [EBiB]:[Cu] = 1117:1). Conversion increases from left to right: conversion = 9%, M_n = 6200 g·mol^{-1}, PDI = 3.01, t = 60 min; conversion = 74%, M_n = 32400 g·mol^{-1}, PDI = 1.46, t = 1400 min.

Poly(MMA) was also prepared by ARGET ATRP using $Sn(EH_2)$ as a reducing agent. The experimental conditions and final properties of the polymer produced are summarized in Table 3.3. As with the poly(BMA) experiments, the use of $[Cu^{II}(TPMA)Br][Br]$ as catalyst produced nearly colourless polymer with living characteristics. Figure 3.3(a) shows the evolution of molecular weights and PDI for the three MMA polymerizations. In all cases, M_n increased linearly while PDI decreased with conversion. The use of anisole in experiments 7 and 8 gave higher polymerizations rates than when using toluene as co-solvent, but control was good and the kinetic plots in Figure 3.3(b) are linear for all three experiments. The polymerization rates were comparable to that of BMA ARGET ATRP, which was expected as the two monomers have similar propagation constants and should have similar ATRP constants. In all, ARGET ATRP was found to be very robust with a high tolerance for impurities in the polymerization of methacrylates.

Table 3.3: Final properties of PMMA prepared by ARGET ATRP.

exp. [a]	Cu [b] (ppm)	t (min)	conv (%)	$M_{n,theo}$ [c] ($g \cdot mol^{-1}$)	$M_{n,GPC}$ ($g \cdot mol^{-1}$)	PDI
7 [d]	50	360	55	11000	14000	1.26
8 [e]	50	360	58	11600	14500	1.25
9 [f]	50	360	43	8600	12400	1.27

[a] monomer was not purified before use, molar ratio of reactants: $[MMA]_0:[EBiB]_0:[CuBr_2]_0:[TPMA]_0:[Sn(EH)_2]_0$ = 200:1:0.01:0.01:0.1; T = 70 °C, solvent content is 30% by mass in all cases. [b] molar ratio vs. monomer. [c] $M_{n,theo} = ([M]_0/[EBiB]_0)$ x conv. x MW_M. [d] anisole used as solvent. [e] benzonitrile was used in the stock solution, with final ratio benzonitrile:anisole 1:14 by mass. [f] benzonitrile was used in the stock solution, with final ratio benzonitrile:toluene 1:14 by mass.

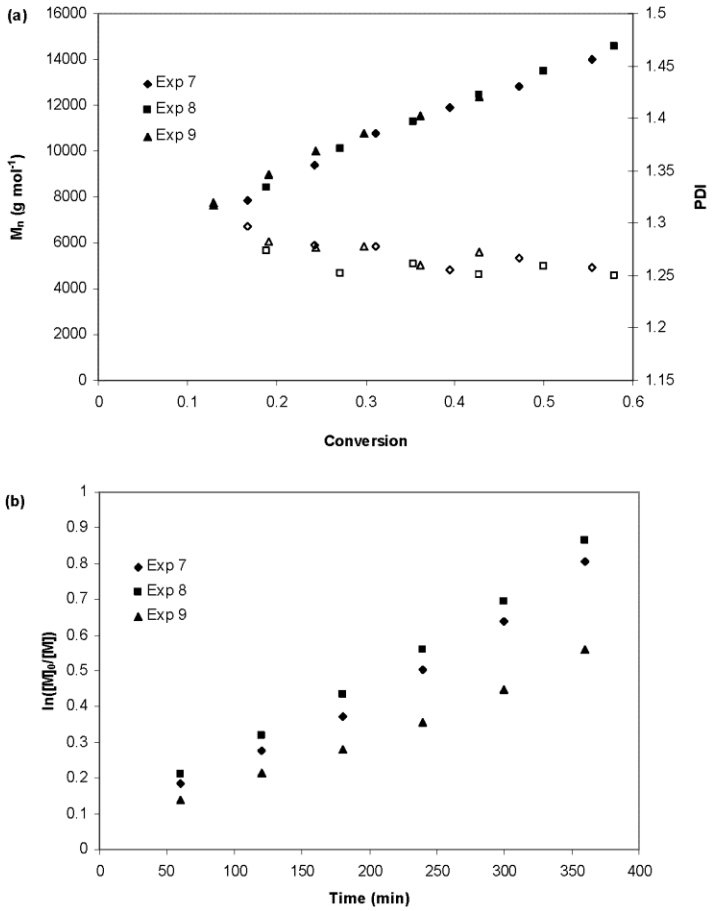

Figure 3.3: Evolution of number-average molecular weight (M_n, filled symbols) and polydispersity index (PDI, open symbols) with conversion (a), and normalized conversion vs. time (b) for methyl methacrylate ARGET ATRP at 70 °C. Experimental conditions are summarized in Table 3.3.

3.3.2 ARGET ATRP of butyl acrylate

ARGET ATRP of butyl acrylate was also carried out with stoichiometric quantities of ligand, along with unpurified monomer and solvent. These results are summarized in experiments 10-12 in Table 3.4. As acrylates have much higher propagation rate constants than methacrylates, these experiments were conducted at 60 °C in order to ensure a higher level of control over the polymerization. All experimental conditions produced polymer with living character, as shown by the linear increase in M_n and decrease in PDI with conversion presented in Figure 3.4(a). Figure 3.4(b) indicates a slight deviation from linear behaviour in the kinetic plot that could be attributed to a number of factors, as discussed previously for BMA. Acrylates are known to complex more strongly than methacrylates and styrenics, and while this complexation is weak relative to halide ion or ligand bonding, at low catalyst concentration this may cause the catalyst to destabilize.[21]

Table 3.4: Final properties of PBA prepared by ARGET ATRP at 60 °C.

exp. [a]	Cu [b] (ppm)	t (min)	conv (%)	$M_{n,theo}$ [c] ($g \cdot mol^{-1}$)	$M_{n,GPC}$ ($g \cdot mol^{-1}$)	PDI
10 [d]	57	310/1260	28/43	6290/10120	5630/8550	1.36/1.21
11 [d, e]	57	300/1270	23/43	4910/9230	5240/9320	1.35/1.26
12 [e, f]	57	300/1720	16/30	3480/6550	3830/7060	1.43/1.27

[a] molar ratio of reactants: $[BA]_0:[EBiB]_0:[CuBr_2]_0:[TPMA]_0: [Sn(EH)_2]_0$ = 156:1:0.009:0.009:0.1; T = 60 °C, solvent content is 30% by mass in all cases. [b] molar ratio vs. monomer. [c] $M_{n,theo} = ([M]_0/[EBiB]_0)$ x conv. x MW_M. [d] benzonitrile used as solvent. [e] monomer not purified before use. [f] benzonitrile was used in the stock solution, with final ratio benzonitrile:toluene 1:14 by mass.

From the conversion data, it can be seen that a considerably larger amount of polymer is formed between initiation and the first sample than compared to any other time step. This indicates a larger active radical concentration at the beginning of the polymerization, and could be attributed to the difference in activation constants between EBiB (a tertiary alkyl halide), and a butyl acrylate chain end (a secondary alkyl halide). In general, tertiary alkyl halides (forming tertiary radicals) have a much higher rate constant of activation than alkyl halides forming secondary radicals.[28] As such, most of the catalyst will preferentially react with the initiator over

dormant polymer chains until all the initiator is consumed, accounting for the higher initial rate of polymerization seen in the kinetic plot.

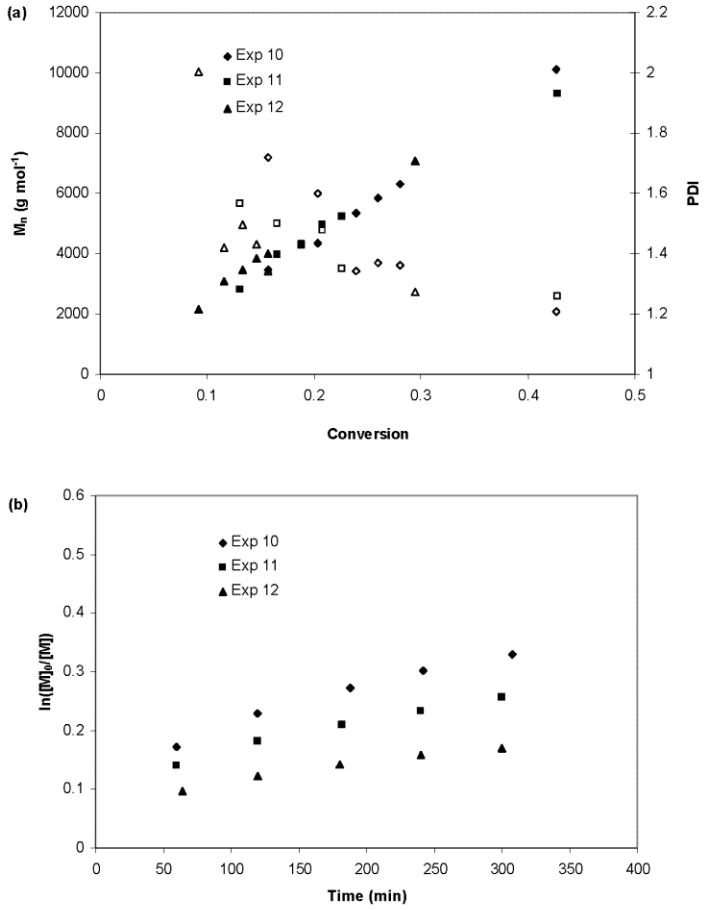

Figure 3.4: Evolution of number-average molecular weight (M_n, filled symbols) and polydispersity index (PDI, open symbols) with conversion (a), and normalized conversion vs. time (b) for butyl acrylate ARGET ATRP at 60 °C. Experimental conditions are summarized in Table 3.4.

In contrast to butyl methacrylate polymerizations, the observed rate for butyl acrylate is higher when benzonitrile is used as the only solvent (experiments 10 and 11). When toluene is used as a co-solvent (experiment 12), polymerization rate decreases but control over molecular weight remains similar. This behaviour seems contradictory at first, but might be explained by competitive complexation between benzonitrile and butyl acrylate. As previously discussed,

benzonitrile can stabilize the copper(I) complex, thereby reducing the ATRP equilibrium constant and decreasing reaction rate. Since acrylates are known to complex more strongly than methacrylates, monomer complexation may block solvent from complexing with the catalyst so that the polymerization rate is not affected to the same degree in butyl acrylate polymerizations. Figure 3.5 shows the GPC trace for experiment 11. A clear shift in the molecular weight distribution can be seen, indicating that the system is indeed living and controlled.

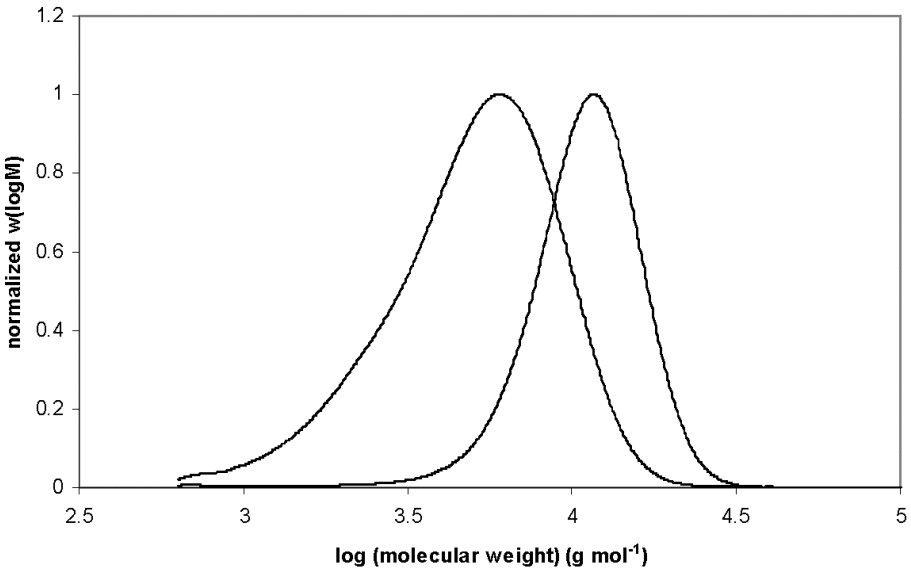

Figure 3.5: Gel permeation chromatography traces for pBA produced in experiment 11 (57 ppm catalyst, [EBiB]:[Cu] = 112:1). Conversion increases from left to right: conversion = 17%, M_n = 3950 g·mol^{-1}, PDI = 1.50, t = 120 min; conversion = 43%, M_n = 9300 g·mol^{-1}, PDI = 1.26, t = 1270 min.

3.3.3 High temperature ARGET ATRP of BMA, MMA, and BA

In order to investigate whether higher temperatures cause catalyst destabilization, styrene ARGET ATRP experiments were conducted with TPMA as ligand under conditions investigated in previous work.[8] In agreement with literature, it was found that with a stoichiometric ratio of ligand to copper, only low molecular weight oligomers were formed. With a 10 fold excess of ligand, polymerization was well controlled at 110 °C. Styrene polymerization was also conducted

at 90 °C with similar results to polymerizations at 110 °C. For all styrene ARGET ATRP runs without excess ligand, it was observed that the reaction mixture quickly became cloudy after the injection of reducing agent. A yellow precipitate then formed on the flask walls, which might indicate the formation of destabilized catalyst.

Given that the same reducing agent, catalyst, and solvents have been used for ARGET ATRP of styrene as for methacrylates and acrylates, it is likely that all systems exhibit the same set of side reactions: complexation with solvent, complexation with monomer, and destabilization by Lewis acid formed from reducing agent. Since acrylates and methacrylates complex more strongly to catalyst than styrene, it is surprising that acrylates and methacrylates, but not styrene, can be successfully polymerized by ARGET ATRP at a 1:1 Cu:ligand ratio. However, from the reaction temperature of BA (60 °C) to that of styrene (90-110 °C), the stability constant of catalyst complexes formed with TPMA can vary by an order of magnitude.[21] To investigate this possible temperature effect, high temperature ARGET ATRP of BMA, MMA, and BA was conducted. Experimental conditions and final properties of polymer are listed in Table 3.5 and Table 3.6.

Table 3.5: Experimental conditions of PBMA, PMMA, PBA prepared by ARGET ATRP at high temperatures.

exp. [a]	monomer	$[M]_0$: $[EBiB]_0$: $[CuBr_2]_0$:$[TPMA]_0$: $[Sn(EH)_2]_0$	T (°C)	solvent [b]
5	BMA	140:1:0.009:0.009:0.1	70	toluene
13	BMA	140:1:0.009:0.009:0.1	90	toluene
14	BMA	140:1:0.009:0.009:0.1	110	toluene
9	MMA	200:1:0.01:0.01:0.1	70	toluene
15	MMA	200:1:0.01:0.01:0.1	90	toluene
12	BA	156:1:0.009:0.009:0.1	60	toluene
16	BA	156:1:0.009:0.009:0.1	90	toluene
17	BA	156:1:0.009:0.009:0.1	110	toluene

[a] monomer was not purified before use, benzonitrile was used in the stock solution, with final ratio benzonitrile:toluene 1:14 by mass. [b] solvent content is 30% by mass in all cases.

Table 3.6: Final properties of PBMA, PMMA, PBA prepared by high temperature ARGET.

exp.	Cu [a] (ppm)	t (min)	conv (%)	$M_{n,theo}$ [b] ($g \cdot mol^{-1}$)	$M_{n,GPC}$ ($g \cdot mol^{-1}$)	PDI
5	64	300/1330	50/96	10600/19000	13300/20700	1.28/1.24
13	64	360	76	14900	17800	1.29
14	64	360	96	19100	20700	1.50
9	50	360	43	8600	12400	1.27
15	50	300	87	17000	18000	1.32
12	57	300/1720	16/30	3480/6550	3830/7060	1.43/1.27
16	57	360	54	10650	11600	1.13
17	57	360	91	18150	15400	1.32

[a] molar ratio vs. monomer. [b] $M_{n,theo} = ([M]_0/[EBiB]_0) \times conv. \times MW_M$.

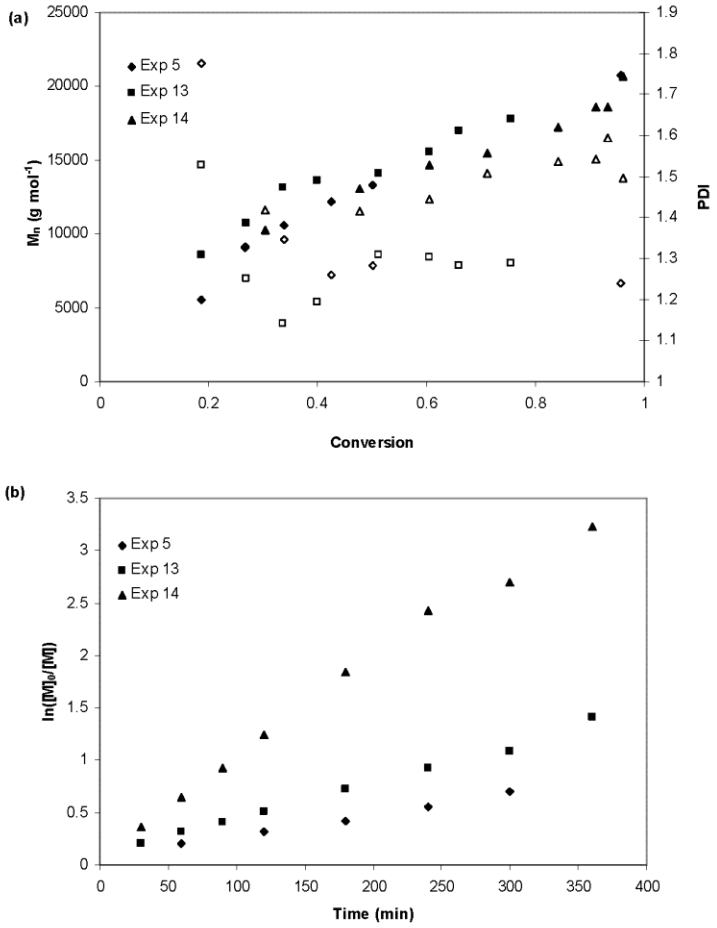

Figure 3.6: Evolution of number-average molecular weight (M_n, filled symbols) and polydispersity index (PDI, open symbols) with conversion (a), and normalized conversion vs. time (b) for butyl methacrylate ARGET ATRP at 70, 90, and 110 °C. Experimental conditions are summarized in Table 3.5.

In all cases, an increase in temperature led to significantly higher polymerization rates, as expected. In addition, all polymerizations produced polymer with living characteristics, and no visible catalyst destabilization was observed. Evolutions of molecular weight and PDI against conversion, as well as normalized conversion for high temperature BMA ARGET ATRP are shown in Figure 3.6. At all temperatures, M_n increases linearly with conversion, and the kinetic plot shows linear behaviour. The PDI of experiment 14 was noticeably higher throughout the polymerization, indicating that there is less control over the polymerization at 110 °C. This could be due to increased propagation and activation at higher temperatures, or destabilization of the catalyst, although no visible precipitate was observed.

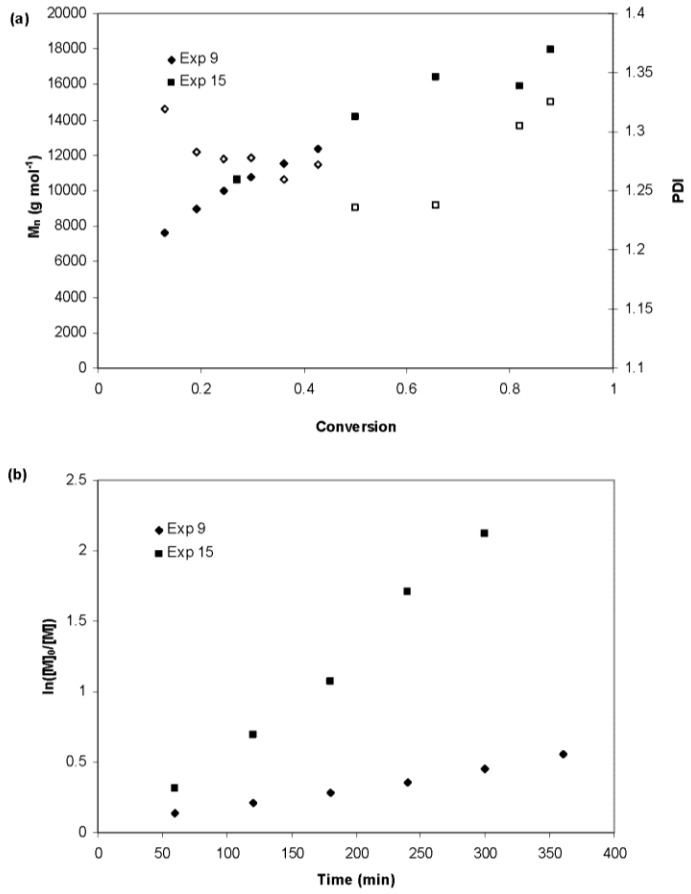

Figure 3.7: Evolution of number-average molecular weight (M_n, filled symbols) and polydispersity index (PDI, open symbols) with conversion (a), and normalized conversion vs. time (b) for methyl methacrylate ARGET ATRP at 70 and 90 °C. Experimental conditions are summarized in Table 3.5.

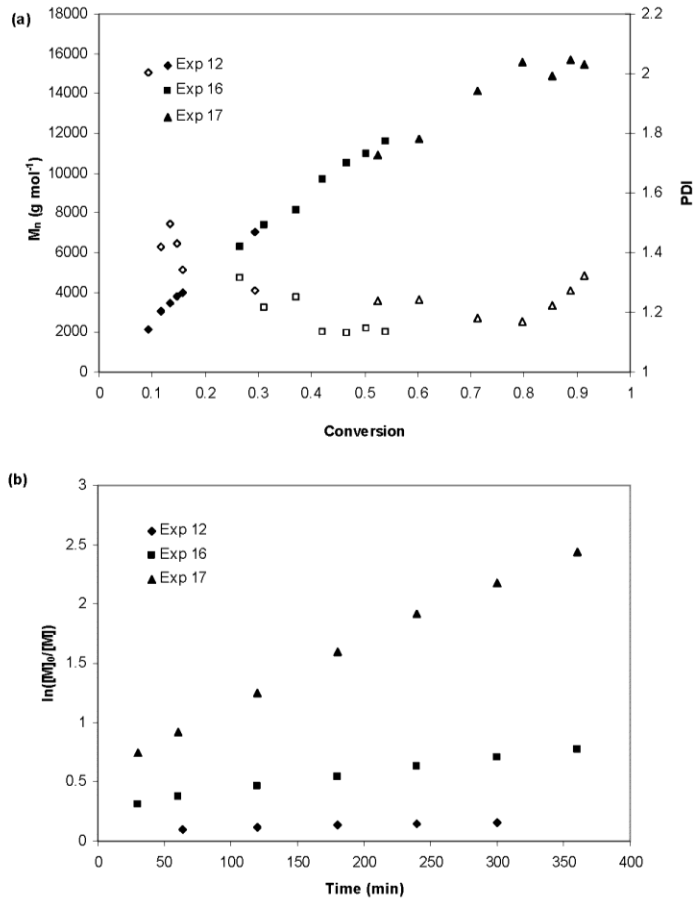

Figure 3.8: Evolution of number-average molecular weight (M_n, filled symbols) and polydispersity index (PDI, open symbols) with conversion (a), and normalized conversion vs. time (b) for butyl acrylate ARGET ATRP at 60, 90, and 110 °C. Experimental conditions are summarized in Table 3.5.

ARGET ATRP of methacrylate and acrylate was successful at high temperature with stoichiometric quantities of ligand, unlike what was found for styrene. This suggests that temperature is not the main factor for catalyst destabilization in styrene polymerizations. Rather, catalyst stability seems to be influenced by monomer choice. Curiously, methacrylates and acrylates are known to complex more strongly to catalyst than styrene, and thus might be expected to destabilize the catalyst to a greater extent. Instead, the opposite trend is observed: monomer complexation seems to help to stabilize the catalyst, allowing controlled polymerization of acrylates and methacrylates to proceed without excess ligand present.

3.4 Conclusions

ARGET ATRP of acrylates and methacrylates was successfully carried out with stoichiometric quantities of ligand, and in unpurified solvent and monomer at temperatures up to 110 °C. The number-average molecular weight increased linearly with conversion, and the polydispersity index decreased with conversion for all experiments. The use of a benzonitrile/toluene co-solvent system for butyl methacrylate polymerization gave fast kinetics and good control down to even 6.4 ppm of catalyst. For butyl acrylate, benzonitrile as the sole solvent gave faster kinetics. The ability to polymerize both representative monomers with small quantities of catalyst and ligand demonstrates the robustness of ARGET ATRP and its potential for industrial applications.

References

(1) Kato, M.; Kamigaito, M.; Sawamoto, M.; Higashimura, T. *Macromolecules* **1995**, *28*, 1721-1723.

(2) Wang, J. S.; Matyjaszewski, K. *Journal of the American Chemical Society* **1995**, *117*, 5614-5615.

(3) Matyjaszewski, K.; Xia, J. *Chemical Reviews* **2001**, *101*, 2921-2990.

(4) Braunecker, W.; Matyjaszewski, K. *Progress in Polymer Science* **2007**, *32*, 93-146.

(5) Tsarevsky, N. V.; Matyjaszewski, K. *Chemical Reviews* **2007**, *6*, 2270-2299.

(6) Tang, W.; Tsarevsky, N. V.; Matyjaszewski, K. *Journal of the American Chemical Society* **2006**, *128*, 1598-1604.

(7) Matyjaszewski, K.; Jakubowski, W.; Min, K.; Tang, W.; Huang, J.; Braunecker, W. A.; Tsarevsky, N. V. *Proceedings of the National Academy of Sciences of the United States of America* **2006**, *103*, 15309-15314.

(8) Jakubowski, W.; Min, K.; Matyjaszewski, K. *Macromolecules* **2006**, *39*, 39-45.

(9) Jakubowski, W.; Matyjaszewski, K. *Macromolecular Symposia* **2006**, *240*, 213-223.

(10) Jakubowski, W.; Matyjaszewski, K. *Angewandte Chemie* **2006**, *45*, 4482-6.

(11) Pietrasik, J.; Dong, H.; Matyjaszewski, K. *Macromolecules* **2006**, *39*, 6384-6390.

(12) Min, K.; Gao, H.; Matyjaszewski, K. *Macromolecules* **2007**, *40*, 1789-1791.

(13) Dong, H.; Tang, W.; Matyjaszewski, K. *Macromolecules* **2007**, *40*, 2974-2977.

(14) Mueller, L.; Jakubowski, W.; Tang, W.; Matyjaszewski, K. *Macromolecules* **2007**, *40*, 6464-6472.

(15) Matyjaszewski, K.; Dong, H.; Jakubowski, W.; Pietrasik, J.; Kusumo, A. *Langmuir* **2007**, *23*, 4528-4531.

(16) Jakubowski, W.; Kirci-Denizli, B.; Gil, R. R.; Matyjaszewski, K. *Macromolecular Chemistry and Physics* **2008**, *209*, 32-39.

(17) Britovsek, G. J. P.; England, J.; White, A. J. P. *Inorganic Chemistry* **2005**, *44*, 8125-8134.

(18) Eckenhoff, W. T.; Garrity, S. T.; Pintauer, T. *European Journal of Inorganic Chemistry* **2008**, *2008*, 563-571.

(19) Beuermann, S.; Buback, M.; Davis, T. P.; Gilbert, R. G.; Hutchinson, R. A.; Kajiwara, A. ; Klumperman, B.; Russell, G. T. *Macromolecular Chemistry and Physics* **2000**, *201*, 1355-1364.

(20) Penzel, E.; Goetz, N. *Angewandte Makromolekulare Chemie* **1990**, *178*, 191-200.

(21) Tsarevsky, N. V.; Braunecker, W. A.; Vacca, A.; Gans, P.; Matyjaszewski, K. *Macromolecular Symposia* **2007**, *248*, 60-70.

(22) Shipp, D. A.; Matyjaszewski, K. *Macromolecules* **2000**, *33*, 1553-1559.

(23) Snijder, A.; Klumperman, B.; van der Linde, R. *Macromolecules* **2002**, *35*, 4785-4790.

(24) Faucher, S.; Zhu, S. *Macromolecular Rapid Communications* **2004**, *25*, 991-994.

(25) Zhang, Z.; Zhu, X.; Zhu, J.; Cheng, Z.; Zhu, S. *Journal of Polymer Science Part A: Polymer Chemistry* **2006**, *44*, 3343-3354.

(26) Zhang, C. X.; Kaderli, S.; Costas, M.; Kim, E.; Neuhold, Y.; Karlin, K. D.; Zuberbuhler, A. D. *Inorganic Chemistry* **2003**, *42*, 1807-1824.

(27) Gnanou, Y.; Hizal, G. *Journal of Polymer Science Part A: Polymer Chemistry* **2004**, *42*, 351-359.

(28) Tang, W.; Matyjaszewski, K. *Macromolecules* **2007**, *40*, 1858-1863.

(29) Fu, Y.; Cunningham, M. F.; Hutchinson, R. A. *Macromolecular Symposia*, **2007**, *1*, 151-163.

Chapter 4

ARGET ATRP in a Continuous Tubular Reactor

Preface

The study conducted in Chapter 3 provided some insights into the intricacies of ARGET ATRP. By showing that polymerizations of methacrylates and acrylates could be conducted with only a stoichiometric ratio of ligand to copper, the investigation helped to resolve the major weakness of ARGET ATRP. In this chapter, the process of adapting ARGET ATRP of butyl methacrylate utilizing a stoichiometric ratio of ligand to copper, to a continuous tubular reactor is documented. The design of a new tubular reactor and the development of troubleshooting experiments to elucidate the differences between batch and continuous polymerizations are discussed. ARGET ATRP was shown to be very tolerant to impurities, and an 850 mL continuous tubular reactor was successfully used to synthesize well-controlled poly(butyl methacrylate). The results demonstrated the industrial potential of ARGET ATRP, as well as the use of continuous tubular reactors for large scale production of novel polymers. The work in this section has been published as a feature article in Macromolecular Reaction Engineering (2009, vol. 3, 222-231).

Abstract

Continuous ARGET ATRP of butyl methacrylate was carried out in an 850mL tubular reactor using parts per million levels of copper catalyst and stoichiometric amounts of ligand to copper under industrially relevant conditions without monomer and solvent purification. A copper(II) bromide/tris(2-pyridylmethyl)amine complex was used as catalyst, and tin(II) 2-ethylhexanoate was chosen as the reducing agent. It was found that stainless steel fittings and/or storage tanks had an adverse effect on polymerization rate, underlining the importance of the choice of chemically inert tubing. The problem of lower rate was solved by increasing the amount of reducing agent in the system fourfold, under which conditions the molecular weight development and polymerization rate in the tubular system compared well to that in a batch reactor. Thus, ARGET ATRP can be made significantly faster and more robust through the judicious use of an inexpensive and non-hazardous reducing agent. The tubular reactor produces polymer with a controlled molecular weight distribution continuously and reliably, demonstrating its potential for industrial adoption.

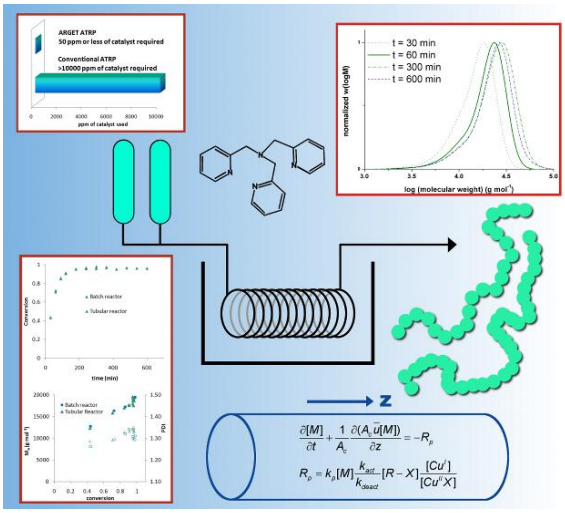

4.1 Introduction

Living radical polymerization techniques have been the object of significant academic and industrial interest over the last 15 years, due to their ability to produce polymers with controlled microstructure. Atom transfer radical polymerization (ATRP) in particular is able to polymerize a wide range of monomers under relatively mild conditions with good control.[1-4] However, industrial adoption of ATRP has been limited because a transition metal catalyst is conventionally used in high concentrations to mediate the polymerization. A high catalyst concentration was typically required due to irreversible radical-radical termination reactions which led to an accumulation of catalyst in its deactivating form, prematurely stopping the reaction. Recently, two method termed "activator regenerated by electron transfer" (ARGET),[5-7] and "initiators for continuous activator regeneration" (ICAR)[5] have been developed by Matyjaszewski *et al.* which allows for the catalyst concentration to be reduced to parts per million (ppm) levels. At such low catalyst levels, material and post-processing costs are considerably reduced, as catalyst separation and processing can be omitted or greatly simplified, making an ATRP process much more industrially attractive.

As illustrated in Scheme 4.1, the key to ATRP lies in a dynamic equilibrium between a small concentration of growing radicals ($R^{\bullet}$) and a majority of dormant species (R-X) which can be reversibly activated to form growing radicals. The majority of chains exist in a dormant (capped) state due to the persistent radical effect (PRE),[8] and as such the active radical concentration is lowered and termination is suppressed. In addition, the rate coefficient for deactivation is often of the same order of magnitude as that for bimolecular termination and, since catalyst concentration is much higher than radical concentration, deactivation becomes the dominant chain stopping event.

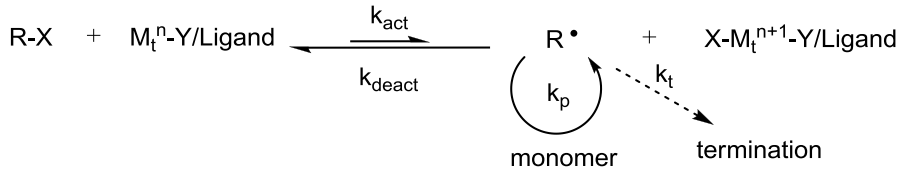

Scheme 4.1: General mechanism for ATRP.

In ARGET ATRP, as shown in Scheme 4.2, an excess amount of reducing agent is added to both initiate polymerization and to convert deactivator, which has accumulated due to radical termination, back into the activating species. A variety of reducing agents such as tin(II) 2-ethylhexanoate ($Sn(EH_2)$), glucose, ascorbic acid, hydrazine, phenols, and tertiary amines have been successfully used in ARGET ATRP.[5,9,10] Unfortunately, one of the reported drawbacks of ARGET is that ligand must be added in 3 to 10 times molar excess (with respect to metal) in order to achieve a controlled polymerization.[5] The excess ligand helps to maintain the catalyst complex and protect it from destabilizing side reactions.

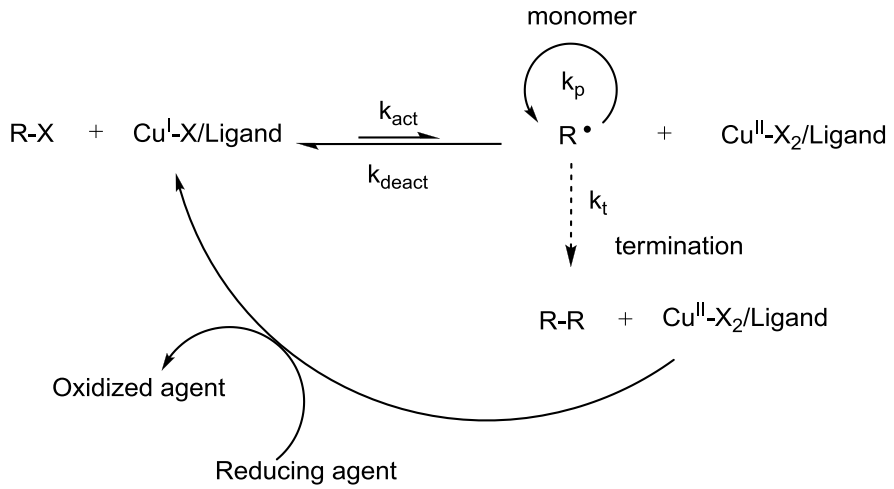

Scheme 4.2: Proposed mechanism for ARGET ATRP.

Alternatively, ICAR ATRP uses a small amount of thermal free radical initiator to reduce copper(II) deactivator into copper(I) activator. The use of a conventional free radical initiator reduces the number of competing side reactions so that ligand can be used in a stoichiometric

ratio to ligand.[5,11] At the same time, the presence of another radical source will generate new homopolymer in a block copolymerization, making ARGET ATRP the more desirable process for copolymerization.

ARGET is an elegant and clean polymerization technique, especially for the preparation of block copolymers, but the requirement for excess ligand can be a considerable hurdle for scale up as the ligands are expensive and not readily available. As such, the first step towards scale up of ARGET ATRP should be to reduce the amount of ligand required. We have recently demonstrated that ARGET ATRP of methacrylates and acrylates can be performed using only stoichiometric amounts of ligand to copper and under industrially relevant conditions where monomer and solvent purification are bypassed.[12]

This work investigates the adaptation of ARGET ATRP to a continuous process. Tubular reactors have a much higher surface area to volume ratio, permitting better control of the temperature profile and heat removal, which allows for simpler and more efficient scale up to larger reactor sizes. In addition, continuous operation allows for more consistent product quality, providing another economic advantage. As reviewed by Müller *et al.*, there are very few studies reporting living radical polymerization in continuous processes.[14] One of the reasons it is difficult to adapt ATRP to a continuous tubular process is catalyst heterogeneity, which can cause plugging. Recently Noda *et al.*[15] reported the synthesis of methyl methacrylate homo and block copolymers in a 10 mL continuous microreactor made from Teflon tubing with a 1.6 mm inner diameter. Presumably, the two ligands used in the study form homogeneous catalyst complexes, and as such reactor plugging was not observed. Polymerizations were conducted at 90 °C and showed good control (i.e., no observed broadening of polymer molecular weight distribution (MWD)). An additional feed point was added to synthesize block copolymers of methacrylates and acrylates. While the copolymerization of two methacrylates was successful, low conversion was observed when butyl acrylate was fed in as the second monomer. As the residence time after

the additional feed point is halved from its original value due to the additional flow rate of the second stream, there may not have been enough reaction time to polymerize the acrylate to high conversion. Another possible cause is that methacrylate capped chain ends are preferentially activated over acrylate capped chain ends. Since both monomers existed simultaneously in solution, methacrylates would have been preferentially consumed.

Müller *et al.* have also recently used ATRP to continuously polymerize butyl acrylate and styrene in a tubular reactor.[14] Unlike Noda, the approach was to demonstrate industrial feasibility by utilizing a large stainless steel reactor (volume of approximately 500 mL, 150 m of stainless steel tubing with an ID of 2.1 mm), and to modify catalyst solubility through monomer and solvent choice. The polymerization of butyl acrylate using acetonitrile as solvent at 80 °C was homogeneous and the tubular experiments showed good agreement with batch experiments. Polymerization of styrene at 110 °C in the tubular reactor was slightly faster than in batch. However, the reactor became plugged even when using a nitrile based solvent, possibly due to precipitation of Cu(II) catalyst complex.

In this work, we use a similar reactor system to produce well-controlled polymer from butyl methacrylate (BMA) using ARGET ATRP with low catalyst concentrations and a stoichiometric ratio of ligand to Cu. In addition to the significant environmental and economic benefits of using low catalyst concentrations, the likelihood of reactor plugging due to catalyst precipitation becomes nearly negligible.

4.2 Experimental

4.2.1 Materials

Butyl methacrylate (BMA) (99%, Aldrich), styrene (99%, Aldrich), copper(II) bromide ($CuBr_2$, 99% Aldrich), anisole (99%, Aldrich), benzonitrile (99%, Aldrich), toluene (99%, Acros), ethyl 2-bromoisobutyrate (EBiB) (98%, Aldrich), tin(II) 2-ethylhexanoate ($Sn(EH)_2$) (95%, Aldrich), and azobisisobutyronitrile (AIBN) (Vazo-64, Dupont) were used as received. Tris(2-pyridylmethyl)amine (TPMA) and $[Cu^{II}(TPMA)Br][Br]$ were synthesized as described previously.[12] A stock solution of $[Cu^{II}(TPMA)Br][Br]$ (0.0630 g) in benzonitrile (5 g) was made for batch polymerizations.

4.2.2 Tubular reactor setup

The reactor setup was adapted from the one used by Müller *et al.*[14] to investigate solution ATRP in a continuous reactor, and similar to the setup used by Enright *et al.* to study nitroxide mediated polymerization in miniemulsion.[16] The reactor consisted of two 1 L stainless steel high pressure storage cylinders, attached to PTFE tubing immersed in an oil bath. The setup was kept under nitrogen overpressure, which was used to push the solution forward. The flow was controlled by a Masterflex L/S peristaltic pump with a PTFE pump head, located at the reactor exit. The mass flow rate was measured by a Mettler Toledo PG 5002s balance also situated at the outlet. A schematic of the reactor is shown in Figure 4.1. The original setup used by Müller *et al.* for solution ATRP employed narrow stainless steel tubing (150 m in length, 3.2 mm outer diameter, 2.1 mm inner diameter, total reactor volume of approximately 520 mL), which was prone to plugging from precipitated catalyst. To proactively eliminate this problem, the stainless steel tubing was replaced with PTFE tubing with a wider inner diameter (48 m in length, 6.35 mm outer diameter, 4.75 mm inner diameter, reactor volume of approximately 850 mL). PTFE tubing

was chosen because it is chemically inert and is easier to clean, and cheaper to replace in the event that the reactor plugs.

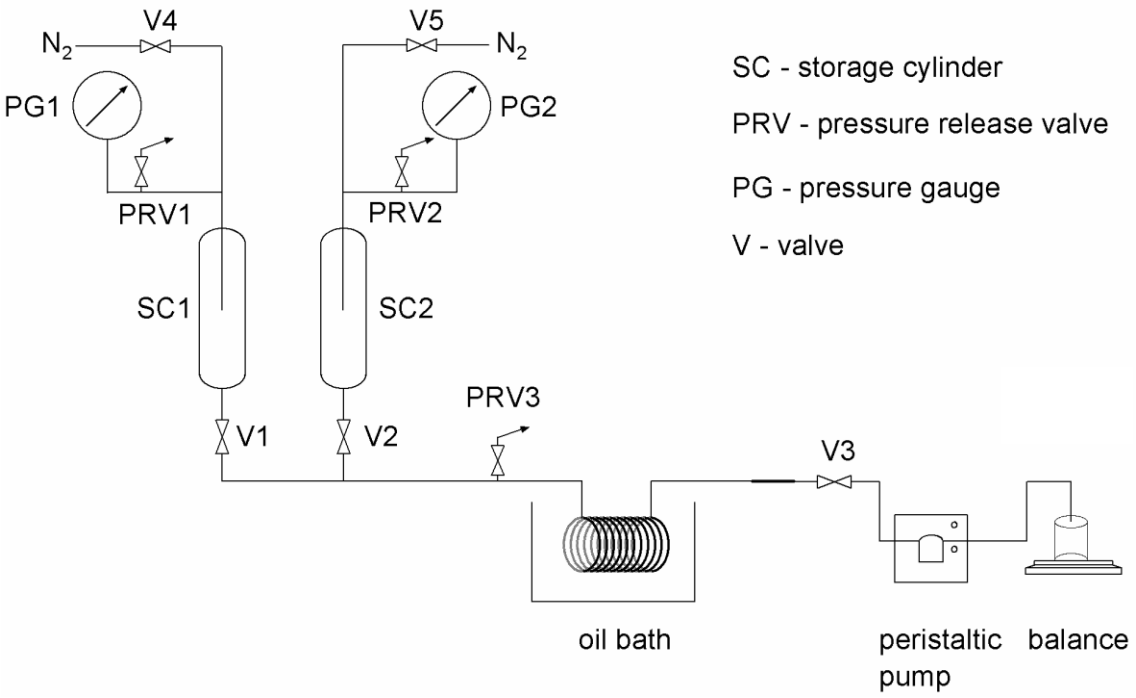

Figure 4.1: Schematic of continuous tubular reactor used for ARGET ATRP polymerizations.

4.2.3 Synthesis procedure for continuous and equivalent batch ARGET polymerization

$[Cu^{II}(TPMA)Br][Br]$ (0.235 g, 0.457 mmol) was combined with 18.57 g of benzonitrile in a small vial and stirred for approximately 30 minutes until the catalyst fully dissolved. The catalyst solution was then mixed with 500 g of anisole and 1300 g BMA (9.14 mol) in a 2 L Erlenmeyer flask and purged with nitrogen for one hour. EBiB (17.83 g, 0.091 mol) was dissolved in 19.25 g of anisole and added to the purging solution. $Sn(EH)_2$ (3.70 g, 9.14 mmol) dissolved in 19.25 g of anisole purged with nitrogen was added to the monomer solution.

Most of the mixture was then poured into the two storage tanks of the tubular reactor setup, and purged with nitrogen for another 30 minutes. After purging the solution, the first tank

was put under nitrogen pressure to quickly fill (typically less than 3 minutes) the tubular reactor with the reactive solution, before the outlet valve V3 was closed. As the tubing was immersed in an oil bath set to 90 °C, this is considered the start of the polymerization. The peristaltic pump head was then closed, V3 opened, and the pump flow rate set to 2.5 $g \cdot min^{-1}$ to give a total residence time of approximately 5 h in the reactor. Then some solvent (acetone) was added to the first tank and both storage cylinders were closed and nitrogen pressure adjusted to 2.5 bars. The second tank was used to push the first half of the reactive solution through the tube and the solvent placed in the first tank was used to push the second half of the reactive solution through the tube. Samples were taken at specified time intervals from the outlet of the reactor.

For the batch equivalent experiment, the remaining solution was transferred from the Erlenmeyer flask to a 100 mL 2 neck round bottom flask. The round bottom flask was purged with nitrogen for 30 minutes before being immersed in an oil bath set to 90 °C to initiate polymerization. Samples were withdrawn using a deoxygenated syringe at specified time intervals.

4.2.4 Batch ARGET ATRP polymerization procedure

Some experiments were run exclusively in batch. 0.50 g of benzonitrile/[Cu^{II}(TPMA)Br][Br] stock solution was diluted by 9.5 g of anisole and mixed with BMA (35 g, 0.246 mol) in a 100 mL two neck round bottom flask. The mixture was purged under nitrogen for one hour, before being heated to 90 °C. EBiB (0.341 g, 1.75 mmol) dissolved in 2.5 g of anisole was purged with nitrogen for ten minutes, and then added to the round bottom flask via a degassed syringe. After approximately 10 minutes, $Sn(EH)_2$ (0.10 g, 0.246 mmol) dissolved in 2.5 g of anisole purged with nitrogen was injected to initiate the polymerization. Samples were withdrawn using a deoxygenated syringe and placed into an ice bath to stop polymerization. The target molecular weight of the polymerization was 14219 $g \cdot mol^{-1}$ (DP_n = 100). Solvent content was 30% by mass, and concentration of $CuBr_2$ was 50 ppm on a molar basis with respect to monomer.

4.2.5 Styrene free radical polymerization (FRP) procedure

Styrene (560 g, 5.37 mol) was mixed with toluene (1307 g, 14.18 mol) in a 2 L Erlenmeyer flask and purged with nitrogen for one hour. AIBN (3.28 g, 0.02 mol) was added to the purged mixture. Most of the solution was transferred to the storage tanks of the tubular reactor setup where it had been purged with nitrogen for another 30 minutes. The storage tanks were then closed, and nitrogen pressure was adjusted to 2.5 bars. The tubular reactor was then quickly filled using one of the two storage cylinders, and the pump flow rate was set to 5 g/min to give a total residence time of approximately 2.5 hours in the reactor. Samples were taken at specified time intervals from the outlet of the reactor.

For the batch equivalent styrene FRP, the remaining monomer solution was transferred from the Erlenmeyer flask to a 100 mL 2 neck round bottom flask. The round bottom flask was purged with nitrogen for 30 minutes before being immersed in an oil bath set to 90 °C to initiate polymerization. Samples were withdrawn using a deoxygenated syringe at specified time intervals.

4.2.6 Analysis methods and characterization

Sample conversion was determined by gravimetry. Gel permeation chromatography (GPC) was used to determine the molecular weight distribution of the polymer samples. Samples were prepared by dissolving approximately 100 mg of dried polymer in 10 mL of distilled THF. The dissolved polymer samples then passed through a column packed with basic alumina to remove remaining copper, before filtering through a nylon filter (0.2 µm pore size). The GPC was equipped with a Waters 2960 separation module containing four Styragel columns of pore sizes 100, 500, 10^3, 10^4 Å, coupled with a Waters 410 differential refractive index (RI) detector (930 nm) operating at 40 °C. THF was used as eluant and the flow rate was set to 1.0 $mL \cdot min^{-1}$. The detector was calibrated with eight narrow polystyrene standards ranging from 347 to 355 000

$g \cdot mol^{-1}$. The molecular weights of poly(BMA) samples were obtained by universal calibration using the Empower software and known Mark-Houwink parameters for polystyrene ($K=11.4 \cdot 10^{-5}$ $dL \cdot g^{-1}$, a = 0.716) and poly(BMA) ($K = 14.8 \cdot 10^{-5}$ $dL \cdot g^{-1}$, a = 0.664).[17]

4.3 Results and Discussion

The final properties of PBMA produced by the ARGET ATRP tubular reactions and their batch equivalents are given in Table 4.1 Polymerizations were run at 90 °C. The concentration of catalyst was 50 molar ppm with respect to monomer in all cases, with a one to one ratio of copper to ligand. The target chain length is 100 repeat units, such that each catalyst molecule mediates 200 chains instead of a more usual 100 chains.[5,12] The molar ratio of $Sn(EH)_2$ reducing agent to initiator was initially set to 0.1, based upon previous work.[12] However, as described below, this ratio was ultimately increased by a factor of four in order to improve polymerization performance in the continuous tubular system. In all experiments, the use of $[Cu^{II}(TPMA)Br][Br]$ as catalyst produced nearly colourless polymer with living characteristics.

Table 4.1: Final properties of PBMA prepared by ARGET ATRP in batch (B) and tubular (T) reactors. All experiments were conducted at 90 °C with 30 wt % anisole solvent.

Exp.	$[M]_0$: $[EBiB]_0$: $[CuBr_2]_0$:$[TPMA]_0$: $[Sn(EH)_2]_0$	conv (%)[a]	$M_{n,theo}$[b] ($g \cdot mol^{-1}$)	$M_{n,GPC}$ ($g \cdot mol^{-1}$)	PDI
B1	100:1:0.005:0.005:0.1	87	12 900	17 700	1.27
B2	100:1:0.005:0.005:0.2	93	13 500	17 400	1.27
B3	100:1:0.005:0.005:0.4	97	13 900	19 500	1.31
T1	100:1:0.005:0.005:0.1	19	2 800	10 500	1.28
T2	100:1:0.005:0.005:0.2	51	7 300	14 600	1.29
T3	100:1:0.005:0.005:0.4	96	13 800	18 700	1.34

[a] conversion and molecular weight data taken at 360 min. [b] $M_{n,theo} = ([M]_0/[EBiB]_0)$ x conv. x MW_M.

4.3.1 Polymerizations with 10 mol percent reducing agent to initiator

From Table 4.1 it can be seen that two of the tubular experiments (T1 and T2) had limited final conversion compared to their batch equivalents. This puzzling behaviour is best shown by Figure 4.2, which compares the conversion profile between experiments B1 and T1. The tubular experiment T1 reaches approximately 20% conversion after 30 min, after which conversion does not increase any further. Figure 4.3 shows the evolution of molecular weights and polydispersity index (PDI) for these two experiments. Measured M_n for both batch and tubular experiments were higher than theoretical values, as is usually observed in ARGET ATRP of methacrylates.[12] Experiment B1 shows a linear increase in number-average molecular weight (M_n) with conversion, as expected in a living polymerization. M_n for T1, however, remains relatively constant at 10500 $g \cdot mol^{-1}$. This value is consistent with the limiting conversion achieved, and matches with the initial data point for B1 (also at ~20% conversion). Both experiments have low PDI values, indicating that the polymerizations are well controlled.

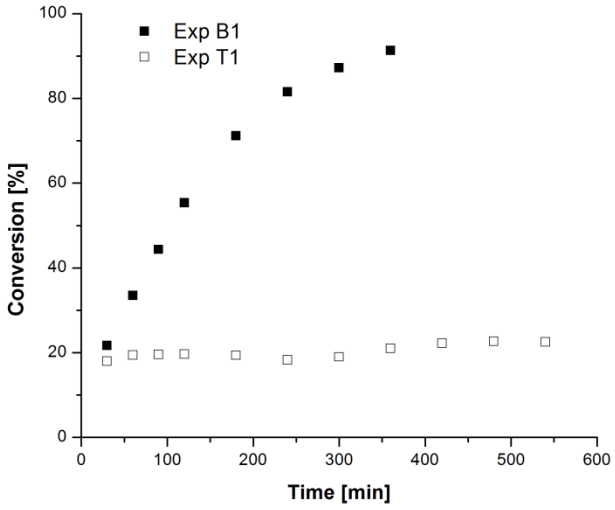

Figure 4.2: Conversion profiles of batch (B1) and tubular (T1) BMA polymerizations with 10 mol percent reducing agent relative to initiator. See Table 4.1 for experimental details.

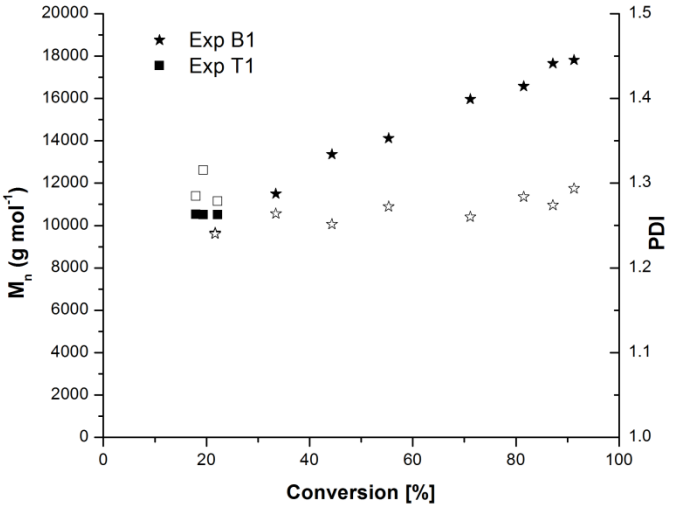

Figure 4.3: Evolution of number-average molecular weight (M_n, filled symbols) and polydispersity index (PDI, open symbols) with conversion for batch (B1) and tubular (T1) experiments with 10 mol percent reducing agent relative to initiator.

Figure 4.4 shows the GPC traces for some samples of experiments B1 and T1. The traces do not exhibit any unexpected characteristics such as a second higher molecular weight peak due to uncontrolled polymerization, or low molecular weight shoulder formed via bimolecular termination by disproportionation. In ATRP, the most common reason for limited conversion is a build-up of deactivator due to radical termination[3] which, at such low catalyst concentrations, will have a significant effect on the overall ATRP equilibrium. However, the distributions provide no indication that T1 was stopped by bimolecular radical termination. As the same starting solution is used in B1 and T1, the unexpected behaviour has to be from the use of the tubular reactor and some factor in the reactor configuration that has not been accounted for. Although this reactor configuration has been previously used for solution ATRP, the use of a high activity catalyst at low concentrations may make the system more sensitive to external impurities.

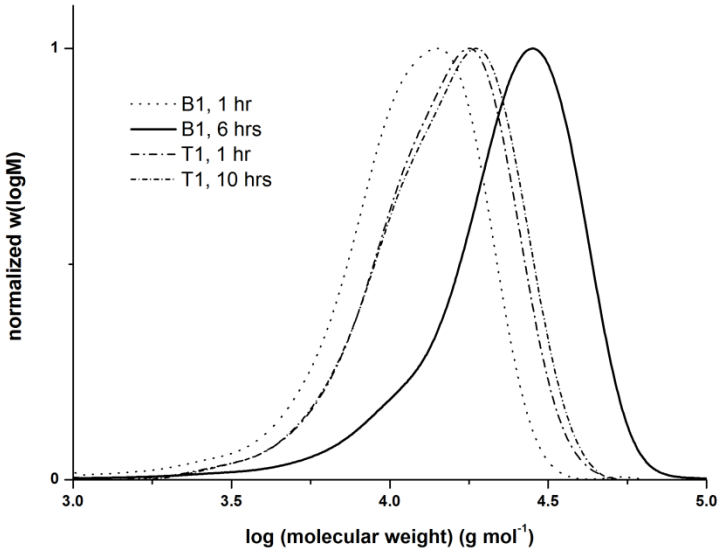

Figure 4.4: Gel permeation chromatography traces for PBMA produced in experiments B1 and T1.

4.3.2 Study of external variables

Several factors were examined which might have led to the limiting conversion in experiment T1.

The tests were conducted using the same recipes as for B1 and T1, as summarized in Table 4.2.

Table 4.2: Summary of external factors examined to diagnose low conversion obtained for ARGET ATRP in the tubular reactor.

Exp.	Factor examined	Method of diagnosis
X1	Chemical leaching from Teflon tubing	Batch polymerization with tubing
X2	Silicone oil leaching in through joints	Batch polymerization with silicone oil
X3, X4	Tubular reactor not operating in plug flow	FRP polymerization of styrene in tubular (X4) and batch reactor (X3)
X5	Reaction between catalyst and storage cylinder	Batch polymerization of solution that has been kept in the cylinder
X6, X7	Loss of catalyst inside the tubular reactor	Batch polymerization of outlet polymer by reheating (X6), and with additional reducing agent (X7)
X8, X9	Reaction between catalyst, metal fittings, and residual metal from past experiments	Batch polymerization with used (X8) and new (X9) stainless steel fitting

Plasticizers contained in the PTFE tubing could leach out upon prolonged exposure to the polymerization solution at relatively high temperature (90 °C). While PTFE tubing is known to be chemically inert, a sizeable amount of surface area is in direct contact with a hot organic solution for an extended period of time. Given the low catalyst concentration being used, only a small quantity of impurities per area could have a considerable effect. To explore this hypothesis, a batch polymerization was run with approximately 5 cm of tubing cut up into small pieces (experiment X1). A less likely impurity could be the presence of silicone oil in the tubular reactor. This was not expected to be the cause as the reactor was under pressure, and as such leakage at the joints should flow outwards from the reactor, and not in the opposite direction. Nevertheless, silicone oil could have entered through the connections between the different tubular sections when the reactor was unused and so not under pressure. Thus, approximately 3 g of silicone oil was added to a batch ARGET polymerization (experiment X2). For both experiments, the conversion and MW profiles were very similar to that found for B1, and thus it is concluded that neither the Teflon tubing nor silicone oil are the cause of the limiting conversion obtained in the tubular reactor.

FRP of styrene was attempted to confirm that the tubular reactor setup was not the cause of the conversion plateau. The conversion profiles for batch (experiment X3) and tubular (experiment X4) styrene FRP experiments exhibit excellent correlation. As such, it was concluded that the configuration of the tubular reactor is not the cause of inhibition.

Another cause of inhibition could be a redox reaction between the catalyst or reducing agent and the stainless steel walls in the storage cylinders. To investigate this possibility, some of the monomer solution used in experiment T1 was withdrawn from SC1 after a few hours of storage via valve PRV3 (see Figure 4.1). The extracted solution was transferred to a 2 neck round bottom flask, purged under nitrogen for 30 minutes, and then submerged in an oil bath heated to 90 °C (experiment X5). X5 polymerized slightly more slowly than B1 (80% conversion after 6 h

compared with 87%). Although molecular weight increased linearly with conversion, the slope of the curve was slightly higher, corresponding to a lower initiator efficiency (64% vs. 72% for B1). This result, combined with a slower polymerization rate, suggests that the effective catalyst concentration may have been lower than expected and supports the theory of a redox reaction within the storage cylinder. However, the 80% conversion is still much higher than the 19% obtained in experiment T1, indicating that the solution entering the heated tube should be active and polymerizable.

Further experiments were performed to explore the possibility of loss of catalyst through deactivation/poisoning within the reactor system, either within the stainless steel connections or on the stainless steel storage vessel walls. To verify this hypothesis, a part of the exit polymer solution collected at the outlet of the tube was purged and reheated in a round bottom flask (experiment X6), while extra reducing agent was also added to another part of the same solution (experiment X7). The conversion profile for T1, X6 and X7 are shown in Figure 4.5.

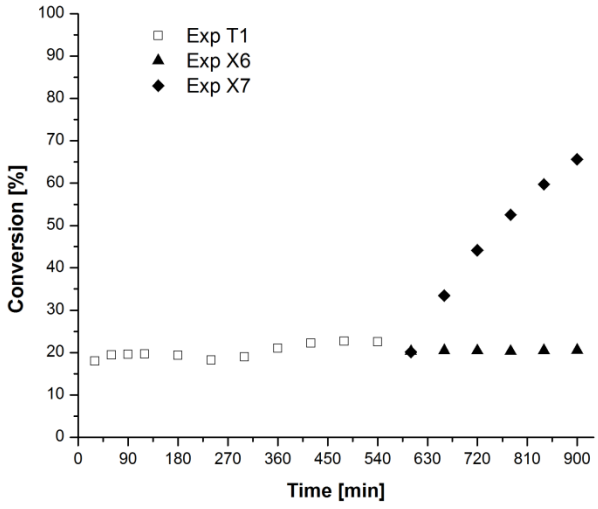

Figure 4.5: Conversion profiles for experiments T1, X6, and X7.

It is clear that simply reheating the outlet polymer is insufficient to reinitiate polymerization. However, if another 10 mol percent of reducing agent is added to the outlet polymer solution, bringing the total reducing agent concentration to 20 mol percent relative to initiator (experiment X7), the outlet conversion can be increased to about 70% in an additional 6 hours.

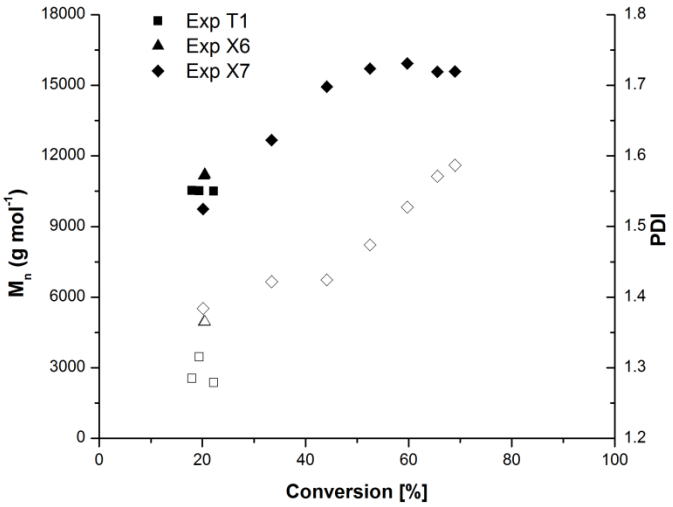

Figure 4.6: Evolution of number-average molecular weight (M_n, filled symbols) and polydispersity index (PDI, open symbols) with conversion for experiments T1, X6, and X7.

Figure 4.6 shows the evolution of molecular weight and PDI with conversion for T1, X6, and X7. Molecular weight increases linearly for the first 4 samples in X7, and then levels off. Similarly, the PDI for X7 increases from 1.36 to 1.6 by the end of the polymerization, resulting from a population of dead low molecular chains. The results show that catalyst was not lost or trapped in the reactor, but rather conversion was limited due to a build-up of deactivator. In the batch ARGET experiment, B1, there was sufficient reducing agent to regenerate activator, but in T1 the reducing agent appears to have been partially consumed prior to the polymerization, ultimately limiting the outlet conversion. These conclusions suggest that higher conversions could be reached in the presence of higher levels of reducing agent. Therefore, the next step was to

increase the initial reducing agent concentration in the recipe from 10 to 20 mol percent with respect to the concentration of initiator.

4.3.3 Polymerization with 20 mol percent reducing agent to initiator

The results for experiment B2 and T2 are summarized in Table 4.1. Figure 4.7 shows the conversion profiles for B2 and T2. Polymerization is faster than previously observed for B1 and T1, reaching 50% conversion in less than 90 minutes. However, conversion in the tubular reactor levels off after 90 minutes (similar to what happened in experiment T1 after 30 minutes). The batch reaction B2 shows a continuous increase in conversion with time, reaching a slightly higher final conversion than B1. The presence of excess reducing agent gave a slight enhancement to polymerization rate, most likely by altering the copper(I)/copper(II) ratio. Figure 4.8 shows the evolution of molecular weight and polydispersity with conversion for B2 and T2. Both reactions were living with a linear increase in molecular weight with conversion and a PDI under 1.3 for most samples.

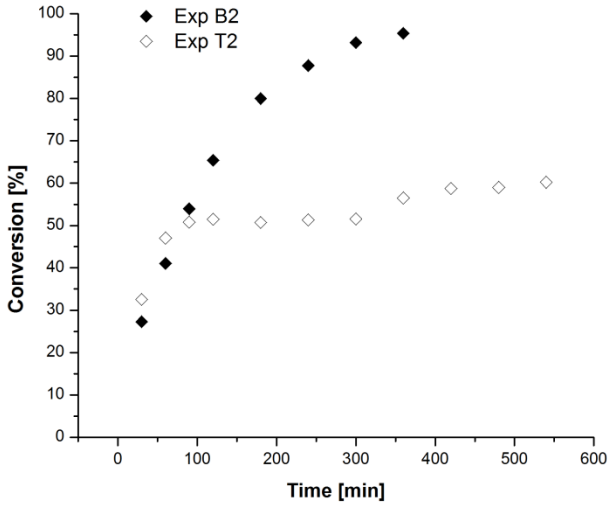

Figure 4.7: Conversion profiles of batch (B2) and tubular (T2) BMA polymerizations with 20 mol percent reducing agent relative to initiator. See Table 4.1 for experimental details.

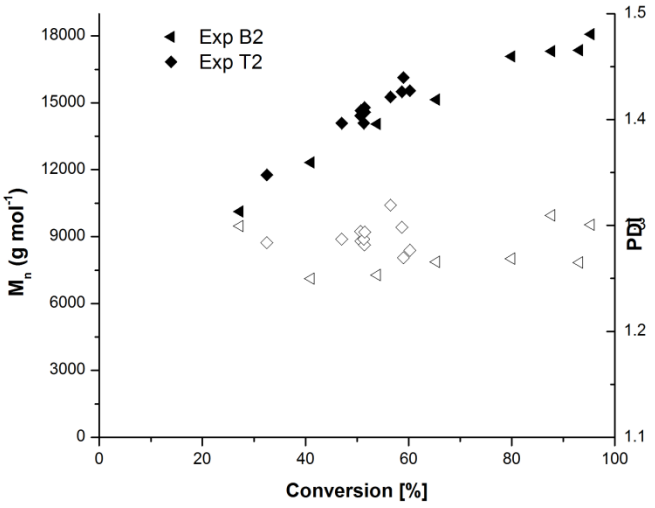

Figure 4.8: Evolution of number-average molecular weight (M_n, filled symbols) and polydispersity index (PDI, open symbols) with conversion for batch (B2) and tubular (T2) experiments with 20 mol percent reducing agent relative to initiator.

Before further increasing the reducing agent concentration, additional batch experiments were conducted at 20 mol percent reducing agent. So far, the evidence collected points towards consumption of reducing agent within the tubular reactor system as the cause of the limiting conversion, partially caused by a redox reaction between catalyst/reducing agent and the stainless steel vessels and fittings. As the storage vessels and many of the fittings had previously been used by Müller *et al.* for solution ATRP,[14] it is possible that there is some residual metal accumulated from previous experiments due to fouling. As such, two batch polymerizations containing a stainless steel fitting were conducted. One of the fittings was taken from the tubular reactor (experiment X8), while the other had never been used before (experiment X9). In addition to testing for residual metal from previous experiments, X8 and X9 should give more evidence towards a redox reaction between catalyst/reducing agent and a stainless steel surface.

Figure 4.9 shows the conversion profiles for X8 and X9 against B2. Both experiments showed lower final conversion and lower polymerization rate than B2, confirming that ARGET

ATRP is sensitive to metal contamination during polymerization. The conversion profiles of X8 and X9 are almost identical, suggesting that there is no residual metal accumulated from fouling from previous experiments.

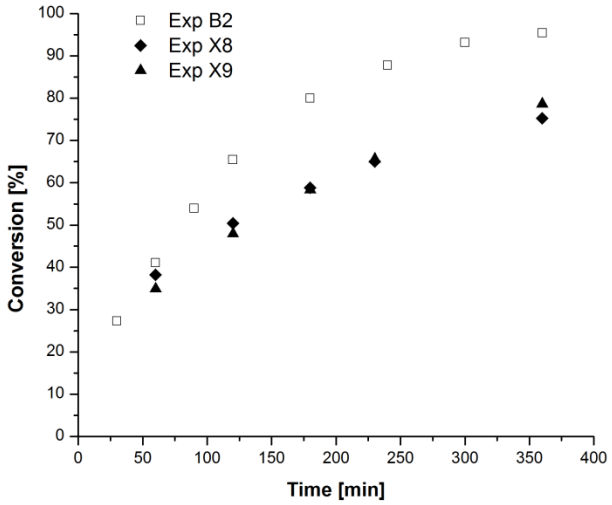

Figure 4.9: Conversion profiles for batch polymerization B2 and troubleshooting experiments X8 and X9.

Figure 4.10 shows a linear increase of molecular weight with conversion for both X8 and X9. There is also an upward drift in PDI in experiment X8 and X9 that was not observed in experiment B2 or T2. However, in the tubular experiments, the reaction medium is not continuously exposed to metal at high temperature like in experiment X8 or X9. It is possible that continued exposure at high temperature helped to enhance a redox reaction between catalyst or reducing agent and metal, or caused destabilization of catalyst. Both of these factors would account for the observed upward drift in PDI.

These results showed that contamination of the reaction mixture by exposure to metal surfaces may significantly affect the reaction kinetics. It should be noted that the grade of stainless steel used may influence sensitivity to the reaction media. The fittings used were in experiments X8 and X9 were Society of Automotive Engineer (SAE) grade 316 stainless steel,

which contains chromium, nickel and manganese. In the subsequent chapters, reactions are carried out in stainless reactor reactors made from SAE grade 316Ti stainless steel without any noticeable issues. Thus, it would appear that the presence of oxygen in the system due to permeability of the PTFE tubing towards oxygen is a more likely cause for inhibition of the polymerization. With the objective of increasing the final conversion reached in the continuous process, another series of experiments was run in the presence of 40 mol percent of reducing agent relative to initiator.

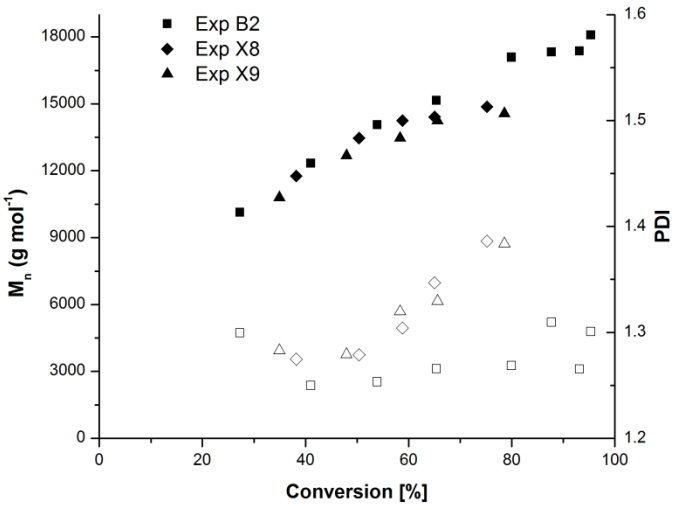

Figure 4.10: Evolution of number-average molecular weight (M_n, filled symbols) and polydispersity index (PDI, open symbols) with conversion for experiments B2, X8, and X9.

4.3.4 Polymerization with 40 mol percent reducing agent to initiator

The final polymer properties of both batch (B3) and tubular (T3) experiments at 40 mol percent reducing agent relative to initiator are summarized in Table 4.1. Doubling the reducing agent concentration gave excellent agreement between the conversion profiles of batch and tubular experiment, as shown in Figure 4.11. Both reactions were fast, reaching approximately 90% conversion in under 3 hours.

The evolution of molecular weight and polydispersity with conversion are shown in Figure 4.12, with both experiments exhibiting a linear increase in molecular weight with conversion. Control for both experiments was good with a final PDI of approximately 1.3. There is some overlap in molecular weight data towards the end, but this was expected as there were numerous data points taken at similar conversions. From the excellent agreement between batch and tubular conversion and molecular weight data, it can be concluded that the adaptation of ARGET ATRP to a continuous tubular for the homopolymerization of BMA was successful.

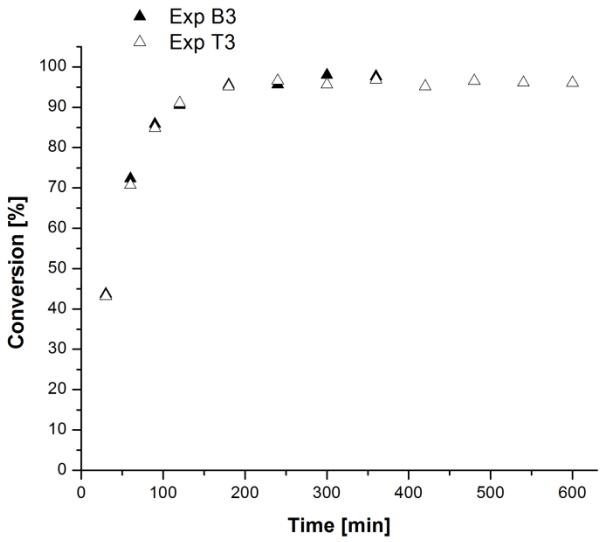

Figure 4.11: Conversion profiles of batch (B3) and tubular (T3) BMA polymerizations with 40 mol percent reducing agent relative to initiator. See Table 4.1 for experimental details.

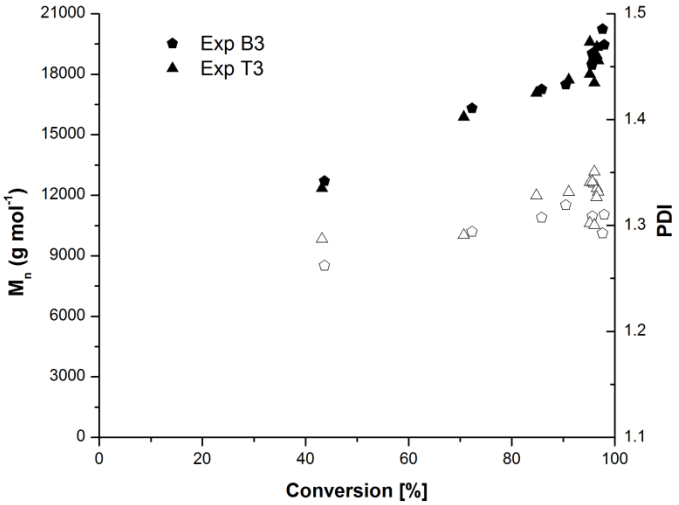

Figure 4.12: Evolution of number-average molecular weight (M_n, filled symbols) and polydispersity index (PDI, open symbols) with conversion for batch (B3) and tubular (T3) experiments with 40 mol percent reducing agent relative to initiator.

The effect of reducing agent on polymerization rate is especially striking when the conversion profiles for batch experiments at 10, 20, and 40 mol percent reducing agent are overlapped, as shown in Figure 4.13. Polymerization rates of B3 are approximately double that of B1 and B2 for the first hour, and the experiment reaches 90% total conversion in less than half the reaction time. The presence of a large excess of reducing agent likely keeps deactivator concentration low (as deactivator would be converted to activator more rapidly), increasing reaction rate. In addition, increasing the amount of reducing agent made the process more robust. The effects of potential redox reactions that could have consumed reducing agent or oxidized catalyst were minimized as the large excess of reducing agent was able to continuously regenerate catalyst. This observation is in agreement with results recently reported in the literature, where the authors use excess reducing agent to polymerize in the presence of air.[10,18,19] Overall, ARGET ATRP was found to be very robust and suitable for scale up.

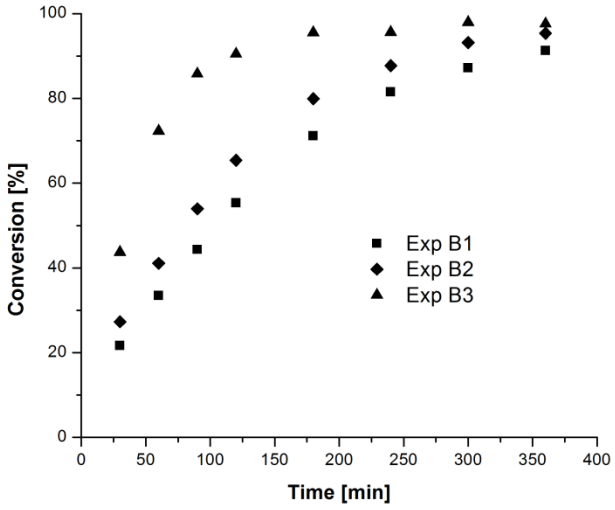

Figure 4.13: Conversion profiles for batch experiments at 10 mol percent (B1), 20 mol percent (B2), and 40 mol percent (B3) reducing agent relative to initiator. See Table 4.1 for experimental details.

4.4 Conclusions

The goal of this study was to investigate the adaptation of ATRP to a continuous process. ARGET ATRP was chosen as the concentration of catalyst required can be reduced to parts per million (ppm) levels. Also, to proactively eliminate plugging issues due to possible catalyst heterogeneity the narrow stainless steel tubing used in a previous study[14] was replaced with PTFE tubing with a wider inner diameter (4.75 mm inner diameter).

First, it was found that the use of stainless steel fittings and storage tanks in the tubular reactor setup had an adverse effect on polymerization rate. At both 10 and 20 mol percent reducing agent relative to initiator, outlet conversion in the tubular reactor was lower than in the equivalent batch polymerization. This result was attributed to the consumption of reducing agent, possibly due to a redox reaction with metal surfaces, as well as due to the unavoidable presence of trace amounts of oxygen. At 40 mol percent reducing agent to initiator, there was good

agreement between batch and continuous polymerizations. Polymerizations were well controlled in all cases, with similar number average molecular weights and polydispersities between batch and continuous experiments.

It was also found that increasing the amount of reducing agent in the system significantly increased reaction rate by changing the copper(I):copper(II) ratio without a corresponding loss of livingness. The results show that ARGET ATRP can be made significantly faster through the judicious use of reducing agent, demonstrating its potential for industrial adoption.

Finally ARGET ATRP of butyl methacrylate was successfully conducted, in a 850 mL continuous tubular reactor, under industrially relevant conditions where monomer and solvent purification were bypassed and using only ppm amounts of catalyst and stoichiometric amounts of ligand to copper. Further studies are planned to modify and apply the reactor system to the production of copolymers.

References

(1) Kato, M.; Kamigaito, M.; Sawamoto, M.; Higashimura, T. *Macromolecules* **1995**, *28*, 1721-1723.

(2) Wang, J. S.; Matyjaszewski, K. *Journal of the American Chemical Society* **1995**, *117*, 5614-5615.

(3) Matyjaszewski, K.; Xia, J. *Chemical Reviews* **2001**, *101*, 2921-2990.

(4) Braunecker, W.; Matyjaszewski, K. *Progress in Polymer Science* **2007**, *32*, 93-146.

(5) Matyjaszewski, K.; Jakubowski, W.; Min, K.; Tang, W.; Huang, J.; Braunecker, W. A.; Tsarevsky, N. V. *Proceedings of the National Academy of Sciences of the United States of America* **2006**, *103*, 15309-15314.

(6) Jakubowski, W.; Min, K.; Matyjaszewski, K. *Macromolecules* **2006**, *39*, 39-45.

(7) Jakubowski, W.; Matyjaszewski, K. *Angewandte Chemie* **2006**, *45*, 4482-6.

(8) Fischer, H. *Chemical Reviews* **2001,** *101*, 3581-3610.

(9) Pintaeur, T.; Matyjaszewski, K. *Chemical Society Reviews* **2008**, *37*, 1087-1097.

(10) Tang, H.; Shen, Y.; Li, B. G.; Radosz, M. *Macromolecular Rapid Communications* **2008**, *29*, 1834-1838.

(11) Mueller, L.; Jakubowski, W.; Tang, W.; Matyjaszewski, K. *Macromolecules* **2007**, *40*, 6464-6472.

(12) Chan, N.; Cunningham, M. F.; Hutchinson, R. A. *Macromolecular Chemistry and Physics* **2008**, *209*, 1797-1805.

(13) Jakubowski, W.; Matyjaszewski, K. *Macromolecular Symposia* **2006**, *240*, 213-223.

(14) Müller, M.; Cunningham, M. F.; Hutchinson, R. A. *Macromolecular Reaction Engineering* **2008**, *2*, 31-36.

(15) Noda, T.; Grice, a; Levere, M.; Haddleton, D. *European Polymer Journal* **2007**, *43*, 2321-2330.

(16) T. E. Enright, M. F. Cunningham, and B. Keoshkerian, *Macromolecular Rapid Communications*, **2005**, *26*, 221-225.

(17) Beuermann, S.; Buback, M.; Davis, T. P.; Gilbert, R. G.; Hutchinson, R. A.; Kajiwara, A. ; Klumperman, B.; Russell, G. T. *Macromolecular Chemistry and Physics* **2000**, *201*, 1355-1364.

(18) Matyjaszewski, K.; Dong, H.; Jakubowski, W.; Pietrasik, J.; Kusumo, A. *Langmuir* **2007**, *23*, 4528-4531.

(19) Min, K.; Jakubowski, W.; Matyjaszewski, K. *Macromolecular Rapid Communications* **2006**, *27*, 594-598.

Chapter 5

ARGET ATRP in a Continuous Stirred Tank Reactor

Preface

With a successful demonstration of ARGET ATRP in a continuous tubular reactor, the next phase of the investigation was to examine the adaptation of ARGET chemistry to continuous stirred tank reactors (CSTR). CSTRs are robust processes and are commonly used in industry for synthesis of commodity polymers. The ability to retrofit ARGET ATRP to existing CSTR infrastructure makes it an economical choice for large scale production of value added polymers. The study was conducted in cooperation with the Eindhoven University of Technology, where I initially spent 6 months as a visiting scientist under the supervision of Prof. Jan Meuldijk. While in Eindhoven, a 100 mL glass CSTR was designed and constructed, and polymerizations of butyl acrylate (BA) and methyl methacrylate (MMA) were attempted at varying reaction conditions. These preliminary results were published as part of a feature article in Macromolecular Reaction Engineering (2010, vol. 4, 369-390) providing an overview of ATRP in continuous processes. The investigation was completed upon my return to Queen's University, utilizing a different CSTR apparatus tailored from a Chemspeed semi-automated reaction platform. The results will be submitted to Industrial & Engineering Chemistry Research in the near future. In the previous chapter, it was thought that polymerization rate in ARGET ATRP was inhibited by the presence of oxygen in the system, and possibly by exposure to stainless steel surfaces. However, the CSTR experiments in this chapter were conducted in a stainless steel tank with no observed adverse effects. It is possible that the grade of stainless steel used can affect the polymerization kinetics due to differences in composition, but the more likely cause of inhibition is the presence of oxygen as briefly explained in Chapter 4.

Abstract

ARGET ATRP of butyl acrylate (BA) and methyl acrylate (MMA) was successfully adapted from a batch process to a continuous stirred tank reactor (CSTR). DMF was first used as a co-solvent in BA and MMA batch polymerizations to enhance the rate of polymerization and to minimize unsteady state behaviour caused by precipitation of copper(II) complexes. BA batch polymerizations in DMF resulted in a doubling of the apparent rate of polymerization (k_{app}) compared to when anisole was used as solvent. The effects of a DMF/anisole solvent mixture in MMA polymerizations were more complex and a product of solvent effects on the ATRP equilibrium as well as initiator efficiency. A high DMF concentration resulted in considerable termination which lowered initiator efficiency as well as polymerization rate. The optimal batch formulations were attempted in a single CSTR at residence times of 60, 90, and 120 minutes. All polymerizations exhibited steady state behaviour in conversion and M_n after four residence times. Surprisingly, k_{app} in CSTR experiments were higher than batch polymerizations, with a 54% increase in polymerization rate for BA experiments and a 30% increase for MMA experiments. This increased rate was most likely due to a higher steady state reducing agent concentration in the CSTR, which shifted the copper(I)/copper(II) ratio in favour of the activating species. Chain extensions were conducted using both BA and MMA, and showed good living characteristics. The results demonstrated CSTRs as a viable platform for industrial scale synthesis of well-defined acrylic and methacrylic polymers.

5.1 Introduction

Controlled radical polymerization (CRP) combines advantages from living polymerization techniques such as anionic or cationic polymerization, with the robust reaction conditions employed in free radical polymerization (FRP). The combination of control over polymer microstructure and tolerance to impurities such as air, water, and trace amounts of chemicals gives CRP techniques large commercial potential for the synthesis of novel polymers with unique properties. Of the CRP techniques available, atom transfer radical polymerization (ATRP) is one of the more dynamic processes due to its ability to tailor polymer architecture for a range of vinyl monomers under mild reaction conditions.[1-4]

The fundamental principle of CRP is minimization of bimolecular termination through suppression of the active radical concentration. In ATRP, this is accomplished through a dynamic equilibrium between dormant and growing radicals, which are reversibly activated and deactivated through halogen exchange mediated by a transition metal complex. Conventional ATRP typically utilizes copper salts bound to nitrogen based ligands in near stoichiometric quantities relative to the initiating alkyl halide. As a consequence, the resulting polymer contains a high concentration of residual copper on the order of 10^4 parts per million (ppm). Such a high concentration of residual metal not only adds undesired colour to the polymer, but as the metal complex is often toxic and expensive, post polymerization treatments are required in order to separate, and if possible recycle the metal complex from the product.[5-7] This complication in process design imposes additional production costs, and has so far hindered the application of ATRP on an industrial scale.[8]

Two variants of ATRP, "activator regenerated by electron transfer" (ARGET),[9] and "initiators for continuous activator regeneration" (ICAR)[10] which allow for a ~2-3 orders of magnitude reduction in the amount of mediator required down to $<10^2$ ppm levels have been recently developed by Matyjaszewski *et al.* In the two systems, a reducing agent or free radical

initiator is added to the polymerization in excess of the copper complex as a means of continuous regeneration of activators from deactivators which have accumulated due to termination. Although both techniques enable low copper concentration ATRP, the use of a small amount of thermal free radical initiator in ICAR makes it less suitable towards the synthesis of block copolymers and polymers with more advanced structures.[11]

The mechanism for ARGET ATRP is shown in Scheme 4.2. The copper complex is added in its oxidatively stable copper(II) state to simplify handling and storage. An excess of reducing agent is then added to initiate polymerization, as well as to regenerate activator through reduction of accumulated deactivating species. A variety of reducing agents such as tin(II) 2-ethylhexanoate ($Sn(EH_2)$),[9,12] ascorbic acid,[13] hydrazine,[10] sugars,[14] and tertiary amines[10,15,16] have been successfully applied to ARGET ATRP. An interesting consequence of the ARGET mechanism is that the choice of reducing agent can influence the rate of polymerization by altering the activator to deactivator ratio. An excess of a strong reducing agent like ascorbic acid can lead to a loss of control if inappropriate reaction conditions are chosen.[13,17,18] Conversely, an excess of a weaker reducing agent like $Sn(EH)_2$ can tilt the ratio in favour of the activator and enhance the rate of polymerization.[19,20]

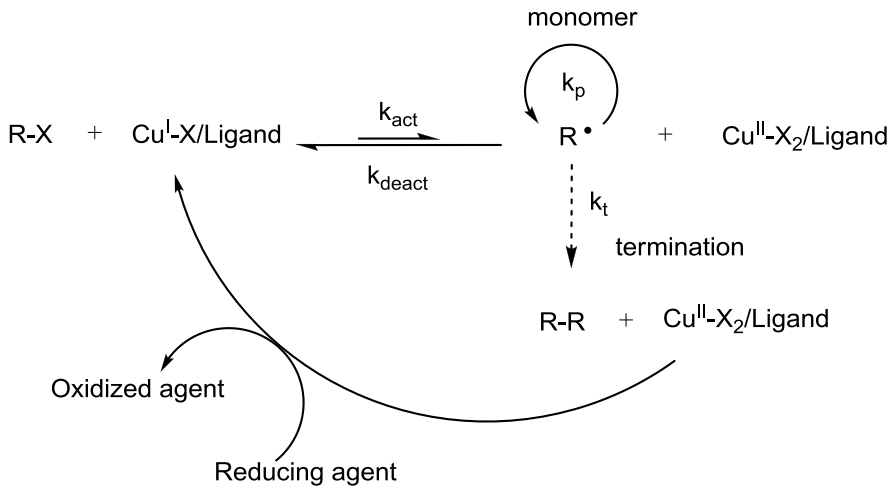

Scheme 5.1: Proposed mechanism for ARGET ATRP.

The advent of ARGET chemistry is an important step towards commercial applications of ATRP. To fully realize the potential of ARGET, it must be studied not only in lab scale batch reactions but also in processes which are more commonly employed in industry. Continuous processes such as tubular reactors and continuous stirred tank reactors (CSTR) yield more consistent product quality once at steady state, and possess higher space time yields compared to batch reactors. CSTRs are commonly used in industry for FRP due to their simple and robust designs. Compared to tubular reactors, they are less prone to fouling and often exhibit better mixing, lending CSTRs an advantage for the production of copolymers.

Despite the advantages that CSTRs can offer, there are very few studies utilizing CSTRs for copper mediated CRP. Zhang and Ray have modeled conventional ATRP of styrene and butyl acrylate (BA) in a series of CSTRs,[21] but no experimental studies of ATRP have been conducted. This is partly due to poor copper solubility in organic solvents that are used in ATRP. In addition, polymerization rates in ATRP and other CRP methods are typically much lower than FRP, thus requiring very long residence times to reach a practical yield. Another contributing factor is the long lifetime of polymer chains in CRP, which combined with the residence time distribution in a CSTR can significantly broaden the molecular weight distribution (MWD) of the resulting polymer.[22] As one of the defining characteristics of a well-controlled CRP is a narrow MWD, a CSTR process for polymer synthesis via CRP appears to be a poor fit. However, a low polydispersity index is only a superficial measure of livingness, and a broad MWD caused by residence time effects can still possess a high degree of chain end functionality.

We have recently demonstrated the use of copper(0) mediated CRP in a CSTR.[23] The use of heterogeneous copper(0) in the reactor as a catalyst source resulted in fast polymerizations at 30 ˚C, with a low concentration of residual copper in the final polymer. Although broad MWDs were obtained, the polymer produced was shown to have strong living characteristics, and the use of DMSO at low copper concentrations mitigated copper solubility issues. In this work, we

present a follow-up to preliminary attempts in adapting ARGET ATRP to a CSTR,[24] by extending the investigation to the production of BA and methyl methacrylate (MMA) homopolymers in different solvent combinations. The results build upon previous ARGET ATRP studies in batch[25] and tubular reactor[20] where well-defined acrylic and methacrylic polymers produced using only stoichiometric amounts of ligand to copper with unpurified monomer and solvent. The results serve as a useful comparison of continuous and batch processes, and demonstrate the potential benefits of utilizing a CSTR in combination with low copper ATRP for the synthesis of novel polymeric materials.

5.2 Experimental

5.2.1 Materials

Butyl acrylate (BA) (99%, Aldrich), methyl methacrylate (MMA) (99%, Aldrich), anisole (99%, Aldrich), benzonitrile (99%, Aldrich), dimethylformamide (DMF) (99.8%, Aldrich), copper(II) bromide ($CuBr_2$) (99%, Aldrich), ethyl 2-bromoisobutyrate (EBiB) (98%, Aldrich), tin(II) 2-ethylhexanoate ($Sn(EH)_2$) (95%, Aldrich) were used as received. Tris(2-pyridylmethyl)amine (TPMA) was synthesized according to literature procedures.[26] To simplify handling, the ligand TPMA and $CuBr_2$ were premixed to form the complex $[Cu^{II}(TPMA)Br][Br]$ as described previously.[27]

5.2.2 Batch ARGET ATRP polymerization procedure for BA

Batch polymerizations of BA were conducted to determine the apparent rate of polymerization for comparison to continuous experiments. $[Cu^{II}(TPMA)Br][Br]$ (6.0 mg, 0.012 mmol) was added to a 20 mL glass scintillation vial. DMF (18.34 g, 0.246 mol) was added to the vial, which was gently shaken until the copper complex was fully dissolved. The contents were pipetted into a 100 mL two neck round bottom flask, and mixed with BA (30 g, 0.234 mol). The mixture was purged

under nitrogen for one hour, before being placed in an oil bath heated to 90 °C. EBiB (0.456 g, 2.34 mmol) dissolved in 0.83 g of anisole was purged with nitrogen for 5 minutes, and then added to the round bottom flask via a degassed syringe. After approximately 10 minutes, $Sn(EH)_2$ (0.19 g, 0.47 mmol) dissolved in 0.83 g of anisole purged with nitrogen was injected to initiate the polymerization. Samples were withdrawn using a deoxygenated syringe, placed in an ice bath and exposed to air to stop the polymerization. The target degree of polymerization (DP_n) was 100, giving a target molecular weight of 12817 $g \cdot mol^{-1}$. Solvent content was 40% by mass, and concentration of $CuBr_2$ was 50 ppm on a molar basis with respect to monomer. For some experiments, a benzonitrile/anisole (2.5/97.5 wt %) mixture was used in place of DMF/anisole as specified in the discussion.

5.2.3 Batch ARGET ATRP polymerization procedure for MMA

A series of MMA batch polymerizations were carried out to assess the effect of DMF concentration on the apparent rate of polymerization. $[Cu^{II}(TPMA)Br][Br]$ (6.4 mg, 0.0125 mmol) was added to a 20 mL glass scintillation vial. DMF (0.5 g, 6.8 mmol) and anisole (19.5 g, 0.18 mol) were added to the vial and the contents were stirred until the copper complex was fully dissolved. The solvent mixture was then transferred to a 100 mL two neck round bottom flask, and mixed with MMA (25 g, 0.250 mol). The solution was purged under nitrogen for one hour, and then placed in an oil bath heated to 90 °C. EBiB (0.487 g, 2.50 mmol) dissolved in 2.5 g of anisole was purged with nitrogen for 5 minutes, and then added to the round bottom flask via a degassed syringe. After approximately 10 minutes, $Sn(EH)_2$ (0.40 g, 0.10 mmol) dissolved in 2.5 g of anisole purged with nitrogen was injected to initiate the polymerization. Samples were withdrawn using a deoxygenated syringe, placed in an ice bath and exposed to air to stop polymerization. The target degree of polymerization (DP_n) was 100, giving a target molecular weight of 10000 $g \cdot mol^{-1}$. Solvent content was 50% by mass, and concentration of $CuBr_2$ was 50

ppm on a molar basis with respect to monomer. The DMF concentration in the sample procedure was 2% by mass of total solvent used.

5.2.4 ARGET ATRP in a CSTR

A Chemspeed MultiPlant M100 semi-automated high output reaction platform was configured to run as a single CSTR. The M100 reaction platform consisted of six 100 mL stainless steel tank reactors, with independently controlled heating, cooling, and mixing for each vessel. Feed rates into and out of each reactor was controlled by six adjustable syringe pumps. By programming the pumps to feed into and pull out of a tank reactor at equal rates, a single tank can be configured as a CSTR.

The formulations for the CSTR experiments are given in Table 5.1. The copper complex was first dissolved in DMF. The copper solution was combined with monomer, initiator, as well as the bulk of the solvent in a 500 mL three neck round bottom flask at a ratio of reactants $[M]_0$:$[EBiB]_0$:$[CuBr_2]_0$:$[TPMA]_0$ of 100:1:0.005:0.005 for a target degree of polymerization of 100 at full conversion. A separate reducing agent feed solution was made by dissolving $Sn(II)EH_2$ in 15 g of anisole. The reducing agent was kept separate from the monomer mixture to prevent polymerization in the feed vessel. Both feeds were purged with nitrogen for 1 hour prior to the start of polymerization. While the feed mixtures were being purged, the reaction vessel and stirrer were carefully cleaned. Once the reactor was reassembled, it was filled with nitrogen for approximately 30 minutes to minimize the presence of oxygen in the reaction. The feed solutions and reactor were all kept under a nitrogen blanket for the duration of the experiment.

To initiate polymerization, 48.5 mL of monomer mixture from the 500 mL round bottom flask was injected into the reactor via a deoxygenated syringe. The reactor contents were stirred at 240 rpm and heated to 90 °C. A deoxygenated $Sn(II)EH_2$/anisole dose was then injected into the reactor to initiate polymerization. The inlet (monomer, reducing agent) and outlet feeds were started and programmed to deliver 400 mL of liquid over a period of 8 residence times. Three

different flow rates corresponding to residence times of 60, 90, and 120 minutes were used, with feed rates automatically calculated. To account for the change in solution density between inlet and outlet, the outlet tube was carefully positioned inside the reactor to only draw from the top of the reaction volume. Limiting the depth of the outlet served as a level control to ensure a consistent residence time over the course of the polymerization. The outlet polymer solution was collected in an Erlenmeyer flask open to the atmosphere, with samples withdrawn over the course of 7 mean residence times via the outlet tube at specified time intervals.

Table 5.1: Formulations used in ARGET ATRP of BA and MMA in a CSTR.

	BA CSTR		MMA CSTR	
	m (g)	n (mol)	m (g)	n (mol)
Monomer	270	2.11	225	2.25
$[Cu^{II}(TPMA)Br][Br]$	5.41×10^{-2}	1.05×10^{-4}	5.77×10^{-2}	1.12×10^{-4}
EBiB	4.11	2.11×10^{-2}	4.38	2.25×10^{-2}
DMF	162	2.26	4.5	6.16×10^{-2}
Anisole (feed)	15	1.39×10^{-1}	220.5	2.04
$Sn(II)EH_2$ (feed)	1.71	4.21×10^{-3}	3.64	8.99×10^{-3}
Anisole (injection)	1.67	1.54×10^{-2}	1.67	1.54×10^{-2}
$Sn(II)EH_2$ (injection)	1.9×10^{-1}	4.7×10^{-4}	4.0×10^{-1}	1.0×10^{-3}

5.2.5 Synthesis procedure for chain extension of outlet polymer

Chain extensions of both BA and MMA polymer solutions were conducted as a qualitative measure of livingness. 25 g of polymer solution from the CSTR outlet was added to a 100 mL three neck round bottom flask. 25 g of additional monomer and solvent were added to the flask in the same proportion as the initial CSTR formulations, giving a DP_n of 200 at full conversion. The diluted polymer solution was purged with nitrogen for 1 hour and placed into an oil bath set at 90 °C. A small amount of $Sn(II)EH_2$ (0.2 g, 0.49 mmol) dissolved in 0.5 g of anisole was injected into the flask to re-initiate polymerization. Samples were withdrawn using a deoxygenated syringe at specified time intervals.

5.2.6 Characterization

Sample conversion was determined by gravimetry. Gel permeation chromatography (GPC) was used to determine the molecular weight distribution of the polymer samples. Samples were prepared by dissolving 30 mg of dried polymer in 3 mL of THF. The dissolved samples were then passed through a column packed with basic alumina to remove any remaining copper, before being filtered through a nylon filter (0.2 µm pore size). The GPC was equipped with a Waters 2960 separation module containing four Styragel columns of pore sizes 100, 500, 10^3, 10^4 Å, coupled with a Waters 410 differential refractive index (RI) detector (930 nm) operating at 40 °C. THF was used as eluant and the flow rate was set to 1.0 $mL \cdot min^{-1}$. The detector was calibrated with eight narrow polystyrene standards ranging from 347 to 355 000 $g \cdot mol^{-1}$. The molecular weights of poly(BA) and poly(MMA) samples were obtained by universal calibration with Mark-Houwink parameters for polystyrene (K=11.4·10^{-5} $dL \cdot g^{-1}$, a = 0.716),[28] poly(MMA) (K = 9.44·10^{-5} $dL \cdot g^{-1}$, a = 0.719),[28] and poly(BA) (K = 7.4·10^{-5} $dL \cdot g^{-1}$, a = 0.750).[29]

5.3 Results and Discussion

5.3.1 ARGET ATRP of BA in a batch reactions

Copper solubility was a prominent issue in our preliminary attempts to adapt ARGET ATRP of BA to a CSTR.[24] Although it was possible to produce well-defined poly(butyl acrylate), problems with catalyst solubility in the monomer feed were observed when operation times were extended at longer residence times. The use of a benzonitrile/anisole (2.5/97.5 wt%) solvent combination was sufficient to temporarily solubilize the copper(II) complex, but after 6-7 hours green particles began to precipitate from solution and were visible on the walls of the monomer feed tank. The problem was compounded by the presence of an inline ceramic filter which efficiently separated the suspended copper complex from solution. These factors combined to give unsteady state

behaviour and poor operational stability as effective copper concentration in the reactor decreased with operation time.

A simple solution to mitigate copper precipitation issues is to use more polar solvents with greater affinity for the copper complexes.[30] Solvent choice is important in ATRP, as the solvent can influence the various stages of halogen transfer and shift the overall ATRP equilibrium.[31-33] Polar solvents generally give higher ATRP equilibrium constants (K_{ATRP}) resulting in greater polymerization rates. DMF is a commonly used solvent with high copper solubility, and according to experimental studies and theoretical calculations, K_{ATRP} in DMF is approximately an order of magnitude higher than in a less polar solvent like anisole.[31] By switching the solvent from anisole to DMF, it is possible to both increase the overall polymerization rate as well as eliminate problems caused by copper precipitation. The use of DMF as a solvent for ARGET ATRP of BA was first investigated in batch reactions. The experimental conditions and final properties of pBA produced in batch ARGET polymerizations are shown in Table 5.2.

Table 5.2: Final properties of poly(butyl acrylate) prepared by ARGET ATRP in batch reactions at 90 ˚C.

Exp.	solvent [a]	k_{app} [b] (min^{-1})	t (min)	conv. (%)	$M_{n,theo}$ [c] ($g \cdot mol^{-1}$)	$M_{n,GPC}$ ($g \cdot mol^{-1}$)	PDI
B1	anisole/2.5% benzonitrile	0.0032	360	88	11280	11700	1.28
B2	DMF	0.0072	360	95	12140	11460	1.36
B3	DMF/10% anisole	0.0069	360	96	12360	12120	1.38

[a] solvent content 40% by mass, ratio of reactants $[BA]_0$: $[EBiB]_0$:$[CuBr_2]_0$: $[TPMA]_0$: $[Sn(EH)_2]_0$ is 100:1:0.005:0.005:0.2 for all reactions. [b] k_{app} calculated from normalized conversion vs. time plot assuming pseudo first order kinetics. [c] $M_{n,theo} = ([BA]_0/[EBiB]_0) \times conv. \times MW_{BA}$.

Polymerizations were conducted at 90 ˚C, and copper concentration was 50 molar ppm with respect to monomer in all reactions, with a stoichiometric ratio of ligand to copper. It can be seen that switching from anisole (B1) to DMF (B2, B3) resulted in higher final conversion, as well as a slightly broader MWD. The reducing agent was found to be insoluble in DMF. As the reducing agent feed will need to be kept separate from the monomer feed in the CSTR

experiments, experiment B3 was conducted with a small amount of anisole to more accurately reflect the experiment conditions in the CSTR experiments. An equivalent batch recipe was left stirring for 48 hours under nitrogen, with no observable copper precipitation. The simple solubility test indicated that DMF would be a suitable solvent choice to prevent precipitation and unsteady state behaviour due to changing copper concentrations.

The conversion profile and molecular weight evolution is better illustrated in Figure 5.1. As expected in CRP, the number-average molecular weight (M_n) increased linearly with conversion. Experimental M_n values were very close to the theoretical figure, indicating high initiator efficiency. The polydispersity index (PDI) decreased with increasing conversion, although at high conversion (>85%), the MWD exhibited an upward drift in PDI. This may have been caused by known acrylate side reactions such as radical backbiting or β-scission, which may have resulted in branching or an increased number of polymer chains resulting in a larger PDI than expected.

The normalized conversion plot is mostly linear, indicating a constant radical concentration. The observed rate constant of polymerization (k_{app}) can be derived from linear regression of the normalized conversion plot. As shown in Table 5.2, k_{app} more than doubled when switching from anisole to DMF or a DMF/anisole mixture due to an increase in K_{ATRP}.[31] An important detail to consider when evaluating k_{app} is that the regression analyses are not fitted to zero conversion at the beginning of the polymerization. This indicates that during the first 20 minutes of polymerization, the radical concentration for all three polymerizations was likely much higher than during the remainder of the reaction time. This discrepancy was likely caused by the higher rate of activation of the initiating alkyl halide (EBiB), compared to the butyl acrylate chain ends. EBiB forms a tertiary radical which is more stable than the secondary radical formed from butyl acrylate.[34,35] The increased stability contributes to an approximate order of

magnitude difference in experimentally measured activation rate constant of similar structural analogues.

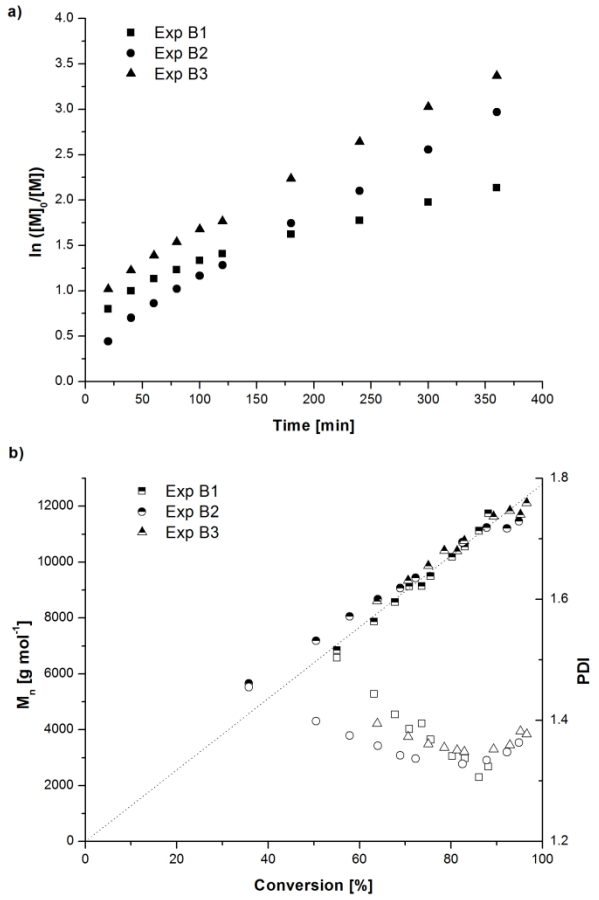

Figure 5.1: Normalized conversion vs. time (a), and evolution of number-average molecular weight (M_n, half-filled symbols) and polydispersity index (PDI, open symbols) with conversion (b) for butyl acrylate ARGET ATRP at 90 °C in different solvents. Experimental conditions are summarized in Table 5.2.

5.3.2 ARGET ATRP of BA in a CSTR

Having confirmed the feasibility of ARGET ATRP of BA in DMF, the formulation was then applied to a CSTR experiment at 90 °C. Three different residence times (60, 90, 120 minutes) were studied and both transient and steady state behaviour was recorded. The experimental conditions and steady state properties for poly(butyl acrylate) produced from ARGET ATRP in a

single CSTR are summarized in Table 5.3. For all three experiments, steady state behaviour was observed after four residence times, with stable outlet conversion and molecular weights. The steady state conversion and M_n values were calculated as an average of the measured values from the 4th to the 7th residence time.

Table 5.3: Steady state properties of poly(butyl acrylate) prepared by ARGET ATRP in a CSTR at 90 °C with 40% DMF as solvent.

Exp. [a]	τ (min)	conv. [b] (%)	$M_{n,theo}$ [c] ($g \cdot mol^{-1}$)	$M_{n,GPC}$ ($g \cdot mol^{-1}$)	PDI	I_{eff} [d] (%)	k_{app} [e] (min^{-1})
S1	60	38.7	4960	5850	1.82	85	0.011
S2	90	47.1	6030	6910	1.84	87	0.010
S3	120	56.1	7190	8500	1.92	85	0.011

[a] solvent content 40% by mass, ratio of reactants $[BA]_0$: $[EBiB]_0$:$[CuBr_2]_0$: $[TPMA]_0$: $[Sn(EH)_2]_0$ is 100:1:0.005:0.005:0.2 for all reactions. [b] conversion and molecular weight data taken as average of steady state values between 4th and 7th residence time [c] $M_{n,theo} = ([BA]_0/[EBiB_0)$ x conv. x MW_{BA}. [d] $I_{eff} = M_{n,theo}/M_{n,GPC}$ x 100% as calculated from steady state averages. [e] k_{app} calculated from average steady state conversion values assuming first order kinetics with respect to monomer concentration.

Conversion, M_n, and PDI as a function of dimensionless residence time (t/τ) for experiments S1-S3 are shown in Figure 5.2. Increasing the residence time from 60 (experiment S1) to 90 (experiment S2) to 120 (experiment S3) gave a corresponding increase in steady state conversion of 39, 47, and 56% respectively. The steady state M_n values also increased from 5850 to 6910 and 8500 $g \cdot mol^{-1}$ for experiments S1-S3 as expected in a controlled polymerization. Broadening of the MWD due to residence time effects can be clearly observed in all three experiments, with an average PDI of 1.82, 1.84, and 1.92 at steady state. The experimental PDI values were lower than the predicted limit of 2 for living polymerization.[22] For CRP in a CSTR, broadening due to residence time effects and termination should contribute to give a PDI greater than 2. The difference between predicted and experimental value may be due to oligomers which fall outside the calibration range of the GPC and are subsequently not accounted for. The GPC is calibrated to 374 $g \cdot mol^{-1}$ by polystyrene standards, which results in a lower limit cut off of ~428 $g \cdot mol^{-1}$ for poly(butyl acrylate) oligomers. Therefore, oligomers below 3-4 monomer units may

be undetected, and can account for a significant portion of the total number of chains. This can lead to artificial inflation of number-average molecular weight, and a narrower molecular weight distribution than expected.

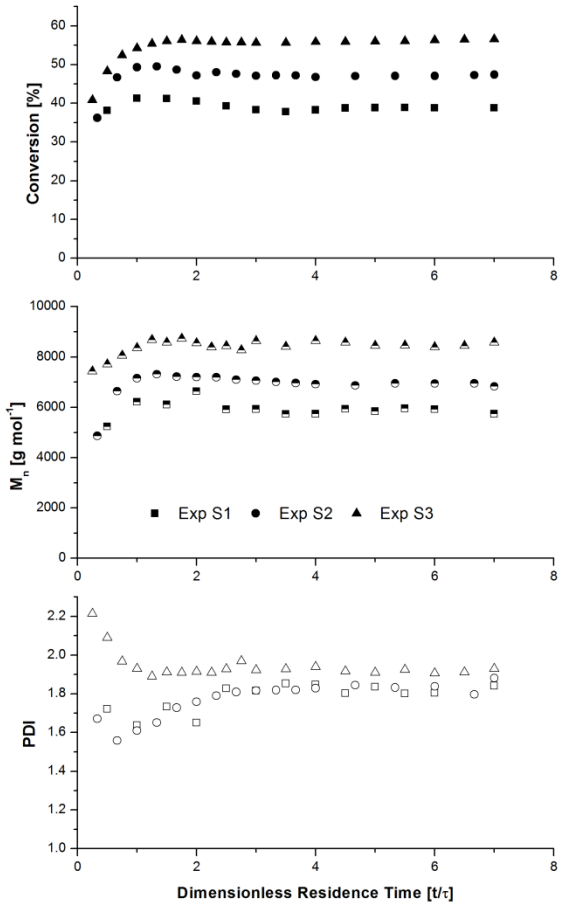

Figure 5.2: Evolution of conversion (closed symbols), number-average molecular weight (half-filled symbols), and polydispersity index (open symbols) as a function of dimensionless residence time for ARGET ATRP of BA experiments S1-S3. Experimental conditions are summarized in Table 5.3.

An ideal Flory distribution has a PDI of 2, and the influence of undetected short chains on the M_n and PDI can be calculated by neglecting oligomers of certain lengths in the Flory distribution to approximate the experimental effects observed. The degree of polymerization (DP_n) has a large influence on the Flory chain length distribution, and DP_n's of 35, 50, and 65 units are used in the calculation to simulate experimentally observed values. Using a molar mass

of 128 $g \cdot mol^{-1}$ for one unit of butyl acrylate, M_n and PDI are calculated based on the full Flory distribution (up to chains of 1000 units), as well as when polymer chains up to 3 or 5 units long are neglected. The results are summarized in Table 5.4, and show that 5% or more of the total population of chains can be unaccounted for in the GPC measurement if oligomers of just 3 units or less are undetected. As the degree of polymerization increases, fewer short chains exist in the population and the PDI begins to approach the ideal value of 2. The trend is similar to that of experiments S1-S3, and provides strong numerical evidence to the presence of undetected oligomeric chains that artificially lowers the expected PDI.

Table 5.4: Effect of undetected oligomers as estimated using a Flory distribution at different degrees of polymerization.

	$DP_n = 35$	$DP_n = 50$	$DP_n = 65$
$M_{n,\ all\ chains}$ $(g \cdot mol^{-1})$	4480	6400	8320
$PDI_{\ all\ chains}$	1.97	1.98	1.98
% chains > 3 units	91.6	94.1	95.5
$M_{n,\ >\ 3\ units}$ $(g \cdot mol^{-1})$	4864	6784	8700
$PDI_{\ >\ 3\ units}$	1.82	1.87	1.90
% chains > 5 units	86.5	90.4	92.5
$M_{n,\ >\ 5\ units}$ $(g \cdot mol^{-1})$	5120	7040	8960
$PDI_{\ >\ 5\ units}$	1.74	1.81	1.85

All three CSTR experiments had high initiator efficiency, with a slight increase in efficiency with longer residence time, as less initiator is washed out of the reactor prior to activation at larger τ's. This can be seen in Figure 5.3, which shows that the observed M_n values increase linearly with conversion and fall almost exactly along the theoretical line.

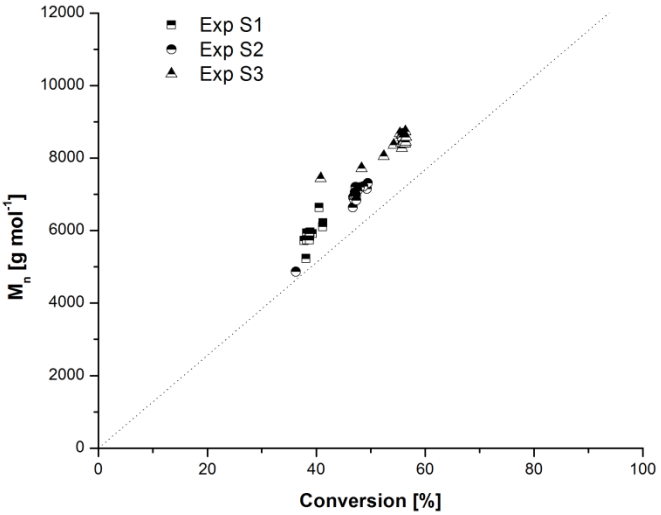

Figure 5.3: Evolution of poly(butyl acrylate) number-average molecular weight (M_n) with conversion for experiments S1-S3.

As with batch polymerizations, the apparent rate constant (k_{app}) can be calculated by assuming a pseudo first order reaction with respect to monomer concentration. For a CSTR at steady state, the conversion is correlated to k_{app} and mean residence time (τ) by the following equation:

$$x_{ss} = \frac{k_{app} * \tau}{\left(1 + k_{app} * \tau\right)} \qquad \textbf{Equation 5-1}$$

The calculated values are shown in Table 5.3, with k_{app} of 0.011, 0.010, and 0.011 min^{-1} for experiments S1-S3. The values are in excellent agreement, suggesting that the pseudo first order assumption used is appropriate. Compared to the batch experiments with DMF as the primary solvent (B2 and B3), k_{app} in a CSTR was approximately 47-54% higher than in batch. This was a rather unexpected result, as the rate of reaction should depend on factors such as copper concentration and target degree of polymerization, and not on the process used. The faster polymerization rate can be partially attributed to the difference in reactivity between EBiB chain ends and butyl acrylate chain ends as discussed above. In a CSTR, there will be two populations

of alkyl halide that can be initiated. EBiB species that are fed in will be preferentially activated and k_{act} and k_{app} for these chains will be higher than the rate constants for existing butyl acrylate chains.[35] In batch polymerizations, this results in a jump in conversion at the beginning of the polymerization. In a CSTR, the overall kinetics will be an average of the polymerization rate of existing butyl acrylate chains as well as newly initiated chains, resulting in a higher k_{app} than observed in batch reactions.

To better understand the difference in kinetics, it is useful to revisit the rate of polymerization in ATRP as well as the ARGET ATRP mechanism. The rate of polymerization for an ATRP system mediated by a copper complex and assuming negligible bimolecular termination can be written as:

$$R_p = k_p[M][P^\bullet] = k_p[M]\frac{k_{act}}{k_{deact}}[R-X]_0\frac{[Cu^I]}{[Cu^{II}X]} \qquad \textbf{Equation 5-2}$$

where: k_p is the monomer propagation rate coefficient; [*M*], [$P^\bullet$], [*R-X*] are monomer, propagating chain, and alkyl halide initiator concentrations respectively; k_{act} and k_{deact} are the rate constants of activation of deactivation which combine to form the ATRP equilibrium constant; and [Cu^I] and [$Cu^{II}X$] are the concentrations of the activator and deactivator species. As the same reactants are used in both batch and CSTR experiments, the activation and deactivation rate constants should be the same. From Equation 2-1, it can be seen that the rate of polymerization is also dependent on the ratio of copper species. As an excess of reducing agent is used in ARGET to continuously reduce copper(II) deactivators, it follows that the concentration of reducing agent in the reactor will have a large effect on copper ratio and as such the polymerization rate.[18-20]

If the reducing agent ($Sn(II)EH_2$) is assumed to react with copper(II) with a second order rate coefficient, k_{reduce}, then the concentration of $Sn(II)EH_2$ at time *t*, [*Sn*], in a batch reactor should follow an exponential decay from the initial concentration $[Sn]_0$ as shown in Equation 5-3:

$$[Sn] = [Sn]_0 \exp(-k_{reduce}[Cu^{II}X]t) \quad \textbf{Equation 5-3}$$

In a CSTR at steady state, the concentration of reducing agent in the reactor, [*Sn*], can be calculated from the inlet tin concentration, $[Sn]_{in}$, as well as the mean residence time (τ) from Equation 5-4:

$$[Sn] = {[Sn]_{in}} \Big/ \left(1 + \tau k_{reduce}[Cu^{II}X]\right) \quad \textbf{Equation 5-4}$$

Although the actual concentration of $Sn(II)EH_2$ in either system is not known from the experimental data, the equations make it possible to examine some general trends. In a batch reactor, the tin concentration is heavily dependent on the speed of the reduction process. If the reduction process is fast, then the tin concentration decreases rapidly due to the exponential function. In a CSTR, the steady state tin concentration is a function of not only the reduction rate but also the reducing agent feed rate and the mean residence time. As such, with a fast reduction process the steady-state tin concentration in a CSTR will likely be higher than that in a batch reactor for most of the reaction time. A higher steady state concentration of reducing agent will shift the copper(I)/copper(II) ratio in favour of the activators and increase the rate of polymerization. This difference in reducing agent concentration, combined with the difference in activation kinetics for newly fed initiators discussed above likely account for the increase in polymerization rate observed in a CSTR when compared to a batch reactor.

5.3.3 ARGET ATRP of MMA with varying DMF concentration

As with BA polymerizations, copper precipitation was also an issue for MMA polymerizations when benzonitrile/anisole (2.5/97.5 wt%) was used as solvent. Since DMF was successfully used as a solvent for BA experiments, a series of batch MMA polymerizations with varying DMF concentration were conducted. The results and solvent conditions are summarized in Table 5.5.

Table 5.5: Final properties of poly(methyl methacrylate) prepared by ARGET ATRP in batch reactions at 90 °C.

Exp.	solvent [a]	k_{app} [b] (min^{-1})	t (min)	conv. (%)	$M_{n,theo}$ [c] ($g \cdot mol^{-1}$)	$M_{n,GPC}$ ($g \cdot mol^{-1}$)	PDI
M1	anisole/2.5% benzonitrile	0.0048	360	86	8600	13000	1.43
M2	DMF	0.0025	360	62	6200	9600	1.65
M3	anisole/50% DMF	0.0055	360	87	8700	9700	1.64
M4	anisole/25% DMF	0.0073	360	93	9300	12000	1.55
M5	anisole/10% DMF	0.010	360	97	9700	11200	1.57
M6	anisole/5% DMF	0.011	360	97	9700	12300	1.49
M7	anisole/2% DMF	0.0070	360	91	9100	12300	1.46

[a] solvent content 50% by mass, ratio of reactants $[MMA]_0$: $[EBiB]_0$:$[CuBr_2]_0$: $[TPMA]_0$: $[Sn(EH)_2]_0$ is 100:1:0.005:0.005:0.4 for all reactions. [b] k_{app} calculated from normalized conversion vs. time plot assuming pseudo first order kinetics. [c] $M_{n,theo} = ([MMA]_0/[EBiB]_0) \times conv. \times MW_{MMA}$.

Although the use of DMF should have increased the ATRP equilibrium constant and increased polymerization rate, the opposite was observed in MMA polymerizations. Conducting ARGET ATRP of MMA in DMF resulted in lower final conversion (experiment M2, 62%) compared to anisole (experiment M1, 86%), along with a broader molecular weight distribution as evidenced by the higher PDI value of 1.65. The molecular weight data and normalized conversion plots for experiments M1 and M2 are shown in Figure 5.4. Both experiments showed an approximately linear increase in M_n with conversion, however there was considerable broadening of the molecular weight distribution with DMF. The normalized conversion plots for both experiments are linear, and k_{app} calculated assuming pseudo first order kinetics are 0.0048 and 0.0025 min^{-1} respectively. The lower conversion and reaction rate, along with the broader molecular weight distribution in M2 indicate that the use of DMF caused a significant decrease in initiator efficiency. It is likely that the use of DMF enhanced k_{act} which resulted in a large radical flux at the beginning of the experiment. This caused an increased amount of radical termination, which generated a population of low molecular weight chains that broadened the molecular weight distribution. Also, with fewer active chains in the experiment the rate of polymerization was lower than expected, despite the enhancement in K_{ATRP} from solvent effects.

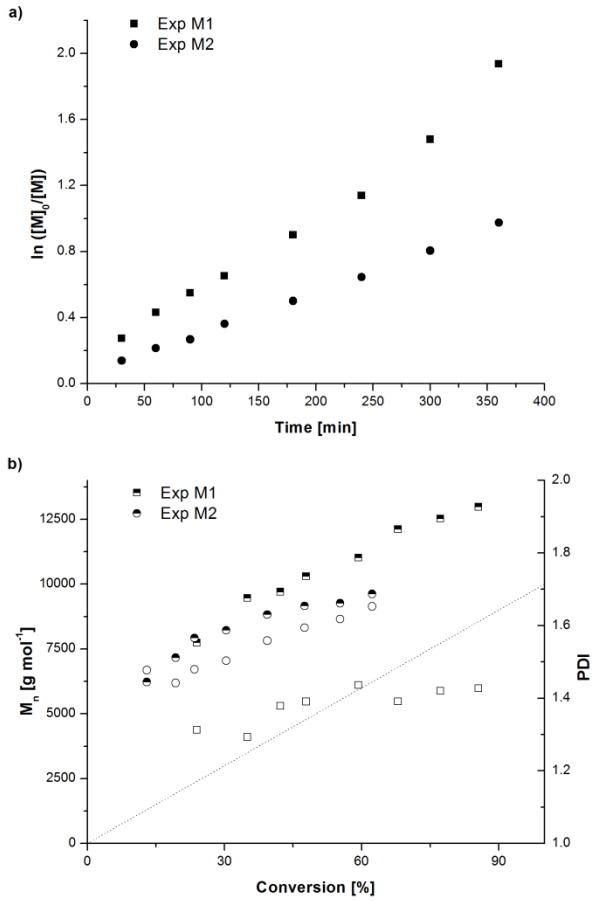

Figure 5.4: Normalized conversion vs. time (a), and evolution of number-average molecular weight (M_n, half-filled symbols) and polydispersity index (PDI, open symbols) with conversion (b) for methyl methacrylate ARGET ATRP at 90 °C in anisole (Exp M1) and DMF (Exp M2). Experimental conditions and final properties are summarized in Table 5.5.

The results from experiment M2 clearly show that DMF cannot be used as the primary solvent for the experimental conditions chosen. However, to ensure stable operation in a CSTR, some DMF is still required to prevent copper precipitation. Mixtures of DMF and anisole were used in ARGET ATRP of MMA in an attempt to obtain a favourable balance between copper solubility, enhanced polymerization rate due to solvent effects, and control over polymerization while minimizing termination. The experiments contained 50% (M3), 25% (M4), 10% (M5), 5% (M6) and 2% DMF (M7) respectively. Looking at the summary in Table 5.5, it can be seen that

all 5 experiments reached high conversion. There molecular weight data for experiments M3-M7 is shown in Figure 5.5.

At high DMF concentration, there was greater deviation from linearity in the M_n vs. conversion plot, indicating the existence of a population of dead chains. There was also an upwards drift in PDI with conversion for all 5 experiments, most likely caused by increased termination as when DMF was used as the primary solvent. As the DMF concentration was decreased, the final PDI also decreased indicating that lowering the DMF concentration will help to enhance control over the polymerization and minimize termination. The molecular weight data in experiment M7 (2% DMF) was similar to experiment M1, when anisole was used as the main solvent, and seemed to contain the least amount of undesired bimolecular termination. A mixture of copper complex, MMA, anisole and 2% DMF was stirred under nitrogen for 48 hours with no observed precipitation, indicating that this would be a suitable formulation for use in a CSTR experiment.

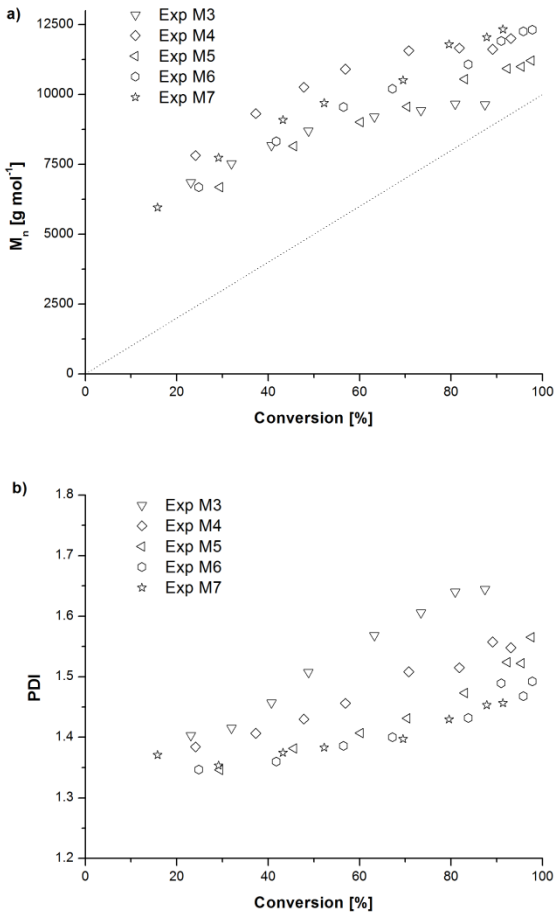

Figure 5.5: Evolution of number-average molecular weight (M_n) (a), and polydispersity index (PDI)) with conversion (b) for methyl methacrylate ARGET ATRP at 90 °C in anisole/DMF binary solvent mixture. Experimental conditions and final properties are summarized in Table 5.5.

The normalized conversion vs. time plots for experiments M3-M7 are shown in Figure 5.6. The kinetic plot exhibits linear behaviour for all 5 experiments, and interestingly the slope of the plot changes with DMF concentration such that there's a maximum observed rate constant at 5% DMF. This is better illustrated when k_{app} is plotted against DMF concentration as shown in Figure 5.7.

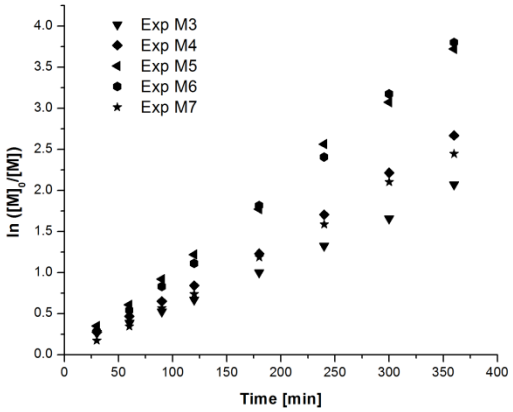

Figure 5.6: Normalized conversion vs. time for methyl methacrylate ARGET ATRP at 90 °C in an anisole/DMF binary solvent mixture. Experimental conditions and final properties are summarized in Table 5.5.

Figure 5.7 suggests that solvent effects on the rate of polymerization are a product of a complex balance between enhancement to the ATRP equilibrium, initiator efficiency, as well as effective copper concentration. Although solvent effects have been extensively investigated in ATRP, studies typically only take into account effects from a single solvent and not a mixture of solvents.[31,32] However, the effects of solvent mixtures which cause disproportionation have been studied in copper(0) mediated CRP.[36,37] It was suggested that solvent effects in copper(0) mediated CRP is a combination of polarity, disproportionation and the solvent mixture's ability to stabilize colloidal copper(0) species.[37] However, disproportionation of copper(I) into copper(0) and copper(II) species is proposed to change the dominant mechanism by which halogen transfer occurs. While DMF may also promote disproportionation, the ligand used (TPMA) forms very stable copper(I) species and as such disproportionation is nearly negligible. Therefore, the observed effect of DMF on polymerization rate and control were likely not due to disproportionation but rather a localized complex coordination effect. The study of other solvent mixtures containing solvents which enhance K_{ATRP} may yield other systems where synergistic and beneficial solvent effects are observed.

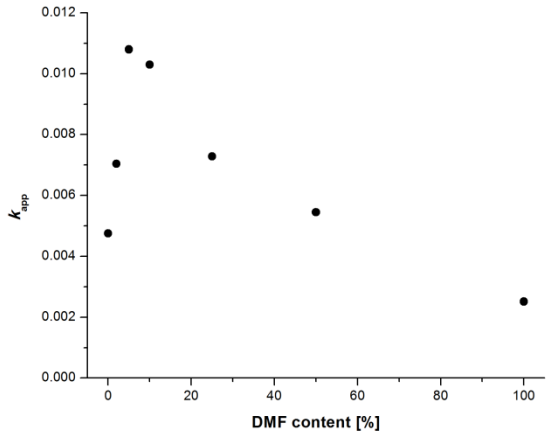

Figure 5.7: Apparent rate constant (k_{app}) as a function of DMF concentration in the anisole/DMF binary solvent mixture for ARGET ATRP of MMA at 90 °C.

5.3.4 ARGET ATRP of MMA in a CSTR

The formulation from experiment M7 was used for a series of MMA polymerizations in a single CSTR at three different residence times (60, 90, 120 minutes). The experimental conditions and steady state properties for pMMA produced from ARGET ATRP are summarized in Table 5.6. For all three experiments, steady state behaviour was observed after four residence times, with stable outlet conversion and molecular weights. The steady state conversion and M_n values were calculated as an average of the measured values from the 4th to 7th residence time.

Table 5.6: Steady state properties of poly(methyl methacrylate) prepared by ARGET ATRP in a CSTR at 90 °C with 50% anisole/DMF as solvent.

Exp. [a]	τ (min)	conv. [b] (%)	$M_{n,theo}$ [c] ($g \cdot mol^{-1}$)	$M_{n,GPC}$ ($g \cdot mol^{-1}$)	PDI	I_{eff} [d] (%)	k_{app} [e] (min^{-1})
S4	60	33.7	3370	10090	1.96	33	0.0084
S5	90	45.7	4570	11740	1.91	39	0.0094
S6	120	53.5	5350	12120	1.89	44	0.0096

[a] solvent content 50% by mass, ratio of reactants $[MMA]_0$: $[EBiB]_0$:$[CuBr_2]_0$: $[TPMA]_0$: $[Sn(EH)_2]_0$ is 100:1:0.005:0.005:0.4 for all reactions. [b] conversion and molecular weight data taken as average of steady state values between 4th and 7th residence time [c] $M_{n,theo} = ([MMA]_0/[EBiB]_0)$ x conv. x MW_{MMA}. [d] $I_{eff} = M_{n,theo}/M_{n,GPC}$ x 100% as calculated from steady state averages. [e] k_{app} calculated from average steady state conversion values assuming first order kinetics with respect to monomer concentration.

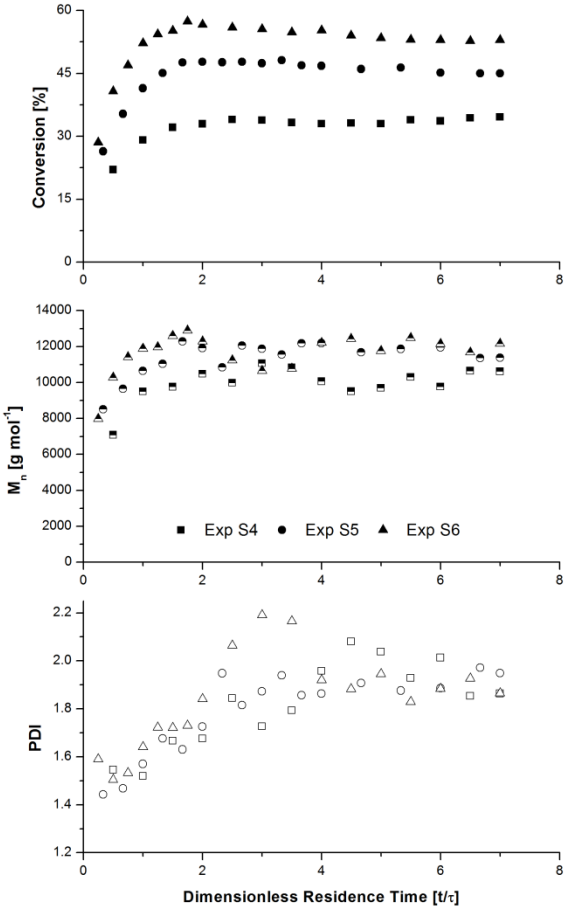

Figure 5.8: Evolution of conversion (closed symbols), number-average molecular weight (half-filled symbols), and polydispersity index (open symbols) as a function of dimensionless residence time for ARGET ATRP of MMA experiments S4-S6. Experimental conditions are summarized in Table 5.6.

Conversion, M_n, and PDI as a function of dimensionless residence time (t/τ) for experiments S4-S6 are shown in Figure 5.8. The steady state values for conversion and M_n are 34%/10090 g·mol^{-1}, 39%/11740 g·mol^{-1}, and 54%/12120 g·mol^{-1} for residence times of 60, 90 and 120 minutes respectively. As with the BA ARGET CSTR experiments, reactor conversion and the outlet molecular weight distribution stabilize after approximately four residence times. The molecular weight distributions in experiments S4-S6 were broader than observed in the BA CSTR experiments. As the activation rate constant for EBiB is similar to that for methyl methacrylate chain ends, the preferential activation which was present in BA polymerizations was

absent in MMA experiments and there was no such effect on the molecular weight distribution. The measured PDI values were still below the predicted limit of 2, likely due to GPC calibration issues as discussed before.

Although there was an increase in steady state conversion with increasing residence time, the observed molecular weights between the three experiments were very similar. This was also observed in batch polymerizations where the experimental M_n values deviate considerably from the theoretical value at low conversion. This may be caused by poor initiator efficiency in the early stages of polymerization and slow gradual activation of EBiB. Figure 5.9 shows a plot of initiator efficiency vs. reaction time for batch experiment M7, where it can be seen that the initiator efficiency increases with reaction time and gradually levels off at approximately 70-75%. The initiator efficiency for experiments S4-S6 is also shown in Figure 5.9 by treating the mean residence time as the equivalent batch reaction time. The initiator efficiency for experiments S4-S6 were lower than batch values at the same reaction time. This may have been caused by EBiB that was washed out of the reactor prior to activation, resulting in a lower concentration of chains than expected.

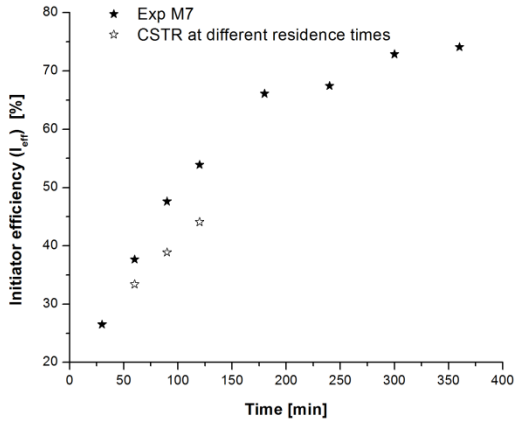

Figure 5.9: Initiator efficiency (I_{eff}) as a function of reaction time (closed symbols) and a function of mean residence time (open symbols) for ARGET ATRP of MMA with 2% DMF in batch and CSTR.

The calculated pseudo first order apparent rate constants for experiments S4-S6 are shown in Table 5.6. The values are in good agreement and increase slightly with residence time, going from 0.0084, to 0.0094, and 0.0096 min^{-1} at residence times of 60, 90, and 120 minutes respectively. This may be due to activation of a larger percentage of EBiB being fed into the reactor at longer residence times, as shown in the increased initiator efficiency at longer residence times (Figure 5.9). As with the BA CSTR experiments, k_{app} in the MMA CSTR experiments was higher than the comparable batch reaction (M7). The average CSTR rate constant was 30% higher than the batch k_{app}, and was likely due to a higher steady state reducing agent concentration as discussed above. However, since EBiB is not preferentially activated over MMA chain ends, the overall activation rate constant was similar to that in batch experiences, and the increase in k_{app} for MMA going from a batch reactor to a CSTR was lower than in BA polymerizations.

5.3.5 Representative chain extensions of outlet polymer

To give a qualitative assessment of the livingness of the polymer produced, the outlet polymer solutions were chain extended with a small amount of additional monomer. Extensions were conducted with both BA and MMA to create homopolymers as well as a gradient block copolymer. The results of the chain extensions are summarized in Table 5.7.

Table 5.7: Experimental conditions and properties of poly(butyl acrylate) and poly(methyl methacrylate) chain extension experiments conducted in batch at 90 °C.

Exp.	Condition	$conv_{init}$ [a] (%)	$M_{n,\,init}$ ($g \cdot mol^{-1}$)	PDI_{init}	$conv_{final}$ (%)	$M_{n,\,final}$ ($g \cdot mol^{-1}$)	PDI_{final}
X1	Extension of S1 (pBA)	22	6100	1.86	87	21900	1.32
X2	Extension of S6 (pMMA)	49	16400	1.54	92	24400	1.47
X3	Extension of S6 with BA at 110 °C	49	16400	1.54	61	17100	1.64

[a] initial conversion after dilution from monomer and solvent addition.

Experiment S1 was chosen as a representative BA CSTR polymerization for chain extension with additional butyl acrylate (X1). Although other monomers could have been used to

create a gradient block copolymer, butyl acrylate was used to simplify analysis. Reinitiation of the outlet polymer solution was successful with a small injection of reducing agent. A substantial increase in conversion and M_n was observed between the initial and final samples, along with narrowing and movement of the entire molecular weight distribution. The GPC traces of chain extension X1 are shown in Figure 5.10.

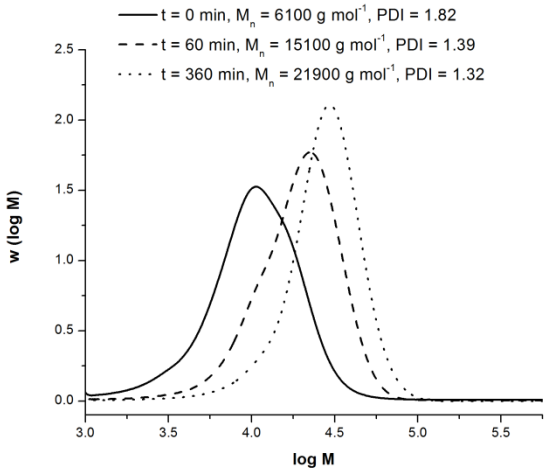

Figure 5.10: Gel permeation chromatography traces for poly(butyl acrylate) chain extension (X1) of experiment S1. The traces are normalized by area, and experimental conditions of the extensions are shown in Table 5.7.

Experiment S6 was chosen for chain extension of MMA CSTR outlet polymer. Chain extension was attempted with additional MMA (X2) at 90 °C, as well as with additional BA (X3) at 110 °C. It should be noted that the initial M_n and PDI of X2 and X3 were different from the steady state values of S6. The M_n had increased from a steady state average of 12120 g·mol^{-1} to 16400 g·mol^{-1} by the time the chain extensions were conducted. The PDI had also decreased from 1.89 to 1.54. Both results suggest that polymerization had occurred at room temperature in the outlet polymer despite exposure to air. The additional polymerization was likely caused by a high level of residual $Sn(EH)_2$ in the outlet polymer that continuously reduced oxidized copper(II) species back into copper(I) activators, which enabled slow polymerization in the outlet polymer at room temperature.

When MMA was used for chain extension of experiment S6 (X2), there was some narrowing and movement of the molecular weight distribution along with an increase in conversion and M_n. Unfortunately, chain extension of S6 with BA (X3) resulted in a broader molecular weight distribution and only a small increase in conversion. The broadening may have been caused by a gradual exchange of MMA chain ends for BA chain ends. Due to the difference in activation rates between the two, the MWD did not experience a uniform growth rate, and more units were added to some chains than expected. The GPC traces for experiments X2 and X3 are shown in Figure 5.11.

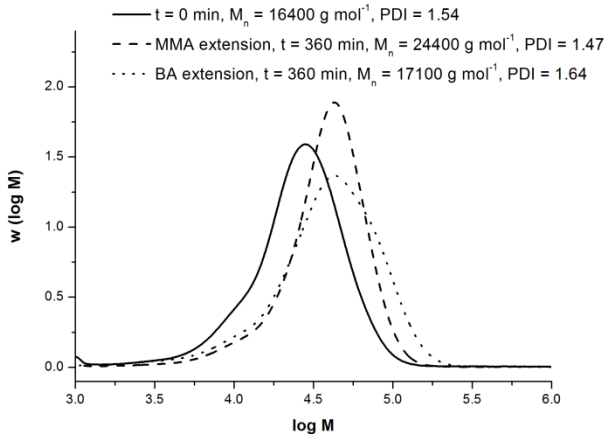

Figure 5.11: Gel permeation chromatography traces for poly(methyl methacrylate) chain extensions (X2, X3) with MMA and BA. The traces are normalized by area, and experimental conditions of the extensions are shown in Table 5.7.

5.4 Conclusions

In order to successfully adapt ARGET ATRP of BA and MMA to a continuous stirred tank reactor, copper solubility issues in the monomer feed had to be overcome. The use of DMF was investigated as a co-solvent in batch ARGET experiments to minimize copper precipitation as well as to test the effects of DMF on polymerization kinetics. BA polymerizations in DMF resulted in an overall polymerization rate more than double that of polymerizations conducted in

anisole, without significant loss of control. However, for MMA polymerizations, the concentration of DMF had a large effect on the polymerization rate as well as the broadness of the molecular weight distribution. The batch results suggested that the solvent effects from DMF on the overall rate of polymerization were a product of enhancement to the ATRP equilibrium and effect on initiator efficiency. A large concentration of DMF resulted in a large initial radical flux and a high degree of termination, lowering the actual number of chains.

The successful batch formulations for BA and MMA were attempted in a single CSTR at 90 °C and at residence times of 60, 90, and 120 minutes. All polymerizations exhibited steady state behaviour in conversion and M_n after four residence times. Differences in activation kinetics between the two monomers resulted in very different initiator efficiencies. In BA polymerizations, EBiB was preferentially consumed and resulted in high initiator efficiency. For continuous MMA experiments, it was likely that a portion of initiator was washed out prior to activation, resulting in lower initiator efficiency than comparable batch experiments.

The apparent rates of polymerization in CSTR experiments were calculated assuming pseudo first order kinetics, and compared to the rates of equivalent batch reactions. Surprisingly, the polymerizations were faster in a CSTR than in a batch reactor, with a 54% increase in polymerization rate for BA experiments and a 30% increase for MMA polymerizations. This was most likely due to a higher steady state reducing agent concentration in the CSTR, as the $Sn(EH)_2$ concentration in a CSTR is a function of residence time as well as the kinetics of the reduction process, while in a batch reactor the reducing agent concentration decays exponentially.

Chain extension experiments conducted in batch using outlet BA and MMA polymer solutions showed good living behaviour with an increase in conversion and M_n along with a narrowing of the molecular weight distribution. The results suggest that although residence time effects in a CSTR cause broadening of the molecular weight distribution, there was no observable detrimental impact on livingness. In combination with the increased polymerization rate

compared to batch reactors, ARGET ATRP in CSTRs may serve as an economical and robust means for large scale production of novel acrylic and methacrylic polymers.

References

(1) Kato, M.; Kamigaito, M.; Sawamoto, M.; Higashimura, T. *Macromolecules* **1995**, *28*, 1721-1723.

(2) Wang, J. S.; Matyjaszewski, K. *Journal of the American Chemical Society* **1995**, *117*, 5614-5615.

(3) Matyjaszewski, K.; Xia, J. *Chemical Reviews* **2001**, *101*, 2921-2990.

(4) Ouchi, M.; Terashima, T.; Sawamoto, M. *Chemical reviews* **2009**, *109*, 4963-5050.

(5) Tsarevsky, N. V.; Matyjaszewski, K. *Journal of Polymer Science Part A: Polymer Chemistry* **2006**, *44*, 5098-5112.

(6) Shen, Y.; Tang, H.; Ding, S. *Progress in Polymer Science* **2004**, *29*, 1053-1078.

(7) Tsarevsky, N. V.; Matyjaszewski, K. *Chemical reviews* **2007**, *107*, 2270-2299.

(8) Destarac, M. *Macromolecular Reaction Engineering* **2010**, *4*, 165-179.

(9) Jakubowski, W.; Min, K.; Matyjaszewski, K. *Macromolecules* **2006**, *39*, 39-45.

(10) Matyjaszewski, K.; Jakubowski, W.; Min, K.; Tang, W.; Huang, J.; Braunecker, W. A.; Tsarevsky, N. V. *Proceedings of the National Academy of Sciences of the United States of America* **2006**, *103*, 15309-15314.

(11) Mueller, L.; Jakubowski, W.; Tang, W.; Matyjaszewski, K. *Macromolecules* **2007**, *40*, 6464-6472.

(12) Pietrasik, J.; Dong, H.; Matyjaszewski, K. *Macromolecules* **2006**, *39*, 6384-6390.

(13) Min, K.; Gao, H.; Matyjaszewski, K. *Macromolecules* **2007**, *40*, 1789-1791.

(14) Jakubowski, W.; Matyjaszewski, K. *Angewandte Chemie* **2006**, *45*, 4482-6.

(15) Tang, H.; Shen, Y.; Li, B. G.; Radosz, M. *Macromolecular Rapid Communications* **2008**, *29*, 1834-1838.

(16) Dong, H.; Matyjaszewski, K. *Macromolecules* **2008**, *41*, 6868-6870.

(17) Paterson, S. M.; Brown, D. H.; Chirila, T. V.; Keen, I.; Whittaker, A. K.; Baker, M. V. *Journal of Polymer Science Part A: Polymer Chemistry* **2010**, *48*, 4084-4092.

(18) Min, K.; Jakubowski, W.; Matyjaszewski, K. *Macromolecular Rapid Communications* **2006**, *27*, 594-598.

(19) Matyjaszewski, K.; Dong, H.; Jakubowski, W.; Pietrasik, J.; Kusumo, A. *Langmuir* **2007**, *23*, 4528-4531.

(20) Chan, N.; Boutti, S.; Cunningham, M. F.; Hutchinson, R. A. *Macromolecular Reaction Engineering* **2009**, *3*, 222-231.

(21) Zhang, M.; Ray, W. H. *Industrial & Engineering Chemistry Research* **2001**, *40*, 4336-4352.

(22) Schork, F. J.; Smulders, W. *Journal of Applied Polymer Science* **2004**, *92*, 539–542.

(23) Chan, N.; Cunningham, M. F.; Hutchinson, R. A. *Polymer Chemistry* **2012**, *3*, 486.

(24) Chan, N.; Cunningham, M. F.; Hutchinson, R. a. *Macromolecular Reaction Engineering* **2010**, *4*, 369-380.

(25) Chan, N.; Cunningham, M. F.; Hutchinson, R. a. *Macromolecular Chemistry and Physics* **2008**, *209*, 1797-1805.

(26) Britovsek, G. J. P.; England, J.; White, A. J. P. *Inorganic chemistry* **2005**, *44*, 8125-8134.

(27) Eckenhoff, W. T.; Garrity, S. T.; Pintauer, T. *European Journal of Inorganic Chemistry* **2008**, *2008*, 563-571.

(28) Beuermann, S.; Buback, M.; Davis, T. P.; Gilbert, R. G.; Hutchinson, R. a.; Kajiwara, A.; Klumperman, B.; Russell, G. T. *Macromolecular Chemistry and Physics* **2000**, *201*, 1355-1364.

(29) Penzel, E.; Goetz, N. *Die Angewandte Makromolekulare Chemie* **1990**, *178*, 191-200.

(30) Faucher, S.; Okrutny, P.; Zhu, S. *Industrial & Engineering Chemistry Research* **2007**, *46*, 2726-2734.

(31) Braunecker, W. A.; Tsarevsky, N. V.; Gennaro, A.; Matyjaszewski, K. *Macromolecules* **2009**, *42*, 6348-6360.

(32) Coullerez, G.; Malmström, E.; Jonsson, M. *The Journal of Physical Chemistry A* **2006**, *110*, 10355-10360.

(33) Lin, C. Y.; Coote, M. L.; Gennaro, A.; Matyjaszewski, K. *Journal of the American Chemical Society* **2008**, *130*, 12762-12774.

(34) Tang, W.; Matyjaszewski, K. *Macromolecules* **2007**, *40*, 1858-1863.

(35) Tang, W.; Kwak, Y.; Braunecker, W.; Tsarevsky, N. V.; Coote, M. L.; Matyjaszewski, K. *Journal of the American Chemical Society* **2008**, *130*, 10702-10713.

(36) Nguyen, N. H.; Rosen, B. M.; Jiang, X.; Fleischmann, S.; Percec, V. *Journal of Polymer Science Part A: Polymer Chemistry* **2009**, *47*, 5577-5590.

(37) Jiang, X.; Fleischmann, S.; Nguyen, N. H.; Rosen, B. M.; Percec, V. *Journal of Polymer Science Part A: Polymer Chemistry* **2009**, *47*, 5591-5605.

Chapter 6

Continuous copper wire mediated CRP in a CSTR

Preface

Although the free radical nature of ATRP has been established, the mechanism of halogen transfer is still a subject of debate. In recent years, another CRP technique called "single electron transfer-living radical polymerization" (SET-LRP) possessing many similarities to ATRP has been proposed. SET-LRP vs. ATRP has been a subject of intense debate in literature, and the specifics are discussed in Chapter 2. Although the mechanistic aspects of SET-LRP are still unclear, the advantages of SET-LRP (high polymerization rates at room temperature, high chain end functionality, compatibility with water soluble polymers, use of copper(0) instead of copper salts) are obvious and make the technique very attractive to industry. As a result of my research into solvent effects on ATRP kinetics copper solubility, I began to experiment with SET-LRP as a tool for the synthesis of various acrylic polymers upon my return from the Eindhoven University of Technology. Ultimately, this led to the work in the following three chapters wherein SET-LRP was applied to different continuous processes. This chapter details the use of SET-LRP to synthesize well-defined poly(methyl acrylate) in a CSTR at 30 °C, using copper wire as a "catalyst" source. The effects of a residence time distribution in a CSTR on polymerization kinetics and the resulting molecular weight distribution are discussed. The results in this section have been published as a full paper in Polymer Chemistry (2012, vol. 3, 486-497).

Abstract

The controlled radical polymerization of methyl acrylate in DMSO mediated by copper wire in a continuous stirred tank reactor (CSTR) was successfully demonstrated. Copper wire proved to be an easy to handle and reusable catalyst source, mediating chain growth through the SET-LRP mechanism. Polymerizations were conducted at 30 °C for three different residence times at varying copper surface area and ligand concentration. Doubling the available copper surface area led to an approximately 30% increase in polymerization rate at the same residence time, in agreement with published literature. Experiments conducted at low ligand concentration showed only a slight drop in polymerization rate with no adverse effect on molecular weight control. Chain extensions were conducted using methyl acrylate to simulate a second polymer block; no significant dead chain fraction was observed, indicating that the polymer produced retained living characteristics. The life time of copper wire as a catalyst source was estimated from experimental data on copper consumption rates. Deviation from expected polydispersities and the effects of utilizing two CSTRs in series on the molecular weight distribution are discussed.

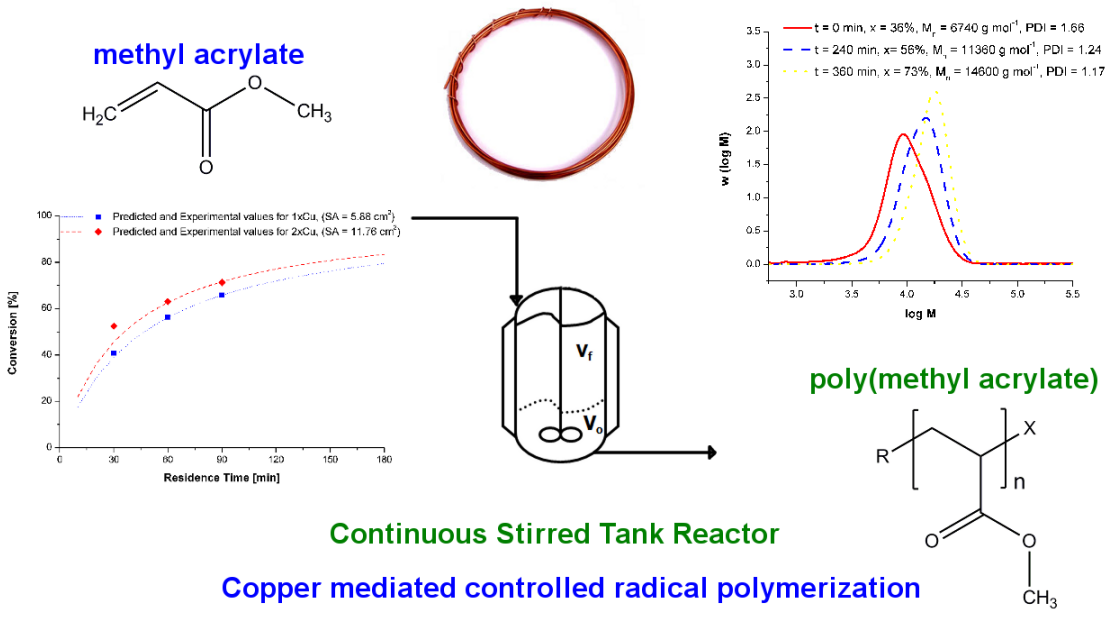

6.1 Introduction

In recent years, controlled radical polymerization (CRP) has been demonstrated to be a promising approach for the synthesis of innovative high-value macromolecules with novel applications. Of the available CRP systems, atom transfer radical polymerization (ATRP) has received a great deal of attention due to its ability to precisely control molecular architecture and its compatibility with a wide range of monomers under mild reaction conditions.[1-4]

ATRP is governed by a dynamic equilibrium between dormant and growing radicals, which are reversibly activated and deactivated by a transition metal catalyst. Copper is one of the more popular metals for ATRP, and copper(I)/copper(II) salts are traditionally used with a nitrogen ligand in stoichiometric or slightly sub-stoichiometric quantities relative to the initiating alkyl halide, leading to a high catalyst concentration in the desired material on the order of 10^4 parts per million (ppm). As the metal and ligand are toxic and add undesired colour to the polymer, the catalyst must be separated from the final product.[5] Due to the high cost of the metal and ligand, it is also preferential to recycle used catalyst to reduce material costs. Unfortunately, neither separation nor catalyst recycling are simple or cost effective tasks, adversely affecting production costs as well as some product applications.[6-8] These factors make the design of an economically feasible ATRP process rather challenging such that, despite its many successes at the laboratory scale, there are still few instances where ATRP is used in an industrial process.[9]

Recently, the catalyst concentration required in ATRP processes has been dramatically reduced by ~2-3 orders of magnitude to $<10^2$ ppm levels through the use of techniques such as "activator regenerated by electron transfer" (ARGET),[10] "initiators for continuous activator regeneration" (ICAR),[11] and "single electron transfer-living radical polymerization" (SET-LRP).[12,13] ARGET and ICAR follow the basic ATRP mechanism, with either a reducing agent or free radical initiator added to the polymerization as a means of continuously regenerating activating species from deactivators which have accumulated due to bimolecular termination.

The proposed mechanism of SET-LRP on the other hand is quite different. Although also a controlled radical polymerization technique involving a dynamic equilibrium between dormant and growing radicals mediated by a transition metal species, Percec *et al*. propose that SET-LRP differs from ATRP in that alkyl halides are activated by copper(0) via outer sphere electron transfer to form copper(I) species.[14] Under certain combinations involving polar or coordinating solvents (DMSO, alcohols, water) and ligands, the copper(I) species undergo near spontaneous disproportionation into copper(0) and copper(II) species.[15,16] This reaction forms the basis of a catalytic cycle that continuously generates copper(0) (activating species) and copper(II) (deactivating species) in pairs, with the mechanism proposed to give greater control over the polymerization and thus greater retention of chain-end fidelity.[17] However, the exact mechanism of SET-LRP is still a subject of debate in the literature.[12,14,15,18,19]

Putting aside the mechanistic implications of SET-LRP vs. conventional ATRP, SET-LRP has several advantageous properties. It can polymerize acrylics at ambient temperature (25 °C) with excellent control and much faster reaction rates than observed in ATRP. In addition, elemental copper in the form of powder or wire can be used instead of copper salts, simplifying handling and catalyst removal.[15,20] Induction times are occasionally observed, however, leading to batch to batch variability under the same process conditions.[20,21] Of larger concern, is the exothermic nature of the SET-LRP batch reactions, with large heat release associated with the rapid polymerization. The internal temperature of SET-LRP of methyl acrylate conducted in a schlenk tube (working volume ~25 mL) in a thermostat oil bath was recorded to be in excess of 60-100 °C, depending on the reaction conditions, due to poor heat removal.[21] This exotherm poses a potential risk of runaway reaction when polymerization is scaled to larger volumes.

This work investigates the adaption of SET-LRP to a continuous stirred tank reactor (CSTR). Continuous processes offer much higher productivity than comparable batch processes and, once at steady-state, yield a product with consistent quality. We have recently demonstrated

the first continuous process utilizing SET-LRP, by using copper tubing to construct a modular tubular reactor for continuous production of well-defined poly(methyl acrylate).[22] Tubular reactors have a high surface area to volume ratio, which facilitates better heat removal and control of the temperature profile, and allows for efficient scale up to larger production volumes. On the other hand, CSTRs are commonly used in industry for free radical polymerization (FRP). Their simplicity in design makes them an economical means to construct a continuous process, and are sometimes preferred over tubular reactors as they are less prone to fouling. While their heat removal capacity is similar to a batch reactor, CSTR have lower instantaneous monomer concentrations and as such generate less heat than similarly sized vessel operating in batch. In addition, CSTRs possess better mixing than tubular reactors, making them potentially more advantageous for the production of copolymers.

The combination of copper catalyzed CRP and CSTRs has not been studied in great detail. Zhang and Ray modeled conventional ATRP of styrene and BA at 110 °C in a series of 4, 8, or 16 reactors,[23] but no experimental studies exist. This can be partly attributed to poor catalyst solubility in ATRP and low reaction rates requiring very long residence times to reach an appreciable yield. Another contributing factor is that polymer chains in CRP have a lifetime of several hours which, combined with the residence time distribution in a CSTR, can significantly broaden the molecular weight of the product.[24] As one of the hallmarks of a well-controlled CRP is narrowly dispersed polymer chains, utilizing a CSTR for CRP appears counterintuitive and a source of deleterious effects. However, a narrow polydispersity index is only one measure of livingness, and a broad molecular weight distribution due to residence time effects does not mean the polymer livingness is low.

In this work, we utilize a Chemspeed Multiplant M100 semi-automated reaction platform configured as a CSTR for the production of living poly(methyl acrylate) in DMSO. This represents the first demonstration of SET-LRP in a CSTR, and the first experimental investigation

of copper mediated controlled radical polymerization in a CSTR. By combining low temperature controlled radical polymerization with a continuous process, SET-LRP in a CSTR is demonstrated to be a simple and economically attractive means for the synthesis of novel polymers.

6.2 Experimental

6.2.1 Materials

Methyl acrylate (MA) (99%, Aldrich), dimethyl sulfoxide (DMSO) (99.9%, Aldrich), methyl 2-bromopropionate (MBP) (98%, Aldrich), and nitrogen gas (Praxair, 99.998%) were used as received. Copper wire (diameter of 0.155 cm) was purchased from a local hardware store, and the surface of the wire was scrubbed with acetone and a non-abrasive material to remove any surface residue before use. Tris[2-(dimethylamino)ethyl]amine (Me_6TREN) was synthesized as described previously.[25]

6.2.2 Continuous copper mediated CRP in a stirred tank reactor

A Chemspeed MultiPlant M100 semi-automated high output reaction platform, consisting of six 100 mL stainless steel tank reactors was used. Each reactor has independently controlled heating, cooling, and stirring as well as feeding via six adjustable syringe pumps. By programming the pumps to feed into and pull out of a tank reactor at equal rates, it was possible to configure a single tank as a CSTR, or multiple tanks into a series of CSTRs.

Methyl acrylate (275 g, 3.20 mol), DMSO (183.33 g, 2.35 mol), Me_6TREN (0.30 g, 1.60 mmol), and MBP (5.34 g, 32.0 mmol) were combined in a 500 mL three neck round bottom flask at a ratio of reactants $[MA]_0$:$[MBP]_0$:$[Me_6TREN]_0$ of 100:1:0.05 for a target degree of polymerization of 100 (target molecular weight of 8640 $g \cdot mol^{-1}$) at full conversion. The reactants were mixed at 60% monomer by mass, to yield a relatively high final polymer content. After the

reactants were combined, the contents were stirred at 300 rpm while being purged with nitrogen for approximately 1 hour before the start of polymerization. While purging the reaction mixture, the reaction vessel and stirrer were carefully cleaned. A piece of copper wire with a length of roughly 12 cm, weighing 2.024 g was scrubbed using acetone and a non-abrasive material. The wire was then wrapped around the stirrer, the reactor reassembled and also purged with nitrogen for approximately 30 minutes to minimize the presence of oxygen in the system.

To initiate polymerization, 50 mL of monomer mixture was injected into the reactor via a deoxygenated syringe. The reactor contents were stirred at 240 rpm at room temperature under nitrogen, until the thermocouple showed an increase in reactor temperature due to heat release from polymerization. At this point, temperature control was initiated to bring the reactor contents to 30 °C and the inlet and outlet feeds were started. The feeds were programmed to deliver 400 mL of liquid over a period of 8 residence times. Three different flow rates corresponding to residence times of 30, 60, and 90 minutes were used, with feed rates automatically calculated. To account for the change in solution density between inlet and outlet, the outlet tube was carefully positioned inside the reactor to only draw from the top of the reaction volume. Limiting the depth of the outlet served as a level control to ensure that residence time did not decrease over the course of the polymerization. The reacted polymer solution was collected in an Erlenmeyer flask open to the atmosphere, with samples periodically withdrawn over the course of 7 mean residence times via the outlet tube. The copper wire was weighed before and after the experiment to determine the amount of copper used.

6.2.3 Continuous copper mediated CRP in two stirred tanks in series

The Chemspeed Multiplant M100 can also be configured to run as two CSTRs in series, by utilizing the outlet of the first tank as the inlet of the second tank. The operating procedure was similar to that of a single tank, with the amount of reactants doubled and a piece of copper wire put into each vessel. To initiate polymerization, 50 mL of monomer mixture was injected into

each reactor via a deoxygenated syringe. The reactor contents were stirred at 240 rpm at room temperature, until the first reactor showed an increased temperature due to the start of polymerization. Temperature control was then initiated to bring the contents of both reactors to 30 °C. The feeds were programmed to deliver 800 mL of liquid over a period of 8 total residence times (sum of both reactors). As before, the outlet tubes were carefully position to act as a level controller and samples were taken from the outlets of both reactors at specified time intervals.

6.2.4 Synthesis procedure for chain extension of outlet polymer

Representative chain extensions were conducted to verify the livingness of the polymer produced. 25 g of polymer solution from the CSTR outlet was added to a 100 mL three neck round bottom flask. Methyl acrylate (15 g, 0.174 mol) and DMSO (10 g, 0.128 mol) were also added to the flask. The combined solution was then purged with nitrogen for 1 hour and placed into an oil bath set at 30 °C. A piece of copper wire (0.155 cm in diameter, 2.024 g) was wrapped around a stir bar and added to the flask to reinitiate polymerization. Samples were withdrawn using a deoxygenated syringe at specified time intervals.

6.2.5 Analytical methods and characterization

Sample conversion was determined by gravimetry. Gel permeation chromatography (GPC) was used to determine the molecular weight distribution of the polymer samples. Samples were prepared by dissolving 30 mg of dried polymer in 3 mL of THF. The dissolved samples were then passed through a column packed with basic alumina to remove any remaining copper, before being filtered through a nylon filter (0.2 µm pore size). The GPC was equipped with a Waters 2960 separation module containing four Styragel columns of pore sizes 100, 500, 10^3, 10^4 Å, coupled with a Waters 410 differential refractive index (RI) detector (930 nm) operating at 40 °C. THF was used as eluant and the flow rate was set to 1.0 $mL \cdot min^{-1}$. The detector was calibrated with eight narrow polystyrene standards ranging from 347 to 355 000 $g \cdot mol^{-1}$. The molecular

weights of poly(MA) samples were obtained by universal calibration with Mark-Houwink parameters for polystyrene (K=11.4·10^{-5} dL·g^{-1}, a = 0.716) and poly(MA) (K = 6.11·10^{-5} dL·g^{-1}, a = 0.799) at low molecular weights.[26]

6.3 Results and Discussion

6.3.1 Initial SET-LRP CSTR experiments

CSTR SET-LRP polymerizations were performed using one piece of copper wire wrapped around the stirrer. Three different residence times (30, 60, 90 minutes) were studied, and both transient and steady-state behaviour was recorded. In all cases, the reactor reached steady-state behaviour after four residence times, with stable outlet conversion and molecular weight as expected. The steady-state values were calculated as an average of the measured values from the 4th to 7th mean residence times. The experimental conditions and steady-state properties for these and all other single CSTR experiments are summarized in Table 6.1.

Table 6.1: Steady-state properties of poly(methyl acrylate) prepared by SET-LRP in a CSTR at 30°C with 40% DMSO as solvent.

Exp.	$[M]_0$:$[MBP]_0$:$[Me_6TREN]_0$	SA_{Cu} (cm^2)	τ (min)	conv [a] (%)	$M_{n,theo}$ [b] ($g \cdot mol^{-1}$)	$M_{n,GPC}$ ($g \cdot mol^{-1}$)	PDI	k_{app} [c] (min^{-1})
S1	100:1:0.05	5.88	30	40.9	3520	4670	1.78	0.023
S2	100:1:0.05	5.88	60	56.2	4837	5870	1.78	0.021
S3	100:1:0.05	5.88	90	65.8	5660	6730	1.79	0.021
S4	100:1:0.05	11.76	30	52.4	4510	4780	1.75	0.037
S5	100:1:0.05	11.76	60	63.0	5420	5960	1.75	0.028
S6	100:1:0.05	11.76	90	71.3	6140	7120	1.74	0.028
S7	100:1:0.01	5.88	60	52.3	4500	6330	1.72	0.018
S8	100:1:0.01	11.76	60	60.8	5230	6190	1.81	0.026
S9	100:1:0.01	23.52	60	61.7	5310	6670	1.77	0.027

[a] conversion and molecular weight data taken as average of steady-state values between 4th and 7th residence time [b] $M_{n,theo}$ = ($[M]_0$/$[MBP]_0$) x conv. x MW_M. [c] k_{app} calculated from average steady-state conversion values assuming first order kinetics with respect to monomer concentration.

Conversion, number average molecular weight (M_n), and polydispersity index (PDI) as a function of dimensionless residence time (t/τ) are shown in Figure 6.1. The data shows that increasing the residence time from 30 (experiment S1) to 60 (S2) to 90 (S3) minutes gives a corresponding increase in steady-state conversion of 41, 56, and 66%, respectively. With increasing conversion comes an increase in molecular weight; the steady-state M_n values are 4670, 5870, and 6730 $g \cdot mol^{-1}$ for experiments S1-S3. By assuming a pseudo first order reaction with respect to monomer concentration, the steady-state conversion (x_{ss}) value can be used with the mean residence time (τ) to calculate an apparent rate constant (k_{app}) using the following equation:

$$x_{ss} = \frac{k_{app} * \tau}{\left(1 + k_{app} * \tau\right)} \qquad \textbf{Equation 6-1}$$

The calculated values are shown in Table 6.1, with an apparent rate constant of 0.023, 0.021, and 0.021 min^{-1} for experiments S1-S3. The values are in very good agreement, providing an accurate measurement of the rate of SET-LRP in a CSTR at a controlled and constant temperature.

The molecular weight data for experiments S1-S3 is also of interest. Figure 6.1 shows that for all three experiments, the M_n starts out at a low value of approximately 3000 g mol^{-1}, and steadily increases to the steady-state value with each passing residence time. The PDI exhibits a similar transient trend; it steadily increases from approximately 1.5 to the steady-state value between 1.7 and 1.8. The observed polydispersities are lower than the theoretical minimum value of 2 for controlled polymerization in a single CSTR.[24] A detailed discussion for this behaviour is provided later. For experiment S3 with a 90 minute residence time, the PDI is broad for the first sample before narrowing considerably prior to its eventual climb to the steady-state value. The second sample in S3 in particular, has a small PDI value of 1.26, which implies a narrow molecular weight distribution.

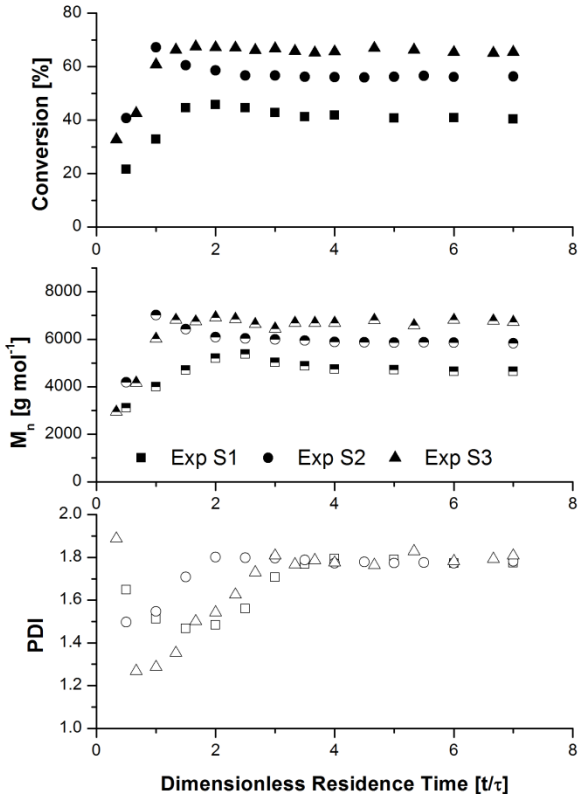

Figure 6.1: Evolution of conversion (closed symbols), number-average molecular weight (half-filled symbols), and polydispersity index (open symbols) as a function of dimensionless residence time for experiments S1-S3. Experimental conditions are summarized in Table 6.1.

Looking at the GPC traces for experiment S3, plotted in Figure 6.2, illustrates clearly what is happening inside the reactor. During startup, the reactor is filled with the monomer mixture until polymerization is detected by a rise in internal temperature. As the reactants are pumped out of the well-mixed vessel, a residence time effect can be observed as new chains are added and existing chains are slowly washed out. In part a) of Figure 6.2, the polymerization is just initializing with low conversion which leads to a broad distribution. As reaction time increases, conversion increases and more monomer is added to the growing chains leading to a more uniform and narrow molecular weight distribution, as would be seen in a batch system. In part b), the effect of the CSTR's residence time distribution becomes evident as two distinct populations emerge – the higher molecular weight chains which were present from the beginning,

and the low molecular weight tail formed by newly fed initiator. The low molecular weight section continues growing, while the higher molecular weight population leaves the reactor in part c), leading to a broad and homogenous distribution at steady-state in part d). Interestingly, while the appearance of the molecular weight distribution changes rather dramatically with time, the number average molecular weight and PDI remain relatively stable even before a homogenous distribution appears inside the reactor.

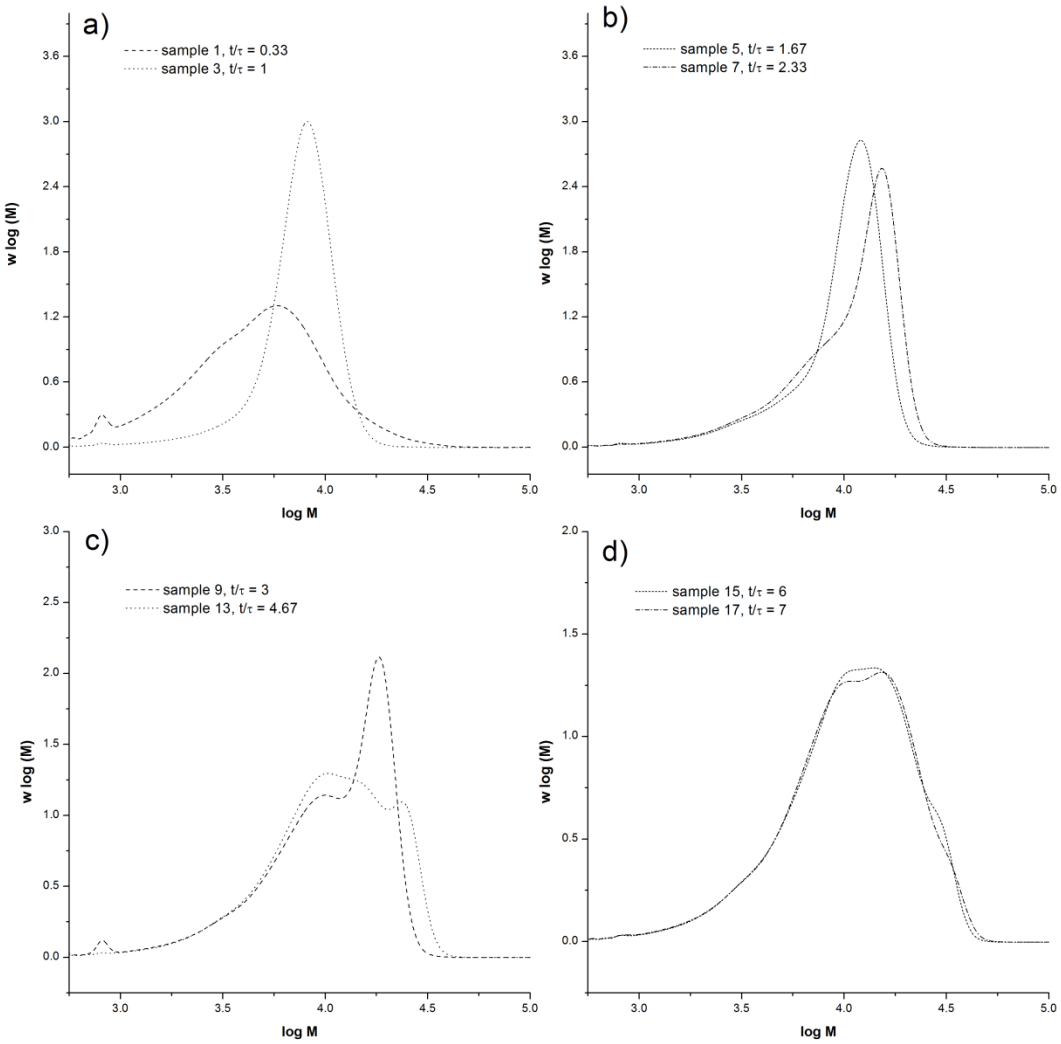

Figure 6.2: Gel permeation chromatography traces for poly(methyl acrylate) produced in experiment S3 at different dimensionless residence times: a) t/τ = 0.33, 1 b) t/τ = 1.67, 2.33 c) t/τ = 3, 4.67 d) t/τ = 6, 7.

6.3.2 Increasing copper surface area

For the production of block copolymers, a high steady-state conversion in the reactor is desirable. One means of achieving this is to increase residence time, as demonstrated by experiments S1-S3. However, the kinetics of a CSTR design imposes a limit on what conversion can be achieved, and to achieve a further marginal increase in conversion requires a substantial increase in residence time. The other approach is to increase the rate constant, k_{app}, by increasing the surface area of copper available for catalysis inside the reactor. Experiments S4-S6 examine this route by utilizing twice the amount of copper as in experiments S1-S3 at the same mean residence times by placing an addition piece of copper wire inside the reactor. Due to the narrow clearance between the stirrer and thermocouple, it was not possible to wrap the additional wire around the stirrer. Instead, the wire was shaped into a loose coil and placed around the periphery of the vessel. With the small reaction volumes, the reactor possesses near ideal mixing and the additional wire proved to serve as an effective site for catalysis.

Conversion, number average molecular weight (M_n), and polydispersity index (PDI) as a function of dimensionless residence time (t/τ) for experiments S4-S6 are shown in Figure 6.3. The steady-state values for conversion and M_n are 52%/4780 $g \cdot mol^{-1}$, 63%/5960 $g \cdot mol^{-1}$, and 71%, 7120 $g \cdot mol^{-1}$ for residence times of 30, 60, and 90 minutes respectively. As with experiments S1-S3, the reactor conversion and molecular weight distribution stabilize after four residence times. With the higher reaction rate due to increased copper surface area, however, there appears to be a shorter period of transient behaviour. For batch experiments, induction times of up to 30 minutes have been reported in the literature.[21] This type of transient behaviour is conveniently eliminated by utilizing a continuous process.

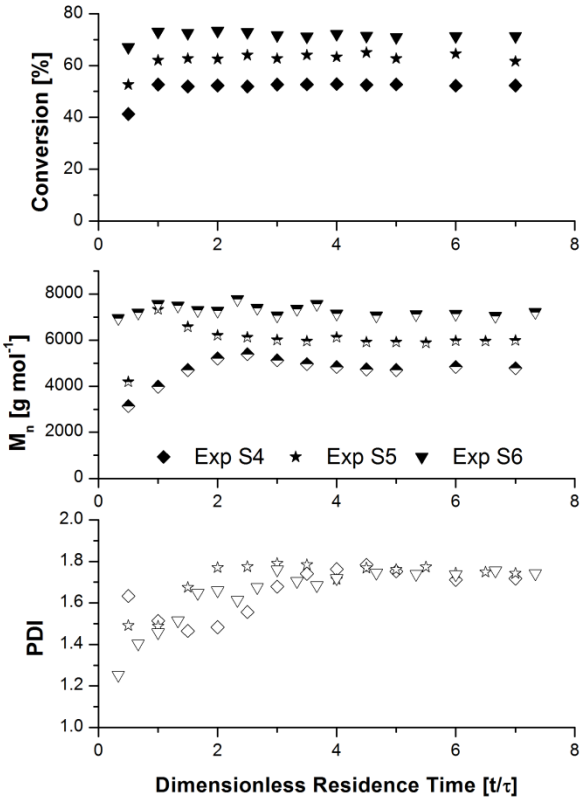

Figure 6.3: Evolution of conversion (closed symbols), number-average molecular weight (half-filled symbols), and polydispersity index (open symbols) as a function of dimensionless residence time for experiments S4-S6. Experimental conditions are summarized in Table 6.1.

A linear relationship between M_n and conversion is one of the properties of a well-controlled polymerization. When M_n is plotted against conversion for experiments S1-S6 as shown in Figure 6.4, it can be seen that the data falls roughly in a straight line above the theoretical molecular weight value. This shows that, even though a CSTR will cause some broadening of the molecular weight distribution, the underlying principle of gradual chain growth with increasing conversion is still valid.

The fact that the data points fall above the theoretical values may indicate reduced initiator efficiency or incomplete initiator activation. The initiator used, methyl 2-bromopropinoate (MBP) is the alkyl halide analogue of a methyl acrylate radical. It has been

shown that in batch reactions under similar conditions, only 28% of the initiator has been activated at 10% conversion, and that MBP is not completely consumed until the reaction has reached 34% conversion.[27] Within a CSTR's residence time distribution, there will be a portion of reactants which possess a very short lifetime. As such, some of the MBP can be washed out prior to activation, leading to a lower radical concentration and initiator efficiency than expected. Additionally, oligomers which fall outside the GPC calibration range will not be included in the measured molecular weight and can artificially inflate the number average molecular weight. The GPC is calibrated to 374 $g \cdot mol^{-1}$ by polystyrene standards, which when converted to poly(methyl acrylate) using Mark-Houwink parameters is 402 $g \cdot mol^{-1}$. Thus, pMA oligomers below 5 units are outside the calibration range of the GPC and may not be accounted for. If a Schulz-Flory distribution is assumed, oligomers that are 1 to 5 units in length can account for 5% of the total number of chains. These two factors together most likely account for the discrepancy between theoretical and observed M_n values.

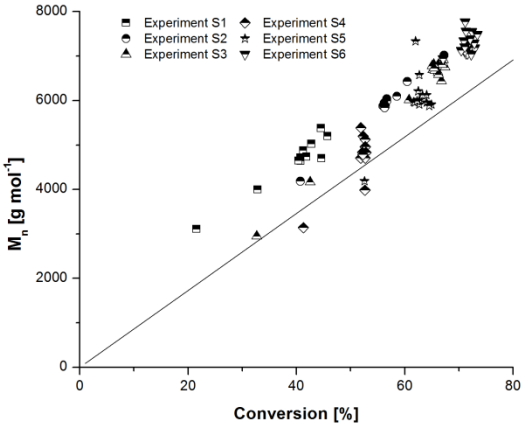

Figure 6.4: Evolution of poly(methyl acrylate) number-average molecular weight (M_n) with conversion for experiments S1-S6.

Intuitively, one would expect that doubling the amount of copper would lead to a doubling of reaction rates. However, literature batch experiments show that k_{app} is linearly proportional to copper surface area to the power of 0.44.[20] By doubling the amount of wire, the surface are is increased from 5.88 cm^2 to 11.76 cm^2, which utilizing the literature relationship should lead to a 36% increase in reaction rate. The experimental results are comparable, with steady-state conversions of 52%, 62%, and 71% for experiments S4, S5, and S6 respectively as summarized in Table 6.1. Utilizing the first order relationship in Equation 6-1, the apparent rate constants are 0.028 min^{-1} for S5 and S6, approximately a 30% increase in reaction rate.

The larger apparent rate constant for S4 (at 0.037 min^{-1} approximately 59% higher) is most likely explained by the reaction temperature. With the higher feed rates associated with the 30 minute residence time, the heat generated for S4 with its higher copper surface area was above the heat removal capacity of the reactor. Instead of operating at 30 °C, the reactor temperature was often in the range of 32-33 °C. The higher temperature leads to an increased propagation rate constant of approximately 5%, in addition to an increase in the activation rate constant of dormant chains. Combined, these factors led to the larger than expected rate increase for experiment S4 over S1.

The rate constants obtained for experiments S2/S3, and S5/S6 are in excellent agreement with each other, and can be assumed to be the representative rate constant at the operating conditions of these experiments. Utilizing the first order relationship in Equation 6-1, the measured rate constant can be used to generate a prediction of steady-state conversion as a function of mean residence time, as shown in Figure 6.5. The predicted conversion illustrates the limitations of utilizing a single CSTR to reach high conversion. Even at a long residence time of 180 min, the steady- state conversion reaches 80%, only 9-15% higher than that achieved with a residence time of 90 minutes. This operating limitation makes the use of a CSTR or a train of CSTRs not suitable for the production of well-defined block copolymers, as a high conversion is

required in the first block. However, gradient copolymers, or even "blocky" gradient copolymers, can be synthesized by placing additional feed streams in a train of CSTRs. The chosen residence times of 30, 60, and 90 minutes seem to be in an optimal region for achieving relatively high steady-state output, without requiring a large mean residence time and long transient behaviour.

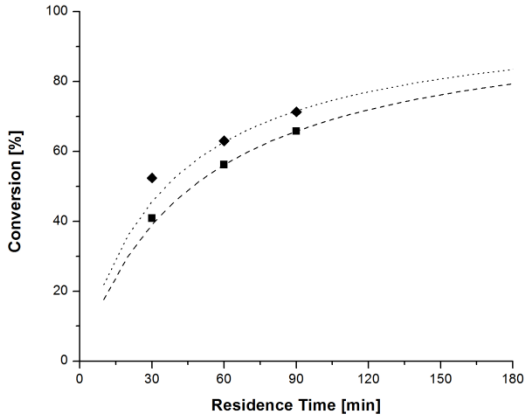

Figure 6.5: Experimental (points) and predicted conversion (lines) as a function of mean residence time for experiments S1-S3 (■, – – –) and S4-S6 (◆, ·····).

It is difficult to directly compare the observed values of the rate constants with any literature values due to differences in reaction temperature, target degree of polymerization, solvent content, ligand concentration, as well as the ratio of copper surface area to reaction volume. In general, the rate constants are lower than reported literature values from batch systems.[20,28] The observed CSTR measurements should be more accurate, however, as they are for isothermal operation. As mentioned previously, a comparable batch reaction was observed to have an internal temperature over 60 °C instead of the assumed 25 °C during the initial phases of polymerization.[21] Such behaviour brings into doubt the accuracy of rate constants calculated from a first order kinetic plot of a batch experiment. On the other hand, the lower instantaneous monomer concentration in a CSTR leads to more readily controlled heat generation, and isothermal operation was maintained at 30 °C during the course of the reaction.

6.3.3 Reducing ligand concentration

A reduction in quantity of ligand used can greatly reduce material cost, as well as lower the amount of copper in the final polymer solution. In batch experiments, the ligand concentration has a strong impact on the reaction rate as well as molecular weight control by controlling the concentration of deactivating species and affecting the extent of disproportionation. In a CSTR, the effect on steady-state conversion may be less obvious due to residence time effects. To test this, a series of experiments (S7-S9) with a residence time of 60 minutes and increasing copper surface area was conducted with low ligand concentration. The ligand concentration was reduced five-fold compared to experiments S1-S6.

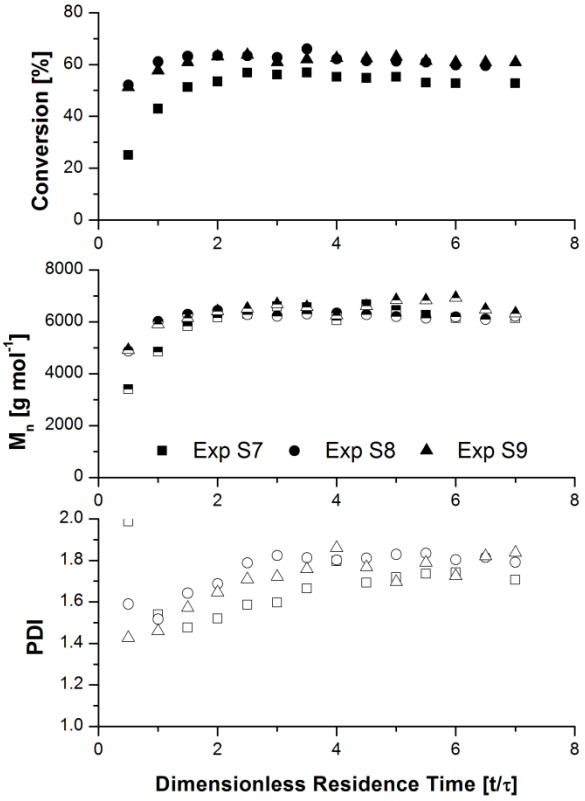

Figure 6.6: Evolution of conversion (closed symbols), number-average molecular weight (half-filled symbols), and polydispersity index (open symbols) as a function of dimensionless residence time for experiments S7-S9. Experimental conditions are summarized in Table 6.1.

Conversion, number average molecular weight and polydispersity index as a function of dimensionless residence time for experiments S7-S9 is shown in Figure 6.6. Experiment S7 reaches a steady-state conversion of approximately 52%, with an average M_n of 6330 g·mol^{-1} and a PDI of 1.72. In comparison, experiment S2 has a slightly higher steady-state conversion of 56% with an average M_n of 5870 g·mol^{-1} and a PDI of 1.78. The apparent rate constant of S7 was found to be 0.018 min^{-1}, a 17% decrease from the value for experiment S2. In all, the five-fold reduction in ligand leads to only a small decrease in steady-state conversion and reaction rate, as well as an increased deviation from calculated theoretical M_n values, most likely related to the factors described previously.

The copper surface area is increased by two fold in experiment S8, giving a steady-state conversion of 61%, with an average M_n of 6190 g mol^{-1} and a PDI of 1.81. The apparent rate constant is 0.026 min^{-1}, which represents an increase of 40% over the reaction rate in S7, a larger increase than observed between experiment S2 and S5, and slightly higher than the predicted literature increase of 36%. In experiment S9, the copper surface area is increased again by a factor of two, to four times higher than in S7. Experiment S9 has a steady-state conversion of 62%, with an average M_n of 6670 g·mol^{-1}, a PDI of 1.77, and an apparent rate constant of 0.027 min^{-1}; all of these values are quite comparable to those found in experiment S8. The similar results suggest that further increasing copper at the reduced ligand level does not lead to any addition rate enhancement, as the combination of copper surfaces and free ligand or deactivating species is already saturated. A previous batch study by Nguyen *et al.* on the effect of ligand concentration on the apparent rate constant in SET-LRP found that the initial ligand concentration has a complex effect on the rate of polymerization.[28] Increasing ligand level led to faster polymerizations, but the observed rate constants plateaued beyond a ligand to initiator ratio of 0.1 to 0.2. Increasing the copper surface area at a constant ligand concentration led to an increase in k_{app}, although it should be noted that the values were calculated assuming isothermal behaviour.

Overall, the reduction in ligand in the CSTR system seems to have no adverse effect on the control of the polymerization, and it is possible to achieve a comparable steady-state conversion. The ability to utilize much lower quantities of ligand while maintaining a highly living polymerization with good reaction rate has positive economic ramifications with regards to material cost as well as post-process product purification.

6.3.4 Quantifying copper levels and catalyst lifetime

As briefly discussed, one of the advantages of utilizing copper wire for SET-LRP is the ease of handling, removal, and recycling of catalyst from the system compared to conventional copper salts. Copper wire is oxidatively stable and does not break apart during polymerization, making addition and removal a simple matter of unwinding the wire that has been wrapped around the stirrer. The gently cleaned copper wire was weighed pre and post polymerization to give an accurate account of how much copper was lost to the system over the polymerization. The results are summarized in Table 6.2.

Table 6.2: Experimental conditions and copper used in each CSTR experiment.

Exp.	$[M]_0$:$[MBP]_0$:$[Me_6TREN]_0$	SA_{cu} (cm^2)	τ (min)	conv [a] (%)	Cu [b] (mg)	dCu/dt [c] ($mg \cdot min^{-1}$)	ppm [d]
S1	100:1:0.05	5.88	30	40.9	12.2	0.0508	110
S2	100:1:0.05	5.88	60	56.2	18.1	0.0431	117
S3	100:1:0.05	5.88	90	65.8	20.3	0.0308	112
S4	100:1:0.05	11.76	30	52.4	25.6	0.106	177
S5	100:1:0.05	11.76	60	63.0	26.3	0.0626	155
S6	100:1:0.05	11.76	90	71.3	30.3	0.0459	155
S7	100:1:0.01	5.88	60	52.3	8.8	0.0210	61
S8	100:1:0.01	11.76	60	60.8	12.9	0.0307	77
S9	100:1:0.01	23.52	60	61.7	14.9	0.0355	88

[a] conversion taken as average steady-state values. [b] mg of copper calculated from weight of copper wire pre and post polymerization. [c] mg of copper used divided by total reaction time, total reaction time = 7 x τ. [d] residual copper, calculated as copper used divided by amount of polymer produced (total monomer multiplied by steady-state conversion).

The copper consumption data can be analysed with respect to the main operating parameters – total reaction time, reactant feed rate, and the apparent rate of polymerization. The total copper consumed increases from 12.2 to 18.1 to 20.3 mg for experiments S1-S3, suggesting

that with increased residence time, and as such increasing reaction time, more copper is consumed. Correspondingly, the rate of copper consumption (estimated by dividing the mass of copper used by the total reaction time), is found to decrease from 0.0508 to 0.0308 $mg \cdot min^{-1}$ with increasing residence time. Residence time is a direct function of feed rate; as feed rates decrease and material passes through the reactor more slowly, the rate of copper usage decreases. Finally, the amount of copper used can be scaled by the amount of polymer produced to give a measure of residual copper. For experiments S1-S3, the measured values of 110-120 ppm are much lower than those found for conventional ATRP and are comparable with other low copper systems. It is important to note that the values reported are in terms of final polymer, and not initial monomer loading. For example, an ARGET ATRP with 50 ppm of copper with respect to monomer would also have 100 ppm of residual copper at 50% conversion. The k_{app} for these three experiments were calculated to be roughly equal (Table 6.1), and the similar agreement in residual copper levels suggests that the rate of polymerization is the determining factor for how much copper will remain in the final material.

Similar trends are observed when the copper surface area is doubled for experiments S4-S6. The total amount of copper consumed is higher and increases from 25.6 to 30.3 mg of copper. The residual copper level is in excellent agreement for experiments S5 and S6 at 155 ppm, a 30-38% increase from the residual copper concentration for experiments S2 and S3. This increase is approximately proportional to the increase in k_{app} (see Table 6.1), which further confirms k_{app} as a driving factor for how much copper is dissipated into the polymer solution. The residual copper for experiment S4 is higher than expected, most likely due to the slightly higher operating reactor temperature that also caused a higher k_{app} value, as discussed before.

When the ligand concentration is decreased 5-fold in experiments S7-S9, a considerable drop in consumed copper is observed. Experiment S7 utilizes 8.8 mg of copper, for a copper concentration of 61 ppm in the final polymer, roughly 52% of the value in experiment S2. While

a significant decrease, the result indicates the amount of copper in solution is not directly proportional to the amount of ligand used, perhaps due to the ability of DMSO to also act as a ligand and coordinate to copper in solution.[29] With increasing copper surface area in S8 and S9, the amount of spent copper increases to 12.9 and 14.9 mg, or 77 and 88 ppm respectively in the product. The amount of copper used in S9 is only marginally higher than in S8, suggesting that the system has become saturated with copper at that ligand concentration. Approximately 47% more copper is used in S8 when compared to S7, corresponding well to the 44% increase in k_{app} (Table 6.1). The residual copper concentration for S8 is approximately 50% of that in experiment S5, in excellent agreement with the relationship between experiments S2 and S7.

Two of the main concerns with a continuous process are stability at steady-state, and the operational time before the reactor has to be taken offline for maintenance. As such, the lifetime and reusability of the copper catalyst is an important factor. The same copper wires were utilized through experiments S4 to S6 with no unexpected change in kinetics or molecular weight, showing that not only can the copper wire be recycled between experiments, but that it has a long operational lifetime. A quick estimate of the actual lifetime of a copper wire utilized in these reactions can be performed by assuming that copper is consumed from the surface of the wire, and that the wire will maintain its shape and length (L) throughout its lifetime. The change in surface area (SA_{cu}), rate constant (k_{app}), and mass of copper (m_{cu}) wire then becomes a function of the change in diameter (d) of the wire shown in Equations 6.2-6.4.

$$SA_{cu} = 2\pi\left(\frac{d}{2}\right)^2 + \pi dL \cong \pi dL \qquad \textbf{Equation 6-2}$$

$$m_{cu} = \rho_{cu}\pi\left(\frac{d}{2}\right)^2 L \qquad \textbf{Equation 6-3}$$

$$k_{app} \propto SA_{cu}^{\,0.44} \qquad \textbf{Equation 6-4}$$

The changes can be normalized by the initial values to give a relative plot of changes in surface area, k_{app} and residual wire mass as a function of wire diameter, as shown in Figure 6.7. The apparent rate constant was calculated by assuming a relationship of $SA^{0.44}$, as previously discussed. The results show that although 37.5% of the original copper mass is consumed as diameter decreases from 0.155 cm to 0.122 cm, k_{app} has only decreased by approximately 10% from the original value.

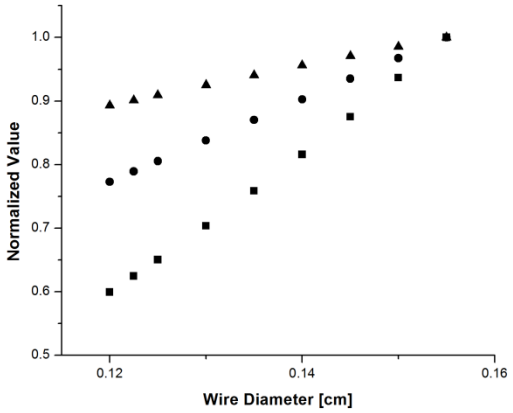

Figure 6.7: Change in surface area (●) and mass of copper wire (■), as well as expected apparent rate constant (k_{app} ▲) as a function of copper wire diameter.

The operational lifetime of a copper wire (t_{life}) can be estimated by setting a 10% decrease in polymerization rate, with a corresponding loss in 37.5% of initial copper mass, as the cutoff level for replacement. Using the observed copper consumption rates in Table 6.2, the time to replacement can be estimated with Equation 6-5. The results of this calculation and relevant terms in Equation 6-5 are explained in Table 6.3.

$$t_{life} = \frac{0.375 m_{cu,0}}{m_{con}} * t_{rxn} \qquad \textbf{Equation 6-5}$$

Table 6.3: Estimated lifetimes of copper wire in a 50 mL CSTR for methyl acrylate polymerization (For experimental details, see Table 6.1).

Exp.	SA_{Cu} (cm^2)	$m_{cu,0}$ [a] (g)	t_{rxn} [b] (min)	m_{con} [c] (mg)	t_{life} (days)
S1	5.88	2.02	210	12.2	9.1
S2	5.88	2.02	420	18.1	12.2
S3	5.88	2.02	630	20.3	16.3
S4	11.76	4.04	210	25.6	8.6
S5	11.76	4.04	420	26.3	16.8
S6	11.76	4.04	630	30.3	21.9
S7	5.88	2.02	420	8.8	25.1
S8	11.76	4.04	420	12.9	34.3
S9	23.52	8.08	420	14.9	59.4

[a] initial mass of copper added. [b] total reaction time, calculated as 7 x mean residence time. [c] copper consumed per experiment, taken from Table 6.2.

The catalyst lifetime increases with increasing residence times, as less polymer is being produced due to the reduction in flow rates. Reducing the ligand usage increases catalyst endurance as less copper is consumed, and an estimated operation time of almost 60 days is predicted. Of course, this simplified treatment is likely to underestimate the catalyst lifetime. In an operational process, the polymerization rate decreases as copper is depleted, and a corresponding drop in copper consumption rate will also be observed.

6.3.5 Representative chain extension of outlet polymer

To confirm livingness of the entire molecular weight distribution, the collected polymer solutions were chain extended with a small amount of additional methyl acrylate. Other monomers could have been used to produce a block copolymer, but for simplicity of analysis methyl acrylate was used to simulate the second block. The results of the chain extensions are summarized in Table 6.4.

Experiments S1, S5, and S8 were chosen as representative polymerizations for chain extension. Reinitiation of the outlet polymer solution was successful, and resulted in considerable narrowing and movement of the entire molecular weight distribution. A drop in PDI was observed with increasing conversion, as expected in well-controlled batch CRP experiments.

Although there is overlap within the molecular weight distribution, there is clear growth from the short polymer chains which are formed due to residence time effects. There is also no observable high molecular weight shoulder caused by bimolecular termination by combination. These qualitative observations indicate good livingness in the polymer produced; NMR and other analytical techniques are required to quantify this analysis. The GPC traces of chain extension X3 are shown in Figure 6.8.

Table 6.4: Experimental conditions and properties of PMA chain extension experiments conducted in batch at 30 °C.

Exp.	Extension of	$conv_{init}$ [a] (%)	$M_{n,\,init}$ ($g \cdot mol^{-1}$)	PDI_{init}	$conv_{final}$ (%)	$M_{n,\,final}$ ($g \cdot mol^{-1}$)	PDI_{final}
X1	S1	36	6740	1.66	73	14600	1.17
X2	S5	45	7270	1.69	89	16190	1.16
X3	S8	26	6170	1.87	75	13420	1.21

[a] initial conversion after dilution from monomer and solvent addition.

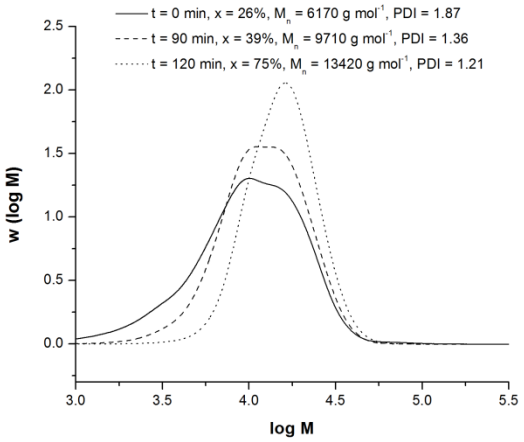

Figure 6.8: Gel permeation chromatography traces for poly(methyl acrylate) chain extensions (X3) of experiment S8. The traces are normalized by area, and experimental conditions of the extensions are shown in Table 6.4.

6.3.6 CSTR in series and residence time distribution

One important element which has not been discussed in great detail so far is the observed polydispersity indices. Calculations and simulations have shown that for a single CSTR, the polydispersity should approach 2 for an ideal living polymerization.[24] The same should hold for controlled radical polymerization, and any termination or non-instantaneous initiation of alkyl halide should only lead to a broadening of the molecular weight distribution and give a polydispersity greater than 2. However, for all the experiments, the observed PDI's are in the range of 1.7-1.8, less than expected. The different residence times also seem to have no impact on the PDI, which indicates the value is not dependent on conversion. Ideal mixing is expected in a reactor this small (working volume 50 mL), and any non-idealities would only result in a segregated CSTR that would give a broader residence time distribution and as such a broader molecular weight distribution. A possible explanation is the presence of a population of short oligomers, which are not detected in the GPC. As previously discussed, pMA oligomers below 5 units are outside the calibration range of the GPC and may not be accounted for resulting in a lower PDI than expected. Assuming a Schulz-Flory distribution, this represents 5% of the total number of chains, and would lower the PDI from an ideal case of 2 to 1.9. If even longer oligomers up to 10 units long are excluded from the calculation, the PDI decreases to 1.8, similar to the observed molecular weight distributions.

One way of reducing broadening is to use a series of CSTRs. The residence time will tighten and approach plug flow behaviour as the number of reactors is increased, and the molecular weight distribution should narrow correspondingly. Zhang and Ray modeled a series of CSTRs, and found that the number of CSTRs increased from 4 to 16, the PDI decreased from 1.6 to 1.3 as the residence time distribution tightened. Since the composition in each tank was different in their copolymerization example, a tapered gradient polymer was suggested as the final product.[23] Schork *et al.* have published several articles on reversible addition fragmentation

chain transfer (RAFT) miniemulsion polymerization in a series of CSTRs.[30,31,32] They were able to produce styrene homopolymer in a series of three CSTRs with a mean residence time of approximately two hours per reactor. A decrease in PDI was observed along the train of CSTRs.[30] Styrene and butyl acrylate copolymerizations were also conducted in a series of four CSTRs with a similar residence time, although bimodality and an increase in PDI was observed.[31]

Given the benefits of operating a train of CSTRs, an additional reactor was added in series to configure a 2 CSTR train. The results are summarized in Table 6.5. Each CSTR had a residence time of 60 minutes, for a total residence time of 120 minutes in the two reactors. Conversion, number average molecular weight and polydispersity index as a function of reaction time for experiment T1 is shown in Figure 6.9. The experiment started without issues, and reactor 2 clearly shows a higher conversion and molecular weight than in the first reactor, demonstrating that the chains exiting the first reactor were living, and continued growing in the second CSTR. Approximately 200 minutes into the reaction, the first CSTR exhibited stirring problems, and the reactor eventually had to be opened. The stirring shaft was cleaned, and the reactor reassembled. During disassembly and cleaning, the reactor contents were exposed to oxygen. This resulted in a sharp decrease in conversion along with unsteady-state behaviour, with a lesser impact on tank 2 performance. From 600 minutes on, the reactor seemed to be functioning normally, although the steady-state conversion was slightly lower than expected from single CSTR experiments. Experiment T2 had similar operational difficulties, but also demonstrated chain extension and narrowing of the molecular weight distribution in the second reactor.

Table 6.5: Experimental conditions and steady state properties of PMA prepared by SET-LRP in a train of 2 CSTRs in series.

Exp.	$[M]_0$:$[MBP]_0$:$[Me_6TREN]_0$	$conv_{CSTR1}$[a] (%)	$M_{n,CSTR1}$ ($g \cdot mol^{-1}$)	PDI_{CSTR1}	$conv_{CSTR2}$[a] (%)	$M_{n,CSTR2}$ ($g \cdot mol^{-1}$)	PDI_{CSTR2}
T1	100:1:0.05	50-55	6090	1.70	69-73	7434	1.55
T2	100:1:0.01	38-42	4900	1.78	57-63	6460	1.52

[a] conversion and taken after 4 residence times, molecular weight data taken as average of values after 4 residence times.

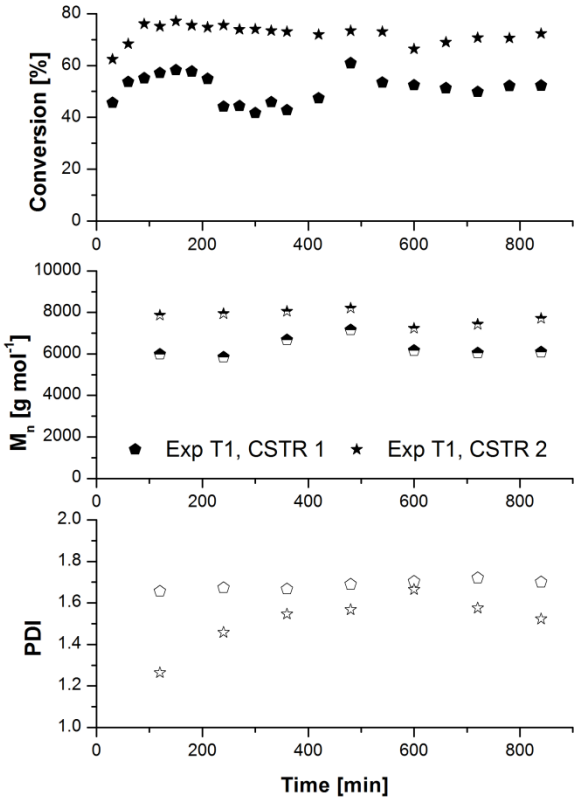

Figure 6.9: Evolution of conversion (closed symbols), number-average molecular weight (half-filled symbols), and polydispersity index (open symbols) as a function of reaction time for experiment T1. Experimental conditions are summarized in Table 6.5.

As shown in Figure 6.9, there is an obvious tightening of the molecular weight distribution between the outlet from reactor 1 and 2, with the PDI decreasing from approximately 1.7 to 1.5. Figure 6.10 gives a GPC trace of the polymer from experiment T1. The chromatogram clearly illustrates a narrowing of the molecular weight distributions and a shift from a broad distribution with a substantial number of short chains to a tighter distribution of higher molecular weight chains, in accordance with expected behaviour.

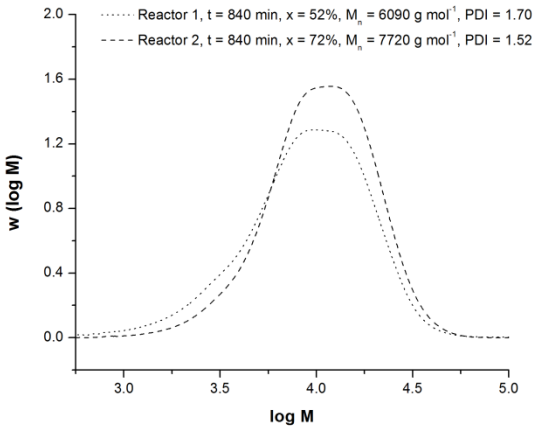

Figure 6.10: Gel permeation chromatography traces for poly(methyl acrylate) samples taken from the two reactors in experiment T1 at *t* = 840 min. The traces are normalized by area and experiment conditions are shown in Table 6.5.

6.4 Conclusions

The SET-LRP of methyl acrylate in DMSO mediated by copper wire in a continuous stirred tank reactor was successfully demonstrated. The polymerizations were conducted at 30 °C and at residence times of 30, 60, and 90 minutes. When one piece of copper wire was used, increasing residence time led to an increase in steady-state conversion from 41 to 66% with a corresponding increase in molecular weight. When additional copper wire was added to double the surface area, a 30% increase in polymerization rate was observed and steady-state conversion increased to 52, 63, and 71% for the three residence times.

Due to the lower instantaneous monomer concentration in a CSTR, effective temperature control was achieved, unlike in a batch reactor where large exothermic responses have been observed.[21] The experimental rate constants were fitted to a first order CSTR kinetic equation, which accurately predicted the observed change in conversion with residence time. Lower ligand levels could also be used with only a slight drop in polymerization rate. Decreasing ligand concentration reduces material costs as well as copper content in the final material, both of which will be advantageous when designing an industrial scale process.

Although a broad molecular weight distribution was expected due to residence time effects in a CSTR, the observed polydispersities between 1.7 and 1.8, were lower than the minimum theoretical value of 2.[24] The narrower than expected PDI was attributed to a population of short oligomers which were undetected in calibrated GPC measurements. Chain extensions were conducted using outlet polymer to verify livingness. Although the initial molecular weight distributions were broad, the polymerization could be reinitiated by addition of copper wire. Well-controlled polymerizations were observed in the chain extension, with no visible population of dead chains. Broadening of the molecular weight distribution due to residence time effects can also be mitigated by operating a train of CSTRs. To demonstrate this, two CSTRs were operated in series and the PDI was observed to drop from 1.7-1.8 down to 1.5-1.6, along with a corresponding increase in outlet conversion in the second reactor.

The rate of copper consumption (monitored by weighing the copper wires before and after each experiment) was low, with approximately 100 ppm of residual copper in the final polymer. Copper wires were reused in several of the experiments with no change in reaction kinetics, demonstrating the reliability and long operational time of this catalyst source. The results demonstrate the use of a CSTR as an economical and facile means to scale-up production of novel acrylic materials via SET-LRP in a continuous process.

References

(1) Kato, M.; Kamigaito, M.; Sawamoto, M.; Higashimura, T. *Macromolecules* **1995**, *28*, 1721-1723.

(2) Wang, J. S.; Matyjaszewski, K. *Journal of the American Chemical Society* **1995**, *117*, 5614-5615.

(3) Matyjaszewski, K.; Xia, J. *Chemical Reviews* **2001**, *101*, 2921-2990.

(4) Ouchi, M.; Terashima, T.; Sawamoto, M. *Chemical reviews* **2009**, *109*, 4963-5050.

(5) Tsarevsky, N. V.; Matyjaszewski, K. *Journal of Polymer Science Part A: Polymer Chemistry* **2006**, *44*, 5098-5112.

(6) Shen, Y.; Tang, H.; Ding, S. *Progress in Polymer Science* **2004**, *29*, 1053-1078.

(7) Tsarevsky, N. V.; Matyjaszewski, K. *Chemical reviews* **2007**, *107*, 2270-2299.

(8) Mueller, L.; Matyjaszewski, K. *Macromolecular Reaction Engineering* **2010**, *4*, 180-185.

(9) Destarac, M. *Macromolecular Reaction Engineering* **2010**, *4*, 165-179.

(10) Jakubowski, W.; Min, K.; Matyjaszewski, K. *Macromolecules* **2006**, *39*, 39-45.

(11) Matyjaszewski, K.; Jakubowski, W.; Min, K.; Tang, W.; Huang, J.; Braunecker, W. A.; Tsarevsky, N. V. *Proceedings of the National Academy of Sciences of the United States of America* **2006**, *103*, 15309-15314.

(12) Percec, V.; Guliashvili, T.; Ladislaw, J. S.; Wistrand, A.; Stjerndahl, A.; Sienkowska, M. J.; Monteiro, M. J.; Sahoo, S. *Journal of the American Chemical Society* **2006**, *128*, 14156-14165.

(13) Rosen, B. M.; Percec, V. *Chemical Reviews* **2009**, *109*, 5069-5119.

(14) Lligadas, G.; Rosen, B. M.; Monteiro, M. J.; Percec, V. *Macromolecules* **2008**, *41*, 8360-8364.

(15) Lligadas, G.; Rosen, B. M.; Bell, C. a.; Monteiro, M. J.; Percec, V. *Macromolecules* **2008**, *41*, 8365-8371.

(16) Jiang, X.; Fleischmann, S.; Nguyen, N. H.; Rosen, B. M.; Percec, V. *Journal of Polymer Science Part A: Polymer Chemistry* **2009**, *47*, 5591-5605.

(17) Monteiro, M. J.; Guliashvili, T.; Percec, V. *Journal of Polymer Science Part A: Polymer Chemistry* **2007**, *45*, 1835-1847.

(18) Matyjaszewski, K.; Tsarevsky, N. V.; Braunecker, W. A.; Dong, H.; Huang, J.; Jakubowski, W.; Kwak, Y.; Nicolay, R.; Tang, W.; Yoon, J. A. *Macromolecules* **2007**, *40*, 7795-7806.

(19) Isse, A. A.; Gennaro, A.; Lin, C. Y.; Hodgson, J. L.; Coote, M. L.; Guliashvili, T. *Journal of the American Chemical Society* **2011**, *133*, 6254-6264.

(20) Nguyen, N. H.; Rosen, B. M.; Lligadas, G.; Percec, V. *Macromolecules* **2009**, *42*, 2379-2386.

(21) Levere, M. E.; Willoughby, I.; O'Donohue, S.; de Cuendias, A.; Grice, A. J.; Fidge, C.; Becer, C. R.; Haddleton, D. M. *Polymer Chemistry* **2010**, *1*, 1086-1094.

(22) Chan, N.; Cunningham, M. F.; Hutchinson, R. A. *Macromolecular Rapid Communications* **2011**, *32*, 604-609.

(23) Zhang, M.; Ray, W. H. *Journal of Applied Polymer Science* **2002**, *86*, 1047-1056.

(24) Schork, F. J.; Smulders, W. *Journal of Applied Polymer Science* **2004**, *92*, 539-542.

(25) Britovsek, G.; England, J.; White, A. J. P. *Inorganic Chemistry* **2005**, *44*, 8125-8134.

(26) Gruendling, T.; Junkers, T.; Guilhaus, M.; Barner-Kowollik, C. *Macromolecular Chemistry and Physics* **2010**, *211*, 520-528.

(27) Nguyen, N. H.; Rosen, B. M.; Percec, V. *Journal of Polymer Science Part A: Polymer Chemistry* **2011**, *49*, 1235-1247.

(28) Nguyen, N. H.; Jiang, X.; Fleischmann, S.; Rosen, B. M.; Percec, V. *Journal of Polymer Science Part A: Polymer Chemistry* **2009**, *47*, 5629-5638.

(29) Monge, S.; Darcos, V.; Haddleton, D. M. *Journal of Polymer Science Part A: Polymer Chemistry* **2004**, *42*, 6299-6308.

(30) Smulders, W. W.; Jones, C. W.; Schork, F. J. *AIChE Journal* **2005**, *51*, 1009-1021.

(31) Smulders, W. W.; Jones, C. W.; Schork, F. J. *Macromolecules* **2004**, *37*, 9345-9354.

(32) Qi, G.; Jones, C. W.; Schork, J. F. *Industrial & Engineering Chemistry Research* **2006**, *45*, 7084-7089.

Chapter 7

Continuous Copper(0) Mediated CRP in a Copper Tubular Reactor

Preface

The use of copper(0) as a catalyst source in SET-LRP lends it two main advantages. Copper(0) is proposed to be more active than copper(I) salts for the activation of alkyl halides, resulting in faster polymerization rates. Also, elemental copper is a cheap and easy to handle catalyst source, with very low residual copper concentrations in the final polymer after removal of the heterogeneous copper. In Chapter 6, the use of copper wire as a catalyst source was investigated for SET-LRP of methyl acrylate in a CSTR. Although copper wire is a simple and elegant material for use in batch or stirred tank reactors, the physical bulk of the wire imposes an upper boundary on the amount of copper that can be put into a reactor, and limits the copper surface area to reactor volume ratio. As SET-LRP kinetics are proposed to be surface area dependent, it may be advantageous to investigate a process with a much higher surface area to volume ratios, such as tubular reactors. Conveniently, copper tubing is commonly used in a while variety of applications and readily available. In this chapter, the use of copper tubing to construct a continuous tubular reactor for copper(0) mediated CRP of methyl acrylate is reported. The reactor walls act as a source of copper, and the high surface area to volume ratio of tubular reactors provides a large surface area for catalysis allowing high conversion to be reached in just minutes. In addition, the surface area to volume ratio greatly improves heat transfer, which is an important design criterion for scale up of exothermic processes. The work in this chapter has been published in Macromolecular Rapid Communications (2011, 32, 604-609).

Abstract

The use of copper tubing as both the reactor and as a catalyst source is demonstrated for continuous controlled radical polymerization of methyl acrylate at ambient temperature and at low solvent content of 30%. The high surface area provided by the copper walls mediates the reaction via the single electron transfer-living radical polymerization (SET-LRP) mechanism. The polymerizations proceeded quickly, reaching 67% conversion at a residence time of 16 minutes. Ligand concentration could also be reduced without a sharp drop in polymerization rate, demonstrating the potential for decreased raw material and post-process purification costs. Chain extension experiments conducted using synthesized polymer showed high livingness. The combination of living polymer produced at high polymerization rates at ambient temperature and low volatile organic solvent content demonstrate the potential of a copper reactor for scale up of SET-LRP.

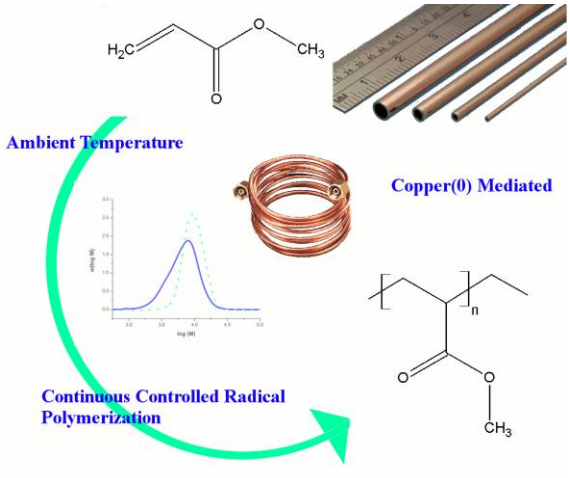

7.1 Introduction

Atom transfer radical polymerization (ATRP) is one of several controlled radical polymerization (CRP) techniques which have been extensively studied in recent years.[1,2] Despite the ability to produce a variety of novel polymers under mild reaction conditions at the laboratory scale, however, there are few instances where ATRP has been adopted to an industrial process.[3-5] The catalyst, generally copper, is toxic and difficult to remove, making the design of an economic process rather challenging. As a result, there is only a limited number of publications on the use of ATRP in continuous processes,[6-12] despite their advantages over batch operation. In general, continuous processes offer more consistent product quality as well as higher reactor productivity. Tubular reactors in particular are advantageous due to their large surface area to volume ratio, which improves heat removal and control of the temperature profile. As such, tubular reactors are more readily scaled to larger reactor sizes than stirred tanks by increasing the reactor size or adding more reactors in parallel.

In recent years, the catalyst concentration required in ATRP processes has been dramatically reduced through the use of techniques such as "activator regenerated by electron transfer" (ARGET),[13] "initiators for continuous activator regeneration" (ICAR),[14] and "single electron transfer-living radical polymerization" (SET-LRP).[15,16] Although SET-LRP is also a controlled radical polymerization technique involving halogen capped chains that are reversibly activated and deactivated by copper species, Percec *et al.* propose that SET-LRP is distinct from ATRP in that it uses Cu(0) as an activating species.[17] Alkyl halides are activated by Cu(0) via outer sphere electron transfer to form Cu(I) species, which with certain polar solvents (DMSO, alcohols, water) and ligand combinations undergo near spontaneous disproportionation into Cu(0) and Cu(II) species.[18,19] This catalytic cycle generates Cu(0) (activating species) and Cu(II) (deactivating species) in pairs, which allows for greater retention of chain end fidelity.[20] The mechanism of SET-LRP is still currently debated in the literature.[15,17,18,21]

Regardless of the SET-LRP mechanism, it can polymerize acrylics at room temperature (25 °C) with excellent control and much faster reaction rates than observed in ATRP, although induction times are occasionally observed.[22,23] As Cu(0) is used as the catalyst source, elemental copper in the form of powder or wire can be used instead of copper salts to make handling and catalyst removal more facile.[17,22] In this work, the use of copper tubing as a catalyst source is investigated in the design of a continuous tubular reactor for SET-LRP. Copper tubing is inexpensive and readily available, making it an ideal copper source for a continuous SET-LRP reactor. A modular copper tubular reactor has been constructed and used to produce well-controlled poly(methyl acrylate) in DMSO with high polymer content. This represents the first demonstration of a continuous process for SET-LRP. The combination of ambient temperature polymerization, continuous operation with residence times of less than 30 minutes, as well as low volatile solvent content makes continuous SET-LRP polymerization in a copper tube an ideal process for environmentally friendly synthesis of novel materials.

7.2 Experimental

7.2.1 Materials

Methyl acrylate (MA) (99%, Aldrich), dimethyl sulfoxide (DMSO) (99.9%, Caledon Laboratories), methyl 2-bromopropionate (MBrP) (98%, Aldrich), and tin(II) 2-ethylhexanoate ($Sn(EH)_2$) (95%, Aldrich) were used as received. Tris[2-(dimethylamino)ethyl]amine (Me_6TREN) was synthesized as described previously.[24]

7.2.2 Copper tubular reactor setup

The reactor was composed of refrigeration grade copper tubing (15.24 m in length, 3.2 mm outer diameter, 1.65 mm inner diameter, total volume of approximately 32 mL). The tubing was split into 4 pieces of equal length to allow for modular assembly into 8, 16, and 32 mL configurations.

A 500 mL three neck round bottom flask was used as a feed vessel, and the feed solution was kept stirring under nitrogen. The flow rate was controlled by an Eldex Recipro VS series high pressure liquid metering pump (B-125-VS), capable of feeding between 0.2 to 10.0 $mL \cdot min^{-1}$. The mass flow rate was measured using a Mettler Toledo PG 5002s balance. The entire reactor was kept in a fume hood and all polymerizations were done at ambient temperature (23-25 °C). The copper coils were weighed before and after each experiment, and mass loss was determined to be negligible (< 0.1% of total weight).

7.2.3 Synthesis procedure for continuous SET-LRP polymerization

Methyl acrylate (140 g, 1.626 mol), DMSO (60 g, 0.768 mol), Me_6TREN (0.153 g, 0.664 mmol), and MBrP (2.717 g, 16.26 mmol) were combined in a 500 mL three neck round bottom flask for a ratio of reactants $[MA]_0$:$[MBrP]_0$:$[Me_6TREN]_0$ of 100:1:0.05. For all continuous experiments, the target degree of polymerization was 100, giving a target number-average molecular weight (M_n) of 8640 $g \cdot mol^{-1}$ and a polymer content of 70 wt% at full conversion. The solution was mixed while being purged with nitrogen for approximately 1 hour before the start of polymerization. At the same time, the copper tubular reactor was flushed with nitrogen to minimize the presence of oxygen in the system.

Once the feed mixture was sufficiently deoxygenated, it was quickly pumped into the copper tubing. Depending on the length of copper tubing used, the reactor was filled in 2-4 minutes. Once the reactor was filled, the flow rate was reduced to the desired level of 1 or 2 $g \cdot min^{-1}$. This was considered the start of the polymerization. The mean residence time was calculated from the reactor volume and experimental flow rate. In total, residence times of 4, 8, and 16 minutes were studied in this work. The flow rate was carefully monitored over the course of the polymerization, and samples were taken at specified time intervals from the outlet of the reactor.

7.2.4 Synthesis procedure for chain extension of outlet polymer

To confirm livingness of the polymer produced, several chain extensions were conducted. In general, 25 g of polymer solution from the reactor outlet was added to a 100 mL three neck round bottom flask. The solution was then purged with nitrogen and placed into an oil bath set at 30 °C. In the control experiment, the purged solution was left at 30 °C with no additional reactants. In all other cases, a small amount of reducing agent, either copper wire (12 cm in length, 1.55 mm outer diameter, 2.0243 g) or tin(II) 2-ethylhexanoate (0.1 g, 2.34 mmol) was added to reinitiate the polymerization. When chain extension of high conversion outlet polymer was conducted, 25 g of polymer solution was combined with methyl acrylate (17.5 g, 0.203 mol) and DMSO (7.5 g, 0.096 mol) to ensure that sufficient monomer units could be added to the existing chains. Samples were withdrawn using a deoxygenated syringe at specified time intervals.

7.2.5 Analytical methods and characterization

Sample conversion was determined by gravimetry. Gel permeation chromatography (GPC) was used to determine the molecular weight distribution of the polymer samples. The GPC was equipped with a Waters 2960 separation module containing four Styragel columns of pore sizes 100, 500, 10^3, 10^4 Å, coupled with a Waters 410 differential refractive index (RI) detector (930 nm) operating at 40 °C. THF was used as eluant and the flow rate was set to 1.0 $mL \cdot min^{-1}$. The detector was calibrated with eight narrow polystyrene standards ranging from 347 to 355 000 $g \cdot mol^{-1}$. The molecular weights of poly(MA) samples were obtained by universal calibration with Mark-Houwink parameters for polystyrene ($K=11.4 \cdot 10^{-5}$ $dL \cdot g^{-1}$, a = 0.716) and poly(MA) ($K = 6.11 \cdot 10^{-5}$ $dL \cdot g^{-1}$, a = 0.799) at low molecular weights.[25]

7.3 Results and Discussion

7.3.1 Effects of changing flow rate and reactor length on reaction kinetics

The experimental conditions and steady state properties of pMA produced by SET-LRP in a continuous copper tubular reactor are summarized in Table 7.1. In all cases, living polymer was produced with high initiator efficiency (74 to 92%) and a narrow molecular weight distribution. As the reaction was catalyzed by the copper wall surface, the steady state conversion was strongly correlated to mean residence time (τ) which was varied by changing the mass flow rate (υ) and/or length of copper tubing used. The polymerization proceeded very rapidly at ambient temperature, reaching 43% conversion with τ=4 min and 67% conversion for τ=16 min. The process was exothermic, with a measured outer wall temperature between 28-32 °C at the inlet, which decreased to slightly over ambient at the outlet.

Table 7.1: Steady state properties of PMA prepared by SET-LRP in tubular reactor. All experiments were conducted at ambient temperature with ratio of reactants $[MA]_0$:$[MBrP]_0$:$[Me_6TREN]_0$ of 100:1:0.05, and 30 wt% DMSO as solvent.

Exp.	Reactor length (m)	Reactor volume (mL)	υ (g min^{-1})	τ (min)	conv [a] (%)	$M_{n,theo}$ [b] (g·mol^{-1})	$M_{n,GPC}$ (g·mol^{-1})	PDI	I_{eff} [c] (%)
T1	3.81	8	2	4	43	3680	4960	1.35	74
T2	7.62	16	2	8	53	4540	4930	1.22	92
T3	15.24	32	2	16	67	5740	6660	1.44	86
T4	7.62	16	1	16	67	5740	6280	1.35	91
T5 [d]	15.24	32	2	16	47	4025	4390	1.30	92

[a] conversion and molecular weight data taken at steady state. [b] $M_{n,theo} = ([M]_0/[EBiB]_0)$ x conv. x MW_M. [c] $I_{eff} = M_{n,theo}/M_{n,GPC}$ x 100%. [d] Experiment T5 was conducted at a lower ligand ratio of $[MA]_0$:$[MBrP]_0$:$[Me6TREN]_0$ of 100:1:0.01.

As tubular reactors possess a greater surface area to volume ratio than batch vessels, improved temperature control is possible for these fast reaction rates. In the case of SET-LRP, use of a copper tube also increases the surface area available for catalysis. The surface area to volume ratio of the reactor is 24.2 $cm^2 \cdot mL^{-1}$, while the use of copper wire in literature

experiments (surface area between 1.17 to 14.40 cm^2, reaction volume approximately 1.5 mL) gives a ratio of 0.8 to 9.6 $cm^2 \cdot mL^{-1}$.[22]

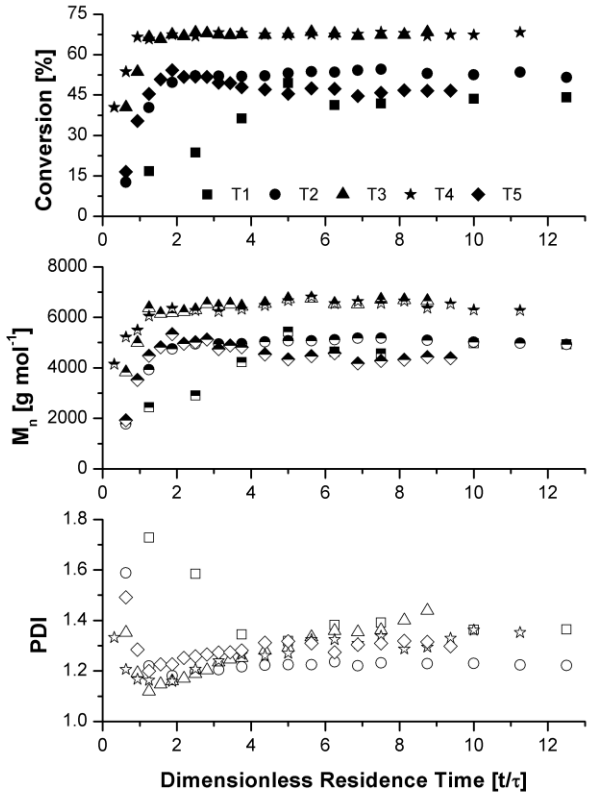

Figure 7.1: Evolution of conversion (closed symbols), number-average molecular weight (half-filled symbols), and polydispersity index (open symbols) as a function of dimensionless residence time for methyl acrylate SET-LRP polymerizations at ambient temperature in a copper tubular reactor. Experimental conditions are summarized in Table 7.1.

Plots of conversion, M_n, and polymer polydispersity index (PDI) as a function of dimensionless residence time (t/τ) are shown in Figure 7.1; as expected for this living system conversion and M_n are highly correlated. Stable steady state operation was achieved over the course of the entire experiment spanning more than 10 residence times. The results were quite reproducible as evidenced from the good agreement between experiments T3 and T4, which have identical residence times. Experiment T1 showed the most scatter in conversion and also had the lowest initiator efficiency (74%), likely due to non-ideal flow behaviour; the short reactor length

and low residence time may have prevented the flow profile from properly developing before the polymer solution exited the reactor. Interestingly, many of the experiments showed transient behaviour past the first residence time, indicating that the copper tubing possessed an activation time. This demonstrates the benefit of conducting SET-LRP in a continuous system as opposed to a batch reactor, where the induction time can vary from experiment to experiment.

Figure 7.1 also shows the evolution of the polymer polydispersity index as a function of dimensionless residence time. PDI for experiments T2-T5 drops quickly within the first residence time, reaching a minimum between the first and second residence times before rising and reaching a steady state value. Experiments T3 and T4, which achieve the highest conversions, show a slight increase in PDI after several residence times, manifested as a higher molecular shoulder in the GPC trace. These observations can best be explained by non-ideal flow behaviour of the viscous non-Newtonian solution. The reactor operates in laminar flow (Reynold's number below 100 in all cases), which results in a parabolic velocity profile with higher velocities near the center. When diffusion is low, as is the case with a viscous polymer solution, the velocity profile will elongate causing further broadening of the residence time distribution. Coiling of the reactor induces radial mixing, and can help alleviate this problem. However, since the reaction proceeds quickly and is catalyzed by the copper walls, it is likely that there will be a small reaction gradient from the wall to the center of the tube as the concentration of copper species will vary in the radial direction. (This effect is mitigated, as the polymerization is not only catalyzed by copper(0) species at the reactor wall, but also by colloidal copper(0) species in solution as well as any transient copper(I) species generated in-situ.) Any gradient would result in more rapid formation of higher molecular weight materials, and thus increased viscosity, at the reactor walls. Combined with the higher coefficient of friction at the reactor walls, the complication is compounded and channelling may occur, with the material at the center of the reactor exiting more quickly than the material at the walls. This deviation from ideal plug-flow

behaviour would cause a non-uniform residence time distribution, leading to an increased PDI. Note that this increase is not observed for Experiment T5, conducted with the same residence time as in T3 and T4 but with lower conversion and lower viscosity, and thus more uniform flow. Experiment T2 represents the most ideal behaviour with stable steady state molecular weight and conversion data. The reactor is short enough that polymer does not accumulate at the walls, and batch to batch variability and induction times have been eliminated.

The ligand level strongly impacts the rate of reaction, controlling the concentration of deactivating species as well as the extent of disproportionation.[26] For experiment T5, the ligand concentration was reduced five-fold compared to the other experiments, with only a resultant 20% decrease in conversion compared to T3 (with identical τ). The reduction in ligand has no adverse effect on the control of the polymerization, as the molecular weight distribution remains narrow despite a lower copper concentration. The ability to significantly decrease ligand use while maintaining control of the polymerization and a reasonable reaction rate has considerable economic implications both in material cost and post-polymerization purification for copper removal.

7.3.2 Chain extension of outlet polymer solution

Table 7.2 summarizes the experimental conditions and properties of a series of chain extension experiments conducted to verify livingness of the polymer produced in the copper tube. Polymer solution from T1 was chosen as it had the highest residual monomer content. Chain extension of T1 was attempted in three ways. First, the solution was simply purged with nitrogen and heated to 30 °C (X1). X1 did not polymerize further, due to oxygen saturation before chain extension, resulting in soluble copper species being converted to inactive states. When copper wire was added (X2), the solution quickly re-initiated and the conversion increased to 86% in the first hour. The M_n increased from 5350 to 8270 $g \cdot mol^{-1}$, and the PDI decreased from 1.32 to 1.14. Tin(II) 2-ethylhexanoate, a commonly used reducing agent in ARGET ATRP was used in chain extension

X3; although reducing agents are typically used in ARGET ATRP to re-initiate a polymerization, they have also been used in SET-LRP to enhance reactivity by converting accumulated copper(II) species into their copper(I) state and to activate copper surfaces.[27] The use of tin resulted in a slower reaction (conversion of 87% after 17 h), but was nonetheless effective at re-activating the dormant chains. GPC traces of chain extensions X1, X2, and X3, the latter examined at various reaction times, are shown in Figure 7.2. As the traces are normalized with respect to area, there is a noticeable narrowing of the distribution upon extension, as well as an increase to higher MW values.

Table 7.2: Experimental conditions and properties of PMA chain extension experiments conducted in batch at 30 °C.

Exp.	Condition	conv $_{init}$ (%)	$M_{n,\ init}$ ($g \cdot mol^{-1}$)	PDI $_{init}$	conv $_{final}$ (%)	$M_{n,\ final}$ ($g \cdot mol^{-1}$)	PDI $_{final}$
X1	T1, purged and heated	52	5350	1.32	52	5350	1.32
X2	T1, purged, heated, with Cu wire	52	5350	1.32	87	8270	1.14
X3	T1, purged, heated, with $Sn(II)EH_2$	52	5350	1.32	86	8200	1.14
X4	T4, purged, heated, with Cu wire	33	6500	1.32	80	13970	1.10

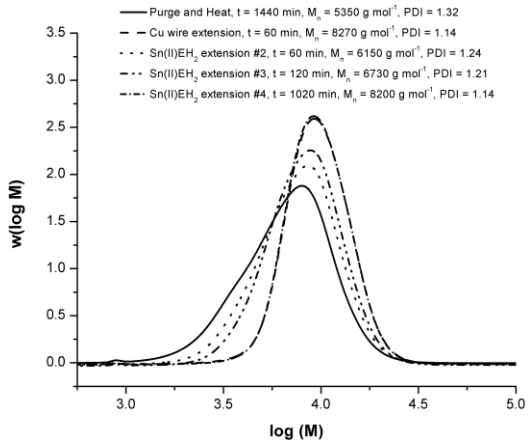

Figure 7.2: Gel permeation chromatography traces for pMA chain extensions of experiment T1. The traces are normalized by area, and experimental conditions of the extensions are shown in Table 7.2.

As an upwards drift in PDI was observed towards the end of experiments T3 and T4, a chain extension with the outlet polymer from one of these experiments was conducted to determine whether the formation of a high MW shoulder indicates a loss of livingness; channelling would form living higher molecular weight polymer while termination would form dead chains. Material from T4 was used for chain extension (X4) with additional monomer, and the GPC traces are shown in Figure 7.3. The high molecular weight shoulder gradually disappears during polymerization and the molecular weight distribution statistically evolves. The molecular weight increases from 6500 to 13960 $g \cdot mol^{-1}$, and the PDI decreases from 1.32 to 1.1. The chain extension of X4 demonstrates that, despite the higher PDI, the polymer produced from the copper tubular reactor is living, and that it is possible to polymerize methyl acrylate in a controlled manner using copper tubing as the catalyst in a continuous process at high solid content.

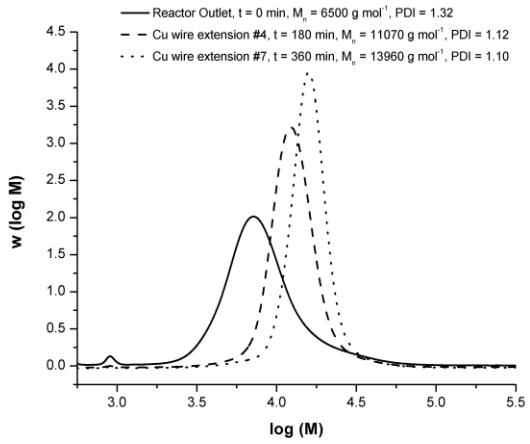

Figure 7.3: Gel permeation chromatography traces for pMA chain extensions of experiment T4. The traces are normalized by area, and experimental conditions of the extensions are shown in Table 7.2.

7.4 Conclusion

The concept of using copper tubing to form a continuous reactor wherein the reactor walls acted as a catalyst in SET-LRP was successfully demonstrated. Methyl acrylate was polymerized at ambient temperature with 30 wt% DMSO as solvent, and Me_6TREN as ligand. The polymerizations proceeded very quickly, reaching 67% conversion for a residence time of 16 minutes. Lower ligand levels could be used without a precipitous decrease in reaction rate, offering the potential to balance the increased reactor volume (residence time) required with decreased raw material and post-process purification costs.

While there was some broadening of the molecular weight distributions due to channelling inside the reactor, chain extension experiments using outlet polymer from the continuous experiments demonstrated that the polymer chains retained a high degree of livingness. The polymer solution could be reinitiated using either copper wire or a reducing agent, with both options giving a well-controlled chain extension with further narrowing of the distributions. The results illustrate the significant potential of using a copper tubular reactor as an efficient means to scale-up production of well controlled polyacrylics in a continuous process. Further studies are being conducted on decreasing ligand concentration, while maintaining a high rate of polymerization for the production of copolymers.

References

(1) Matyjaszewski, K.; Xia, J. *Chemical Reviews* **2001**, *101*, 2921-2990.

(2) Ouchi, M.; Terashima, T.; Sawamoto, M. *Chemical reviews* **2009**, *109*, 4963-5050.

(3) Matyjaszewski, K.; Spanswick, J. *Materials Today* **2005**, *8*, 26-33.

(4) Matyjaszewski, K. "Controlled radical polymerization: state of the art in 2008", in: *Controlled/Living Radical Polymerization: Progress in ATRP*, K.Matyjaszewski, Ed., ACS Symp. Ser. 1023, 2009, chap. 1, p. 3.

(5) Destarac, M. *Macromolecular Reaction Engineering* **2010**, *4*, 165-179.

(6) Shen, Y.; Zhu, S.; Pelton, R. *Macromolecular Rapid Communications* **2000**, *21*, 956–959.

(7) Shen, Y.; Zhu, S. *AIChE Journal* **2002**, *48*, 2609-2619.

(8) Müller, M.; Cunningham, M. F.; Hutchinson, R. A. *Macromolecular Reaction Engineering* **2008**, *2*, 31-36.

(9) Noda, T.; Grice, a; Levere, M.; Haddleton, D. *European Polymer Journal* **2007**, *43*, 2321-2330.

(10) Chan, N.; Boutti, S.; Cunningham, M. F.; Hutchinson, R. A. *Macromolecular Reaction Engineering* **2009**, *3*, 222-231.

(11) Chan, N.; Cunningham, M. F.; Hutchinson, R. A. *Macromolecular Reaction Engineering* **2010**, *4*, 369-380.

(12) Bally, F.; Serra, C. A.; Hessel, V.; Hadziioannou, G. *Macromolecular Reaction Engineering* **2010**, *4*, 543-561.

(13) Jakubowski, W.; Min, K.; Matyjaszewski, K. *Macromolecules* **2006**, *39*, 39-45.

(14) Matyjaszewski, K.; Jakubowski, W.; Min, K.; Tang, W.; Huang, J.; Braunecker, W. A.; Tsarevsky, N. V. *Proceedings of the National Academy of Sciences of the United States of America* **2006**, *103*, 15309-15314.

(15) Percec, V.; Guliashvili, T.; Ladislaw, J. S.; Wistrand, A.; Stjerndahl, A.; Sienkowska, M. J.; Monteiro, M. J.; Sahoo, S. *Journal of the American Chemical Society* **2006**, *128*, 14156-14165.

(16) Rosen, B. M.; Percec, V. *Chemical Reviews* **2009**, *109*, 5069-5119.

(17) Lligadas, G.; Rosen, B. M.; Bell, C. a.; Monteiro, M. J.; Percec, V. *Macromolecules* **2008**, *41*, 8365-8371.

(18) Lligadas, G.; Rosen, B. M.; Monteiro, M. J.; Percec, V. *Macromolecules* **2008**, *41*, 8360-8364.

(19) Jiang, X.; Fleischmann, S.; Nguyen, N. H.; Rosen, B. M.; Percec, V. *Journal of Polymer Science Part A: Polymer Chemistry* **2009**, *47*, 5591-5605.

(20) Lligadas, G.; Percec, V. *Journal of Polymer Science Part A: Polymer Chemistry* **2007**, *45*, 4684-4695.

(21) Matyjaszewski, K.; Tsarevsky, N. V.; Braunecker, W. A.; Dong, H.; Huang, J.; Jakubowski, W.; Kwak, Y.; Nicolay, R.; Tang, W.; Yoon, J. A. *Macromolecules* **2007**, *40*, 7795-7806.

(22) Nguyen, N. H.; Rosen, B. M.; Lligadas, G.; Percec, V. *Macromolecules* **2009**, *42*, 2379-2386.

(23) Levere, M. E.; Willoughby, I.; O'Donohue, S.; de Cuendias, A.; Grice, A. J.; Fidge, C.; Becer, C. R.; Haddleton, D. M. *Polymer Chemistry* **2010**, *1*, 1086-1094.

(24) Britovsek, G.; England, J.; White, A. J. P. *Inorganic Chemistry* **2005**, *44*, 8125-8134.

(25) Gruendling, T.; Junkers, T.; Guilhaus, M.; Barner-Kowollik, C. *Macromolecular Chemistry and Physics* **2010**, *211*, 520-528.

(26) Nguyen, N. H.; Jiang, X.; Fleischmann, S.; Rosen, B. M.; Percec, V. *Journal of Polymer Science Part A: Polymer Chemistry* **2009**, *47*, 5629-5638.

(27) N. H. Nguyen and V. Percec, Journal of Polymer Science Part A: Polymer Chemistry, 2010, 48, 5109-5119.

Chapter 8

Copper Mediated CRP in the Presence of Ascorbic Acid in a Continuous Tubular Reactor

Preface

In Chapter 7, the concept of using copper tubing to construct a continuous tubular reactor where the copper walls acted as a catalyst source was presented. The high copper surface area enabled room temperature polymerizations of methyl acrylate to a moderate conversion in very short residence times. Although the proof of concept was successful, concerns were raised over the viability of the reactor for long term operation as copper was leeched from the reactor wall into solution. In addition, higher molecular weight material seemed to form along the reactor walls due to preferential activation by the copper surface, which broadened the final molecular weight distribution and may cause fouling. In this chapter, an improved reactor design using a combination of copper and stainless steel tubing is proposed to address the shortcomings with an all copper design. The effect of ascorbic acid in SET-LRP is also investigated for the first time. The results provide insight into the SET-LRP mechanism, and demonstrate a process design that may be viable for larger scale production of novel multiblock copolymers. The contents of this chapter have been published as a full paper in Polymer Chemistry (2012, vol. 3, 1322-1333).

Abstract

Controlled radical polymerization of methyl acrylate catalyzed by copper was conducted in a continuous tubular reactor. A length of copper tubing was used to initiate polymerization and generate soluble copper species, while the bulk of polymerization took place in inert stainless steel tubing. To mediate polymerization in the absence of copper surface, environmentally benign ascorbic acid was used for the first time in single electron transfer-living radical polymerization (SET-LRP) as a reducing agent to regenerate activating copper species. Polymerizations were conducted at ambient temperature with 30 wt% DMSO as solvent, producing well defined living polymer at a steady state conversion of 78% for a residence time of 62 minutes. Chain extensions using outlet polymer solutions were well-controlled and proceeded to high conversion in a short period of time, with a final concentration of 10 ppm of residual copper. The results illustrate the significant potential of using a continuous tubular reactor with ascorbic acid as a reducing agent as an efficient means to scale-up production of well controlled polyacrylics and other multiblock copolymers.

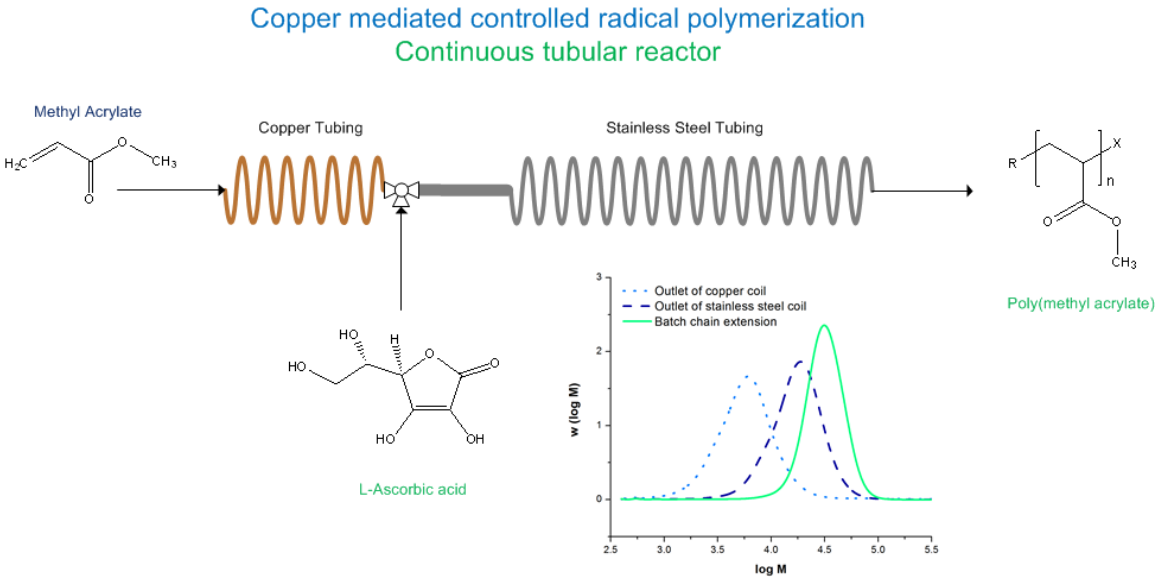

8.1 Introduction

Controlled radical polymerization (CRP) has been the subject of intense academic interest as an attractive route towards the synthesis of novel polymeric materials that cannot be produced using conventional free radical polymerization methods. Atom transfer radical polymerization (ATRP) is an effective and dynamic technique for the controlled polymerization of many vinyl monomers under mild conditions.[1-4] A transition metal catalyst is used in ATRP to mediate reversible activation and deactivation of dormant and growing radicals. Conventional ATRP utilises copper(I) and copper(II) salts with nitrogen based ligands in stoichiometric or slight sub-stoichiometric ratios relative to the initiating species, which results in a high catalyst concentration on the order of 10^4 parts per million (ppm) in the final polymer. This high concentration of transition metal leads to difficulties in process design as post polymerization treatments are required to remove residual catalyst which is often toxic and adds undesired colour to the final product.[5] This complication imposes increased production cost, and has hindered the adoption of ATRP on an industrial scale.[6-9]

Improved understanding of the electrochemistry involved in ATRP has led to the development of more active catalyst complexes and novel ATRP techniques such as "activator regenerated by electron transfer" (ARGET),[10] "initiators for continuous activator regeneration" (ICAR),[11] and "single electron transfer-living radical polymerization" (SET-LRP).[12,13] All three variants allow for reduction in catalyst concentrations by 2-3 orders of magnitude to below 10^2 ppm levels in the final polymer. Of the three techniques, ARGET and ICAR are most similar to conventional ATRP, with a reducing agent or a free radical initiator added to the polymerization to regenerate copper(I) activating species from copper(II) deactivators that have accumulated due to bimolecular radical termination.

At first glance, SET-LRP bears a strong resemblance to ATRP, as copper species are used in both systems to govern the equilibrium between activation and deactivation species.

However, Percec *et al.* propose that in SET-LRP, copper(0) acts an activating species via outer sphere electron transfer to form transient copper(I) species.[14] Under appropriate combinations of polar or coordinating solvents (DMSO, alcohols, water) and ligands that favour disproportionation, copper(I) species undergo near instantaneous disproportionation into copper(0) and copper(II) species to form activators and deactivators in pairs.[15,16] This catalytic cycle is proposed to give greater control over the polymerization and retention of chain end fidelity compared to ATRP, for which copper(I) species are the primary activators via inner sphere electron transfer.[17]

Recent studies into SET-LRP have suggested that copper(0) has a dual role as reducing agent and activator.[18-20] The duality of copper(0) suggests that it may be possible to utilise reducing agents common to ARGET ATRP to enhance the polymerization rate and increase tolerance to air in SET-LRP by changing the amount of reducing agent that is added. It has been established that changing the ratio of reducing agent to copper species can alter the ratio of activating to deactivating species, to increase the rate of polymerization in ATRP.[21-24] There has been very little research done, however, combining SET-LRP with reducing agents. It was found that SET-LRP polymerizations with hydrazine, a commonly used reducing agent in ATRP, showed a higher rate of polymerization as well as increased tolerance to air.[25,26] However, the mode of activation for hydrazine was attributed to reduction of Cu_2O generated by the oxidation of copper(0) with air in the system. The use of hydrazine was later extended to activation of copper(0) surface to increase the rate of polymerization.[27] Unfortunately, hydrazine is a highly reactive and toxic chemical and poses a hazard even in small quantities. In a previous study, we were able to re-initiate a SET-LRP reaction using a non-toxic reducing agent, tin(II) 2-ethylhexanoate, in the absence of additional copper(0) metal.[28] While the effect of reducing agent concentration was not investigated, the results demonstrate the potential for other non-toxic and environmentally benign reducing agents such as ascorbic acid to be beneficial for SET-LRP.

Although the mechanistic nature of SET-LRP is still a subject of scrutiny in literature,[12,14,15,29,30] it has been established that SET-LRP processes offers several advantages when compared with ATRP systems. Compatibility with polar solvents such as alcohols and water offer the use of more environmentally friendly reaction media, in addition to making SET-LRP more suitable for the polymerization of water-soluble or amphiphilic materials. Catalyst can be added in the form of elemental copper powder or wire, greatly simplifying catalyst handling, removal and recycling.[15,31] Furthermore, it can polymerize acrylics at low temperature with excellent control and much faster reaction rates than observed in ATRP. Soeriyadi *et al.* have used this level of enhanced control and reactivity to synthesize high-order multi-block copolymers via an iterative SET-LRP procedure.[32] The polymerizations proceeded to high conversion, and it was possible to polymerize additional blocks without isolating the existing polymer, greatly simplifying the number of steps required when compared to ATRP or other CRP techniques.

At the same time, SET-LRP is not without its own set of issues. Induction times in laboratory scale reactions are occasionally observed which can lead to batch to batch variability in polymer properties under the same process parameters.[31,33] Additionally, due to the large heat release associated with rapid polymerization, SET-LRP reactions are highly exothermic. Levere *et al.* observed internal temperatures in excess of 60-100 °C for SET-LRP of methyl acrylate conducted initially at room temperature in a small Schlenk tube (working volume of approximately 25 mL) due to insufficient heat removal.[33] This behaviour poses risk of runaway reaction when polymerization is scaled to larger volumes, and might make it difficult to conduct SET-LRP in batch reactors on a commercial scale.

While there is only a limited number of publications studying the use of ATRP in continuous processes,[34-36,24,37] the engineering challenges surrounding SET-LRP can be readily remedied by the use of continuous reactors. Inconsistencies between start-up are conveniently

eliminated in continuous processes, and once at steady state, continuous processes yield more consistent product quality and higher productivity than comparable batch reactors. Continuous flow tubular reactors in particular are ideal for scale up due to their large surface area to volume ratio, which greatly improves heat removal and temperature control. We have recently demonstrated the use of copper tubing as both reactor and catalyst source in the design of a continuous tubular reactor for SET-LRP.[28] Although the proof of concept was a success, some concerns remained about the long term structural integrity of the reactor, as copper was leached from the reactor walls into solution. In addition, to synthesize multi-block copolymers in a continuous process, a higher conversion would need to be reached in a reasonable residence time.

In this work, we aim to improve upon the original reactor design and address some of the shortcomings observed. To that end, a combination of copper tubing and stainless steel tubing is used to construct a continuous tubular reactor. A short copper coil is used to initiate polymerization and generate soluble copper species *in-situ*. The majority of the reaction is then carried out in a longer segment of inert stainless steel tubing. The effects of environmentally benign and non-toxic ascorbic acid to enhance the rate of SET-LRP in the absence of copper(0) surface while maintaining good control over chain end fidelity are investigated in batch and continuous reactors and reported for the first time. The combination of an environmentally friendly additive that can be used in combination with “green” solvents, along with an improved and more robust process design makes a continuous tubular reactor an ideal platform for the synthesis of novel polymeric materials.

8.2 Experimental

8.2.1 Materials

Methyl acrylate (MA) (99%, inhibited by less than 100 ppm monomethyl ether hydroquinone, Aldrich), dimethyl sulfoxide (DMSO) (99.9%, Aldrich), methyl 2-bromopropionate (MBP) (98%, Aldrich), L-ascorbic acid (AscA) (99%, Aldrich), and nitrogen gas (Praxair, 99.998%) were used as received. Tris[2-(dimethylamino)ethyl]amine (Me_6TREN) was synthesized as described previously.[38]

8.2.2 Continuous tubular reactor setup

A schematic of the reactor setup is shown in Figure 8.1. The reactor was split into two sections. Section 1 was composed of an Eldex Recipro VS series high pressure liquid metering pump (B-125-VS), capable of feeding between 0.2 to 10.0 mL·min^{-1}. The pump was connected to a series of refrigeration grade copper tubing (3.2 mm outer diameter, 1.65 mm inner diameter). The tubing was split into four pieces of equal length, for a total length of 15.24 m and a total volume of approximately 32 mL. The modular nature of the copper tubing allowed for facile assembly into reactor configurations ranging from 8 to 32 mL. A 500 mL three neck round bottom flask was used as a feed vessel, and the feed solution was kept stirring under nitrogen.

The outlet solution from the copper tubing was mixed continuously with material from Feed Tank 2 in a three way Tee union U1, designated as the beginning of Section 2. The flow rate of the second feed was also controlled by an Eldex Recipro VS series high pressure liquid metering pump (B-125-VS). U1 was connected to a 10 cm section of stainless steel tubing (6.35 mm outer diameter, 4.57 mm inner diameter). A small piece of copper wire (0.155 mm in diameter, 1.44 g) was inserted into the tubing and valve to act as a baffle and enhance mixing between the two feeds. This section of the reactor was designated as the mixing junction as shown in the schematic. A narrower set of stainless steel tubing (15.24 m in length, 3.2 mm outer

diameter, 2.1 mm inner diameter) was connected to the mixing junction. The total mass flow rate out of the stainless steel tubing was controlled as the sum of the two metering pumps, and the flow rate was measured using a Mettler Toledo PG 5002s balance. The entire reactor configuration was kept in a fume hood and all polymerizations were done at ambient temperature (23-25 °C). The copper coils and copper wire baffle were weighed before and after each experiment, and mass loss was determined to be negligible (< 0.1% of total weight).

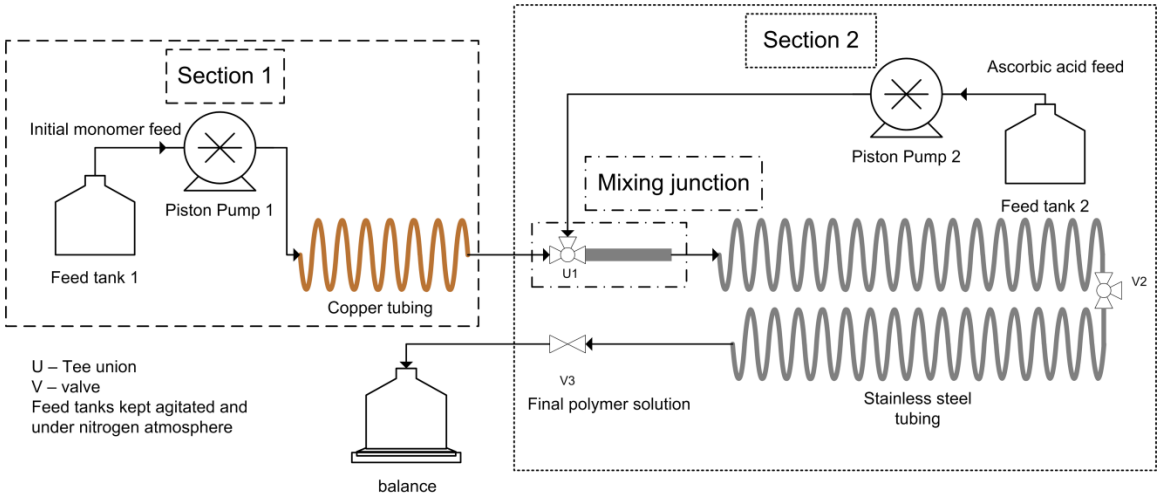

Figure 8.1: Schematic of continuous tubular reactor used for copper(0) mediated polymerization.

8.2.3 Synthesis procedure for continuous SET-LRP polymerization in copper tubing

MA (210 g, 2.44 mol), DMSO (90 g, 1.15 mol), Me_6TREN (0.046 g, 0.244 mmol), and MBP (4.08 g, 24.4 mmol) were combined in a 500 mL three neck round bottom flask for a ratio of reactants $[MA]_0$:$[MBP]_0$:$[Me_6TREN]_0$ of 100:1:0.01. The initial recipe gave a target degree of polymerization of 100, a target number-average molecular weight (M_n) of 8640 $g \cdot mol^{-1}$ and a polymer content of 70 wt% at full conversion. The feed solution was kept agitated and purged with nitrogen for approximately 1 hour before the start of polymerization. At the same time, the copper tubing was flushed with nitrogen to minimize inhibition from the presence of oxygen in the system.

After deoxygenation, the reactants were pumped into the copper tubing at a high flow rate to fill the reactor, typically taking 2-4 minutes. Once the reactor was filled, the flow rate was reduced to 1 $g \cdot min^{-1}$. This action was considered the start of the polymerization. The flow rate was carefully monitored over the course of the polymerization, and samples were taken at specified time intervals from the outlet of the copper tubing (outlet of Section 1).

8.2.4 Synthesis procedure for continuous SET-LRP with entire reactor

As with the procedure above, a feed solution was prepared for section 1 of the reactor. MA (175 g, 2.03 mol), DMSO (75 g, 0.96 mol), Me_6TREN (0.038 g, 0.203 mmol), and MBP (3.40 g, 20.3 mmol) were combined in a 500 mL three neck round bottom flask. The feed solution (F1) was stirred and purged with nitrogen for approximately 1 hour before the start of polymerization. At the same time, MA (175 g, 2.03 mol), DMSO (75 g, 0.96 mol), and ascorbic acid (0.036 g, 0.203 mmol) were combined in another 500 mL three neck round bottom flask. This second feed solution (F2) was also stirred and purged with nitrogen for approximately 1 hour before the start of polymerization.

While the feed solutions were being purged, nitrogen was flushed through both the copper and stainless steel tubing to minimize the impact of oxygen in the system. After the feed solutions were deoxygenated, the first feed solution F1 containing monomer, ligand and initiator was fed into the copper tubing at a flow rate of 1 $g \cdot min^{-1}$. After approximately 15 minutes, the copper tubing, the mixing junction, and the inlet section of the stainless steel tubing have all been saturated with reagents. At that time, feeding of F2 was started at the same flow rate of 1 $g \cdot min^{-1}$. This action was considered the start of the polymerization. The total flow rate out of the reactor was carefully monitored to be the sum of the individual metering pumps for a total of 2 $g \cdot min^{-1}$. Samples were taken at specified time intervals from the outlet of the reactor. The target molecular weight of the polymerization was 17280 $g \cdot mol^{-1}$ (DP_n = 200), for a ratio of reactants $[MA]_0$:$[MBP]_0$:$[Me_6TREN]_0$:$[AscA]_0$ of 200:1:0.01:0.01. Solvent content was 30% by mass.

8.2.5 SET-LRP batch polymerization procedure with ascorbic acid

A few batch polymerizations were conducted to study the effects of adding ascorbic acid to a SET-LRP reaction. MA (35 g, 0.407 mol), DMSO (12.5 g, 0.16 mol), Me_6TREN (0.0077 g, 0.0407 mmol), and MBP (0.68 g, 4.07 mmol) were combined in a 100 mL three neck round bottom flask. The mixture was purged under nitrogen for one hour, before being submerged in an oil bath set to 30 °C. Ascorbic acid (7.2 mg, 0.0407 mmol) was dissolved in 2.5 g of DMSO, purged with nitrogen for ten minutes and then transferred to the round bottom flask via a degassed syringe. A piece of copper wire (0.155 m in diameter, 2.024 g) was gently scrubbed with acetone and a non-abrasive material to remove any surface residue, wrapped around a stir bar and then added to the flask to initiate polymerization. Samples were withdrawn using a deoxygenated syringe at specified time intervals, cooled and exposed to air to stop polymerization. The target molecular weight of the polymerization was 8640 $g \cdot mol^{-1}$ (DP_n = 100). Solvent content was 30% by mass.

8.2.6 Synthesis procedure for chain extension of outlet polymer

Chain extensions using outlet solution from the tubular reactor were conducted to verify the livingness of the polymer produced. 25 g of polymer solution from the outlet was added to a 100 mL three neck round bottom flask. MA (17.5 g, 0.203 mol) and DMSO (5 g, 0.064 mol) were also added to the flask. The polymer solution was then purged with nitrogen for 1 hour and placed into an oil bath set at 30 °C. Me_6TREN (7.7 mg, 0.0407 mmol) was mixed with 1 g of DMSO, purged with nitrogen and then injected into the system via a degassed syringe. After approximately 10 minutes, ascorbic acid (1.8 mg, 0.010 mmol) dissolved in 1.5 g of DMSO purged with nitrogen was also injected via a degassed syringe to reinitiate polymerization. Samples were withdrawn using a deoxygenated syringe at specified time intervals.

8.2.7 Analytical methods and characterization

Sample conversion was determined by gravimetry. Gel permeation chromatography (GPC) was used to determine the molecular weight distribution of the polymer samples. Samples were prepared by dissolving 30 mg of dried polymer in 3 mL of THF. The dissolved samples were then passed through a column packed with basic alumina to remove any remaining copper, before being filtered through a nylon filter (0.2 µm pore size). The GPC was equipped with a Waters 2960 separation module containing four Styragel columns of pore sizes 100, 500, 10^3, 10^4 Å, coupled with a Waters 410 differential refractive index (RI) detector (930 nm) operating at 40 °C. THF was used as eluant and the flow rate was set to 1.0 mL·min^{-1}. The detector was calibrated with eight narrow polystyrene standards ranging from 347 to 355 000 g·mol^{-1}. The molecular weights of poly(MA) samples were obtained by universal calibration with Mark-Houwink parameters for polystyrene (K=11.4·10^{-5} dL·g^{-1}, a = 0.716) and poly(MA) (K = 6.11·10^{-5} dL·g^{-1}, a = 0.799) at low molecular weights.[39]

8.2.8 Residual copper concentration measurements

Residual copper concentration in the polymer solution was measured by flame atomic absorption spectroscopy using a Varian Spectra AA-20 Plus Flame Atomic Absorption Spectrometer, with a copper lamp set to a wavelength of 324.9 nm. The outlet polymer solution was diluted in methyl isobutyl ketone (MIBK) at a ratio of 1:20. Calibration standards were prepared from 500 ppm 21 Elemental Standard in MIBK in a range of dilutions from 0.5 ppm to 5.0 ppm. A calibration check solution was prepared from 300 ppm 21 Element Standard at a concentration of 3.0 ppm.

8.3 Results and discussion

8.3.1 Limitations of an all copper tubular reactor

As briefly discussed in the introduction, there were three impediments for use of the original all copper tubular reactor for large scale production of polymeric materials:

1. Structural integrity of the reactor as copper leaches from the reactor walls.
2. Reaching a high steady state conversion with a reasonable residence time for the product of block copolymers.
3. Broadening of the molecular weight distribution with operation time due to possible radial gradient of reactants across the diameter of the tube at higher conversions.

In the original study,[28] the three problems were correlated and difficult to separate. The copper reactor wall acts as a catalyst source for the activation of dormant chains, and activation of a polymer chain or initiating alkyl halide species generates a copper(I) species on the reactor wall which becomes more readily soluble in solution. As such, the amount of copper that leaches into solution is proportional to the number of activations along the length of the reactor. It is possible to limit the amount of soluble copper species by decreasing the ligand concentration, but doing so will generally slow the reaction rate.[40]

To reach a higher steady state conversion in a continuous tubular reactor, process operating parameters such as temperature or residence time can be altered. Increasing the residence time, either by lowering the flow rate or increasing the length of the reactor, leads to higher conversion.[28] However, solution viscosity also increases, slowing transport of copper species across the radius of the reactor. This makes it likely that chains which are closer to the reactor wall and catalyst source will grow more quickly, leading to a population of higher molecular weight chains and broadening the outlet molecular weight distribution, as was observed experimentally.

In addition, increasing the length of copper tubing increases the available surface area for catalysis. As activation can occur anywhere along the reactor wall, the increased length of copper tubing makes it more difficult to detect where structural integrity may be compromised due to copper leaching. Therefore, it is beneficial that the copper surface area and amount of copper which can leach into solution be limited to improve reactor operation and reduce maintenance.

To illustrate this interdependent behaviour, three experiments were conducted in copper tubing of various lengths. The experimental conditions and steady state properties of the poly(methyl acrylate) (pMA) produced are summarized in Table 8.1. The experiments were conducted with a low ligand ratio of 1:100 with respect to initiator, to limit the amount of soluble copper in order to prolong the longevity of the reactor as well as to reduce the need for removal of residual copper in a post polymerization treatment.

Table 8.1: Steady state properties of pMA prepared by SET-LRP in copper tubular reactor with a single feed. All experiments were conducted at ambient temperature with ratio of reactants $[MA]_0$:$[MBP]_0$:$[Me_6TREN]_0$ of 100:1:0.01, and 30 wt% DMSO as solvent.

Exp.	Reactor length (m)	Reactor volume (mL)	τ (min)	conv [a] (%)	$M_{n,theo}$ [b] ($g \cdot mol^{-1}$)	$M_{n,GPC}$ ($g \cdot mol^{-1}$)	PDI	I_{eff} [c] (%)
T1	3.81	8	8	41	3550	3960	1.48	89
T2	7.62	16	16	53	4310	5120	1.37	90
T3	15.24	32	32	59	5100	5360	1.45	95
T4 [d]	19.05	62	62	55	4780	5020	1.34	95

[a] conversion and molecular weight data taken as average steady state values after 3 residence times. [b] $M_{n,theo} = ([M]_0/[MBP]_0) \times conv. \times MW_M$. [c] $I_{eff} = M_{n,theo}/M_{n,GPC} \times 100\%$ as calculated from steady state averages. [d] Experiment T4 was conducted using a combination of copper tubing (3.81 m) and stainless steel tubing (15.24 m).

In all three experiments, living polymer was produced with high initiator efficiency (89 to 95%), although the molecular weight distributions were broadened due to the relatively low conversion. The changes in conversion, number average molecular weight (M_n), and polymer polydispersity index (PDI) as a function of dimensionless residence time (t/τ) are shown in Figure 8.2. The three experiments all showed some transient behaviour at the beginning of the experiment, with the reactor reaching steady state after an activation time of approximately 30 minutes. This type of activation behaviour has also been observed in batch reactions,[31,33] and

demonstrates the benefit of conducting SET-LRP in a continuous process as opposed to a batch reactor.

The data showed that increasing the reactor length and the residence time (τ) from 8 (T1) to 16 (T2) to 32 (T3) minutes gave a corresponding increase in steady state conversion of 41, 53, and 59%, respectively. With increasing conversion an increase in molecular weight was observed, with average steady state M_n values of 3960, 5120, and 5360 $g \cdot mol^{-1}$ for experiments T1-T3. It would seem that a residence time of 16 minutes (T2) is more favourable for this polymerization recipe, as increasing the residence time to 32 minutes yields only a small increase in steady state conversion, with the molecular weight distribution becoming broader most likely due to the previously discussed concentration gradients across the radial direction of the reactor.

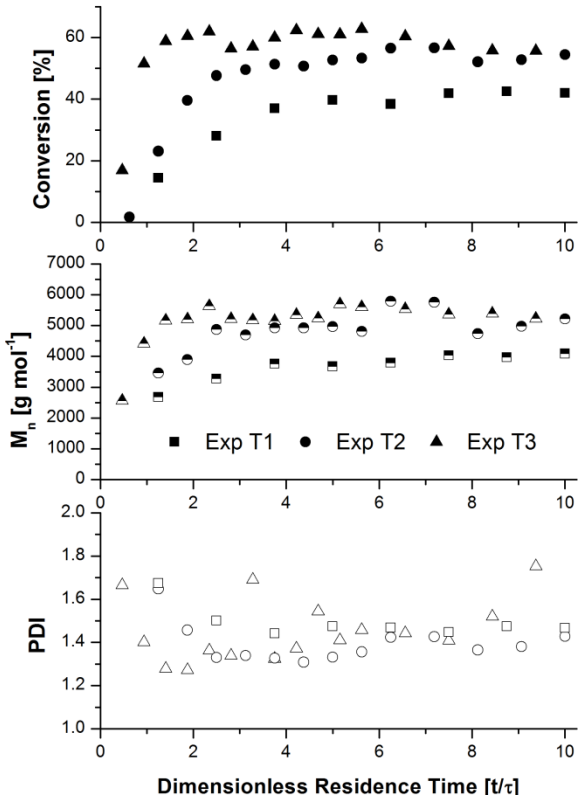

Figure 8.2: Evolution of conversion (closed symbols), number-average molecular weight (half-filled symbols), and polydispersity index (open symbols) as a function of dimensionless residence time for methyl acrylate SET-LRP polymerizations at ambient temperature in a copper tubular reactor. Experimental conditions are summarized in Table 8.1.

8.3.2 Extending the reactor using inert stainless steel tubing

A possible means to achieve higher steady state conversion at ambient temperatures with a continuous flow reactor is to use a combination of copper and stainless steel tubing. With this design, a short coil of copper tubing initiates polymerization and generates soluble or "nascent" copper species *in-situ*. The soluble copper species can then mediate the polymerization in a section of the reactor constructed of inert stainless steel. As there is no reaction between the steel walls and polymer chains, the presence of reaction gradients across the radial direction of the reactor are largely eliminated. This concept was demonstrated in experiment T4 by using a short segment of copper tubing (3.81 m) at the beginning of the reactor connected to a longer segment of stainless steel tubing (15.24 m) of the same diameter. Conversion, M_n, and PDI as a function of reaction time for experiment T4 and T1 are compared in Figure 8.3.

As the residence time of T4 was much longer than experiment T1, it took a longer period of time (>180 min) before the reactor exhibited steady state behaviour. By using an inert material to increase the reactor length, the steady state conversion was increased from 41% (T1) to 55% (T4), with a corresponding increase in M_n from 3960 to 5020 $g \cdot mol^{-1}$. The PDI decreased from 1.48 to 1.34, demonstrating that the increased reactor length did not negatively impact the PDI as observed in experiment T3. This result demonstrates that copper(0), copper(I), and copper(II) species generated *in-situ* are capable of mediating the activation and deactivation equilibrium in the absence of a heterogeneous copper surface.

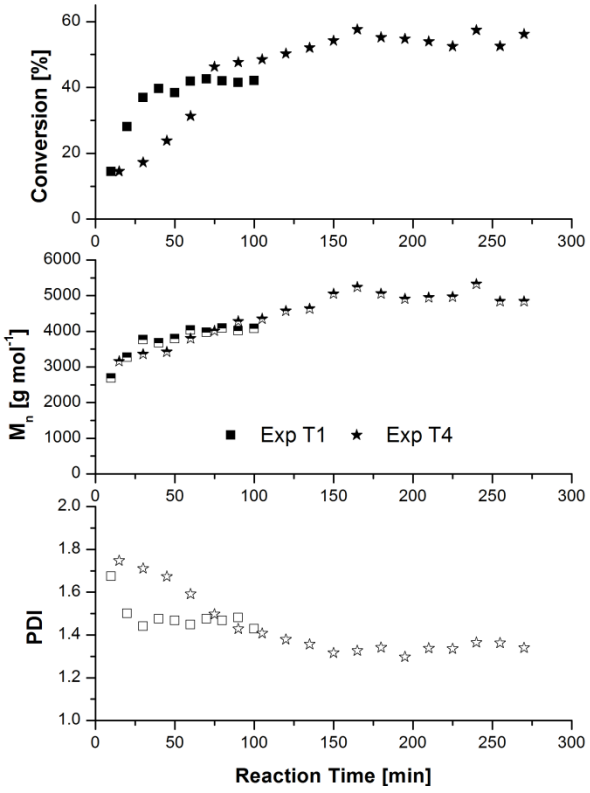

Figure 8.3: Evolution of conversion (closed symbols), number-average molecular weight (half-filled symbols), and polydispersity index (open symbols) as a function of reaction time for methyl acrylate SET-LRP polymerizations at ambient temperature in a copper and stainless steel tubular reactor. Experimental conditions are summarized in Table 8.1.

Interestingly, Lligadas *et al.* conducted a similar type of experiment in batch where they attempted to resolve the role of nascent copper(0) and copper(I) species, but achieved very different results. In their experiment, two Schlenk tubes under inert atmosphere were connected. A polymerization catalyzed by copper powder was initiated in one tube, and upon reaching 20% conversion the polymer solution was decanted to the second vessel while the copper powder was left in the first flask. In the absence of copper powder, polymerization did not continue within the bounds of experimental error. When the reaction mixture was transferred back to the flask with copper powder, polymerization restarted and reached high conversion in a short period of time. It was concluded that low levels of copper(I) species generated from activation of polymer chains

by copper(0) was unable to contribute to chain activation, and that polymerization can only proceed in the presence of an elemental copper surface as an activating species.[15]

Although contradicting the findings by Lligadas *et al.*, the result from experiment T4 provides some insight into the SET-LRP mechanism. While not possible to identify the primary activating species in the stainless steel section of the reactor, the results suggested that copper(0) was playing a role as both activator and reducing agent as suggested in literature.[18,19,29] As ATRP studies have established, bimolecular termination will lead to a build-up of copper(II) deactivating species when a low concentration of copper is used. This accumulation will alter the copper(I) to copper(II) ratio and slow or eventually stop the polymerization. It is likely that the same phenomenon was occurring in the stainless steel tubing. Independent of whether copper(0) or copper (I) was the activating species, a small amount of termination would lead to an increase in copper(II) concentration. Without the presence of a copper surface to act as activator or reducing agent, the equilibrium would thus shift towards deactivation and the build-up of dormant chains. In our previous study on copper(0) mediated CRP, several chain extensions of outlet polymer solution containing in-situ generated copper species were conducted.[28] The addition of copper wire led to fast activation of dormant polymer chains and polymerization reached high conversion in a short period of time. When no copper wire was added, polymerization did not re-initiate. Most interestingly, the addition of tin(II) 2-ethylhexanoate, a common reducing agent used in ARGET ATRP, was successful in re-initiating the polymerization although the rate of polymerization was slower. Based on this result, it was decided to investigate the effects of ascorbic acid, a stronger, non-toxic and environmentally benign reducing agent in this study.

8.3.3 Effects of ascorbic acid on SET-LRP in batch

Ascorbic acid has been used extensively as a reducing agent in ATRP for the polymerization of many water soluble polymers and in dispersed phase systems.[21,41-43] As a reducing agent for ARGET ATRP, it was found that the solvent played a large role in the reaction kinetics and

control over polymerization. When ascorbic acid was added in 10-100 fold excess to copper(II) bromide in anisole, the reducing agent remained insoluble and well controlled polymerizations were achieved. However, when a polar solvent like DMF was used, ascorbic acid was fully dissolved and fast reduction of copper(II) deactivating species led to a loss of control over the polymerization.[44] Paterson *et al.* found that for the polymerization of 2-hydroxyethyl methacrylate in methanol, an 80 fold excess of ascorbic to copper(II) bromide was required to achieve a well-controlled polymerization. A 60 fold excess gave only low conversion, and a 120 fold excess led to a loss of control over the reaction.[45] As such, it seems that for the polar solvents used in SET-LRP where ascorbic acid will be readily dissolved, a fine balancing act is required to achieve a concentration of ascorbic acid that will yield the desired polymerization kinetics.

The experimental conditions and final properties of poly(methyl acrylate) produced by SET-LRP with ascorbic acid are summarized in Table 8.2. Batch experiments B1 to B3 were conducted with a short length of copper wire as catalyst source. Experiment B1 can be considered the standard batch SET-LRP experiment, showing good control over the molecular weight distribution. The experiment reached a conversion of 73% after 180 min, with a final molecular weight of 8140 $g \cdot mol^{-1}$ and a PDI of 1.28. As the available copper surface area was much lower in a batch vessel, the rate of polymerization in experiment B1 was lower than a comparable reaction in a tubular reactor.

Table 8.2: Final properties of pMA prepared by SET-LRP in batch reactions at 30 °C.

exp.	$[M]_0$: $[MBP]_0$:$[Me_6TREN]_0$:$[AscA]_0$	t (min)	conv (%)	$M_{n,theo}$ [a] ($g \cdot mol^{-1}$)	$M_{n,GPC}$ ($g \cdot mol^{-1}$)	PDI
B1	100 : 1 : 0.01 : 0	180	73	6320	8140	1.28
B2	100 : 1 : 0.01 : 0.01	180	80	6880	6980	3.17
B3	100 : 1 : 0.01 : 0.02	180	79	6830	7880	3.57
B4 [b]	200 : 1 : 0.01 : 0.01	60	80	13780	14050	1.16
B5 [b]	200 : 1 : 0.01 : 0.02	60	96	16520	16590	1.21

[a] $M_{n,theo} = ([M]_0/[MBP]_0) \times conv. \times MW_M$. [b] Experiments B4 and B5 were conducted using outlet polymer solution from experiment T1 as explained in the synthesis procedures.

As the effects of ascorbic acid in a SET-LRP reaction were not known, it was decided to test the response by starting with a low concentration. Since there was no copper salt added to the system, the ratio was scaled with respect to ligand; experiment B2 and B3 both used a small amount of ascorbic acid, at ratios of 1:1 and 2:1 to Me_6TREN. Figure 8.4 shows the effect of ascorbic acid on the reaction kinetics. Even with a small amount of ascorbic acid present, there was a boost in polymerization rate and higher conversion was achieved. Unfortunately, ascorbic acid had a detrimental effect on polymerization control. The molecular weight distributions of two samples from experiment B2 are shown in Figure 8.5. As the GPC traces show, polymerization was initially uncontrolled and higher molecular weight polymer was formed. As polymerization continued, a low molecular weight distribution was established corresponding to activation and more controlled growth of alkyl halide initiator. Experiment B3 showed similar results, indicating that the presence of ascorbic acid, a strong reducing agent, quickly reduced any copper(II) species initially generated via the SET-LRP catalytic cycle and extinguished control over the polymerization in its early stages.

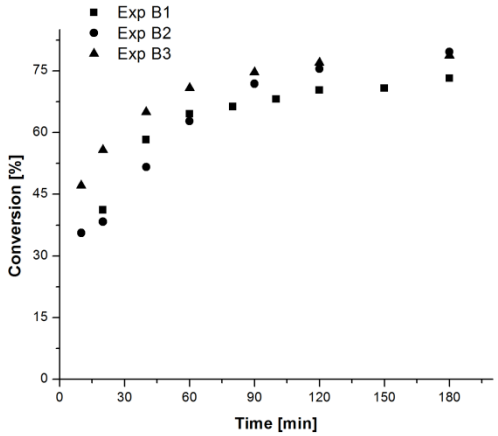

Figure 8.4: Evolution of conversion as a function of reaction time for batch experiments of methyl acrylate with copper wire and ascorbic acid. Experimental conditions are summarized in Table 8.2.

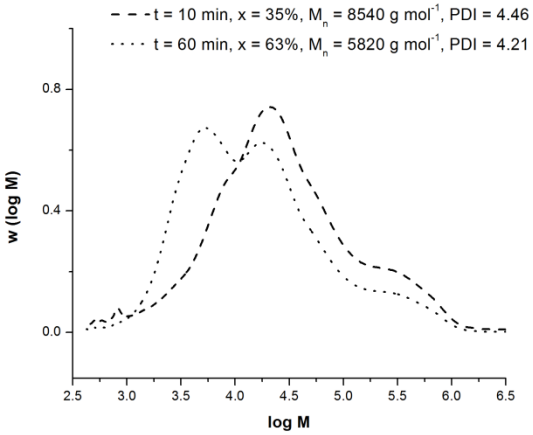

Figure 8.5: Gel permeation chromatography traces for poly(methyl acrylate) from experiment B2. The traces are normalized by area, and experimental condition of the experiment is shown in Table 8.2.

While ascorbic acid added before the SET-LRP catalytic cycle is established has an unfavourable effect over control of the polymerization, the effect is beneficial when added to a polymer solution with existing copper species in the absence of copper wire. The outlet polymer solution from experiment T1 was used to test this effect; the procedure was similar to a chain extension with a small amount of ascorbic acid added to reinitiate polymerization with additional monomer. Experiments B4 and B5 both polymerized rapidly once ascorbic acid was injected, with excellent control over the polymerization. The conversion and molecular weight data for B4 and B5 are shown in Figure 8.6 along with that of experiment B1 as a comparison.

With a one to one ratio of ascorbic acid to ligand, experiment B4 reached 80% conversion in 60 minutes, while experiment B5, with double the amount of ascorbic acid, reached 95% conversion in the same time. Both experiments showed a linear growth in molecular weight with conversion, falling almost exactly along the theoretical line and almost reaching the target molecular weights. The polydispersity decreased to a final value of 1.16 for experiment B4 and 1.21 for experiment B5. These experiments show that with an existing population of copper(II) species in solution, a small amount of ascorbic was sufficient to reduce copper(II) into copper(I)

species, which then acts as activators or undergoes the SET-LRP catalytic cycle to generate copper(0) activating species.

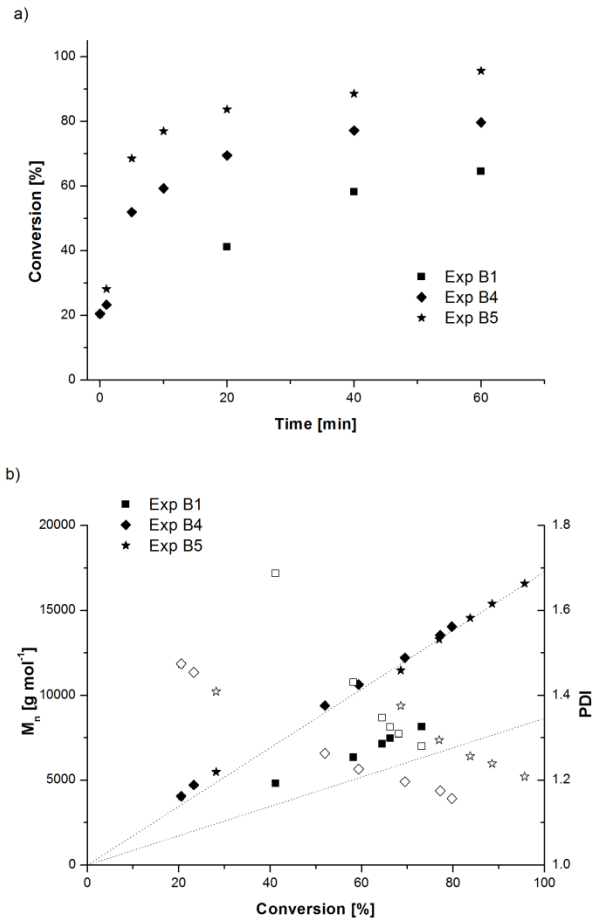

Figure 8.6: Evolution of conversion vs. time (a), and number-average molecular weight (M_n, filled symbols) and polydispersity index (PDI, open symbols) with conversion (b) for poly(methyl acrylate) prepared by SET-LRP with ascorbic acid at 30 °C. Experimental conditions are summarized in Table 8.2.

8.3.4 Effects of ascorbic acid on SET-LRP in a continuous tubular reactor

By utilizing ascorbic acid and an inert reactor, it is now possible to solve the three challenges originally discussed. The improved design is shown in Figure 8.1 in the Experimental section. Rather than constructing the entire reactor out of copper tubing, a short copper coil is used to continuously initiate polymerization and generate soluble copper species. The reaction can then be carried to higher conversion in inert stainless steel tubing, using ascorbic acid fed separately as a reducing agent to drive the activation and deactivation equilibrium. This configuration limits the amount of tubing vulnerable to copper leaching and minimizes the amount of copper in the system. In addition, the residence time and reactor length can now be extended, as the concentration gradients that occur at high conversion in the copper reactor are eliminated in the inert stainless steel tubing as the catalysis is now homogeneous across the radial direction of the reactor.

The experimental conditions and average steady state properties of poly(methyl acrylate) polymerized in the new reactor are summarized in Table 8.3. Experiments T5, T6, and T7 were conducted to test the effect of ascorbic acid concentration on reaction kinetics and polymer properties, with the ascorbic acid level increasing from 1:1, to 2:1, and finally 4:1 with respect to ligand. Note that the feed for the copper reactor was 100:1:0.01 without any added ascorbic acid. Thus, the properties of the polymer exiting the copper tube are similar to those reported for experiment T1 in Table 8.1. The 40% conversion at the outlet of the copper tube is diluted by the addition of the feed from Section 2 such that the inlet conversion for the stainless steel reactor is 20%, and the target DP_n is doubled to 200. All three experiments produced living polymer with high initiator efficiency and predictable molecular weights well in excess of what was possible with only a copper reactor.

Table 8.3: Steady state properties of pMA prepared by SET-LRP in copper and stainless steel tubular reactor with two feeds. All experiments were conducted at ambient temperature and 30 wt% DMSO as solvent.

Exp.	$[M]_0$:$[MBP]_0$:$[Me_6TREN]_0$:$[AscA]_0$	Reactor length [a] (m)	τ (min)	conv [b] (%)	$M_{n,theo}$ [c] ($g \cdot mol^{-1}$)	$M_{n,GPC}$ ($g \cdot mol^{-1}$)	PDI	I_{eff} [d] (%)
T5	200 : 1 : 0.01 : 0.01	19.05	35	65	11240	12230	1.45	92
T6	200 : 1 : 0.01 : 0.02	19.05	35	65	11180	11800	1.47	95
T7	200 : 1 : 0.01 : 0.04	19.05	35	67	11550	11800	1.42	98
T8 [e]	200 : 1 : 0.01 : 0.02	3.81	8	27	4650	4670	1.35	99
T9 [f]	200 : 1 : 0.01 : 0.02	34.29	62	78	13500	13840	1.27	98

[a] Reactor was composed of a short copper tube (3.81 m) and a longer stainless steel section (15.24 m), details as described in the Experimental section. [b] conversion and molecular weight data taken as average steady state values after 3 residence times. [c] $M_{n,theo} = ([M]_0/[MBP]_0)$ x conv. x MW_M. [d] $I_{eff} = M_{n,theo}/M_{n,GPC}$ x 100% as calculated from steady state averages. [e] Experiment T8 was conducted without stainless steel tubing after the mixing junction. [f] Experiment T9 utilized a short copper coil (3.81 m) and two sections of stainless steel tubing (30.48 m).

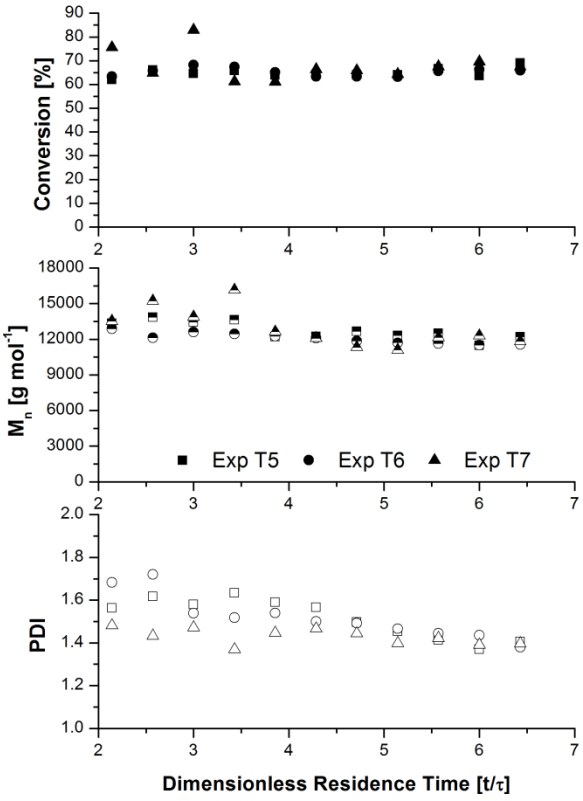

Figure 8.7: Evolution of conversion (closed symbols), number-average molecular weight (half-filled symbols), and polydispersity index (open symbols) as a function of dimensionless residence time for methyl acrylate SET-LRP polymerizations at ambient temperature in a copper tubular reactor with ascorbic acid at a residence time of 35 minutes. Experimental conditions are summarized in Table 8.3.

Conversion, M_n, and PDI as a function of dimensionless residence time (t/τ) for experiments T5-T7 are shown in Figure 8.7. The steady state values for conversion and M_n are 65%/12230 $g \cdot mol^{-1}$, 65%/11800 $g \cdot mol^{-1}$, and 67%/11800 $g \cdot mol^{-1}$ for ratios of 1:1, 2:1 and 4:1 ascorbic acid to ligand, respectively. The steady state conversion and molecular weight for all three experiments were approximately equal, indicating that for these conditions additional ascorbic acid had a negligible effect on reaction kinetics. Conversion and number average molecular weight were relatively stable over several residence times.

A peculiar observation was the slow decrease in PDI with increasing dimensionless residence time for all three experiments. Since M_n remained relatively stable, the downwards drift in PDI indicated a decrease in the weight average molecular weight. One possible explanation for this behaviour is poor mixing in the junction where the two feeds meet. A schematic of the mixing junction, constructed using a Tee union and a 10 cm piece of stainless steel tubing with a total volume of approximately 4 mL, is shown in Figure 8.8. The simple flow through design is intended to provide additional mixing time for the two feeds to equilibrate before the polymer solution entered the stainless steel reactor. However, without active agitation the mixing behaviour is most likely non-ideal, leading to a broadening of the residence time distribution. Any polymer build-up in the dead space would lead to a gradual elution of higher molecular weight polymer until the reactants in the mixing junction become almost homogeneous.

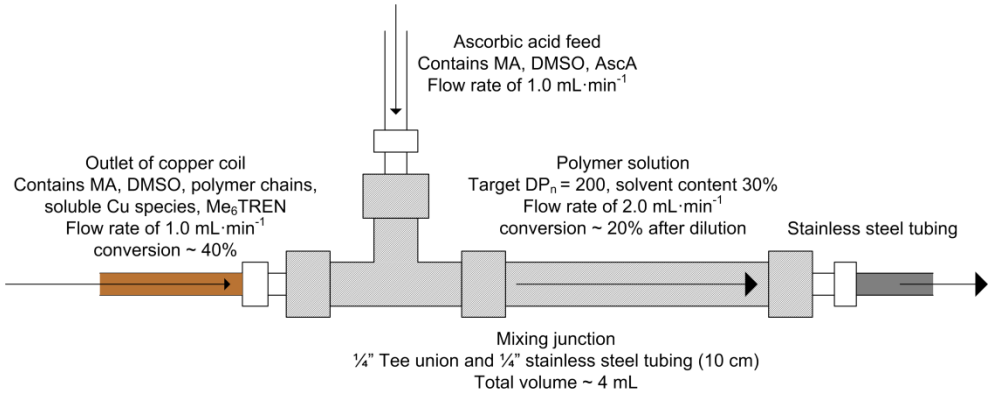

Figure 8.8: Schematic of mixing junction between the outlet of the copper reactor, the inlet of the ascorbic acid feed and the stainless steel reactor.

To test this theory, an experiment (T8) was conducted to sample the material exiting the mixing junction. Conversion, M_n, and PDI as a function of reaction time for experiment T6 (exit of stainless steel reactor) and T8 (exit of mixing junction) are shown in Figure 8.9. The first sample at time 0 of experiment T8 was taken before ascorbic acid was fed into the mixing chamber to confirm that the conversion out of the copper coils was approximately 40% as observed in experiment T1. Once the ascorbic acid feed was started, the reaction mixture was diluted and steady state conversion stabilized at approximately 27%, with an M_n of 4670 g·mol^{-1}. Although the PDI drift was not as significant as in experiment T6, the PDI of T8 decreased from 1.45-1.50 to 1.40 after approximately 150 minutes, providing support for poor mixing in the junction as a cause of PDI drift.

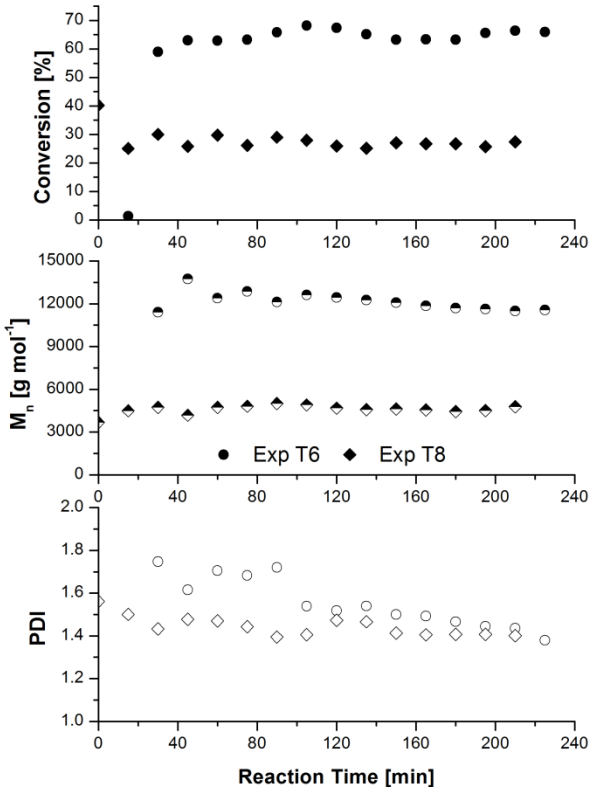

Figure 8.9: Evolution of conversion (closed symbols), number-average molecular weight (half-filled symbols), and polydispersity index (open symbols) as a function of reaction time for poly(methyl acrylate) samples at the outlet of the mixing junction and the outlet of the stainless steel reactor. Experimental conditions are summarized in Table 8.3.

Since increasing the concentration of ascorbic acid had little effect on steady state conversion values, the residence time was increased by adding another section of stainless steel tubing to give a total residence time of 62 minutes (experiment T9). Figure 8.10 shows the evolution of conversion, M_n, and PDI for experiment T6 and T9 as a function of dimensionless residence time (t/τ). As expected, increasing the residence time led to an increase in conversion to 78% along with an increased M_n of 13840 $g \cdot mol^{-1}$ and a decrease of PDI to 1.27. The narrower molecular weight distribution can be attributed to the higher outlet conversion and a corresponding larger number of activation/deactivation cycles.

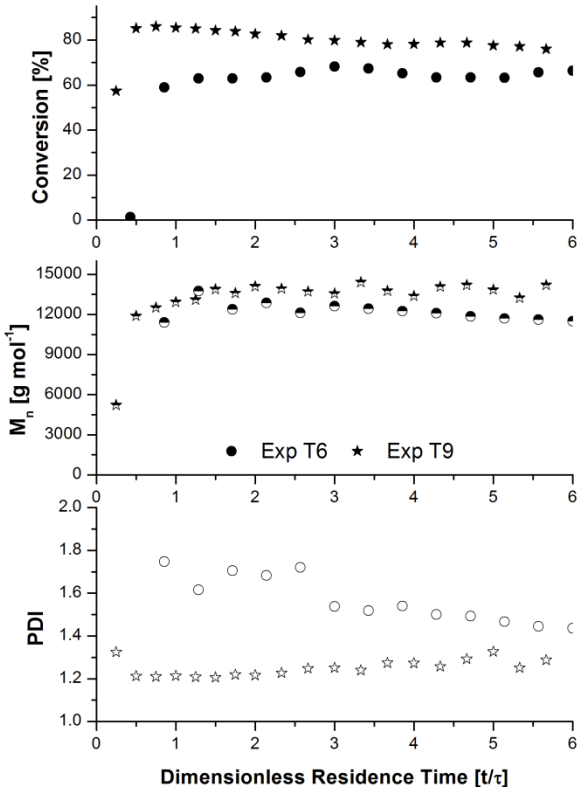

Figure 8.10: Evolution of conversion (closed symbols), number-average molecular weight (half-filled symbols), and polydispersity index (open symbols) as a function of dimensionless residence time for methyl acrylate SET-LRP polymerizations at ambient temperature in a copper tubular reactor with ascorbic acid at residence times of 35 and 62 minutes. Experimental conditions are summarized in Table 8.3.

The results from experiment T9 demonstrate that ascorbic acid can be used as reducing agent to drive a controlled SET-LRP polymerization to high conversion in the absence of copper surface. The use of stainless steel tubing to construct a continuous tubular reactor was validated, and the proposed reactor design could be used as a continuous process to produce well controlled and living polymer chains. Although methyl acrylate was used as monomer in both feeds in the study, a second monomer could have been used in the second feed to produce a block gradient copolymer instead. One can readily envision the use of a water soluble monomer such as *N*-isopropylacrylamide in the first feed to produce an amphiphilic block/gradient copolymer in one continuous process.

8.3.5 Chain extension of outlet polymer

Although ascorbic acid was shown to work well as a reducing agent, it was necessary to keep the ascorbic acid flow separate from ligand until the start of polymerization, as the basic nitrogen based ligand was prone to protonation by ascorbic acid. Additionally, during the reduction process, ascorbic acid was presumably oxidized to form dehydroascorbic acid as well as two quantities of hydrogen halide.[46,47] Since the initiator contained bromide, the reduction process would have formed hydrogen bromide or hydrobromic acid. As the products of the reduction process may also have protonated the ligand, the series of reactions may have been detrimental to retention of chain end functionality. To demonstrate the livingness of the polymer produced from the tubular reactor, chain extensions of the outlet polymer solutions from experiments T5-T9 were conducted with additional monomer. Although other monomers could have been used to produce a block copolymer, for simplicity methyl acrylate was again used to simulate the additional block. The results of the chain extension are summarized in Table 8.4.

Table 8.4: Experimental conditions and properties of pMA chain extension experiments conducted in batch at 30 °C.

Exp.	$[M]_0$:$[MBP]_0$:$[Me_6TREN]_0$:$[AscA]_0$ [a]	conv $_{init}$ [b] (%)	$M_{n,\,init}$ ($g \cdot mol^{-1}$)	PDI $_{init}$	conv $_{final}$ (%)	$M_{n,\,final}$ ($g \cdot mol^{-1}$)	PDI $_{final}$
X1	Ext. of T5, 400 : 1 : 0 : 0.01	30	11200	1.46	31	11200	1.46
X2	Ext. of T5, 400 : 1 : 0.02 : 0.01	30	11200	1.46	88	28990	1.22
X3	Ext. of T6, 400 : 1 : 0.04 : 0.01	43	13800	1.38	88	27810	1.19
X4	Ext. of T7, 400 : 1 : 0.08 : 0.01	45	15320	1.35	90	29390	1.19
X5	Ext. of T9, 400 : 1 : 0.04 : 0.01	44	14200	1.30	91	25750	1.20

[a] concentrations of Me_6TREN and AscA shown are for reactants added during the chain extension procedure and exclude the concentrations initially present in the polymer solution. [b] initial conversion after dilution from monomer and solvent addition.

The chain extension experiments were performed using outlet polymer solution that had been exposed to air for greater than 48 hours. The first chain extension X1 was prepared with no additional ligand. The injection of ascorbic acid to reinitiate polymerization was unsuccessful, as the remaining ligand was likely protonated by residual acid generated in the reduction process. Chain extension of the same polymer solution was performed with the addition of a small amount of ligand (X2) and fresh ascorbic acid. Supplemental ligand was added in a 2 fold excess to the amount of ascorbic acid that would have been present in the solution from the original polymerization. The additional ligand was able to complex to existing copper species and displaced any protonated ligand to form active complexes. Upon injection of fresh ascorbic acid, the polymerization was successfully reinitiated and the conversion increased to 88% in 90 minutes. The M_n increased from 11200 to 28990 $g \cdot mol^{-1}$, and the PDI decreased from 1.46 to 1.22. Chain extensions of the other outlet polymer solutions (X3-X5) were likewise successful, as all the experiments exhibited a clear growth in molecular weight with increasing conversion in a short period of time. The GPC traces of chain extension X2 are plotted along with a molecular weight distribution from experiment T8 (outlet of copper coil) in Figure 8.11. The traces are normalized with respect to area, and show a noticeable narrowing of the molecular weight distribution upon extension, as well as a clean shift to higher molecular weight values.

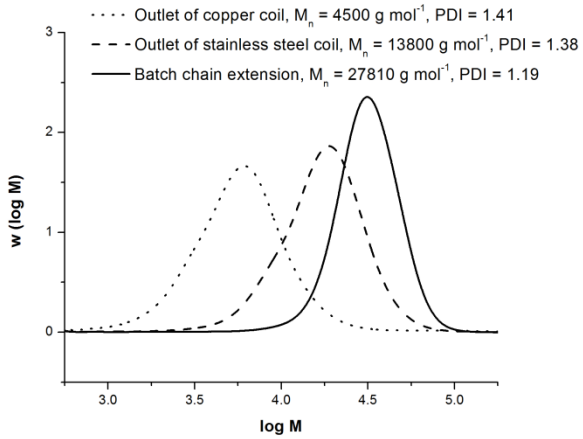

Figure 8.11: Gel permeation chromatography traces for pMA chain extensions of experiment T6. The traces are normalized by area, and experimental conditions of the extensions are shown in Table 8.4.

These chain extensions show that the polymer chains produced are highly living, and that storage with ascorbic acid (and by-products from the reduction process) for an extended period of time had a negligible impact on the chain end functionality. Although a small amount of ligand had to be added to re-initiate polymerization, no additional copper was added to the solution. The copper concentrations in the polymer solutions coming out of the stainless steel reactor were measured by flame atomic absorption spectroscopy and found to be approximately 15-20 ppm. The values were in agreement with those found in a previous SET-LRP study utilizing copper wire as a catalyst source in a continuous stirred tank reactor.[48] With the additional dilution by subsequent monomer addition, the chain extensions were mediated by less than 10 ppm of copper in solution. At such a low copper concentration, the final polymer may be usable in a variety of applications without further purification. With two reactor feeds and the subsequent chain extension, the methodology could be used to produce a triblock gradient copolymer. Conceptually the chain extension could also be added to the continuous process with additional feed points and stainless steel tubing.

8.4 Conclusions

An innovative design for a flow reactor was proposed for the continuous production of uniform polymer with high livingness using SET-LRP, improving upon the initial concept.[28] Instead of using copper tubing to construct the entire reactor, a short copper coil was used to initiate polymerization and generate soluble copper species. The bulk of the reaction then took place in inert stainless steel tubing, using ascorbic acid as a reducing agent to drive the catalytic cycle and mediate the polymerization. The study is the first investigation into the use of ascorbic acid in SET-LRP reactions. The addition of ascorbic acid into a batch reaction with copper wire gave uncontrolled polymerization, likely due to very fast reduction of copper(II) generated at the onset of polymerization such that insufficient deactivators were in solution. However, when a small amount of ascorbic acid was added to a polymer solution with soluble copper species, such as the material exiting the copper tubing, the ascorbic acid was able to regenerate active copper(I) and copper(0) species to re-initiate polymerization in the absence of copper(0) surface.

The improved tubular system was able to continuously polymerize methyl acrylate at ambient temperature with 30 wt% DMSO as solvent, reaching a steady state conversion of 65-67% with a residence time of 35 minutes. The residence time was extended to 62 minutes by adding another length of stainless steel tubing. Using this reactor configuration, it was possible to reach a steady state conversion of 78% and produce well defined living polymer with a narrow molecular weight distribution.

Chain extension experiments were conducted on the outlet polymer solution. It was found that additional ligand was required to re-initiate polymerization, likely due to protonation of ligand already existing in the polymer solution by residual ascorbic acid and the derivatives generated in the reduction process. With a small excess of ligand, the chain extensions were well-controlled and showed a clean shift and narrowing in molecular weight distribution with increasing conversion. Although methyl acrylate was used in in all stages in this study to simplify

analysis, other monomers could have been substituted at any of the feed points or in the chain extension to generate triblock gradient copolymers. The chain extension could also be easily adapted to the continuous reactor by the addition of two feed points, and additional stainless steel tubing. The results illustrate the significant potential of using a continuous tubular reactor as an efficient means to scale-up production of well controlled polyacrylics and other multiblock copolymers.

References

(1) Kato, M.; Kamigaito, M.; Sawamoto, M.; Higashimura, T. *Macromolecules* **1995**, *28*, 1721-1723.

(2) Wang, J. S.; Matyjaszewski, K. *Journal of the American Chemical Society* **1995**, *117*, 5614-5615.

(3) Matyjaszewski, K.; Xia, J. *Chemical Reviews* **2001**, *101*, 2921-2990.

(4) Ouchi, M.; Terashima, T.; Sawamoto, M. *Chemical Reviews* **2009**, *109*, 4963-5050.

(5) Tsarevsky, N. V.; Matyjaszewski, K. *Journal of Polymer Science Part A: Polymer Chemistry* **2006**, *44*, 5098-5112.

(6) Shen, Y.; Tang, H.; Ding, S. *Progress in Polymer Science* **2004**, *29*, 1053-1078.

(7) Tsarevsky, N. V.; Matyjaszewski, K. *Chemical Reviews* **2007**, *107*, 2270-2299.

(8) Mueller, L.; Matyjaszewski, K. *Macromolecular Reaction Engineering* **2010**, *4*, 180-185.

(9) Destarac, M. *Macromolecular Reaction Engineering* **2010**, *4*, 165-179.

(10) Jakubowski, W.; Min, K.; Matyjaszewski, K. *Macromolecules* **2006**, *39*, 39-45.

(11) Matyjaszewski, K.; Jakubowski, W.; Min, K.; Tang, W.; Huang, J.; Braunecker, W. A.; Tsarevsky, N. V. *Proceedings of the National Academy of Sciences of the United States of America* **2006**, *103*, 15309-15314.

(12) Percec, V.; Guliashvili, T.; Ladislaw, J. S.; Wistrand, A.; Stjerndahl, A.; Sienkowska, M. J.; Monteiro, M. J.; Sahoo, S. *Journal of the American Chemical Society* **2006**, *128*, 14156-14165.

(13) Rosen, B. M.; Percec, V. *Chemical Reviews* **2009**, *109*, 5069-119.

(14) Lligadas, G.; Rosen, B. M.; Monteiro, M. J.; Percec, V. *Macromolecules* **2008**, *41*, 8360-8364.

(15) Lligadas, G.; Rosen, B. M.; Bell, C. a.; Monteiro, M. J.; Percec, V. *Macromolecules* **2008**, *41*, 8365-8371.

(16) Jiang, X.; Fleischmann, S.; Nguyen, N. H.; Rosen, B. M.; Percec, V. *Journal of Polymer Science Part A: Polymer Chemistry* **2009**, *47*, 5591-5605.

(17) Monteiro, M. J.; Guliashvili, T.; Percec, V. *Journal of Polymer Science Part A: Polymer Chemistry* **2007**, *45*, 1835-1847.

(18) Zhang, Y.; Wang, Y.; Matyjaszewski, K. *Macromolecules* **2011**, *44*, 683-685.

(19) West, A. G.; Hornby, B.; Tom, J.; Ladmiral, V.; Harrisson, S.; Perrier, S. *Macromolecules* **2011**, *44*, 8034-8041.

(20) Zhang, Y.; Wang, Y.; Peng, C.-how; Zhong, M.; Zhu, W.; Konkolewicz, D.; Matyjaszewski, K. *Macromolecules* **2012**, *45*, 78-86.

(21) Min, K.; Jakubowski, W.; Matyjaszewski, K. *Macromolecular Rapid Communications* **2006**, *27*, 594-598.

(22) Matyjaszewski, K.; Dong, H.; Jakubowski, W.; Pietrasik, J.; Kusumo, A. *Langmuir* **2007**, *23*, 4528-4531.

(23) Tang, H.; Shen, Y.; Li, B. G.; Radosz, M. *Macromolecular Rapid Communications* **2008**, *29*, 1834-1838.

(24) Chan, N.; Boutti, S.; Cunningham, M. F.; Hutchinson, R. A. *Macromolecular Reaction Engineering* **2009**, *3*, 222-231.

(25) Fleischmann, S.; Rosen, B. M.; Percec, V. *Journal of Polymer Science Part A: Polymer Chemistry* **2010**, *48*, 1190-1196.

(26) Fleischmann, S.; Percec, V. *Journal of Polymer Science Part A: Polymer Chemistry* **2010**, *48*, 2243-2250.

(27) Nguyen, N. H.; Percec, V. *Journal of Polymer Science Part A: Polymer Chemistry* **2010**, *48*, 5109-5119.

(28) Chan, N.; Cunningham, M. F.; Hutchinson, R. A. *Macromolecular Rapid Communications* **2011**, *32*, 604-609.

(29) Matyjaszewski, K.; Tsarevsky, N. V.; Braunecker, W. A.; Dong, H.; Huang, J.; Jakubowski, W.; Kwak, Y.; Nicolay, R.; Tang, W.; Yoon, J. A. *Macromolecules* **2007**, *40*, 7795-7806.

(30) Isse, A. a; Gennaro, A.; Lin, C. Y.; Hodgson, J. L.; Coote, M. L.; Guliashvili, T. *Journal of the American Chemical Society* **2011**, *133*, 6254-64.

(31) Nguyen, N. H.; Rosen, B. M.; Lligadas, G.; Percec, V. *Macromolecules* **2009**, *42*, 2379-2386.

(32) Soeriyadi, A. H.; Boyer, C.; Nyström, F.; Zetterlund, P. B.; Whittaker, M. R. *Journal of the American Chemical Society* **2011**, *133*, 11128-11131.

(33) Levere, M. E.; Willoughby, I.; O'Donohue, S.; de Cuendias, A.; Grice, A. J.; Fidge, C.; Becer, C. R.; Haddleton, D. M. *Polymer Chemistry* **2010**, *1*, 1086-1094.

(34) Shen, Y.; Zhu, S. *AIChE Journal* **2002**, *48*, 2609-2619.

(35) Müller, M.; Cunningham, M. F.; Hutchinson, R. A. *Macromolecular Reaction Engineering* **2008**, *2*, 31-36.

(36) Noda, T.; Grice, a; Levere, M.; Haddleton, D. *European Polymer Journal* **2007**, *43*, 2321-2330.

(37) Chen, H.; Zhang, M.; Yu, M.; Jiang, H. *Journal of Polymer Science Part A: Polymer Chemistry* **2011**, *49*, 4721-4724.

(38) Britovsek, G. J. P.; England, J.; White, A. J. P. *Inorganic chemistry* **2005**, *44*, 8125-8134.

(39) Gruendling, T.; Junkers, T.; Guilhaus, M.; Barner-Kowollik, C. *Macromolecular Chemistry and Physics* **2010**, *211*, 520-528.

(40) Nguyen, N. H.; Jiang, X.; Fleischmann, S.; Rosen, B. M.; Percec, V. *Journal of Polymer Science Part A: Polymer Chemistry* **2009**, *47*, 5629-5638.

(41) Stoffelbach, F.; Griffete, N.; Bui, C.; Charleux, B. *Chemical Communications* **2008**, 4807-4809.

(42) Oh, J. K.; Min, K.; Matyjaszewski, K. *Macromolecules* **2006**, *39*, 3161-3167.

(43) McCullough, L. A.; Dufour, B.; Matyjaszewski, K. *Journal of Polymer Science Part A: Polymer Chemistry* **2009**, *47*, 5386-5396.

(44) Min, K.; Gao, H.; Matyjaszewski, K. *Macromolecules* **2007**, *40*, 1789-1791.

(45) Paterson, S. M.; Brown, D. H.; Chirila, T. V.; Keen, I.; Whittaker, A. K.; Baker, M. V. *Journal of Polymer Science Part A: Polymer Chemistry* **2010**, *48*, 4084-4092.

(46) Taylor, M. J. W.; Eckenhoff, W. T.; Pintauer, T. *Dalton transactions* **2010**, *39*, 11475-82.

(47) Casolari, R.; Felluga, F.; Frenna, V.; Ghelfi, F.; Pagnoni, U. M.; Parsons, A. F.; Spinelli, D. *Tetrahedron* **2011**, *67*, 408-416.

(48) Chan, N.; Cunningham, M. F.; Hutchinson, R. A. *Polymer Chemistry* **2012**, *3*, 486.

Chapter 9

Conclusions and Recommendations

9.1 Conclusions

Atom transfer radical polymerization (ATRP) is a dynamic and versatile technique for the synthesis of value-added polymers with novel applications. While ATRP possesses significant commercial potential, industrial adoption of ATRP has been encumbered by practical concerns over low polymerization rates, material costs and availability of ligands and metal complexes, toxicity of the compounds used, as well as post-polymerization purification costs associated with removal of the high level of residual metal in the final product.

The solution to these two problems requires a combination of innovative chemistry and engineering practicality. Recent advances in ATRP chemistry have resulted in the development of low copper variants of ATRP which enable significant reduction in the amount of copper metal complex used down to almost negligible levels. The purpose of this thesis was to study two of these novel ATRP systems - “activator regenerated by electron transfer” (ARGET), and “single electron transfer-living radical polymerization” (SET-LRP), and to adapt the chemistry to continuous processes. As continuous processes offer higher productivity and more consistent product quality at steady state than comparable batch reactors, the amalgamation of low residual copper concentration with the increased space-time yield achieved through continuous processes should provide practical proof of concepts for scale-up considerations.

The principal weakness of ARGET ATRP as first introduced was the requirement for ligand in 3-10 fold excess to the amount of copper used. The excess ligand was proposed to stabilize the copper complex against competing side reactions that become relevant at low copper concentrations. As the ligands typically used for ARGET are expensive and only available in

small quantities, the need of a large excess of ligand was seen as a key barrier to the feasibility of ARGET ATRP. Tris(2-pyridylmethyl)amine (TPMA) has been observed in literature studies to form very stable copper complexes in both copper(I) and copper(II) oxidation states. As such, it was thought that ARGET polymerizations may be possible using only a stoichiometric ratio of TPMA to copper. This was studied in batch solution polymerizations of butyl methacrylate (BMA), methyl methacrylate (MMA), and butyl acrylate (BA) using a stoichiometric ratio of TPMA to copper. Polymerizations were conducted under industrially relevant conditions using unpurified monomer and solvent, and remained well-controlled at high temperature (up to 110 °C).

ARGET ATRP was then adapted to a continuous tubular reactor constructed from PTFE tubing. Polymerization of BMA at 90 °C was attempted in the tubular reactor, and it was found that at low reducing agent content (10 mol% to initiator) the polymerization reached only 20% conversion in the tubular reactor compared to 87% in a batch reactor. The cause of inhibition was determined to be the presence of oxygen which oxidized the copper complex to its copper(II) state. Thus additional reducing agent (40 mol% to initiator) was required to regenerate the copper(I) activating species and achieve high conversion (>95%) in batch and continuous reactors with excellent agreement between the two conversion profiles. Increasing the reducing agent concentration led to an increase in polymerization rate by shifting the copper(I)/copper(II) ratio in favour of the activating copper(I) complex. This study was the first experimental demonstration of ARGET ATRP in a continuous process, and showed that ARGET ATRP could be made significantly faster and more robust through judicious use of an inexpensive reducing agent.

There have been no experimental studies of ATRP in a CSTR, due to problems with copper heterogeneity in the reactor and also because of broadening of the molecular weight distribution caused by residence time effects. As the narrowness of the molecular weight distribution is often used as a measure of livingness in controlled radical polymerization (CRP),

conducting CRP in a CSTR seems counterproductive. However, broadening due to a residence time distribution does not necessitate poor livingness, and as CSTRs are commonly employed in industry, it was decided to adapt ARGET ATRP to a CSTR.

ARGET ATRP of MMA and BA was first conducted in a CSTR using anisole as solvent. As a result of the long operation times required to reach steady state behaviour in a CSTR, precipitation of the less soluble copper(II) species was observed in the monomer feed vessel over the course of a polymerization. To ensure that the copper complex remained in solution, DMF was used as a co-solvent in BA and MMA batch polymerizations to enhance the rate of polymerization and prevent copper precipitation. Although DMF prevented copper precipitated and gave a higher rate of polymerization for BA experiments, the effects of a DMF/anisole solvent mixture in MMA polymerizations were more complex. The resulting MMA polymerization rate was found to be a balance between enhancement of activation kinetics, and initiator efficiency due to bimolecular termination. A high DMF concentration resulted in considerable termination which lowered initiator efficiency and subsequently the polymerization rate. CSTR experiments were conducted with optimal batch formulations at residence times of 60, 90, and 120 minutes. All polymerizations exhibited steady state behaviour in conversion and molecular weight data after four residence times. Interestingly, the apparent rates of polymerization in CSTR experiments were higher than equivalent batch polymerizations, with a 54% increase in polymerization rate for BA experiments and a 30% increase for MMA experiments. This increased rate was most likely due to a higher steady state reducing agent concentration in the CSTR compared to batch reactors, which shifted the copper(I)/copper(II) ratio in favour of the activating species. Chain extensions conducted using outlet polymer solutions showed good living characteristics, and suggested that residence time effects did not negatively impact livingness.

SET-LRP is a robust technique that enables low temperature synthesis of polyacrylates with high polymerization rates. SET-LRP utilizes elemental copper(0) as a catalyst source which limits the amount of residual copper in the final polymer and provides facile removal of the bulk of the heterogeneous copper metal. The difficulty with utilizing SET-LRP for large scale production lies in the batch to batch startup variability that have been observed in literature, and the design of a reactor that has sufficient heat removal to cope with the highly exothermic reaction. Both factors can result in variation in product quality and operational inefficiency, and poor heat removal can be a significant safety concern as it can result in runaway reactions. Fortunately, the engineering challenges surrounding SET-LRP can be efficiently remedied by utilizing continuous processes.

Although having similar heat removal capacity to batch reactors, CSTRs have lower instantaneous monomer concentration and as such instantaneous heat generation in a CSTR is lower than a similarly sized batch reactor. SET-LRP of methyl acrylate (MA) was adapted to a CSTR by using copper wire as an easy to handle and reusable catalyst source. Polymerizations exhibited steady state behaviour in conversion and molecular weight after 4 residence times, and with high polymerization rates at only 30 °C. As activation in SET-LRP is proposed to be mediated by copper(0), polymerizations rates could be increased by increasing the copper surface area. A doubling of the available copper surface area resulted in an approximately 30% increase in polymerization rate. Two CSTRs were connected in series to increase the total residence time, and an increase in conversion was observed between the first and second reactors. More importantly, polymer synthesized in a train of 2 CSTRs had a narrower molecular weight distribution than when just one CSTR was used due to narrowing of the residence time distribution. This result along with batch chain extension experiments demonstrated that residence time effects in a CSTR did not negatively impact chain end functionality of the polymer produced.

Readily available copper tubing was used to construct a modular tubular reactor. The walls of the reactor acted as a catalyst source for SET-LRP of methyl acrylate at ambient temperature. The high surface area to volume ratio resulted in higher polymerization rates than in comparable batch or CSTR experiments. The large surface area in tubular reactors also facilitates efficient heat removal, and is an attractive option for scale-up of SET-LRP. Although the modular copper reactor was an efficient design, there were concerns over long term stability due to copper leeching from the reactor walls. As such, the tubular reactor design was modified by incorporating a short copper coil to initiate polymerization and generate soluble copper species, while utilizing inert stainless steel tubing for the majority of the reactor volume. To mediate polymerization in the absence of copper surface, ascorbic acid was used as a reducing agent for the first time with SET-LRP to regenerate activating copper species. Polymerizations were well controlled and reached high conversion in a reasonable residence time. Chain extensions of the outlet polymer were possible with a small amount of fresh ligand, and showed highly living characteristics with only 10 ppm of residual copper. The improved reactor design can be theoretically used to continuously produce novel multiblock copolymer .

9.2 Recommendations for future work

The investigations in this thesis resulted in the first ever experimental demonstrations of ARGET ATRP and SET-LRP in continuous processes. In addition to successful proof of concepts, the process of adapting these chemistries to different reactor designs generated some insights into the kinetics and utilization of the two low copper ATRP systems that can be further explored.

9.2.1 Systematic study of ARGET ATRP

Although ARGET ATRP and SET-LRP both enable a significant decrease in copper concentration required down to below 100 ppm, further reduction down to below 10 ppm in the final polymer may be required for the residual metal concentration to be truly negligible. As such,

the limits of both ARGET and SET-LRP should be explored to see if copper levels can be further decreased while still maintaining a reasonable polymerization rate. The absolute lower limit of copper complex may be physically limited by the deactivation kinetics. The rate constant of deactivation approaches diffusion limitations for some monomers, and in these systems the concentration of copper required to maintain control over the polymerization can be calculated based on the activation rate constant and active radical concentration.

The type of reducing agent and the concentration used in ARGET should also be explored. A tin compound was used for the ARGET polymerizations in this thesis; however there are many other reducing agents available which can enable different kinetic profiles. Further, it may be possible to use a combination of two or more reducing agents to maintain a constant and high rate of polymerization without sacrificing control.

Some ARGET polymerizations were conducted to investigate solvent effects, and the results from varying DMF concentration on MMA polymerization kinetics were very interesting. Since the overall polarity of a solvent mixture should be proportional to the volume fraction of the solvents in the mixture, the enhancement to polymerization rate at 2-5% DMF was unexpected. Investigating other solvent combinations may yield an explanation of the results, and possibly provide a set of selection criteria towards enhancing the rate of polymerization in ATRP with only a small amount of polar solvent.

9.2.2 Reactor design and operating strategy

The chain end functionality of the polymer produced in the CSTR studies was only qualitatively analyzed with chain extension experiments. A more rigorous quantitative analysis of the polymer using proton NMR and mass spectroscopy can provide an accurate evaluation of livingness, and this can be compared to batch polymerizations or even continuous tubular experiments at similar reaction conditions and conversions. If the analysis shows that CSTRs actually possess higher livingness than a batch or continuous process, it would provide strong incentive towards the use

of CSTRs for the production of block copolymers where self-assembly into more complex structures is not required.

On the subject of block copolymers, most literature reports are focused on distinct block copolymers purified during synthesis by precipitation of the first block in a large excess of organic solvent. On an industrial scale that becomes impractical, and it is likely that block gradient copolymers will be produced in commercial processes. The homogeneity and the degree of transition from one block to the next will likely have an impact on the polymer properties, and it may be interesting to synthesize some block gradient copolymers in batch and CSTR processes to compare their performance.

The limits of the SET-LRP tubular reactor should also be explored. The current set of experiments was conducted at room temperature with no temperature control. With the high surface area to volume ratio, the reactor can be maintained at a constant temperature in an oil bath, and it is possible to explore higher reaction temperatures and perhaps higher ascorbic acid concentrations in order to increase the polymerization rate while maintaining control.

9.2.3 Ligand design and other metal complexes

Dispersed phase polymerizations yield considerable operating advantages in viscosity and heat transfer, as well as facilitating adherence to increasingly stringent environment guidelines to reduce the usage of volatile organic solvents. Although TPMA works well for solution ARGET ATRP, it is less effective for dispersed phase polymerizations as the copper complex will partition into the water phase. The hydrophobicity of the copper complex can be tuned by changing the ligand structure, and while there are some ligands that form hydrophobic copper complexes, one has not been found to effectively mediate ARGET ATRP. Therefore, the design of a ligand that forms an active hydrophobic copper complex, and that is stable against disproportionation may enable ARGET ATRP in dispersed phase polymerization.

Beyond copper mediated ATRP, other transition metal complexes are being investigated. Iron in particular is a cheap and non-toxic metal that has received considerable attention as an ATRP mediator. As with copper mediated ATRP, tuning the ATRP activity of iron complexes will require improvements in ligand design. If a suitable iron complex cannot be found for ARGET ATRP, it may be useful to investigate the use of a strong magnetic field to remove residual iron.